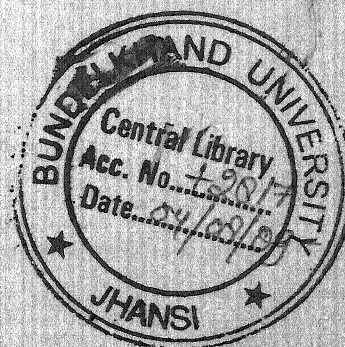


**SYNTHESIS, STRUCTURE AND PROPERTIES OF
CATIONIZED, HYDROLYZED AND UNHYDROLYZED
POLYACRYLAMIDE GRAFTED CHITOSAN**

A Thesis Submitted to
BUNDELKHAND UNIVERSITY, JHANSI
For the Award of the Degree
of
DOCTOR OF PHILOSOPHY
IN
POLYMER SCIENCE



Submitted By
SK. AKBAR ALI

Under the Supervision of

Prof. Sanjay Palsule
Former Head
Department of Polymer Science
Bundelkhand University, Jhansi
Presently at DPT, IIT Roorkee

Prof. Ram Prakash Singh
Vice Chancellor
University of Lucknow
Lucknow

**DEPARTMENT OF POLYMER SCIENCE
BUNDELKHAND UNIVERSITY, JHANSI, INDIA**

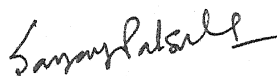
CERTIFICATE

This is to certify that the research work embodied in the Thesis entitled

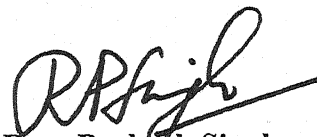
**“Synthesis, Structure and Properties of
Cationized, Hydrolyzed and Unhydrolyzed
Polyacrylamide Grafted Chitosan”**

submitted for the Degree of Doctor of Philosophy in Polymer Science, of Bundelkhand University, Jhansi is the record of the original work performed by **Mr. Sk. Akbar Ali** under our guidance and supervision.

The candidate has worked for the period required under the ordinance and put in the required attendance.



Prof. Sanjay Palsule
Former Head, Department of Polymer Science.
Bundelkhand University,
Jhansi.



Prof. Ram Prakash Singh
Vice Chancellor,
University of Lucknow,
Lucknow.

DEDICATION

“A student who can weave his technology into the fabric of society can claim to have a liberal education.”

Dedicated to those who helped me to weave the technology.

∞ ACKNOWLEDGEMENT ∞

At the successful completion of the work I sincerely acknowledge cooperation and support of Prof. R P Agarwal, Vice-Chancellor, Bundelkhand University, for his kind help. I also acknowledge help of Prof. Ramesh Chandra, Former Vice-Chancellor, Bundelkhand University.

I am thankful to Prof. Ram Prakash Singh, Vice-Chancellor, University of Lucknow, for his guidance, encouragement, support in performing experiments, fruitful discussions and valuable comments that led to successful completion of this project. I am heartily thankful to Dr. Sanjay Palsule, Associate Professor, IIT-Roorkee, (Former Head, Department of Polymer Science, Bundelkhand University) for his guidance and help.

I am thankful to Prof. Chapal Kumar Das, Head, Materials Science Centre, IIT-Kharagpur, for providing laboratory facility and support.

I also acknowledge my friends and colleague in Polymer Science Department for their valuable comments.

I am also thankful to the Registrar, Dy. Registrar and Administrative officers of Bundelkhand University for their sincere and active support.

SK. Akbar (AQ)
(SK. AKBAR ALI)

CONTENTS

<u>Index</u>	<u>Page No.</u>
CERTIFICATE	I
DEDICATION	II
ACKNOWLEDGEMENT	III
CONTENTS	IV-XI
LIST OF FIGURES	XII-XVI
LIST OF TABLES	XVII
ABSTRACT	XVIII-XX
 CHAPTER I INTRODUCTION	 1-9
1.1 Introduction	2
1.2 Plan of Work	7
1.3 Overview	8
 CHAPTER II LITERATURE REVIEW	 10-68
2.1 Introduction to chitosan	11
2.1.1 Chitosan – a deacetylated form of chitin	11
2.1.2 Physiochemical Characteristics of Chitosan	12
2.1.2.1 Degree of N-acetylation	12
2.1.2.2 Solubility	12
2.1.2.3 Crystallinity	13
2.1.3 Industrial Production	13
2.1.4 Use of Chitosan	14
2.2 Graft Copolymers	15
2.3 Synthesis of Polysaccharides based Graft Copolymers	16
2.3.1 Chemical Initiation	16
2.3.1.1 Initiation by Ceric Ion	16

2.3.1.2	Initiation by Trivalent Manganese	18
2.3.1.3	Initiation by Hydrogen Peroxide / Fe^{2+} System (Fenton's Reagent)	18
2.3.1.4	Initiation by Cu (II) ions	18
2.3.1.5	Initiation by Chromium (VI) ions	18
2.3.1.6	Initiation by Vanadium(V) ions	18
2.3.1.7	Initiation by Xanthate Process	19
2.3.1.8	Initiation by Azo-bis-isobutyro Nitrile (AIBN)	19
2.3.1.9	Initiation by Metal Chelates	19
2.3.2	Initiation by Irradiation	19
2.3.3	Initiation by Mastication	20
2.4	Proof of Grafting	20
2.4.1	IR Spectra of Graft Copolymers	20
2.4.2	Molecular Weight of Grafted Chains	21
2.4.3	Calculation of Grafting Parameters	22
2.5	Particle Interaction Studies	23
2.6	Coagulation and Flocculation	24
2.6.1	Coagulation	24
2.6.2	Flocculation	25
2.6.3	Stability of the Colloids	26
2.6.4	Electrical Double Layer	27
2.7	Zeta Potential	30
2.7.1	Principle of Measuring Zeta Potential	31
2.7.2	Significance of the Measured Zeta Potential	32
2.8	Flocculation Mechanisms	33
2.8.1	Polymer Bridging	33
2.8.1.1	Synthetic Bridging Polymer	35
2.8.1.2	Natural Bridging Polymer	35
2.8.2	Charge Neutralization	36
2.8.3	Electrostatic Patch Mechanism	36
2.8.4	Polymer Complex Formation	37
2.8.5	Flocculation by Free Polymers	37

2.9	Flocculating Materials	38
2.9.1	Inorganic Flocculants	38
2.9.1.1	Aluminum Compounds	38
2.9.1.1.1	Aluminum Chloride Hydroxide	39
2.9.1.1.2	Sodium Aluminates	39
2.9.1.2	Iron Compounds	39
2.9.1.3	Calcium Salts	39
2.9.1.4	Sodium Silicates	39
2.9.2	Polymeric Flocculants	40
2.9.2.1	Cationic Polymers	40
2.9.2.1.1	Polyacrylamide-Based Cationic Polymers	40
2.9.2.1.2	Polyamines, Polyimines and Poly Vinyl Pyridines	42
2.9.2.2	Anionic Polymers	43
2.9.2.2.1	Polymers Containing Carboxyl Groups	43
2.9.2.2.2	Poly(Acrylic Acid) and its Salts	43
2.9.2.2.3	Anionic Polyacrylamide	44
2.9.2.2.4	Polymers Containing Sulfonic Acid Group	44
2.9.2.2.5	Poly (Vinyl Sulfonic Acid) (PVSA)	44
2.9.2.2.6	Poly (Styrene Sulfonic Acid)(PSSA)	45
2.9.2.3	Nonionic Polymers	46
2.9.2.3.1	Polyacrylamide (PAM)	46
2.9.2.3.2	Poly (Ethylene Oxide) (PEO)	46
2.9.2.4	Natural Polymers	47
2.9.2.4.1	Starch	47
2.9.2.4.2	Gum	48
2.9.2.4.3	Cellulose and its Derivatives	49
2.9.2.4.4	Dextran	49
2.9.2.4.5	Glycogen	49
2.9.2.5	Graft Copolymers	49
2.9.2.5.1	Anionic/Nonionic Graft Copolymers	50
2.9.2.5.2	Cationic Graft Copolymers	51
2.10	Polymeric versus Inorganic Flocculants	51
2.11	Natural versus Synthetic Flocculants	52

2.12	Flocculation: The Test Methods	52
2.12.1	The Settling Test	53
2.12.2	The Jar Test	54
2.13	Factors Affecting the Flocculation	55
2.13.1	Effects of Molecular Weight and Charge Density of Polymer	55
2.13.2	Effect of Polymer Dosage, Critical Concentration and Optimum Dose	56
2.13.3	Conformation of Polyelectrolyte in Solution	58
2.13.4	Solution Properties	58
2.13.4.1	Effect of Ionic Strength	58
2.13.4.2	Effect pH	59
2.13.4.3	Effect of Particle Size	60
2.13.4.4	Effect of Temperature	60
2.14	Applications of Flocculant	61
2.14.1	Water Clarification	61
2.14.2	Paper Making	61
2.14.3	Mineral Processing	62
2.14.4	Selective Flocculation	63
2.15	Partial Alkaline Hydrolysis	63
2.16	Cationization	64
2.17	Summary	68
CHAPTER III	SYNTHESIS AND CHARACTERIZATION	69-90
3.1	Materials	70
3.2	Synthesis	70
3.3	Purification of the Graft Copolymers by Solvent Extraction	73
3.4	Characterization of Graft Copolymers	73
3.4.1	Elemental Analysis	73
3.4.2	Measurement of Intrinsic Viscosity	73
3.4.3	IR Spectroscopy	74
3.4.4	Thermal Analysis	74

3.4.5	Scanning Electron Microscopy (SEM)	74
3.4.6	X-ray Diffraction Analysis (XRD)	74
3.5	Results and Discussion	75
3.5.1	Synthesis	75
3.5.2	Elemental Analysis	77
3.5.3	Intrinsic Viscosity	77
3.5.4	Calculation of Approximate Molecular Weight	79
3.5.5	IR Spectroscopy	80
3.5.6	Scanning Electron Microscopy (SEM)	83
3.5.7	Thermal Analysis	84
3.6.7.1	Differential Scanning Calorimetry (DSC)	84
3.6.7.2	Thermogravimetric Analysis (TG and DTG)	85
3.5.8	X-ray Diffraction (XRD)	88
3.6	Summary	89
CHAPTER IV	FLOCCULATION STUDIES	91-112
4.1	Materials	92
4.2	Experimental	92
4.2.1	Measurement of Zeta Potential	92
4.2.1.1	Measurement Procedure	92
4.2.2	Measurement of Particle Size Distribution	92
4.2.3	Average Chemical Composition of the Colloidal Particles	94
4.2.4	Scanning Electron Micrograph Analysis of Particles	94
4.2.5	Flocculation Studies	96
4.2.5.1	Settling Test	96
4.2.5.2	Jar Test	96
4.2.6	Measurement of Supernatant Turbidity	97
4.2.6.1	Preparation of Stock Turbidity Suspension	97
4.2.6.2	Preparation of Standard Turbidity Suspension	97
4.2.6.3	Measurement Procedure	97
4.3	Results and Discussion	99
4.3.1	The Settling Test Results	99

4.3.1.1	Flocculation of the Kaolin Suspension	99
4.3.1.2	Flocculation of the Iron Ore Suspension	102
4.3.1.3	Flocculation of the Silica Suspension	104
4.3.1.4	Flocculation of the Bentonite Suspension	106
4.3.2	Jar Test Results	108
4.3.2.1	Flocculation of the Kaolin Suspension	108
4.3.2.2	Flocculation of the Iron Ore Suspension	109
4.3.2.3	Flocculation of the Silica Suspension	110
4.3.2.4	Flocculation of the Bentonite Suspension	111
4.4	Summary	112
CHAPTER V	PARTIAL ALKALINE HYDROLYSIS	113-140
5.1	Introduction	114
5.2	Materials	114
5.3	Alkaline Hydrolysis of Chitosan-g-PAM	114
5.4	Characterization of Hydrolyzed Products	115
5.4.1	Determination of Neutralization Equivalent (N.E.) of the Hydrolysed Copolymers	115
5.4.2	Elemental Analysis	116
5.4.3	IR Spectroscopy	116
5.4.4	Scanning Electron Microscopy	116
5.4.5	Thermal Analysis	116
5.4.6	X-ray Diffraction	117
5.5	Flocculation Studies	117
5.6	Results and Discussion	117
5.6.1	Synthesis	117
5.6.2	Characterization	118
5.6.2.1	Neutralization Equivalent Value	118
5.6.2.2	Elemental Analysis	118
5.6.2.3	IR Spectroscopy	119
5.6.2.4	Scanning Electron Microscopy (SEM)	120
5.6.2.5	Thermal Analysis	122
5.6.2.5.1	Differential Scanning Calorimetry (DSC)	122

5.6.2.5.2	Thermogravimetric Analysis (TG and DTG)	123
5.6.2.6	X-ray Diffraction	125
5.7	Flocculation Studies	126
5.7.1	The Settling Tests	126
5.7.1.1	Flocculation of the Kaolin Suspension	126
5.7.1.2	Flocculation of the Iron Ore Suspension	128
5.7.1.3	Flocculation of the Silica Suspension	130
5.7.1.4	Flocculation of the Bentonite Suspension	133
5.7.2	Jar Test Results	134
5.7.2.1	Flocculation of the Kaolin Suspension	135
5.7.2.2	Flocculation of the Iron Ore Suspension	136
5.7.2.3	Flocculation of the Silica Suspension	137
5.7.2.4	Flocculation of the Bentonite Suspension	138
5.8	Summary	139
CHAPTER VI	CATIONIZATION OF CHITOSAN	141-165
6.1	Introduction	142
6.2	Materials	143
6.3	Synthesis	144
6.4	Characterization of the Cationized Chitosan	145
6.4.1	Elemental Analysis	145
6.4.2	Measurement of Intrinsic Viscosity	145
6.4.3	IR Spectroscopy	146
6.4.4	Scanning Electron Microscopy (SEM)	146
6.4.5	Thermal Analysis	146
6.4.6	X-ray Diffraction	146
6.5	Flocculation Studies	146
6.6	Results and Discussion	147
6.6.1	Synthesis and Intrinsic Viscosity measurement	147

6.6.2	Elemental Analysis	148
6.6.3	IR Spectroscopy	149
6.6.4	Scanning Electron Spectroscopy (SEM)	151
6.6.5	Thermal Analysis	152
6.6.5.1	Differential Scanning Calorimetry (DSC)	152
6.6.5.2	Thermogravimetric Analysis (TG and DTG)	153
6.6.6	X-ray Diffraction	155
6.7	Flocculation Studies	156
6.7.1	The Settling Tests	156
6.7.1.1	Flocculation of the Kaolin Suspension	157
6.7.1.2	Flocculation of the Iron Ore suspension	158
6.7.1.3	Flocculation of the Silica Suspension	159
6.7.1.4	Flocculation of the Bentonite Suspension	160
6.7.2	Jar Tests	161
6.7.2.1	Flocculation of the Kaolin Suspension	161
6.7.2.2	Flocculation of the Iron Ore suspension	162
6.7.2.3	Flocculation of the Silica Suspension	163
6.7.2.4	Flocculation of the Bentonite Suspension	164
6.8	Summary	165
CHAPTER VII CONCLUSIONS AND FUTURE SCOPES		166-170
7.1	Conclusion	167
7.2	Future Scope of the work	170
REFERENCES		171-187

LIST OF FIGURES

<u>Figure No.</u>	<u>Description</u>	<u>Page No.</u>
Figure 1.1	Structure of chitin	5
Figure 1.2	Structure of chitosan	5
Figure 2.1	Deacetylation of chitin by alkali	12
Figure 2.2	Structure of graft copolymer	15
Figure 2.3	Schematic representation of ceric ion initiation graft copolymerization	17
Figure 2.4	Schematic diagram showing the nature of electrical forces around a colloidal particle in blank solution	28
Figure 2.5	Schematic diagram showing energy barrier of the colloidal particle	29
Figure 2.6	Graphical representation of Zeta Potential showing isoelectric point	31
Figure 2.7	Schematic representation of Zeta meter	32
Figure 2.8	Schematic illustration of (a) bridging flocculation and (b) restabilisation of the adsorbed polymer	34
Figure 2.9	Schematic illustration of flocculation by electrostatic patch mechanism	37
Figure 2.10	Schematic representation of anionic polymer particle interaction	64
Figure 6.11	Schematic illustration of the adsorbed polycation conformation for (a) highly charged polycation on a highly charged anionic surface; (b) highly charged polycation on a surface of low anionic charge; (c) highly charged polycation on a small, negatively charged particle	66

<u>Figure No.</u>	<u>Description</u>	<u>Page No.</u>
Figure 2.12	Schematic illustration of electrostatic patch flocculation mechanism. Flocculation occurs when polycation-rich surfaces collide with polycation free surfaces	67
Figure 3.1	Schematic representation of the purification of the graft copolymer	72
Figure 3.2	Variation of viscosity of chitosan with concentration	78
Figure 3.3	Variation of viscosity of PAM with concentration	79
Figure 3.4	IR Spectrum of chitosan	81
Figure 3.5	IR Spectrum of PAM	82
Figure 3.6	IR Spectrum of product	82
Figure 3.7	Scanning Electron Micrographs of (a) chitosan, (b) PAM and (c and d) grafted chitosan	83
Figure 3.8	DSC curves of chitosan and Chito-g-PAM6	84
Figure 3.9	TG curve of chitosan	86
Figure 3.10	TG curve of Chito-g-PAM6	86
Figure 3.11	DTG curve of chitosan	87
Figure 3.12	DTG curve of Chito-g-PAM6	87
Figure 3.13	X-ray diffraction pattern of chitosan	88
Figure 3.14	X-ray diffraction pattern of Chito-g-PAM6	89
Figure 4.1 (a, b)	Scanning electron micrograph of kaolin powder	94
Figure 4.1 (c, d)	Scanning electron micrograph of iron ore	95
Figure 4.1 (e, f)	Scanning electron micrograph of silica powder	95
Figure 4.1(g, h, i)	Scanning electron micrograph of bentonite powder	95/96
Figure 4.2	Settling curves for kaolin suspension with addition of PAM grafted chitosan copolymers	100
Figure 4.3	Settling curves for kaolin suspension with addition of chitosan, PAM and Chito-g-PAM6	101
Figure 4.4	Settling curves for iron ore suspension with addition of PAM grafted chitosan copolymer	102

<u>Figure No.</u>	<u>Description</u>	<u>Page No.</u>
Figure 4.5	Settling curves for iron ore suspension with addition of chitosan, PAM and Chito-g-PAM6	103
Figure 4.6	Settling curves for silica suspension with addition of PAM grafted chitosan copolymers	104
Figure 4.7	Settling curves for silica suspension with addition of chitosan, PAM and Chito-g-PAM6	105
Figure 4.8	Settling curves for bentonite suspension with addition of PAM grafted chitosan copolymers	106
Figure 4.9	Settling curves for bentonite suspension with addition of chitosan, PAM and Chito-g-PAM6	107
Figure 4.10	Jar test results for kaolin suspension (0.25wt %) with addition of PAM grafted chitosan copolymers	108
Figure 4.11	Jar test results for iron ore (0.25wt %) suspension with addition of PAM grafted chitosan copolymers	109
Figure 4.12	Jar test results for silica suspension (0.25wt %) with addition of PAM grafted chitosan copolymers	110
Figure 4.13	Jar test results for bentonite suspension (0.25wt %) with addition PAM grafted chitosan copolymers	111
Figure 5.1	IR Spectrum of Chito-g-PAM6	119
Figure 5.2	IR Spectrum of Chito-hyd-3	120
Figure 5.3	SEM of Chito-g-PAM6 (a, c) and Chito-hyd-3 (b, d, e, f)	121
Figure 5.4	DSC curves of Chito-g-PAM6 and Chito-hyd-3	122
Figure 5.5	TG curve of Chito-g-PAM6	123
Figure 5.6	TG curve of Chito-hyd-3	123
Figure 5.7	DTG curve of Chito-g-PAM6	124
Figure 5.8	DTG curve of Chito-hyd-3	125
Figure 5.9	X-ray diffraction of Chito-g-PAM6	126
Figure 5.10	X-ray diffraction of Chito-hyd-3	126
Figure 5.11	Settling curves for kaolin suspension with addition of partially hydrolyzed graft copolymers	127

<u>Figure No.</u>	<u>Description</u>	<u>Page No.</u>
Figure 5.12	Settling curves for kaolin suspension with addition of chitosan, PAM, Chito-g-PAM6 and Chito-hyd-3	128
Figure 5.13	Settling curves for iron ore suspension with addition of partially hydrolyzed graft copolymers	129
Figure 5.14	Settling curves for iron ore suspension with addition of chitosan, PAM, Chito-g-PAM6 and Chito-hyd-3	130
Figure 5.15	Settling curves for silica suspension with addition of Partially hydrolyzed graft copolymers	131
Figure 5.16	Settling curves for silica suspension with addition of chitosan, PAM, Chito-g-PAM6 and Chito-hyd-4	132
Figure 5.17	Settling curves for bentonite suspension with addition of partially hydrolyzed graft copolymers	133
Figure 5.18	Settling curves for bentonite suspension with addition of chitosan, PAM, Chito-g-PAM6 and Chito-hyd-4	134
Figure 5.19	Jar test result for kaolin suspension (0.25wt %) with addition of partially hydrolyzed graft copolymers	135
Figure 5.20	Jar test results for iron ore suspension (0.25wt %) with addition of partially hydrolyzed graft copolymers	136
Figure 5.21	Jar test results for silica suspension (0.25wt %) with addition of partially hydrolyzed graft copolymers	137
Figure 5.22	Jar test results for bentonite suspension (0.25wt %) with addition of partially hydrolyzed graft copolymers	138
Figure 6.1	Schematic representation of the synthesis of cationized chitosan	144
Figure 6.2	Mechanism for the synthesis of CHPTAC grafted chitosan	149
Figure 6.3	IR Spectrum of CHPTAC	164
Figure 6.4	IR Spectrum of chitosan	164
Figure 6.5	IR Spectrum of CHPTAC grafted chitosan	151
Figure 6.6	SEM of chitosan (a) and Chito-cat-2 (b, c, and d)	152

<u>Figure No.</u>	<u>Description</u>	<u>Page No.</u>
Figure 6.7	DSC thermograph of chitosan and Chito-cat-2	153
Figure 6.8	TG curves of chitosan and Chito-cat-2	154
Figure 6.9	DTG Curves of chitosan and Chito-cat-2	154
Figure 6.10	X-ray diffraction of (a) chitosan, (b) CHPTAC and (c) Chito-cat-2	155
Figure 6.11	Settling curves for Kaolin suspension with all the cationized chitosan solutions	157
Figure 6.12	Settling curves for iron ore with addition of all the cationized chitosan solutions	158
Figure 6.13	Settling curves for silica suspension with addition of all the cationized chitosan solutions	159
Figure 6.14	Settling curves for bentonite suspension with addition of all the cationized chitosan solutions	160
Figure 6.15	Jar test results for kaolin suspension (0.25wt%) with addition of all the cationized chitosan solutions	161
Figure 6.16	Jar test results for kaolin suspension (0.25wt%) with addition of all the cationized chitosan solutions	162
Figure 6.17	Jar test results for silica suspension (0.25wt%) with addition of all the cationized chitosan solutions	163
Figure 6.18	Jar test results for bentonite suspension (0.25wt) with addition of all cationized chitosan solutions	164

LIST OF TABLES

<u>Table No.</u>	<u>Description</u>	<u>Page No.</u>
Table 2.1	Schematic representation of the conformational state of adsorbed polymer at different pH	59
Table 3.1	Synthetic details of the graft copolymers	72
Table 3.2	Elemental analysis of chitosan and grafted chitosan	77
Table 4.1	Zeta potential of the colloidal suspensions	93
Table 4.2	Average particle size of the colloidal suspensions	93
Table 4.3	Average chemical composition of the colloidal particles	94
Table 4.4	Settling rate of chitosan and PAM grafted chitosan copolymers	112
Table 5.1	Synthetic details of alkaline hydrolysis of Chito-g-PAM6	115
Table 5.2	Determination of Neutralization Equivalent (N.E) of Chito-g-PAM6 and its partially hydrolyzed products	118
Table 5.3	Elemental analyses of partially hydrolyzed and unhydrolysed Chito-g-PAM6	119
Table 5.4	Settling rate of Chito-g-PAM6 and partially hydrolyzed graft copolymers	139
Table 6.1	Synthetic details of cationized chitosan	145
Table 6.2	Intrinsic viscosities of various grades of cationized chitosan	147
Table 6.3	Elemental analysis of cationized chitosan	148
Table 6.4	Settling rate of chitosan and cationized chitosan	165

ABSTRACT

The polysaccharides play an important role in the field of science and technology due to their unique properties. The polysaccharides are renewably available from natural and microbial resources. They are biodegradable and nontoxic. Water-soluble polymers based on grafted polysaccharides have drawn much attention in the recent decades because of their controlled biodegradability, shear stability and high efficiency as turbulent drag reducers, viscosifiers and flocculants. The graft copolymers show better flocculation performance than the ungrafted polysaccharides, which is due to the better approachability of the grafted chains to the colloidal particles. The viscosity of the graft copolymers also increases than that of the base polysaccharides, because of the presence of the longer grafted chains.

The aim of the present investigation is to graft polyacrylamide (PAM) onto the backbone of chitosan in presence of ceric ammonium nitrate (CAN) as initiator. Further, it was envisaged to synthesize a series of graft copolymers with variation in the number and length of PAM chains by varying the concentration of acrylamide and CAN.

The chitosan, PAM and the synthesized graft copolymers were characterized by various materials characterization techniques, like, elemental analysis, viscometry (intrinsic viscosity), infrared spectroscopy (IR), thermal analysis (TGA/DSC), scanning electron microscopy (SEM), and X-ray diffraction (XRD). The flocculation characteristics of graft copolymers were evaluated in four synthetic effluents of namely, kaolin, iron ore, silica and bentonite suspensions.

The best flocculation performing PAM grafted chitosan was partially hydrolysed by the treatment with certain amount of alkali. A series of hydrolysed products were synthesized with varying the experimental conditions in order to establish the flocculation efficiency with expansion and straightening of the grafted flexible PAM chains. During hydrolysis, the $-\text{CONH}_2$ groups of PAM chains are converted to $-\text{COO}^-$ groups. The repulsion between the adjacent negatively charged groups leads to chain expansion.

In some cases the hydrolysed graft copolymers shows better flocculation performance than the corresponding graft copolymers. The hydrolysed products were characterized by elemental analysis, IR spectroscopy, neutralization equivalent, SEM, thermal analysis, and XRD.

By varying the concentration of acrylamide and CAN, seven grades of chitosan based graft copolymers were synthesized (Chitosan-g-PAM 1 to Chitosan-g-PAM7). The variation of synthetic parameters is reflected in the intrinsic viscosity of graft copolymers. The results of elemental analysis, IR spectroscopy, thermal analysis, XRD, SEM etc. establish the proof of grafting. In the series of graft copolymer based on Chitosan, the one with fewer and longer PAM chains was found to be most effective flocculant in all the four suspensions.

During partial alkaline hydrolysis of PAM grafted chitosan, it is possible to control the carboxyl content by controlling the reaction parameters, e.g. time, temperature and concentration of alkali. The hydrolysed products show better flocculation performance than the unhydrolysed product in kaolin suspension. Further the hydrolysed product, which has certain amount of carboxyl content but is still having flexible grafted chains showed better flocculation performance than others having the higher carboxyl content and complete loss of flexibility. On hydrolysis, the $-\text{CONH}_2$ groups of the graft copolymer were converted to $-\text{COO}^-$ groups and the chain extension takes place. The negative charges on grafted chains also increase. The former enhances the flocculation and the latter decreases the flocculation due to increasing repulsion between flocculant and negatively charged particles. Even though the former effect is dominant, only at optimum hydrolysis, there will be larger enhancement in flocculation characteristics. Among all the hydrolysed graft copolymers Chito-hyd-3 exhibited best flocculation performance for Kaolin and Iron Ore suspensions. Whereas Chito-hyd-4 showed best flocculation performance for silica and bentonite suspensions.

It is found that cationic polysaccharides are widely used as wet end additives in paper making industries. This is because they provide many benefits like improvement of the mechanical strength of the flocs, better retention of the fines and fillers, faster draining; reduction of waste water pollution.

The aim of this part of investigation was to synthesize some water-soluble cationic Chitosan where a cationic monomer *N* – (3-chloro-2-hydroxypropyl) trimethyl ammonium chloride (CHPTAC) has been incorporated onto the backbone of chitosan in presence of NaOH. Further, a series of cationic chitosan have been synthesized by varying the reaction parameters like concentration of the CHPTAC monomer and reaction time. It has been observed that with increase in CHPTAC concentration, flocculation performance increases, but after optimum CHPTAC concentration, with further increase in monomer concentration, the flocculation performance decreases.

The CHPTAC and synthesized cationic chitosan were characterized by various materials characterization techniques such as elemental analysis, IR spectroscopy, SEM, thermal analysis, viscometry and X-ray diffraction analysis. All techniques provided unambiguous proof of chemical loading of cationic moiety on chitosan. The flocculation characteristics of these cationised chitosans were evaluated in four synthetic effluents of namely, kaolin, iron ore, silica and bentonite suspensions. Cationic polymers are more efficient as flocculating agents for highly negatively charged colloidal particles suspensions due to their positively charged side chains. So, it is expected that the cationic polymers will work as a better flocculant for the particles having highly negative Zeta potential. Apart from the obvious explanation of simple ionic attraction leading to the flocculation, the flocculation also takes place due to polymer bridging mechanism. So, there would be a competition between the bridging and charge neutralization mechanisms, which effectively invites the particles to come closer leading to flocculation.

CHAPTER-I

INTRODUCTION

1.1 INTRODUCTION

In day-to-day life, the need of water is very much essential for the survival of human beings and almost all industries. To meet the need of potable, industrial and agricultural water, it is important to treat wastewater, particularly the municipal sewage, sludge, slime and industrial effluents. These effluents are highly undesirable and unsafe to use. The wastewater contains solid particles with various shapes and sizes. Some time the industrial wastewater contains heavy metals, which is not only toxic to us but also toxic to plants. So removal of these solid particles from the water is of great interest and our need. Many of the inorganic contaminants and biological organisms are found adsorbed on or incorporated in these particles [1, 2]. Therefore, to prevent the toxic effect of these inorganic chemicals like arsenic, lead, and mercury, and to prevent the water borne diseases, treatment of the wastewater is must prior to use.

The waste-water contains both dissolved materials and suspended particles. Large portions of these suspended particles are too small ($10\mu\text{m}$) to remove by usual filtration techniques. Also the sedimentation rate of these particles is very slow for practical use in industries. Most of these particles are negatively charged in water, which is the major cause of stability of the suspended particles in aqueous media. So the usual techniques to remove these fine particles from water is by addition of inorganic or organic chemicals that accelerates the aggregation of these fine particles to large aggregates and enhance the sedimentation rate. The inorganic chemicals used in this process vary from aluminium to iron. These inorganic chemicals are low in cost and that makes them attractive for industrial use. These metal ions hydrolyzed easily to form insoluble particles and natural or synthetic organic polyelectrolytes rapidly adsorbed on the surface of these particles. But the residues of these large amounts of inorganic chemicals are now becoming threat to us. Disposal of these effluents are the major problem now a day all over the world. The disposal coming from toxic chemicals has created hazardous environmental problem. Not only that, even the minute residues of these chemicals caused toxic effect to human being. Among all the inorganic chemicals available aluminium sulfate and poly aluminium chloride (PAC) are the most widely used because they are cheap, effective and easy to handle. Most important of all, aluminium can be overdose to ensure coagulation efficiency. However, over-use of aluminium salt coagulants elevates the aluminium concentration and turbidity in the treated water, which in turn devaluated the treatment process. Some scientists relating the use of aluminium to Alzheimer disease [3, 4]. They found high level of aluminium in the brain of deceased Alzheimer's patient.

Epidemiological evidences [3] linking the aluminium level in drinking water with the incidence of Alzheimer disease. In 1990 the EPA maintained a list of chemicals suitable for potable water treatment in the United States. The standard has been turned over to a group of organizations headed by the National Sanitation Foundation, which has issued standard in 1992 for the principal inorganic chemicals. At that time only two polymers have been certified for use. These are poly (DADMAC) and Epi-DMA. But even at that time a question of disposal was there.

This concerning matter has forced the scientists and technologists to develop organic materials and materials from renewable sources and plant resources to protect the environment from health threat. They developed different types of organic material, named flocculants. These materials do their work in low amount. These organic materials remove the suspensions of the effluent by coagulation and flocculation. Coagulation and flocculation require a unique combination of chemical and physical phenomena for water treatment process.

These organic materials can be classified into two categories; e.g. natural organic materials (polysaccharides) and synthetic organic materials. Polysaccharides today play a major role as alternative to inorganic materials due to both their generally non-toxic nature and the constantly rising global demand for energy and raw materials. The polysaccharides mainly, starch, different types of gums, algalic acid, cellulose and its derivatives, dextran, glycogen, CMC, chitosan etc. These polymers are large organic molecules that occur in a variety in nature. Depending upon the source, these polysaccharides have many impurities and molecular distributions. However, purification and grafting can make useful products, which can be used as water treatment material. Synthetic materials are broadly divided into non-ionic, cationic and anionic categories. Among the natural and synthetic polymers used in water treatment application, synthetic polymers are much more effective than natural polymers, which are attributed to the easy tailorability of the polymers. But the biggest drawback of these polymers is their shear degradability. It is well known that polyacrylamide and its copolymers are used as good water treatment agent for the beneficiation of the mineral and paper industries. The drawback of polyacrylamide lies in the fact that it is degraded by shear forces. However the great advantage of natural polymers over synthetic polymers is their low cost, non-toxicity, biodegradability and shear resistant characteristics [5], but the biodegradability of natural polymers comes as a drawback in that it reduces the storage life as well as performance.

It is evident in all the polymers, be it natural or synthetic, have one or another disadvantage. Therefore, many attempts have been made in the past by grafting synthetic polymers onto natural ones in order to combine the best properties of both. The great advantages thus obtained are high flocculation efficiency, control biodegradability and shear resistant characteristics of the grafted copolymers [6-8]. Here, the word flocculation is used to describe the water treatment process where agglomerates are formed with the polymers used.

Various types of graft copolymers have been synthesized by grafting polyacrylamide onto the polysaccharides (amylose, amylopectin [9], guar gum [10], hydroxypropyl guar gum [11] P. psyllium [12], sodium alginate [13], starch [14], CMC [15]) backbone. It has been observed that these graft copolymers exhibit better flocculation characteristics in various aqueous suspensions than the polyacrylamide (PAM). The better efficiency of these graft copolymers over PAM can be attributed to the closer approachability of the grafted PAM chains to the colloidal particles in compare to the PAM, as proposed by Singh [6-8].

In this study the author used chitosan as a base polymer. Chitosan is the deacetylated derivative of chitin [16]. Chitin is one of the most abundant organic materials, being second only to cellulose in the amount produced annually by biosynthesis. It occurs in animals, particularly in crustacean, molasses and insects, where it is a major constituent of the exoskeleton, and in certain fungi, where it is the principal fibrillar polymer in the cell wall. It is manufactured from crab and prawn shells [16-22], in countries such as Japan, China, Taiwan, the U.S. and India, which have long coastlines where fishing and fish processing are major industries. The availability, manufacturing process, production economics, chemistry and possible applications of chitosan are all documented by Muzzarelli [23]. The estimated cost of production is about two dollars per kg. Chitin has a crystalline structure and it constitutes a network of organic fibres. This confers rigidity and resistance to organisms that contain it. Chitin is poly [β - (1-4)-2-acetamido-2-deoxy-d-glucopyranose] and its idealized structure is shown in **Figure 1.1**.

Chitosan is produced by alkaline deacetylation of chitin. Chitosan also occurs naturally in some fungi [24, 25] but its occurrence is much less widespread than that of chitin. Chitosan is poly [β -(1-4)-2- amino-2-deoxy-D glucopyranose] and its idealized structure is shown in **Figure 1.2**.

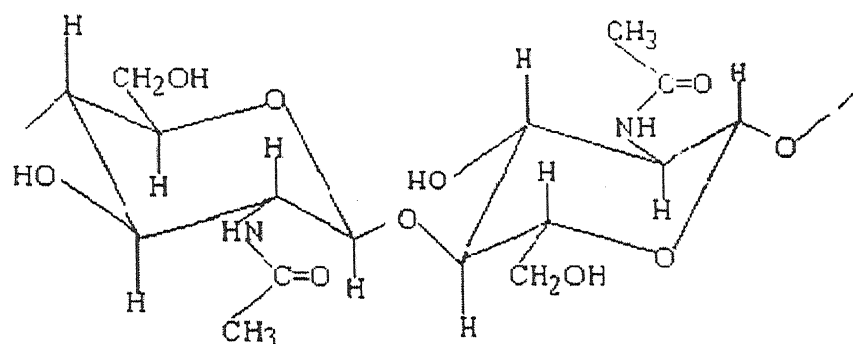


Figure 1.1 Structure of chitin

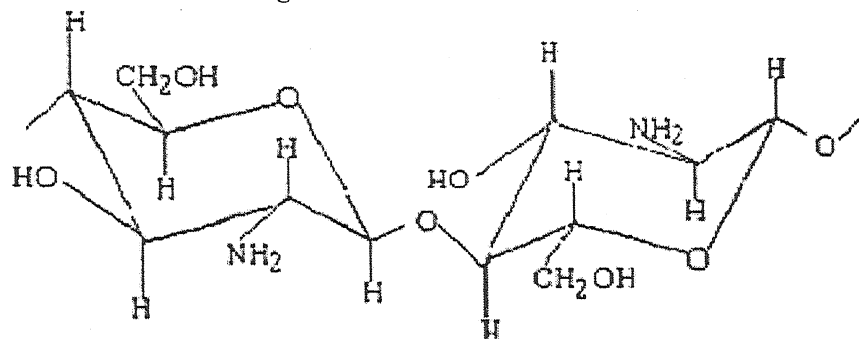


Figure 1.2 Structure of chitosan

The structure of chitosan reveals the high percentage of nitrogen (6.9%), amino and hydroxyl groups on the back bone of chitosan, where they act as chelating sites for metal ions. This attracts a large amount of academic and industrial interest. The typical commercially available chitosan has approximately 85 % deacetylation. Even it is possible to get 100 % deacetylated product depending on the method of deacetylation and the duration of the treatment [26-29].

Keeping in mind renewable resources of this polymer and its biodegradability and non-toxicity [20], it is very attractive in the field of applications like water treatment and biomedical applications [24, 25, 26, 29]. Knorr [30] discovered that chitosan was an effective agent for flocculation of suspended solids from various food processing wastes. Gylíene, et al. (2002) and Ngah and Isa (1998), [19, 21] stated that chitosan could be effective adsorbent for collection of Cu(II) ions from aqueous solution. Huang et al. (1996) [31] stated that chitosan could be a potent coagulant for source water having medium and low turbidity. Since chitin is the second most abundant biopolymer, the application in flocculation not only avoids the health threat from alum treatment, but also allows recycling of a large amount of crab shells. But the use of chitosan is limited because of its insolubility in neutral water. Due to the presence of amino groups on chitosan backbone the material is soluble in dilute acid

solution and opens some of the interesting application of chitosan like as flocculant in water treatment, as viscosifier etc.

In its protonated form, chitosan has a high charge density and is very effective in interacting with negative charged molecules. In its neutralized form it produced complexes with metal.

The potential applications of chitosan can be increased and its chemical and physical properties can be improved by grafting various monomers onto chitosan backbone [32-36]. Various studies have been reported where vinyl monomers were grafted [37-39] onto chitosan backbone to evaluate its flocculation and ion exchange properties.

In the authors' laboratory, grafting of monomers onto polysaccharide backbone has been carried out with the help of ceric ammonium nitrate (CAN). CAN is a redox ion initiator and generates active radical sites onto polysaccharide backbone.

In the recent study PAM has been grafted onto chitosan backbone using the ceric ion initiated polymerization technique.

More investigations are carried out by hydrolysis of this grafted copolymer with alkali with a view that on hydrolysis, the grafted product will become more straightened and at the same time it will remain flexible enough, so that they show better flocculation property.

CHPTAC (3 chloro 2 hydroxyl propyl trimethyl ammonium chloride) was grafted onto chitosan backbone to increase its cationic characteristics. Characterization and flocculation studies of these copolymers were also studied. In all these above cases, best flocculants grades were found. The aim was to study the flocculation efficiency of these cationized products.

To the best of the author's knowledge, the synthesis, characterization and flocculation study was not reported so far.

1.2 PLAN OF WORK

The plans of our present work are as follows:

1. To synthesize a series of graft copolymers based on chitosan and PAM by using ceric ammonium nitrate (CAN) as initiator. By changing the amount of the monomer as well as the ceric ion in the reaction chamber, different grades of copolymers with variation in the number and length of the PAM chains were obtained. The aim was to investigate the variation in the number and length of the PAM chain onto chitosan backbone on their flocculation characteristics.
2. To purify these graft copolymers Soxhlet extraction method was applied to remove even the trace amount of PAM homopolymer in the graft copolymer.
3. To characterize the graft copolymers, various characterization techniques such as elemental analysis, viscometry, IR spectroscopy, SEM, thermal and XRD were used. These techniques directly and indirectly prove the grafting of PAM onto chitosan backbone.
4. To study the flocculation characteristics of the grafted copolymers in four different synthetic effluents, such as kaolin, iron ore, silica and bentonite suspensions. The results were compared to find the best performing graft copolymer.
5. To prepare partially hydrolyzed grafted chitosan by NaOH treatment. The aim in both of these cases was to find the optimal condition for effective flocculation.
6. To characterize the partially hydrolyzed grafted copolymer, elemental analysis, IR-spectroscopy, SEM, thermal analysis and XRD were performed.
7. To synthesize a series of cationic graft copolymers CHPTAC monomer was grafted onto chitosan backbone.
8. The CHPTAC grafted products were also characterized by IR spectroscopy, elemental analysis, SEM, thermal analysis and XRD studies.
9. The flocculation characteristics of all the CHPTAC grafted chitosan copolymers were investigated. The best performing grade was also determined.

1.3 OVERVIEW

Chapter-I is the introduction of this thesis. Water is very much essential for the survival of any industry. To meet the need it is important to treat the waste-water, particularly the municipal sewage, sludge, slime and industrial effluents. These effluents are highly undesirable and unsafe to use. This chapter describes the plan to synthesize a new type of polymeric material based on chitosan which could be used as effective flocculant to remove these contaminants from waste-water.

Chapter-II presents the literature review of the thesis. It provides the physiochemical properties of chitin and chitosan. This chapter gives the details of the different types of physical and chemical methods for graft copolymerization on to the backbone of polysaccharides. This chapter also gives the details of the different kinds of flocculants and their flocculation mechanism. Chapter-II also describes the flocculation mechanism of partially hydrolyzed graft copolymers and cationized copolymers.

Chapter-III is confined to the details on the synthesis of polyacrylamide (PAM) grafted chitosan copolymer. The grafting was done by ceric ion initiation technique. This chapter also gives the details of the synthesis parameters. The PAM grafted chitosan copolymers were characterized by different materials characterization techniques, namely, elemental analysis, viscometry, IR-spectroscopy, thermal analysis (DSC, TG, and DTG), SEM and XRD analysis.

Chapter-IV compares the flocculation behaviour of all the grades of PAM grafted chitosan copolymers and as well as the ungrafted chitosan in aqueous suspension of four particles, namely: kaolin, iron ore, silica and bentonite. The best performing flocculant was identified.

In Chapter-V, the best flocculant (among the PAM grafted chitosan copolymers) was partially hydrolyzed by alkali. The details of the synthesis parameters are given in this chapter. A series of partially hydrolyzed graft copolymers were synthesized. They were characterized by similar material characterization techniques described above. The flocculation characteristics of all the grades were compared and the best flocculation performing grade was identified.

In Chapter-VI, a series of cationized chitosan have been synthesized by grafting a cationic monomer N-(3-chloro-2-hydroxy propyl) trimethyl ammonium chloride (CHPTAC) onto the backbone of chitosan. The details of the synthesis parameters are given in this chapter. These cationized copolymers were characterized by various material characterization techniques

described above. The flocculation performance of all the grades was compared and the best performing grade was identified.

Chapter –VII concludes the successful synthesis of unhydrolyzed, hydrolyzed and cationized products. It also comments on the feasibility of the above mentioned grades as flocculant. The future scope of this work is also given in this chapter.

CHAPTER-II

**LITERATURE
REVIEW**

2.1 INTRODUCTION TO CHITOSAN

Chitosan is a natural carbohydrate biopolymer derived from chitin. The main sources of chitin are the exoskeletons of various crustaceans, principally crab and shrimp. Chitosan is also prepared from squid pens. Squid pen chitosan is synthesized from β -chitin (amine group aligned with the $-\text{OH}$ and $-\text{CH}_2\text{OH}$ groups) and crustacean exoskeleton chitosan is synthesized from α -chitin (anti parallel chain alignment) [40]. Raw chitin is closely associated with proteins, inorganic materials (mainly CaCO_3), pigments and lipids that make it yellowish in colour. Various procedures have been adopted to remove these impurities. Demineralization is most frequently carried out by treatment with HCl and deproteinisation by treatment with strong NaOH . The use of enzymes for protein removal has been examined by a number of workers [41,42] suggested the use of enzymes such as pepsin or trypsin if the chitin is required to be as fully N-acetylated as possible but no experimental details were found. The choice of processing conditions may be governed to some extent by the purpose for which the chitin is required.

The exoskeletons of crustaceans contain colouring matter, principally carotenoids which do not appear to be complexes either inorganic materials or proteins, since treatments, which remove these components, do not remove the carotenoids. However, they may be removed by extracting the shell with ethanol or acetone after demineralization. Alternatively, the colouring matter may be bleached by the use of KMnO_4 or H_2O_2 [41, 42].

2.1.1 Chitosan – a deacetylated form of chitin

Chitosan is produced from the deacetylation of chitin by the use of alkali. The most frequently used alkali is NaOH . The conversion of chitosan from chitin is represented in Figure 2.1. The extent of deacetylation is governed by the alkali concentration, temperature, and time of reaction, particle size and density. Even 100% deacetylated product can be achieved. However this was at the expense of a considerable decrease in solution viscosity indicating chain degradation [41].

To avoid the chain degradation by alkali, a water miscible solvent such as 2-propanol has been used as diluent to ensure ease of stirring [43]. 2-propanol helps to distribute alkali in the reaction mixture.

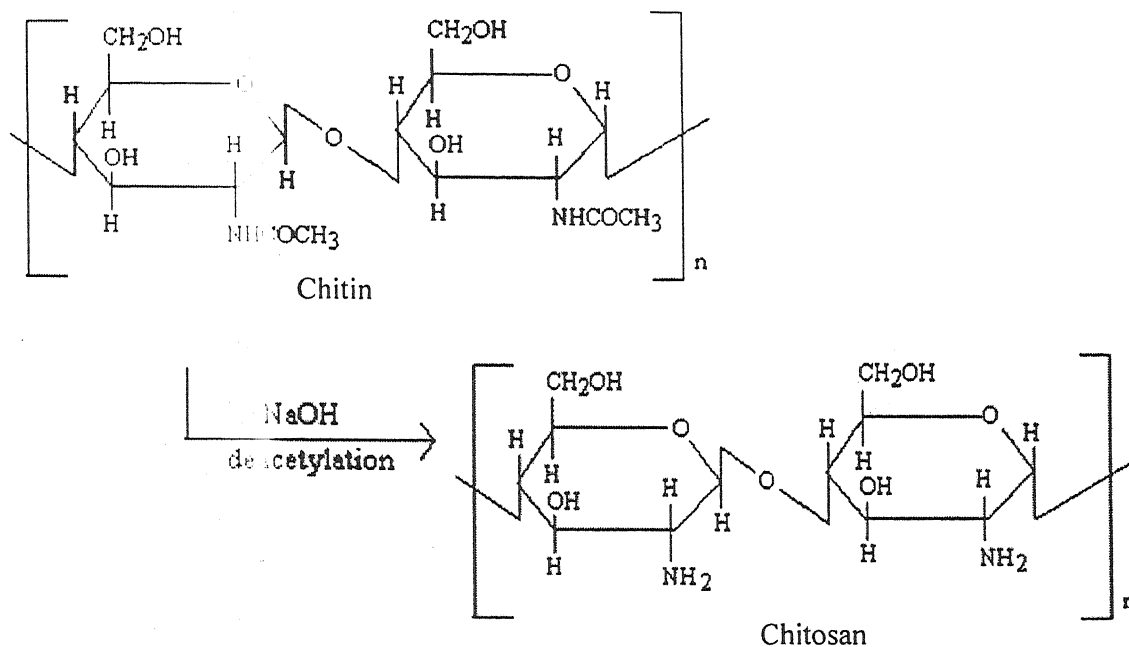


Figure 2.1 Deacetylation of chitin by alkali

2.1.2 Physicochemical Characteristics of Chitosan

2.1.2.1 Degree of N-acetylation

Chitosan is characterized by either the degree of acetylation (DA), which corresponds to the N-acetylamine groups, or the degree of deacetylation (DDA) [$DDA=1000-DA$], which corresponds to the D-glucosamine groups.

The degree of acetylation has an influence on all the physicochemical properties (molecular weight, viscosity, solubility, etc) so; it is one of the most important parameters. Practical grade chitosan from crab shells has a minimum of 85% deacetylation and a viscosity greater than 200 cps (in 1% acetic acid solution).

2.1.2.2 Solubility

Chitosan is insoluble in neutral water. It is soluble in dilute acetic acid, HCl, HI, HNO_3 , $HClO_4$ and H_3PO_4 . It is not soluble in dilute H_2SO_4 . It should be noted here that the solubility of chitosan depends upon its dissociation and the method of deacetylation used. Chitosans primary amino groups have pK_a 's of about 6.3. Below the pK_a , the amino groups are

protonated making chitosan a water-soluble cationic polyelectrolyte. Above the pK_a , chitosan's amino groups are unprotonated.

Interestingly, the pH responsive solubility of chitosan allows to be modified under either heterogeneous or homogeneous conditions. For instance chitosan can be cast into insoluble films at neutral pH.

2.1.2.3 Crystallinity

Ogawa et al. [44, 45] examined the three soluble forms of chitosan. The hydrated crystalline forms show a strong reflection at an angle (2θ) of 10.4 degrees and other peaks at 20 and 22 degrees. The hydrated crystalline form shows a strong peak at 15 degree and another supplementary peak at 20 degree.

Piron et al. [46] reported that the dissolution of chitosan involves the progressive disappearance of the peak at 22 degree. Kurita et al. [47] observed that in nonaoyl substituted chitosan, the value of crystallinity decreases at lower substitution level while it increases at higher substitution level. Guibal et al. [48] stated that the sorption capacity molybdate depends not only on the degree of deacetylation of chitosan but also on the value of crystallinity. The most sorbents are characterized by higher crystallinity index.

2.1.3 Industrial Production

According to the most recent OPD Chemical Buyers Dictionary [49], chitosan is now manufactured or distributed by 45 companies; these are AIDP, Inc., ALFA Chem, AllChem Industries, Inc., Americal Ingredients, Inc., American International Chemical Inc., Arrow Chemical Inc., Ashland Chemical Company, Fine Ingredients Division, Beckmann Chemikalien KG, Belmont Chemicals Inc., Biopolymer Engineering, Buckton Scott USA, Inc., CPB International, Inc., Chemical Industries Services, Inc., Chugai Boyeki (America) Corp., Citi USA, Continental Trading, Co., DCV Bionutritionals, DNP International Co., Inc., FabriChem, Inc., G.C.I. Nutrients, H & A Industrial Inc., IRMA Corp., Infinity Marketing Group, Inc., JC company, Inc., K3 Corp., Kaltron/Pettibone, M.M.P., Inc., Marcor Development Corp., Maypro Industries, Inc., Mini Star International Inc., Pharma Nutrients, Pharmline, Inc. Pronova Biopolymers, Inc., RIA International, Paul Schueller international Inc., Schwerzerhall, Inc., Seltzer Chemicals, Inc., Serra international Trading Inc., Stauber performance Ingredients, Inc., Stryka Botanics Co., Inc., Tanabe USA Inc., Union carbide Corporation. Universal Prevervachem Inc., Vanson Inc., and Wilke International, Inc.

2.1.4 Uses of Chitosan

Many potential products using chitosan have been developed, including flocculating agents for waste water treatment, chelating agent for removal of traces of heavy metals from aqueous solutions, coatings to improve dyeing characteristics of glass fibers, wet strength additives for paper, adhesives, photographic and printing applications, thickeners, and fiber and films [50].

From the literature survey it is found that between 1976 and 1999, a stunning 2064 patents involving chitosan were approved by the US Patent and Trademark Office [51]. Some novel applications involving chitosan include biodegradable fish hooks and surgical sutures, coated papers and transparencies for inkjet ink, biodegradable implants and vascular prostheses, and low-fat whipping cream and ice cream.

Chitosan is used as an excipient for oral drug formulations, primarily as a diluent. Chitosan is also being evaluated as a potential vehicle for orally administered controlled release drugs. Chitosan has also been evaluated for the manufacture of ocular bandage lenses and biodegradable surgical implants [52].

Cosmetic applications based upon chitosan derivatives are suitable for treatment of hair and skin. They can be provided as hair washes, body washes, colouring shampoos, hair dressing creams, hair tonics, blow-dry lotions, hair setting lotions, hair conditioners, agents for permanent hair deformation, and as cosmetic agents for the care, protection, or cleaning of skin.

Chitosan has several agricultural uses. It acts as a preservative and coating for biofungicide when sprayed on fresh fruits and vegetables. Chitosan fertilizers increase the number of useful soil microorganisms and decrease harmful ones. Plant seeds are soaked in chitosan solution to prevent microbial infections and increase plant production.

2.2 GRAFT COPOLYMERS

Polymers have their unique properties. But all the polymers in one or another way are lacking some of the properties. So, to get a polymer with the properties we need, modification is needed. One of the most common methods of modification is copolymerisation. For our own need graft copolymerisation is used in this study. The graft copolymers of polysaccharides are of additional interest for their potential use as viscosifiers and flocculants for treatment of mining and wastewater. The method of graft copolymerisation has been utilizing as a special technique in the recent years [53] for modifying the physical and chemical nature of natural and synthetic polymers. A graft copolymer is consisting of primary backbone chain to which side chains containing different atomic constituents are attached at various points. A simple structure of graft copolymer is represented in **Figure 2.2**. The sequential arrangement of the monomer unit A is referred to as the main chain or the backbone. The sequence of B units is the side chain or graft.

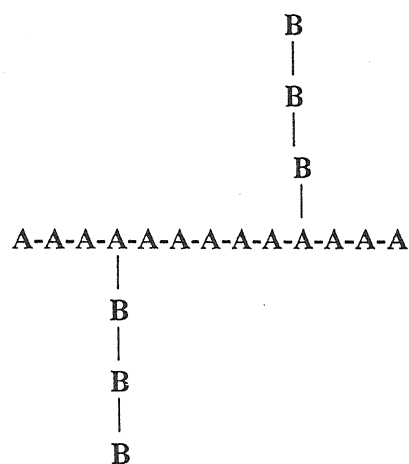


Figure 2.2 Structure of graft copolymer

Both the backbone and the side chain polymer can be homopolymers or copolymers. Among the various polymers onto which grafting can be done, polysaccharide based polymers are most interesting and promising. It is because they are abundant in nature and cheap in cost. The actual properties of the graft copolymer will vary according to the number and length of the grafted side chains. Therefore, it is most important to control the graft frequency and graft segment length in order to activate desired characteristics.

Numerous methods have been developed to initiate the graft copolymerisation. They are classified into three categories: (i) free radical (ii) ionic (iii) condensation and ring opening polymerization. Because of the practicability free radical polymerization reaction got the most importance among the all. Duke et al. [54, 55] provide evidence for the formation of vinyl monomer grafting on 1, 2-diol substituted groups through ceric ion initiation. Mino and Kaizerman [56] showed that the free radicals formed during the disproportionation of these complexes could initiate vinyl polymerization. A vast quantity of research work has since been directed towards ceric ion initiated graft copolymerization of vinyl monomers onto suitable substrates containing 1, 2-diol groups: the polysaccharides being the majority of them.

2.3 SYNTHESIS OF POLYSACCHARIDE BASED

GRAFT COPOLYMERS

The graft copolymers based on polysaccharides have been synthesizing by generating free radical sites on the backbone of the polysaccharides and allowing these radicals to act as micro-initiators. Generally two types of reaction methods have been proposed for the initiation of free radicals on the polysaccharide sites. These are chemical initiation and initiation by irradiation. In some cases free radicals are developed by mastication of the polysaccharides. It is assumed that mastication will rupture the backbone and produce free radicals.

2.3.1 Chemical Initiation

2.3.1.1 Initiation by Ceric ion

For graft copolymerisation of polysaccharides ceric ion initiation method is most widely used [57-59]. The common ceric ion initiators are ceric ammonium nitrate (CAN) and ceric ammonium sulfate (CAS). CAN is best used for low temperature reactions. At higher temperature CAN become unstable and dissociates [60]. However, at elevated temperature CAS is found most efficient. Many more methods have been proposed [54, 55] for the generation of free radicals by oxidation of 1, 2-diols with ceric ions. Mino and Kaizerman [56] have introduced for the first time the formation of graft and block copolymers on these reaction sites. The mechanism by which Ce(IV) ion generates free radicals are believes to be involving in the formation a complex between the hydroxyl group of the polysaccharide and the oxidant. The complex so formed disproportionate forming free radicals on the backbone

of the polysaccharides. Several investigations proposed the formation of complex between cellulose and Ce(IV) ions [61-69]. It has been observed from the study of model compounds that the ceric ion oxidation takes place most probably at C₂-C₃ glycol units of polysaccharides and at C₅ hydroxyl groups [70, 71]. Muhammad and Rao [72] suggested a mechanism for the direct oxidation in sulfuric acid. Hinz and Jonson [71] have pointed out that the oxidation process proceeds through an intermediate complex formation when the equilibrium constant for the complex formation is small. The complex formed in between Ce(IV) and 1,2-glycols may be either a chelated or an acrylic species. However, the oxidation of monohydric alcohols, which does not form complex shows larger value of equilibrium constant. This concludes that the intermediate formation of coordinated complex proceeds through a chelate formation and this will also minimizes the involvement of hydroxyl group at 6-position. On the basis of this complex forming mechanism, following mechanism has been proposed for Ce(IV) ion initiation graft copolymerisation [56,73]. The schematic mechanism is described in Figure 2.3.

The mechanism also supports the grafting of poly [N, N-dimethyl-N-methacryloxyethyl-N-(3-sulfopropyl) ammonium] onto chitosan by ceric ion initiation [74].

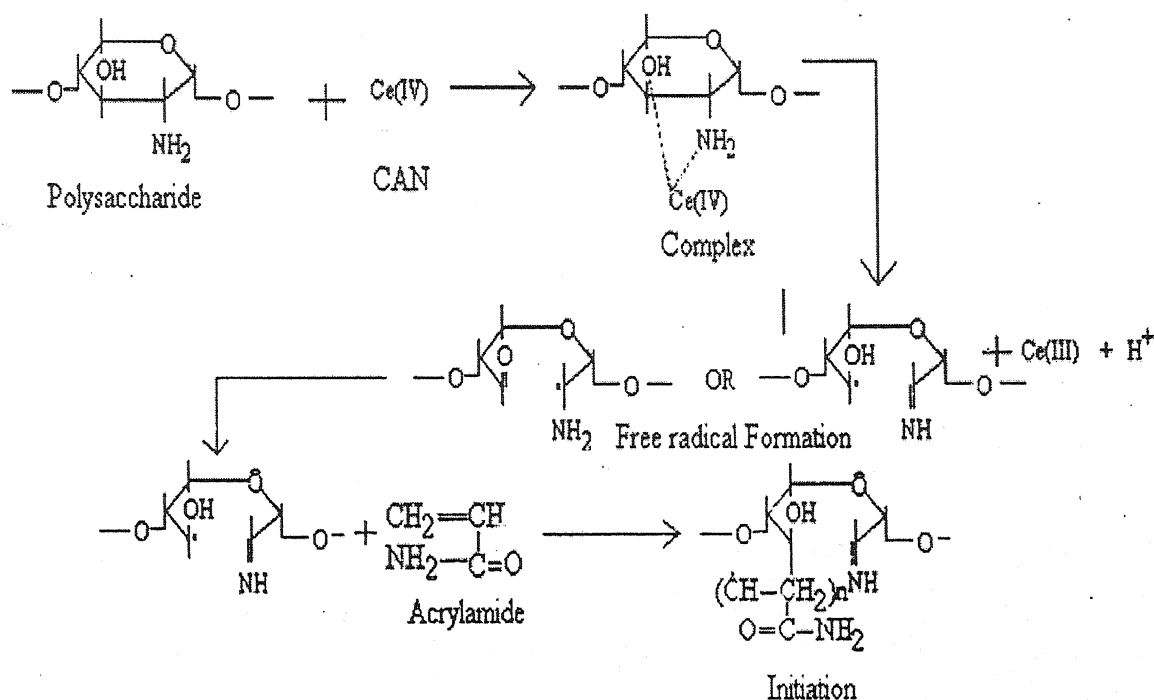


Figure 2.3 Schematic representation of ceric ion initiated graft copolymerisation

2.3.1.2 Initiation by Trivalent Manganese

Singh et al. [75] and Duke; F.R. [76] have developed a method for graft copolymerisation by using manganic sulfate – sulfuric acid system as a source of Mn^{3+} ion. This reaction involves in electron transfer via free radical formation. As Mn^{3+} is unstable at lower acid medium, a phosphate complex is being used to serve the purpose [77-80].

2.3.1.3 Initiated by Hydrogen Peroxide / Fe^{2+} System (Fenton's Reagent)

Hydrogen peroxide- Fe^{2+} system, commonly known as Fenton's reagent can be used for the graft copolymerisation. This reaction also involves in the free radical formation. Brockway and Moser [81, 82] have studied the grafting of MMA onto starch by using this hydrogen peroxide –ferrous sulfate system. Uri [83] has used bisulfate reducing agent instead of ferrous ion. Brockway and Mehrotra et al. [84, 85] have studied the similar system with ascorbic acid.

2.3.1.4 Initiation by Cu (II) ions

Imato et al. [86, 87] have studied the grafting of MMA onto the backbone of starch by Cu(II) ion initiation process. According to Imato [88], this reaction proceeds through the hydrophobic ends in aqueous phase.

2.3.1.5 Initiation by Chromium (VI) ions

Many scientists have studied graft copolymerisation onto polysaccharide backbone with Cr(VI) ion as an initiator. Nayek et al. [89, 90] used Cr(VI) ions for graft copolymerisation as well as for homopolymerisation [91]. Mishra et al. [92, 93] reported the feasibility of Cr(VI) ions to induce graft copolymerisation of MMA onto cellulose.

2.3.1.6 Initiation by Vanadium (V) ions

Lenka et al. [94] carried out graft copolymerisation of MMA onto the backbone of cellulose by vanadium ion initiation process. They observed that the increase of V^{5+} ion concentration upto 0.0025 mole/liter increases the grafting yield and with further increase of the initiator concentration, the grafting yield decreases. Mohanty et al. [95] have reported the grafting of MMA onto jute fibers using redox system consisting vanadium (V) ion.

2.3.1.7 Initiation by Xanthate process

The Xanthate initiation process has got some extraordinary advantages over the processes discussed so far for the grafting of monomers onto the backbone of polysaccharide. In this process the initiating species formed onto the polysaccharide backbone. Also, in this process the formation of homopolymer is minimum, which on the other hand increases the grafting efficiency. The method does not require any inert atmosphere. The study of Dimov and Pavlov [96] was unique among the various methods of xanthate initiation process. They found low percentage of homopolymer formation in the grafting reaction of acrylonitrile with cellulose (Cell), especially in the high xanthate containing substrates.

2.3.1.8 Initiation by Azo-Bis-Isobutyro Nitrile (AIBN)

The use of AIBN as initiator for grafting of vinyl monomer onto cellulose backbone [97-99] and modified cellulose backbone [100] was reported. It was believed that the reaction proceeds through the formation of macro-radicals resulting from a chain transfer reaction between the growing vinyl homopolymer chain and the polysaccharide substrate present in the polymerisation reaction. It was also reported that the extent of grafting varies significantly with the type and amount of solvent used.

2.3.1.9 Initiation by Metal Chelats

The initiation of graft copolymerisation by transition metal chelating process has drawn much attention. The initiation species is assumed to be ligand radicals formed by the homolytic cleavage of the metal-oxygen bond of metal acetylacetonates. At the same time the formal valence of the metal is reduced by one. This was confirmed by spectral and ESR studies. Kasting et al. [101] reported the copolymerisation of MMA by $Mn(acac)_3X$ compounds (X is halogen). Tripathy et al. [102] reported grafting of MMA onto cellulose using acetylacetonato manganese (III) complex.

2.3.2 Initiation by Irradiation

Studies showed that the free radical formation onto polysaccharide backbone not only done by chemical initiation but also by irradiation. Free radical formation onto starch backbone was reported through ^{60}Co and electron beam irradiation [103,104]. Two techniques were

generally used for graft copolymerisation, the simultaneous irradiation and pre irradiation. In simultaneous irradiation mixture of starch and monomer were irradiated together, whereas in pre irradiation, starch is irradiate first alone and the activated starch is allowed to react with the monomer. The percentage of homopolymer formation is less in pre irradiation technique. The advantages of simultaneous technique over pre irradiation one is the possibility of short-lived free radical reaction of the monomer with irradiated starch and the absence of the formation of homopolymer during the irradiation step. Some photosensitisers have been used in radical irradiation process. For example, anthraquinone [105] has been used for grafting monomers onto cellulose. CAN [106] have been used for UV radiation induced graft copolymerisation of styrene and acrylonitrile onto cotton cellulose. Recently photo irradiated graft copolymerisation of polyacrylamide onto cellulose was reported using a novel photo system [107]. Morita et al. [108] have reported the photo induced graft copolymerisation of vinyl monomers onto deoxy chitin.

2.3.3 Initiation by Mastication

Free radicals onto starch have been created by mechanochemical means such as mastication, ball milling and freezing of the starch dispersions. When starch is subjected to shear force, the starch molecules are broken apart producing free radical sites at the broken points. If such application of shear is done in the presence of monomers, copolymerisation is initiated and block copolymers are formed, attached to the starch at the site of free radical formation. Mixture of starch with methyl methacrylate, styrene, vinyl acetate and acrylonitrile result in grafting [109].

2.4 PROOF OF GRAFTYING

2.4.1 IR-spectra of Graft Copolymers

Among the various methods studied by polymer chemists, IR has served as one of the most important technique for proof of grafting. The IR spectra of grafted branches (isolated after depolymerisation of starch) of polyacrylonitrile (PAN) and PAM [110], all showed bands due to carbohydrate end groups. The carbohydrate end groups on PAN have also been benzoylated and the resulting benzoyl groups have been detected by both IR and UV spectroscopy [111]. Under conditions that lead to poor grafting efficiency, selective solvent extraction of crude reaction products with a good solvent easily removes the ungrafted

homopolymers of polyacrylonitrile [111,112]. The ungrafted starch could be removed by water extraction. The inability to achieve such separation with other polymers thus provides evidence for chemical bonding between starch and the acrylic content.

2.4.2 Molecular Weight of Grafted Chains

If quality control standard are sought for properly characterized grafted polysaccharides, especially for use in speciality applications, a reliable method of molecular weight determination is desirable.

More recently, Size Exclusion Chromatography (SEC), also known as Gel Permeation Chromatography (GPC) or Gel Filtration Chromatography (GFC) has been applied to the study of molecular weight and molecular weight distribution of synthetic polymers and biopolymers.

The most commonly used method for molecular weight determination is intrinsic viscosity $[\eta]$ measurement using Mark-Houwink relationship:

$$[\eta] = KM^\alpha$$

Where 'K' and ' α ' are constants for a particular polymer /solvent/temperature system. For instance; for polyacrylamide [113-115],

$$[\eta] = 6.8 \times 10^{-4} (M_n)^{0.66}$$

$$[\eta] = 6.31 \times 10^{-5} (M_w)^{0.80}$$

For polyacrylonitrile [111],

$$[\eta] = 3.92 \times 10^{-4} (M_n)^{0.75}$$

For poly(vinyl alcohol) [116],

$$[\eta] = 0.96 \times 10^{-4} (M_n)^{0.69}$$

For CMC [117,118],

$$[\eta] = 5.36 \times 10^{-4} (M_w)^{0.73}$$

For chitosan [23, 24, 25],

$$[\eta] = 5.48 \times 10^{-4} (M)^{0.715} \text{ when ionic strength is } 0.01(M)$$

$$[\eta] = 2.04 \times 10^{-3} (M)^{0.521} \text{ when ionic strength is } 0.03(M)$$

Here, M_n is the number average molecular weight.

M_w is the weight average molecular weight.

M is the viscosity average molecular weight.

2.4.3 Calculation of Grafting Parameters

Various grafting parameters can be calculated by using the following equations.

1. % of Graft Level [119] (P_g) = (Weight of the Polymer / Weight of the Polysaccharide) x 100
2. Rate of Grafting [119] (R_g) = [(Weight of Graft polymer) x 1000 / {(Molecular Weight of Graft Polymer) x (Reaction Time) x (Reaction Volume)}]
3. Frequency of Grafting [119] (F_g) = [{(Weight of Graft Polymer) x (Molecular Weight of AGU) x 10^4 } / (Molecular Weight of Grafted Polymer)]
4. % of Conversion [120] = [{Weight Product – Weight of Polysaccharide} / (Weight of Monomer) x 100]
5. % Add-on [120] = [(Weight of Pure Copolymer - Weight of Polysaccharide) / Weight of Pure Copolymer] x 100
6. % of Polymer Grafted [120] = [(Weight of grafted Polymer) / (Weight of Grafted Polymer + Weight of Ungrafted Polymer)] x 100
7. Grafting Frequency (AGU/Graft) [121] = [{(%Add-on) / Weight of AGU}] / (%Add-on / Molecular Weight Grafted)
8. Rates of Homopolymerisation [121] (R_h) = [(Weight Of Homopolymer x 1000) / (Mw of Monomer x Reaction Time (sec) x Reaction Volume (ml))]
9. Rate of Total polymerization [121] (R_p) = (R_g + R_h)

2.5 PARTICLE INTERACTION STUDIES

The following definitions are used in this thesis to make the sedimentation process clear. COLLISION is refers to as a procedure in which two particles in a suspension interact so closely that their behaviour affects each other. When two particles are closed enough in a suspension, hydrodynamic interaction influence their behaviour at substantial separation distance due to the flow of water around the settling particles.

The effects of interparticle distance on sedimentation behaviour are significant even when settling particles are not closed enough to form an aggregate. The term AGGREGATION is referred to as a group of fine particles held together. Aggregation is called COAGULATION when it is induced by simple electrolytes. It is called FLOCCULATION when it is induced by high molecular weight polymers or by organic surfactants. When it is induced by non-polar liquid in aqueous suspension it is referred as AGGLOMERATION.

Stoke described that the effect of interparticles at reasonable greater distance is positive. He illustrated that this effect are applicable at several size ratio. Qualitatively the effect on larger particles is small, but the effect on smaller particles is quite large.

For a non-porous, rigid, isolated particle falling under the action of a uniform gravitational field through an incompressible, continuous fluid of infinite extent, the sum of all the forces acting on the particle can be express as:

$$\Sigma F = F_{\text{gravity}} + F_{\text{buency}} + F_{\text{drag}} \text{ [MLt}^{-2}\text{]}$$

Here, F_{gravity} is the weight of the particle. F_{buency} is the weight of volume of fluid displaced by the particle and F_{drag} is the friction force developed by the movement of the particle in the fluid.

When the settling particle is not isolated in the fluid but surrounded by a significant concentration of other particles (more than 0.1% by vol.), its terminal velocity is affected by several effects. Changes in fluid density and viscosity are observed, since it is now a suspension. Closeness of particles gives rise to dragging of smaller particles by a larger one.

Studies showed that the properties of the suspended particles also influenced the sedimentation process [122-124]. Studies of many different mineral water systems over the years have established that the characteristics properties of the suspended slurry, such as particle charge [125,126], particle size distribution [127], and particle shape [128-130];

suspended slurry concentration [131], liquid surface tension [132] and particle hydrophobicity [133] can all influence the flocculation process.

2.6 COAGULATION AND FLOCCULATION

It is evident from the study [127] that settling velocities will be minimal in most of biological suspension, unless some procedure for increasing particle size or density or decreasing fluid density or viscosity is applied. All these effects can be achieved by coagulation and flocculation. Both these techniques are currently used. Particle aggregation not only markedly increases medium solids size but also removes them from the bulk liquid leading to significant improvement of rheological properties.

In any case flocculation characteristics are always significantly different from those of rigid particles of equal size and density. Brown et al. [134] proposed a correction to calculate terminal settling velocities to account for both the concentration effect and that of the liquid carried by the particles.

$$V^{corrected} = V^{calculated} \times \frac{0.123}{1-C} (1+a)^2 \left\{ C - \frac{a}{1+a} \right\}^3$$

Here V is the velocity, C is the volume fraction of solids in the suspension and small a is the volume of liquid retained by the solid per unit of solid (both variables dimension less). The value of a ranges from zero (solid particle) to above unity for highly porous flocs.

2.6.1 Coagulation

In colloidal suspensions the major repulsive forces result from electrically charged particle surfaces, while the main attractive forces are of the Van der Waals type. Surface charges create a layer of electrostatic potential gradient around each particle, which tends to prevent them from approaching one another. The thickness of this layer can be reduced by increasing ionic strength in the liquid, through the addition of electrolytes. In this way, allowable inter particle distances fall to the point where attractive forces dominate and coagulation occurs. This mechanism is called double layer compression. The double layer mechanism has been discussed later in great details.

Particle charge neutralization by adding counter ions is a common coagulation process. The most effective ionic species are the ones with multiple unit charges, such as Al^{3+} , Fe^{3+} and Ca^{2+} ; used in their sulfate, chloride and oxide or hydroxide forms, respectively. In

determining dosages and other particle parameters for the employment of such coagulants, several points must be under taken. As electrostatic interaction is the basis of the method, counter ion over dosage leads to particle charge reversal and reforming of the colloidal suspension. A good part of the coagulation effect often result from the precipitation of counter ion hydroxides, which then adsorb to particle surfaces. The solubility and net precipitate charge of these hydroxides are markedly pH and alkalinity dependent. Control of these two parameters is therefore, necessary. Initial suspension concentration is also important variable. Its increase normally leading to low optimum coagulant concentration. Here it should be noted that the metal hydroxides forms short polymer chain, which enhance microfloc formation.

2.6.2 Flocculation

Flocculation of fine particle suspensions using high molecular weight polymer flocculants is an important step for solid-liquid separation in many mineral processing, hydrometallurgical operations, wastewater treatment process etc. Inspite of the significant improvement made in recent years, the understanding of the mechanism of flocculation is far from complete. Several factors affecting the particles, reagents, and medium influence flocculation process [135-150]. It is well documented in the literature that polymer-induced flocculation of particulate separations involves many steps, namely mixing of polymer molecule among the particles; adsorption of the polymer chains on the particles; rearrangements of the adsorbed chains; collision between polymer-adsorbed particles; and the floc formation and also break up of flocs [151-153].

The process of flocculation primarily involves two basic steps (i) transport of particle to the closest distance of approach of another particle leading to collision, and (ii) adhesion of the particles resulting in aggregation.

Other factors related to the success of the flocculation process are the surface chemistry of particles as well as on the ionic nature, molecular weight, and charge density and bulk properties of the flocculants in solution. But as it is said above, the most important influence affecting the extent and mechanism of flocculation is the nature of the adsorption of the polymer on the particle surface and the conformation of the adsorbed polymer.

The flocculation process has been described [151] by three characteristic time scales: t_a (polymer adsorption), t_r (rearrangement of the adsorbed polymer) and t_c (particle collision).

While the polymer reconfiguration time (t_r) may depend on the chemistry of the polymer and the characteristics of the particle and medium; t_a and t_c can be well estimated using the classical second-order reaction kinetics [152,154-156]. There are some other literatures too [153,154] showing that the order of coagulation/flocculation process is mostly bimolecular. Based on Smoluchowski's classical equation [157-159],

$$\frac{N_1}{N_0} = (1 + \frac{1}{2} KN_0 t)^{-2}$$

Here, N_1 = concentration of singlets at time t , N_0 = concentration of the singlet at $t=0$ and k = rate constant for collisions between the singlets; a plot of $(N_1/N_0)^{1/2}$ against t should give a straight line with an intercept of 1 for a bimolecular process. Here it is assumed that the portion of particles, which did not flocculate, is a singlet.

It is also been established from theoretical calculations and experimentation that flocculation does not require high or complete coverage of the particle surface by the polymer. An ideal flocculant is one, which is able to neutralize a part of the surface charge responsible for repulsion, and adsorb with loops and tails extending into solution for bridging with other particles. La Mer and Healy [160], Hogg [161], Deason [162] and many others proposed that not all the collisions of particles are effective in producing flocculation and have related the collision factor (E) to the fractional surface coverage (θ) by polymer. The selection of flocculants depends upon the requirements [163], as for example, sedimentation requires dense and large flocs with regularity in shape (preferably spherical), centrifugation requires strong dense and large flocs and floc floatation requires low-density flow with narrow size distribution [164].

2.6.3 Stability of Colloids

Particles suspended in an aqueous phase constantly encounter each other via the random Brownian motion and/or the velocity gradient generally by the applied force field such as flowing, agitation, electric and magnetic fields.

Interaction between the particles occurs as they approach together with the applied fields; govern the stability of the colloid and the rate of aggregation. Many types of particle interaction have been revealed. Their occurrence and importance to colloids stability depends on the characteristics of the dispersed particles and the dispersing medium. For the colloids

stability from the viewpoint of particles dispersion-aggregation technology, the following interactions are assumed.

- Van der Waals interaction.
- Electric double layer interaction.
- Solvation or hydration interaction.
- Steric interaction, mainly due to the adsorbed polymer layers.
- Bridging force due to crossover adsorbed polymer molecules.
- Liquid bridging via spreading of a polar liquid (oil) over the particles.

2.6.4 Electrical Double Layer

Colloidal particles are usually contaminated by electrostatic adsorption of ions to the surface. This primary adsorption layer gives rise to a substantial surface charge (i.e. electric potential at the surface). This surface charge does two important things: (i) causes a repulsion to exist between two precipitate particles when they approach each other i.e. fundamentally responsible for particles not sticking together and (ii) attracts counter ions into the vicinity of the particle [165]. These two opposite forces; electrostatic attraction and ionic diffusion, produce a diffuse cloud of ions surrounding the particulate, which can be extended up to 300 nm into the solution. This co-existence of original charged surface and the neutralizing excess of counter ions over co-ions distributed in a diffuse manner are known as the electrical double layer [166]. Thus, an "ion cloud" extends into solution around a charged surface effectively balancing the surface charge over some distance away from particles. The thickness of this electric double layer (ion cloud) around colloidal particles determines how close two particles can get to each other before they start experiencing repulsive forces. The size of this "ion cloud" depends on several factors: (i) the magnitude of the surface charge which depends on the solution concentration of the adsorbing ion, and (ii) the concentration of electrolyte in solution. The higher the concentration, the more compact the double layer and the closer two particles can approach to each other. The double layer is an electrical cloud near the solid surface composed of both a rigid zone, known as the STERN LAYER, and a diffuse layer called GOUY-CHAPMAN LAYER. Ions having the opposite charge as the solid are immediately attracted to the surface of the solid and attach, forming the Stern layer.

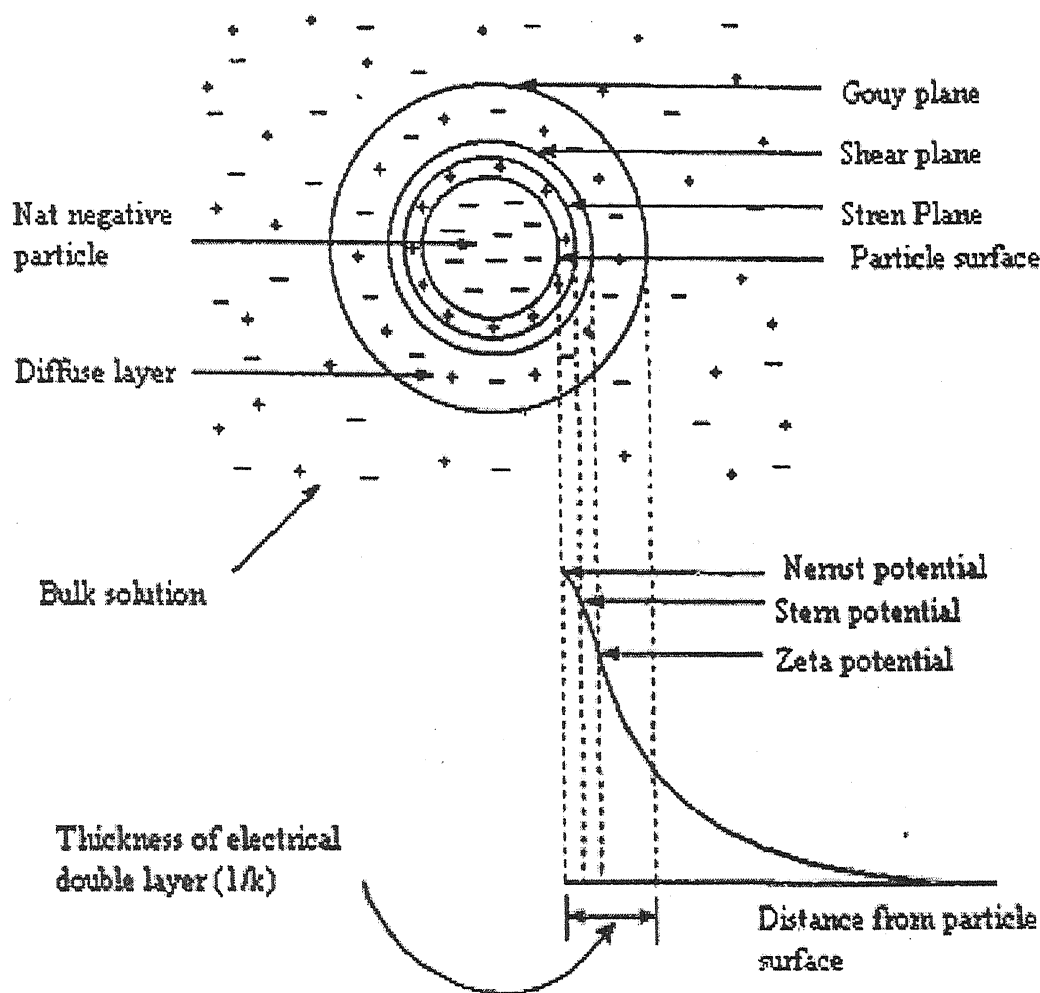


Figure 2.4 Schematic diagram showing the nature of electrical forces around a colloidal particle in blank solution

Additional ions of the same charge as the Stern layer are also attracted by the oppositely charged solid's surface but are simultaneously repelled by the like charges in the Stern layer. This dynamic equilibrium results in the formation of a diffuse layer. The diffuse layer is also composed of ions with the same sign of charge as the solid with the concentration of these ions decreasing with distance from the solid. Together the Stern layer and the diffuse layer form the double layer. The thickness of the double layer is a function of the pH and ionic strength of the solution. The schematic diagram is shown in Figure 2.4.

Both the diffuse layer and inner layer have several important impacts on the behaviour of particulate surfaces in aqueous medium. The stability of colloidal suspension is greatly influenced by the potential of the stern layer. Though the potential cannot be measured directly but approximated to the zeta potential representing the electrical potential between the surface plane and the bulk solution. According to Deryagin and Landau [167], Verwey and Overbeek [168], if the kinetic energy of the particle is large enough to surmount the potential hump created between them by way of double layer formation, the particles would coalesce otherwise they would remain as a stable suspension. This is popularly known as DLVO theory. This theory states that stability of a colloidal system is determined by the sum of the electrical double layer repulsive and Van der Waals attractive forces which the particles experience as they approach one another. The theory also proposes that an energy barrier resulting from the repulsive force prevents two particles approaching one another and adhering together. But if the particles collide with sufficient energy to overcome that barrier, the attractive force will pull them into contact where they adhere strongly and irreversibly together. It is well represented in Figure 2.5.

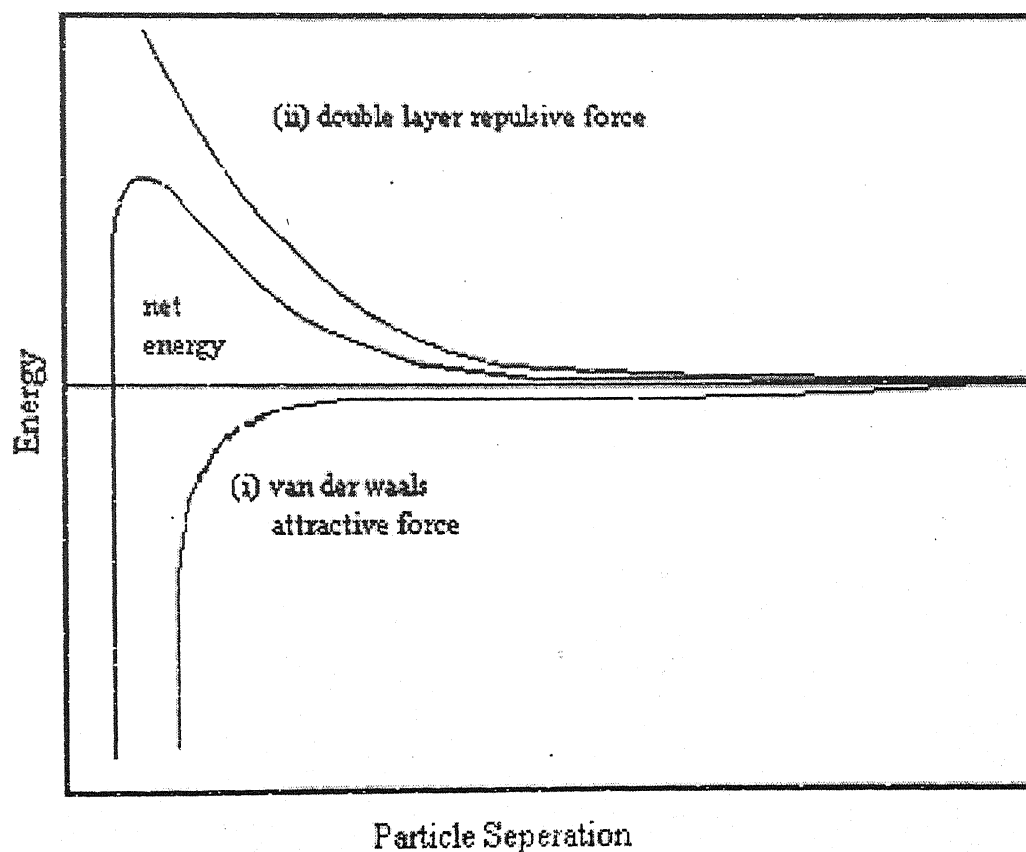


Figure 2. 5 Schematic diagram showing energy barrier of the colloidal particle

2.7 ZETA POTENTIAL

Almost all particulate or macroscopic materials in contact with a liquid acquire an electronic charge on their surfaces. Zeta potential is an important and useful indicator of this charge, which can be used to predict and control the stability of colloidal suspensions or emulsions. A charged particle dispersed in an ionic medium tends to have a concentration of oppositely charged ions attracted towards it, i.e. a negatively charged particle collects a number of positive counter ions. Therefore, the concentration of counter ions decreases as we move further away from the particle due to diffusion until ionic equilibrium is reached. The plot of the charge contributed by these ions versus distance from the particle surface (Figure 2.4) reveals an exponential decay. When a particle is moving, it withdraws its counter ions towards itself and leaving behind the ions that are further away from its surface. This would set up a plane of shear and the potential difference, which is called the zeta potential (ζ).

The greater the zeta potential the more likely the suspension is to be stable because the charged particles repel one another and thus overcome the natural tendency to aggregate. The measurement of zeta potential is often the key to understanding dispersion and aggregation processes in applications as diverse as water purification, ceramic slip casting and the formulation of paints, inks and cosmetics. The magnitude of the zeta potential gives an indication of the potential stability of the colloidal system. If all the particles in the suspension have a large negative or positive zeta potential they will repel each other and there will be dispersion stability. Similarly, if the particles have low zeta potential values then there would be no force to prevent the particles coming together and there is dispersion instability. A dividing line between stable and unstable aqueous dispersions is generally taken at either +30 mV or -30 mV. Particles with zeta potentials more positive than + 30 mV are normally considered stable, where as particles with zeta potentials more negative than -30 mV are normally considered stable.

The most important factor that affects zeta potential is pH of the suspension. A zeta potential value quoted, without a definition of its environment (pH, ionic strength, concentration of any additives) is a meaningless number. Suppose a particle with negative zeta potential is in a suspension. When more alkali is added to this suspension, the particles tend to acquire more negative charge, and on addition of acid to this suspension, a point will be reached where the charge will be neutralized. Excess addition of acid will cause a build up of positive charge. In general, a zeta potential versus pH curve will be positive at low pH and lower or negative at

high pH (Figure 2.6). The point at which the curve passes through zero zeta potential is called the isoelectric point (IEP). At isoelectric point the colloidal system is least stable.

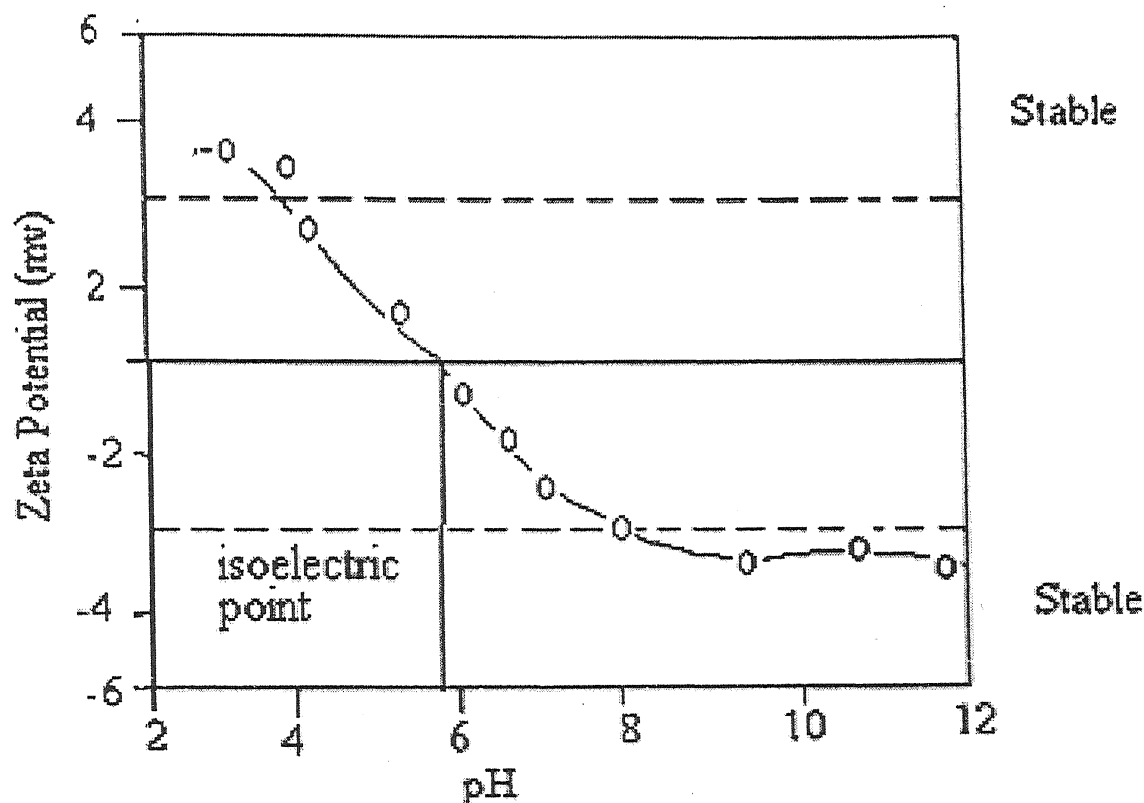


Figure 2.6 Graphical representation of Zeta Potential showing isoelectric point

2.7.1 Principle of Measuring Zeta Potential

The zeta potential is a measure of the magnitude of the repulsion or attraction between particles. The measurement of zeta potential is an extremely important parameter across a wide range of industries including brewing, ceramics, pharmaceuticals, medicine, mineral processing and water treatment. Many industries use large quantities of water, which become contaminated during the production process. Dewatering is now becoming important as the cost of disposal increases. Measurement of zeta potential can be used to optimize the use of expensive flocculants and speed up the flocculation process. Zeta potential is measured [169] using the technique of micro-electrophoresis, invented by Wane and Flygene and independently by Uzgiris in the early 1970s. However, as per Friend and Kitchener [170], zeta potential was calculated using Smouluchowski equation as early as 1903. The sample to be measured is immersed in a suitable liquid phase and subjected to the path of a laser beam.

A pair of electrodes should be dipped into the sample. Under the influence of applied electric field, the charged particles inside the sample will move towards the electrodes and the direction of motion indicates the charge carrying out by the particles, i.e. the positively charged particle will move towards the negative electrode and vice-versa. A schematic representation of Zeta meter is given in **Figure 2.7**.

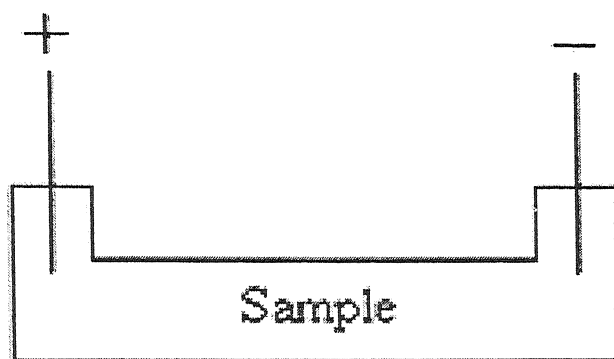


Figure 2.7 Schematic representation of Zeta meter

The velocity of the particles per unit electric field, called the electrophoretic mobility (u), can be measured by the following equation:

$$u = V/E$$

Here, V is the particle velocity and E is the applied field strength.

2.7.2 Significance of the Measured Zeta Potential

The zeta potential is best seen as the potential at the surface of the 'electrokinetic unit' moving through the solution. The electrokinetic entity may well include ions specifically adsorbed from the solutions and this will be reflected in the value of zeta potential. Certainly the double layer on the solution side of zeta potential will be purely diffused so that zeta potential is the relevant potential for all the effects that depend on diffuse layer effects (e.g. inter plate repulsion). Calculation of particle charge from zeta potential is also possible [171].

2.8 FLOCCULATION MECHANISMS

The performance of polymer can be examined on the basis of nature of flocs formed. It is now recognized that several mechanism can be involved in polymer flocculation [172]. These are classified as below:

- I. Polymer bridging.
- II. Charge neutralization.
- III. Electrostatic Patch Mechanism.
- IV. Polymer complex formation.
- V. Flocculation by free polymer (depletion flocculation).

These mechanisms are described in below:

2.8.1 Polymer Bridging

Polymer bridging flocculation occurs because segments of a polymer chain gets adsorbed on more than one particle surface thus linked the particles together [172,173]. Some favourable interaction between polymer segments and particle surface is required for adsorption to occur and this can occur in a number of ways. When the particles and polymers are oppositely charged (e.g. negative particles and cationic electrolytes) the electrostatic attraction leads to a very strong adsorption. When the particles and the polymers have the same sign of charge, or when the polymer has no charge as in the case of non ionic polymers, then there must be some specific interaction responsible for adsorption. Some of these interactions are discussed here.

- Hydrophobic bonding: This is responsible for the adsorption of non-polar segments on to hydrophobic surfaces.
- Hydrogen bonding: When particle surface and polymer molecules have suitable H-bonding sites, adsorption of an appreciable fraction of polymer segments occurs by such process. Hydroxyl groups on oxide surfaces can interact in this way with the amide groups of polyacrylamide.
- Dipole crystal field effects: Here the polar group on the polymer may interact with the electrostatic field at a crystal surface.

An effective bridging flocculation required the adsorbed polymer to be extended far enough from the particle surface to attach on to other particles and that there is a sufficient free surface available for adsorption of these extended chains [174]. If excess molecule is

adsorbed, the particles can become restablised because of surface saturation or by steric stabilization. This concept of flocculation by adsorbed polymers is schematically illustrated in Figure 2.8.

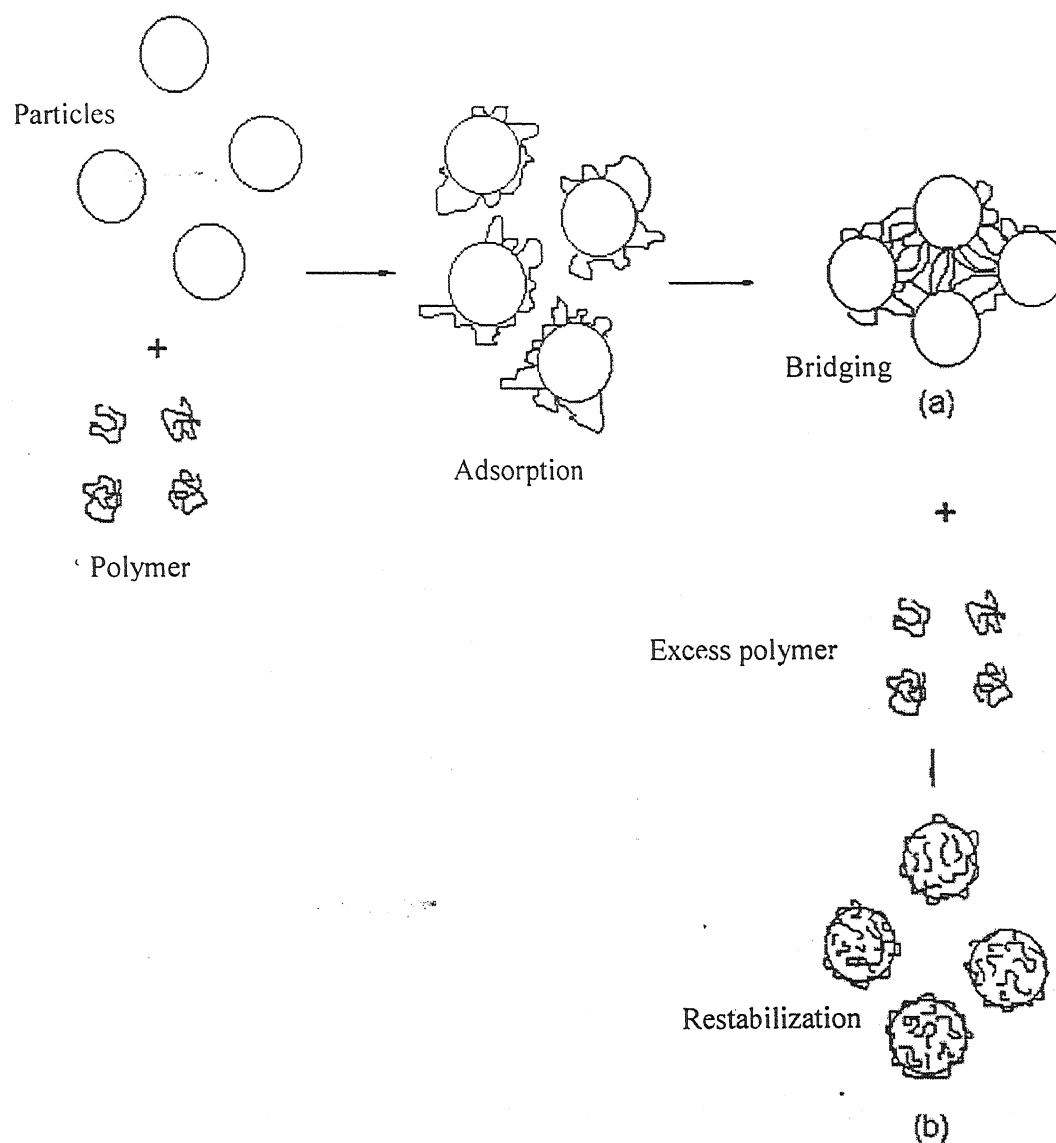


Figure 2.8 Schematic illustration of (a) bridging flocculation and (b) restabilisation of the adsorbed polymer

Most solid particles in contact with water become charged and the electrical repulsion between them depends on the ionic strength of the solution. At low electrolyte concentrations, the electrical double layer around a charged particle can be quite extensive (up to about 100 nm) and particles cannot approach closed to each other. For bridging flocculation to occur, it does not require reduction of the electrical repulsive forces between the particles. However it requires the effective end-to-end distance of polymer be long enough and the particle polymer collision be strong enough to penetrate the double layer of approaching particles [175]. Thus at low ionic strength, high molecular weight polymers and high particle concentration of through mixing are required for better flocculation.

2.8.1.1 Synthetic Bridging Polymer

These are synthetic, water-soluble, organic polymers of very high molecular weight. The bridging flocculants are strongly adsorbed onto the particles, and they are capable of spanning the gap between the particles. Synthetic polymers of high molecular weight are long enough for one end to adsorb onto one particle and the other end onto a second particle. Higher molecular weight polymers adsorb on several particles at once, forming a three-dimensional matrix. With bridging polymers in general, the higher the molecular weight the better the flocculant. Most synthetic flocculants are based on polyacrylamide and its derivatives. For bridging, the polymer must be strongly adsorbed and adsorption can be promoted by chemical groups having good adsorption characteristics, e.g. amide groups.

2.8.1.2 Natural Bridging Polymer

Natural polymers such as starch, gums, glues, alginates, etc., function as bridging flocculants, but they have much lower molecular weight than synthetic polymers and are only capable of a much lower degree of flocculation. Polysaccharides such as starch, dextran, etc are effective in neutral and slightly alkaline conditions. Organic colloids like glue, gelatin, albumin, casein, chitosan, etc, which consist of aggregates of giant molecules, are effective in acid solution. These polymers have several disadvantages, such as the dosages required, unstable solutions, variable quality, and loss of floc strength on storage of sedimented slurries. Natural polymers are generally non-ionic, but may be rendered slightly anionic or cationic by chemical treatment. However, ionic character is of little importance since they have little effect on zeta potential and appear to function by hydrogen bonding.

2.8.2 Charge Neutralization

In many practical applications, the effective flocculants are those having a charge opposite to the particles. In water most particles are negatively charged. Hence, it is likely that the cationic polymers adsorb with a rather flat configuration, which would limit the possibility of bridging. The adsorption of oppositely charged could reduce or eliminate the repulsion and cause flocculation simply for this reason. There are considerable evidences that for cationic polymers and negative particles, charge neutralization plays a major part in the flocculation process. The most direct evidence comes from the measurement of electrophoretic mobility (Zeta Potential). With many different types of particles, including clays [176,177], it has been reported that the optimum flocculant dosage for cationic polymers correspond quite closely to the amount required for giving zero electrophoretic mobility (i.e. to neutralize the particles). However there are instances where with the cationic polymers, bridging appears to be desirable (when strong flocs are required) as in the paper industries and conditioning of waste water sludge to enhance their filterability [178].

2.8.3 Electrostatic Patch Mechanism

Although charge neutralization explains the behaviour of cationic polymers in many systems of interest, the effect of molecular weight and ionic strength do not fit to this simple picture. They can be better explaining by electrostatic patch mode! [172,174]. When the particles have a fairly low density of immobilize surface charges and adsorbing polymer has a high charge density, it is not physically possible for each charge group on the polymer chain to be adjacent to a charge surface site and in this regions of excess charge develop even though the particles as a whole may be electrically neutral. Particles having the 'mosaic' type of charge distribution may interact in this way so that the positive and negative 'patches' come in contact giving rise to quite strong attachment. A schematic illustration of this type of interaction is presented in Figure 2.9.

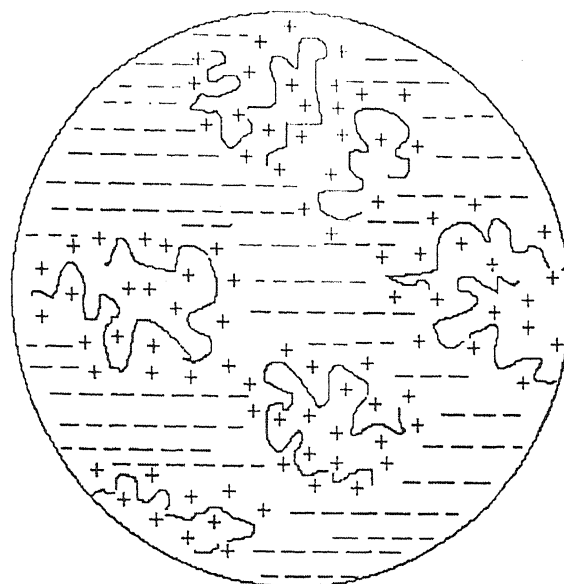


Figure 2.9 Schematic representation of flocculation by electrostatic patch mechanism .

2.8.4 Polymer Complex Formation

In some systems, apart from polymers, there are other components, which are either naturally present or deliberately added. They may interact with the polymer to enhance flocculation. In such cases, polymer complex formation may occur [179,180]. Complex formation and enhanced flocculation can also occur by sequential addition of oppositely charged polymers [181].

2.8.5 Flocculation by Free Polymers

In certain systems, flocculation may occur by exclusion of non-adsorbing large polymer molecules from the narrow zone between closely approaching particles due to geometric reasons [182]. This leads to an osmotic pressure difference between the contact zone and the bulk solution, which tends to pull the particles together. This is sometimes called '*Depletion Flocculation*'.

2.9 FLOCCULATING MATERIALS

The materials being used as flocculating agents can be broadly divided into two categories; inorganic and organic. The organic materials include polymers, which are further classified into natural and synthetic. The synthetic polymers may be nonionic, cationic or anionic, while most of the natural polymers are nonionic except in few cases. A new class of polymeric flocculants has been developed by combining synthetic and natural polymers, known as graft copolymers.

2.9.1 Inorganic Flocculants

The use of various chemicals [183,184] for coagulation of particles in suspension depends upon the characteristics of water being used. The inorganic flocculants are mostly based upon hydrolysable salts of aluminium, iron calcium and silicates. They are mostly used in their divalent and trivalent water-soluble metallic compounds. The principal materials mostly used are described in the following:

2.9.1.1 Aluminium Compounds

Dry and liquid alum are generally used for removal of suspended solids. The dry alum so used for wastewater treatment has the formula $\text{Al}_2(\text{SO}_4)_3 \cdot 14 \text{H}_2\text{O}$ with molecular weight of about 600 dalton. Activated alum contains about 9% sodium silicate, which improves the coagulation. Black alum is the alum containing activated carbon. It is more effective in the pH range of 5 to 8. The more quantities of sodium silicate in activated alum improve the coagulation behaviour in water. It is inexpensive and has high substance removal rate. The flocs, which are formed by using dry alum, are lightweight and loosely bound. It is known that alum formed various polymeric species. They formed short polymeric chains upon hydrolysis. These hydrolyzed compounds thus formed micro flocs with suspended materials. Their rate of floc formation is controlled by the pH of the medium and presence of other ionic species. Alum is not only used in treatment of municipal wastewater but it is also used for drinking water treatment and paper industries [185]. The principal disadvantage of alum is that it lowers the pH of the medium, which often necessitates addition of base and it leaves suitable amount of aluminium in effluent.

2.9.1.1.1 *Aluminium Chloride Hydroxide*

It is commonly called poly aluminium chloride or PAC. PAC is made by partial hydrolysis of aluminium chloride to form mixture of polymeric species. It is more expensive than alum on weight basis. Unlike alum it does not lower the pH of the medium and is also cost effective in some applications.

2.9.1.1.2 *Sodium Aluminates*

It is made by leaching bauxite with caustic soda. As with alum, the active species are the hydrolysis products. It tends to raise the pH of the medium.

2.9.1.2 Iron Compounds

Iron compounds possess flocc characteristics similar to aluminium sulfate. The cost of iron compounds may often be less than that of alum. The iron salts most commonly used as coagulants include ferric chloride, ferric sulfate, ferrous sulfate and ferric chloro-sulfate. In acidic pH condition, these compounds produce better coagulation than alum. However, the corrosiveness and difficulty in dissolution may result in high soluble iron concentration hampering the process of effluent treatment.

In recent years iron salts have replaced aluminium salts particularly in treatment of drinking water.

2.9.1.3 Calcium Salts

The principal calcium salt used as a flocculant is calcium hydroxide or lime. Its use in water treatment is declining [186]. It is now used for pH modifier and to precipitate metals as insoluble hydroxide.

2.9.1.4 Sodium Silicates

It is usually added to slurry as a dispersant. Small amount of sodium silicate is as flocculant. The active species of polymeric silicate is formed by hydrolysis.

2.9.2 Polymeric Flocculants

Generally, water-soluble high molecular weight linear polymers [187-191] are used as flocculants. The cationic and anionic counterparts of these polymers are known as polyelectrolytes endowed with many characteristic attributes. Some of the nonionic water-soluble polymers at times bear some ionic groups as a result of inadvertent hydrolysis.

2.9.2.1 Cationic Polymers

Water-soluble cationic polymers are a class of polyelectrolytes that derive their unique properties from the density and distribution of positive charges along the macromolecular backbone. Chain conformation and solubility of such flocculants depend on the extent of ionization and interaction with water. Cationic functional groups can strongly interact with suspended, negatively charged particles or oil droplets and hence are useful in many applications, including waste water treatment and paper making process. Water-soluble polymers containing cationic charge can be divided into three categories: ammonium (including amines), sulphonium and phosphonium quaternaries.

2.9.2.1.1 *Polyacrylamide-Based Cationic Polymers*

Cationic monomers can be homo or copolymerised with acrylamide to yield water-soluble polymers with varying positive charge (1-100%). Cationic monomers are, in general, more expensive than acrylamide or anionic acrylic monomers.

Random copolymers of acrylamide and acryloyloxyethyltrimethyl ammonium chloride, quaternisation of dimethyl aminoethyl acrylate with methyl chloride are exclusively used in water industry. The methacrylate analogue with variation of cationic content is also commercially available. The quaternised aminoacrylate copolymer having charge density (CD) of 30 mole % has been used for clay flocculation studies. In copolymers with acrylamide, hydrolysis of the ester groups has been investigated and found to be CD and pH dependent with hydrolysis increasing under more alkaline conditions.

Cationic polyacrylamides (PAM) can be prepared by post polymerization functionalization of PAM. In a Mannich-type reaction, PAM reacts with formaldehyde forms N-methylol groups. These can be treated with a dialkyl amine such as dimethyl amine yielding pendant amine groups [192]. Pelton et al [193] describe the synthesis of a model cationic polymer based on the Mannich reaction of PAM. Tanaka [194] describes another approach to introduce amine

groups into PAM by reaction with polyamines or by sodium hypochlorite degradation (Hoffman reaction).

Synthesis and characterization of homo and copolymers of 2-acrylamide-2-methyl propane dimethyl ammonium chloride (AMPDAC) with acrylamide have been reported [195]. Redox polymerisation of a quaternary ammonium acrylic monomer with acrylamide has also been reported [196]. Solberg and Wagberg have been reported the adsorption and flocculation behaviour of cationic polyacrylamide [197]. Besra et al. [198] have synthesised cationic polyacrylamide and used as flocculants.

One of the cationic systems that have been the subject of some basic research [199,200] is poly (diallyl dimethyl ammonium chloride) and its copolymer with acrylamide. The monomer is referred as DADMAC or DADAAC. Zemaitaitiene et al. [201] have used the polyquaternary ammonium salts poly (diallyl dimethyl ammonium chloride) (poly-DADMAC) and poly (vinyl benzyl trimethylammonium chloride) poly (VBTMAC) as flocculants for treatment of dye removal from textile waste water. Besra et al. [198] also studied the flocculation behaviour of cationic polyacrylamide in presence and absence of surfactants. Gill and Herrington [202,203] have also studied the effect of surface charge and effect of colloid concentration and pH on kaolin suspension by using cationic polyacrylamide as flocculants. Butler and Angelo [199] have established that free radical polymerization of DADMAC is intramolecular and involves a cyclization mechanism to produce a five membered ring. Potentiality of these polymers as coagulants and flocculants to silica suspension is due to high cationicity. High molecular weight copolymers of poly (DADMAC) with acrylamide [204,205] have found extensive application in sludge conditioning. Lin et al. [206] have made graft copolymers of acrylamide onto poly (DADMAC) by first making a copolymer of DADMAC with 1-10 % of acrylic acid and then testifying it with 3-chloro-1, 2 propane diol to introduce cis-diol groups, which serve as grafting sites in presence of ceric ion. Deng et al. [207] have studied the temperature sensitive flocculation characteristics of a copolymer of poly (N-isopropyl acrylamide) and poly (DADMAC) with colloidal TiO_2 .

Recently it has been observed that the flocculation efficiency of the colloidal suspension increases by using oppositely charged polyelectrolytes. Petzold et al. [208] have investigated that the flocculation efficiency of the clay suspensions increases by using a dual systems of highly charged polycation poly (diallyl dimethyl ammonium chloride) in combination with

different high molecular weight polyanions of polyacrylamide type. The polyanions are modified polyacrylamide e.g. poly (acrylamide-co-sodium acrylate).

2.9.2.1.2 *Polyamines, Polyimines and Poly vinyl pyridines*

Four types of cationic monomers are involved in this class:

- Polyamines that are condensation products of amines and halogenated compounds.
- Polyamidoamines that result from the formation of a polyamide followed by reaction with a halogenated compound (e.g. epichlorohydrin).
- Polyethylene imines made by ring-opening polymerization of aziridine and
- Polyvinylpyridinium systems.

• Polyamines

Polyamines are prepared by step-growth polymerization of polyfunctional amines and alkyl halides or bifunctional alkyl epoxides and alkyl epoxide derivatives. These are relatively of low molecular weight ($< 10^5$) and have high level of cationicity. Typically in the first case, a poly (ethyl amine) is produced by the reaction of ammonia or low molecular weight alkyl polyamine with ethylene chloride in the presence of aqueous base. This is sometimes followed by the reaction with epichlorohydrin. Reaction variables need to be controlled carefully to meet the molecular weight requirements.

• Polyamidoamines

Polyamidoamines are produced by the reaction of adipic acid with diethylene triamine, yielding a polyamide with secondary amine groups, which further react with epichlorohydrin. The pendent epoxide group may react with the secondary amine group of another polymer chain resulting in cross-linking. This must be controlled to render the polymer water-soluble.

• Poly (ethylene imine) (PEI)

Poly (ethylene imine) is a special type of cationic polymer produced commercially from ethylene amine (aziridine) in an aqueous medium by ring-opening polymerization using CO_2 , a mineral acid or ethylene dichloride as initiator. This product (PEI or polyaziridine) is highly branched with primary, secondary and tertiary amine groups. PEI has been used in a number of model investigations of flocculation [209].

- **Poly (2-vinyl pyridine) and Poly (4-vinyl pyridine)**

These can be prepared by conventional free radical techniques. The polymers are quaternized with alkyl derivatives to form strong polyelectrolytes in solution. Cardoso et al. [210] have studied the flocculation characteristics with bentonite clay suspension of N-oxide type zwitterionic polymeric flocculant derived from isomers of poly (vinyl pyridine) and poly (N, N – dimethylaminoethyl methacrylate) by oxidation. The resulting polymers have high water solubility, chemical stability and ability of chain expansion with increased ionic strength, a property highly desirable in the process of flocculation by polymers. Asanov et al. [211] have studied the flocculation characteristics of an aqueous suspension of bentonite with a water-soluble polyelectrolyte based on 2-methyl-5-vinyl pyridine, methacrylic acid and its amides to show that the presence of functional groups like amines and amides strengthen the flocculation attributes.

2.9.2.2 Anionic Polymers

In anionic flocculants, 1-100 % of the monomer units contribute to the charge and the molecular weight tends to be very high or very high range. Although several types of anionic sites are possible, the major type in commercial flocculants is the polymer having carboxylate ions.

2.9.2.2.1 Polymers containing Carboxyl Groups

High molecular weight PAM based carboxylic acid polymers are extensively used as flocculating agents in the water and various process industries, where a low charge density is the general rule. Homo poly (acrylic acid), poly (acrylic acid-co-acrylamide) and hydrolyzed PAM dominate the anionic flocculant market; where as hydrolyzed PAN has been found to be playing a less important role.

2.9.2.2.2 Poly (acrylic acid) and its salts

Anionic poly (acrylic acid) can be synthesised by direct polymerisation or through hydrolysis. In direct method, salts of acrylic acid are homopolymerised or copolymerised by free-radical initiation in aqueous media. Usually the rate of polymerisation in case of ionic monomer is slower than the corresponding nonionic monomer, owing to the charge repulsion between the growing chains as well as the incoming monomer. The advantages of direct

polymerisation are because of the non-volatility of acrylic acid salts, which allows simultaneous polymerisation and spray drying leading to high molecular weight polymers.

Anionic poly (acrylic acid) can also be prepared indirectly by hydrolysis with alkali (usually sodium hydroxide or sodium carbonate) in aqueous medium. Copolymers with variation in the percent of amide and carboxylic acid groups can be prepared either by copolymerisation of acrylamide and acrylic acid or its salts, or by polymerisation of acrylamide followed by partial hydrolysis. The former route gives random copolymer, whereas some clustering can occur in the alkaline hydrolysis approach. The rate of addition copolymerisation of acrylic acid with acrylamide is pH dependent and the reactivity decreases with increasing pH. Mpofu et al. [212] have used a copolymer of sodium acrylate and carboxyl substituted PAM for flocculation study.

2.9.2.2.3 Anionic Polyacrylamide

Anionic polyacrylamide can be prepared by hydrolysis of acrylamide. Besra et al. [213] and, Petzold and Herrington [214] studied the flocculation and dewatering of Kaolin suspension by using anionic PAM flocculants. Taylor et al. [215] also studied the flocculation process of anionic PAM onto Kaolinite. The stabilization and destabilization of hematite suspension are studied by Zhang et al. [216] by using neutral and anionic polyacrylamide.

2.9.2.2.4 Polymers containing Sulfonic acid group

The sulfonic acid group is an inherently stronger acid than the carboxyl. Polymers with sulfonic acid moieties, therefore, retain their anionic charge in media with low pH. The major representatives of polymers containing sulfonic acid are poly (vinyl sulfonic acid) (PVSA) and poly (styrene sulfonic acid) (PSSA).

2.9.2.2.5 Poly (vinyl sulfonic acid) (PVSA)

It is the simplest example of this family of fully ionized strong electrolyte polymers. It is prepared by polymerisation of ethylene sulfonic acid or its sodium salts under free radical conditions and purified by precipitating aqueous solutions of the sodium salt form with methanol or dioxane. The ion binding selectivity of the polymer with alkali metals has been observed in viscosity and phase separation studies. The homopolymers and its copolymers with methacrylic acid are reported to be useful in deposit control as are the copolymers of allylsulfonic acid and fumaric acid.

2.9.2.2.6 Poly (styrene sulfonic acid) (PSSA)

Poly (styrene sulfonic acid) is prepared by free radical polymerisation of the monomer in solution using the acid, sodium or potassium salt form. PSSA may also be prepared by sulfonation of polystyrene or by hydrolysis of poly (n-propyl p-vinyl benzenesulfonate). The sulfonation route requires a careful choice of the sulfonating conditions necessary to minimize cross-linking and the formation of insoluble gel. The best reagent used to be a sulfur trioxide-trialkyl phosphate complex, with the para-isomer as the major product. Very high products of PSSA have been investigated as flocculants for the so-called red muds in the Bayer process for bauxite to demonstrate the effect of molecular weight on that substrate [217].

Several acrylate or acrylamide polymers containing sulfonate groups are commercially relevant as high molecular weight flocculants or low molecular weight deposit control agents [218]. These include homopolymers of sodium 2-methacryloyloxyethyl sulfonate (SEM) [219] and sodium 2-acrylamido 2-methyl propyl sulfonate (AMPS) [218]. Among these monomers, 2-sulfoethyl methacrylate is of limited commercial value owing to the hydrolytic instability of the ester linkage. The same factor has been a major drawback with 3-sulfo-2-hydroxypropyl methacrylate (SHPM).

However, 2-Acrylamide-2-methyl propyl sulfonic acid (AMPS) prepared by the reaction of SO_3 with isobutylene followed by Ritter reaction with acrylonitrile [220,221] is hydrolytically quite stable. AMPS is highly reactive in both homo and copolymerisation and can be incorporated by homogeneous, solution or emulsion polymerisation technique. Its applications include improving emulsion stability, flocculation, improving dry strength of paper, sludge disposal in boil-water treatment etc. Qin et al. [222] have copolymerised sodium allyl sulfonate onto acrylamide in an aqueous solution using ammonium persulfate as initiator and studied their flocculation behaviour in Kaolin suspension in presence of Calcium ion. Yu et al. [223] have prepared an anionic copolymer with reactive functional groups of amido, carboxyl and sulfonate and studied its flocculation characteristics in lysozyme solution.

2.9.2.3 Nonionic Polymers

For the purpose of classifying as flocculants, a polymer is considered nonionic if less than 1% of the monomer units are charged. In aqueous systems such polymers function as flocculants primarily by the bridging mechanism. Hence, they must be of high or very high molecular weight for practical applications. The important members of this class include polyacrylamide (PAM) and polyethylene oxide (PEO).

2.9.2.3.1 *Polyacrylamide (PAM)*

Acrylamide monomer is polymerized by free radical initiators, e.g. azo compounds, redox initiator, light and radiation. Acrylamide is unique among vinyl and acrylic monomers as it can be polymerised to ultra-high molecular weight (10^6 - 10^7 dalton). This extraordinary feature of acrylamide polymerization is attributed to the high ratio of its propagation to termination rate constants (K_p/K_t). In fact acrylamide has the highest K_p/K_t of any free radically polymerisable monomer. PAM can be prepared via solution inverse emulsion, inverse microemulsion or precipitation techniques. Low temperature initiation, high monomer concentration and a small amount of the added 2-mercaptobenzimidazole radical scavengers are reported to be the optimal reaction conditions for preparing high molecular weight polymers. Pure nonionic polymers or copolymers from acrylamide are difficult to prepare due to the rapid hydrolysis of amide groups. The basic advantage of investigations is the stability of dilute aqueous solutions on ageing. Rahman have studied the flocculation of phosphatic clay waste by using polyacrylamide [224]. Besra et al. [225] also studied the flocculation and dewatering of Kaolin suspension using polyacrylamide flocculants.

2.9.2.3.2 *Poly (ethylene oxide) (PEO)*

PEO resins are commercially made by the catalytic polymerization of ethylene oxide in the presence of one of the several existing catalyst systems. They are available with average molecular weight ranging from 200 to 5×10^6 dalton. The products with a molecular weight below 25,000 dalton are viscous liquids or waxy solids, commonly referred to as poly (ethylene glycols). Those with a molecular weight range from about 1×10^5 to 5×10^6 dalton are called poly (ethylene oxide) (PEO) resins. They are dry, free flowing, and white powders completely soluble in water at temperature upto 98°C and completely soluble in certain organic solvents. Aqueous solutions of PEO display increasing pseudoplasticity with

increasing molecular weight. High molecular weight polymers of ethylene oxide are susceptible to severe auto-oxidative degradation and loss of viscosity in aqueous solution. The mechanism involves the formation of hydroperoxides that decompose and cause cleavage of the polymer chain. The rate of degradation is increased by heat, UV light, strong acids and certain transition metals particularly Fe^{3+} , Cr^{3+} and Ni^{2+} . Ethyl, isopropyl or allyl alcohols, ethylene glycol or Mn^{2+} ions are known to be effective stabilizers of aqueous PEO solutions. The major commercial uses of PEO include adhesives, water soluble films, textile sizes, rheology control agents and thickeners, water-retention aids, lubricants, hydrodynamic drag reducing agents, flocculants, [226] dispersants and additives in medical and pharmaceutical products. The unique combination of properties of these polymers have led to developing applications in detergents, solids transport, control of sewer surcharges, dredging and metal-forming lubricants.

2.9.2.4 Natural Polymers

Several naturally derived substances are used as flocculants, most of them being based on a polysaccharide skeleton, while some of them contain ionic groups.

2.9.2.4.1 Starch

Among natural flocculants the most widely used are starch and its derivatives. Starch isolated from different sources is all used to some degree as flocculants, but some work better with certain substrates than others. Basic starch consists of two constituents, e.g. amylose and amylopectin. The amylose fraction of starch shows better flocculation in red mud treatment when compared to amylopectin and the native starch. The efficiency can be improved by incorporation of cationic and anionic substituent. Järnström et al. [227] have studied the effect of temperature and ionic strength on the flocculation of a kaolin suspension with cationically modified starch and its efficiency is compared [228] with that of poly (vinyl alcohol) and CMC. Weissenborn et al. [229,230] have investigated the mechanism of adsorption of wheat starch and its components (amylopectin and amylose) onto hematite ore. It was observed that wheat starch and amylopectin are adsorbed strongly onto hematite which was proposed to be due to the formation of a surface complex between the carbonyl groups attached to C-2 and C-3 atoms of AGUs and surface iron atom of hematite. A comparison of the selective flocculation performance with adsorption results established that flocculation occurs by the classical bridging mechanism. Application of starch as a selective flocculant

has been reported [231]. Nyström et al. [232,233] have investigated the flocculation characteristics of calcium carbonate by using the mixture of cationic starch and anionic polyacrylate. The application of cationic amylopectin as a selective and efficient flocculant has been reported [234-238].

2.9.2.4.2 Gum

Guar gum (GG), which structurally comprises of a straight chain of D-mannose with a D-galactose side chain on approximately every alternate mannose unit, has a molecular weight of the order of 220,000. As a result of its wide range properties, guar gum is the most extensively used gum, both in food and industrial applications. It is nonionic and hence is an effective flocculant over a wide range of pH and ionic strengths. In the mining industry GG is used as a flocculant or flotation agent, foam stabilizer, filtration and water-treating agent. In the textile industry, it is used as a sizing agent and as a thickener for dyestuffs. However, one disadvantage of GG is its relatively rapid biological decomposition in aqueous solutions, which of course, can be controlled by addition of chelating agents and grafting with PAM chains [239, 240].

Xanthan gum (XG) is a high molecular weight extracellular polysaccharide produced by bacteria of the genus *Xanthomonas* [241]. Xanthan gum may be chemically considered as an anionic polyelectrolyte, with a backbone chain consisting of (1→4) β-D-glucan cellulose [241]. The polymer backbone is substituted at C-3 on alternate glucose residues with a trisaccharide side chain. The side chain consists of β-D-mannopyranosyl - (1→4) - (α-D-glucoropyranosyl)-(1→2) - β-D-mannopyranoside 6-acetate. A pyruvic acid residue is linked to the 4 and 6 positions between 31-56% of the terminal D-mannose residues [242-244]. The flocculation studies of allophanic clay system with xanthan gum and several of its hydrolytic intermediates have been reported [245, 246].

Hydroxypropyl guar gum (HPG) is a derivatized form of guar gum. It is composed of a linear backbone of (1-4)-β-linked D-mannose units with (1-5)-α-linked D-galactose units randomly attached as side chains. HPG is extensively used in oil field operations [247].

2.9.2.4.3 Cellulose and its Derivatives

Cellulose and its derivatives, e.g. sodium carboxymethyl cellulose [248] and sodium carboxyethyl cellulose are also used as flocculating agents. Unlike many flocculants derived from natural products, it is relatively resistant both to biological and hydrolytic degradation.

2.9.2.4.4 Dextran

Dextran is a class of polysaccharide synthesized from sucrose by bacterial enzymes (dextransucrases, glucansucrases, or glucosyltransferases) to give D-glucans with contiguous α -1 \rightarrow 6 glucosidic linkages in the main chains and a variable amount of α -1 \rightarrow 2, α -1 \rightarrow 3, or α -1 \rightarrow 4 branch linkages [249, 250]. Dextran also acts as a flocculating agent due to its branched structure.

2.9.2.4.5 Glycogen

Glycogen is similar to amylopectin. It is heavily branched molecule containing straight chains of glucose units connected by α -1 \rightarrow 4 linkages. The branching that results from α -1 \rightarrow 6 linkages is much more frequent in glycogen than in amylopectin, occurring every 8-12 units. It has high molecular weight. It is a better flocculant than other polysaccharides [251].

2.9.2.5 Graft Copolymers

Graft copolymerization has been successfully used to alter significantly the solution properties of both natural and synthetic polymers. The viscosity, gelling characteristics, solution rheology, e.g. degree of pseudoplasticity, ion compatibility etc. can be drastically changed through graft copolymerization reaction. Enhanced functionality can also be imparted to substrates which will allow them to be more effective in flocculation, dispersion and other applications such as retention aids in paper, dry strength additives etc. Polyelectrolyte side chains can be introduced onto suitable substrates by either grafting an ion-containing monomer or a suitable monomer, which can then be transformed to an electrolyte by a simple chemical reaction.

2.9.2.5.1 *Anionic and Nonionic Graft Copolymers*

Most of the graft copolymerization reactions have been started with starch and celluloses substrate using styrene, acrylamide and acrylic acid as monomer by ceric ion or radiation initiation method. The alkaline hydrolysis of starch-g-polyacrylamide produces a mixture of carboxylic acid and carboxamide groups, but these are slightly effective in flocculation. Acrylic acid/methyl cellulose graft copolymers have been used as clay binders in foundry sands. Water soluble graft copolymers with exceptionally high molecular weight grafted side chains using acrylamide and acrylic acid have been prepared using ionizing radiation as the grafting mechanism. These materials are excellent flocculating agents.

Many graft copolymers have been synthesized by grafting PAM branches onto natural polymers like amylose [252,253], amylopectin [252], guar gum [254], hydroxypropyl guar gum [255], P-psyllium [256], sodium alginate [257] etc. The drag reducing properties as well as the shear stability of the graft copolymers were studied. It was found that grafting of PAM, which is highly prone to shear degradation onto polysaccharide backbones not only results in efficient drag reducing agents but also makes the graft copolymers reasonably shear resistant [258,259]. Further, variation in the number and length of PAM chains were affected by varying the synthetic parameters. It was observed that in a series of graft copolymers with a particular polysaccharide, the one with fewer but longer PAM chains performed the best [260]. The study of the flocculation behaviour of the graft copolymers showed the same trend. In another study, Karmakar [261] studied the flocculation and rheological studies of starch-g-polyacrylamide and amylose-g-polyacrylamide. Starch-g-polyacrylamide was found to be the better in performance. When the performance of amylopectin-g-polyacrylamide was investigated by Rath and Singh [252,262], it was found to perform better than any other graft copolymers and various commercial flocculants. This behaviour was explained by Singh's Easy Approachability Model [263-267], which is based on easy approachability of dangling PAM branches on rigid amylopectin to contaminants in the industrial effluents. Since in amylopectin-g-polyacrylamide the PAM branches are grafted on backbone as well as on amylopectin branches, this provides better approachability of grafted PAM branches to contaminants.

2.9.2.5.2 Cationic Graft Copolymers

Various quaternary ammonium monomers have been graft copolymerized onto starch in attempt to prepare improved flocculants and pigment retention aids useful in papermaking. The work of Fanta et al. [268] on the graft copolymerization of 2-hydroxy-3-methacryloyloxypropyl trimethylammonium chloride onto starch and its evaluation as flocculating agents is of particular interest. Fanta et al. [269] also investigated the graft copolymers of starch with mixtures of acrylamide and the nitric acid salt of dimethylaminoethyl methacrylate and evaluated their flocculation performance. Jones and Jordan [270] investigated the graft and terpolymers of starch with 2-hydroxy-3-methacryloyloxypropyl trimethyl ammonium chloride and acrylamide for use as silica depressants in the flotation-beneficiation of silaceous ores. However and Sinkovitz [271] developed some new cationic graft copolymers made by the graft copolymerization of diallyldimethylammonium chloride or 2-hydroxy-3-methacryloyloxypropyl trimethylammonium chloride and acrylamide onto dextran substrate and their use as additives for improving the dry strength of paper. Walldal et al. [272] have synthesized cationic polymers of amylopectin and polyacrylamide and studied its interaction with colloidal silicic acid. Levy et al. [273] have synthesized cationic guar gum and study its flocculation behaviour in bentonite suspension. First they fragmented the guar gum using ammonium persulphate as a degrading agent, followed by precipitation of the products with ethanol. The cationic charge was added to the guar molecule by reacting it with 2,3-epoxypropyltrimethylammonium chloride. Gu et al. [274] have synthesised cationic graft copolymers of poly diallyldimethyl ammonium chloride (poly DADMAC) and PAM using organic peroxide initiators. Larsson et al. [275] have synthesised cationic amylopectin using 3-chloro-2-hydroxypropyl trimethyl ammonium chloride (QUAB) as the monomer and studied its flocculation performance in colloidal silica suspension.

2.10 POLYMERIC VERSUS INORGANIC FLOCCULANTS

Polymeric flocculants offer some distinct advantages over inorganic flocculants. The flocs are larger and stronger and are more rapidly formed. The salt concentration is not increased and much less sludge is generated. The dosage requirement is quite low (typically 1 % on a dry weight basis) whereas that of inorganic flocculants may be as high as 20 %. The inorganic flocculants frequently require pH adjustment, which is not necessary with polymeric

flocculants. Further, the polymeric flocculants are more convenient and easier to use. However, inorganic flocculants are inexpensive and often used for economic reasons.

2.11 NATURAL VERSUS SYNTHETIC FLOCCULANTS

The principal advantages of natural polymers are that they are non-toxic and readily available from renewable natural resources. Unfortunately, their efficiency is low, thus requiring a high dosage that varies with origin of natural polymers. The biggest advantage of natural polymers is their biodegradability. But this very advantage becomes a drawback in reducing its storage life and tells upon their efficiency as a result of molecular breakdown. The synthetic polymers on the other hand are highly efficient with product consistency and uniformity, biological as well as chemical stability. These can be tailored in terms of functional groups, structure and molecular weight to suit to a particular application. However, their disadvantages are that they are mostly non-biodegradable, highly expensive and may be toxic [276,277] (it may be noted that the synthetic polymers are not toxic but the associated monomers may be toxic).

2.12 FLOCCULATION: THE TEST METHODS

The principal purpose of a flocculation test procedure is to establish the optimal conditions for floc formation, but the nature of test may be greatly influenced by the process considerations [278]. If the aim of flocculation process is to clarify turbid water, then the optimum conditions might be judged in terms of minimum supernatant turbidity after sedimentation of flocs. On the other hand, if solids recovery is the main purpose, settling rate could be the chosen parameter. In case of sludge dewatering, flocculants are used to increase filterability, so that filter cake permeability or specific resistance to filtration (SRF) is considered as the desired parameter.

It seems reasonable to assume that optimum flocculation condition determined on the basis of different tests should coincide, especially if thorough mixing of additives could be achieved rapidly. However, there is very little evidence on this point in practical systems. In fact where flocculation is carried out for some specific purpose such as colour or phosphate removal, then it is the best to monitor the removal directly. Ideally, a flocculation test procedure should simulate the operation of a full-scale unit and be capable of predicting plant performance on the basis of laboratory trials. But due to various reasons, such prediction is difficult to

achieve and a more realistic aim is to establish optimal chemical conditions in laboratory trials which correspond closely to those giving optimum plant performance. The actual performance of the plant, in terms of clarification, settling rate or other parameters may not be the same as that found in the laboratory test under the same chemical conditions, but it is possible to establish an empirical relationship, which can be used for predictive purposes. Usually, measurement of three parameters, namely sedimentation rate, settled volume and supernatant turbidity give information on the state of aggregation of a suspension.

Sedimentation (at fairly high solids concentration) can most conveniently be measured in the zone-settling region, where the movement of the boundary layer can be followed with time. Settled volume of flocs is sometimes used in laboratory evaluation of polymeric flocculants, but is not usually employed in routine tests.

Measurement of supernatant turbidity is frequently employed as an indicator of flocculation performance. Ideally, a well-flocculated suspension should settle leaving no suspended solids in the supernatant liquid and hence a very low turbidity. Turbidity measurements are based on transmitted light or light scattering, the latter being more effective. For very low turbidities, some other measures of solids content like Silting Density Index (SDI) may be more appropriate. The supernatant turbidity, although a directly relevant parameter in applications like water clarification, some difficulties may arise in interpreting the results. For instance, the result may be greatly influenced by a residual haze, which may represent an extremely small proportion of the original solids. Incomplete mixing of the flocculant may result in local overdosing and restabilization of a small number of particles, giving rise to a persistent haze in the supernatant liquid. This effect is likely to occur with polymeric flocculants.

2.12.1 The Settling Test

Settling test is conventionally conducted according to the International Standard Organization (ISO), in 100 ml standard measuring cylinders (2.8 cm inner diameter and 25 cm long) [279]. A suspension of high solids content is taken in the cylinder and mixed well by shaking. Required dosage of flocculant solution is added so as to make the total volume up to 100 ml mark. The cylinder is inverted up side down ten times and is allowed resting to form interface between flocs and supernatant. Settling curves showing fall of the interface height vs. settling time. Many research workers [280, 281] performed settling studies in 100 ml graduated

cylinders. Sometimes, narrow glass tubes (20 cm long and 0.48 cm diameter) are used for settling study of clay materials [282]. One-meter high glass jars are also used for the study of wastewaters of pulp and paper mill [283].

2.12.2 The Jar Test

One of the most common pieces of bench test apparatus found in water treatment laboratories to identify potential coagulation-flocculation conditions in liquid suspensions is the jar test apparatus. The test is used to confirm the preferred chemicals and also to identify the best concentrations. The batch-test consists of using six identical jars containing the same volume and concentration of feed, which are charged simultaneously with six different doses of a potentially effective flocculant. The six jars can be stirred simultaneously at known speeds. The treated feed samples are mixed rapidly and then slowly and then allowed to settle. These three stages correspond respectively to the fundamental processes of dispersing the flocculant onto the particle surface, gently sweeping the colloidal particles together to form large flocs, and allowing the flocks to settle. These three stages are also an approximation of the sequences based on the large-scale plants of rapid mix, coagulation-flocculation and settling basins. At the end of the settling period test samples are drawn from the jars and turbidity of supernatant liquid is measured. A plot of turbidity against flocculant dosage gives an indication of the optimum dosage (i.e. the minimum amount required to give acceptable clarification). The criteria thus obtained from a bench jar test are the quality of resultant floc and the clarity of the supernatant liquid after settling. The design of the full-scale plant process is then done based on the bench-scale selection of chemicals and their concentrations.

Unfortunately, the jar test suffers from a number of disadvantages, despite its widespread application. It is a batch test, which can be very time-consuming. A thorough exploration of optimum flocculation conditions for raw water can easily take a few days. Such an extensive series of trials would require very large volume of sample, which may be inconvenient if testing is to be carried out remote from the raw water source. Finally, the results obtained from a series of jar tests might not correspond to the results obtained on a full-scale plant. Many new methods [284] have been developed to substitute the conventional jar test including techniques [285, 286] for characterization of floc structure.

2.13 FACTORS AFFECTING THE FLOCCULATION

2.13.1 Effects of Molecular Weight and Charge Density of Polymer

When a low molecular weight polymer is used, there is a tendency for each polymer molecule to adsorb on to a single particle. The degree of flocculation is then lessened by further polymer addition. With a polymer of the same type, but higher molecular weight, a greater amount can be adsorbed and utilized by the flocs. Optimum dosage and settling rate both increase with increasing molecular weight. In the treatment of coal wash plant refuse, the trend has been towards the very high molecular weight anionic flocculants since it has become increasingly important to obtain faster sedimentation rates. However, lower molecular weight products are more suitable for filtration applications as has already been stated. The effects of polymer molecular weight on flocculation [287-289] are best described in terms of bridging and electrostatic patch mechanisms. For systems in which bridging predominates irrespective of charge, an increase in molecular weight improves flocculation. At higher molecular weight, as the polymer gets adsorbed, it can extend further away from the particle surface and is slower to reach equilibrium. This in turn, increases particle radius and collision number and hence flocculation rate. Although anionic charge on polymer can impede adsorption onto a negative surface, it serves to promote extension of polymer chain through mutual charge repulsion, enhancing its approachability. It has been observed that beyond an optimum molecular weight, flocculation efficiency decreases, which is attributed to steric repulsion between polymer molecules. On the other hand, molecular weight effects are less well defined in systems where the electrostatic patch mechanism is rate controlling. Optimum flocculant concentration has been found to be independent of molecular weight but dependent on ionic strength. Adachi et al. [290] observed the rate of initial flocculation of polystyrene latex to be remarkably enhanced by the addition of polyelectrolytes, but the extent of this enhancement decreased with an increase in ionic strength. Equally important is the configuration of the solvated polymer, particularly in bridging flocculation. Molecular effects are more apparent when the polymer has a rod-like character.

Overall molecular weight is not the only criterion for effective flocculation, since two products with the same apparent molecular weight may have different molecular weight distributions.

2.13.2. Effect of Polymer Dosage, Critical Concentration and Optimum Dose

The flocculation performance of flocculants primarily lies on the types of flocculants, their molecular weight [291], ionic nature, content [292,293], on the suspended solid content [294] in the waste water and the type of waste water [295] etc.

However the shape of the polymer chain in solution mainly depends on the conformation of the polymer in solution for a given polymer-solvent system. In other words, the concentration could alter the chain shape, and further result in changing the solution properties [296,297], its function [298,299] and even the solid properties [300,301] and its polymer solution. Moreover, the changing in solution properties is not linear with concentration; thus several critical concentrations [302-306] exist from extremely dilute solution to concentrated solution.

One of the most important critical concentration C^* is introduced by Gennes [307], at which the polymer coils start to develop. At $C < C^*$, polymer chains are isolated or with some intra-chain interaction, when $C \geq C^*$, the polymer coils start to contact and inter-chain interaction occurs. Some of the solution properties like viscosity are apparently different in this region. Critical concentration is generally defined as follows:

$$C^* = \frac{3M}{4\pi N_A R_G^3}$$

Where N_A , M and R_G are the Avogadro Constant, molecular weight and the radius of gyration, respectively. Using the Fox-Flory equation,

$$[\eta] = \frac{\phi' R_G^3}{M}$$

Here, $[\eta]$ is intrinsic viscosity, $[\phi'] = 6^{3/2} \phi$ and $\phi = 2.5 \times 10^{23}$ (ml/g), we have:

$$C^* = \frac{1.23}{[\eta]}$$

In general [308], the value of C^* can be approximately written as:

$$C^* = \frac{1}{[\eta]}$$

It means that C^* is inversely proportional to the intrinsic viscosity $[\eta]$, which represents the chain dimension or the segment density of the chain coil.

Experimental results showed that flocculation rate from a given system cannot be increased beyond a certain dose, called the optimum dose (C_{od}) of the polymer and further addition results in decreased efficiency. It has been suggested that [309,310] optimum flocculation occurs when half of the surface area of the solid particle is covered with the flocculants.

Optimum dose cannot be easily predicted since they are known to be varying not only with ionic character and degree, but also with molecular weight. Optimum dosages increased with increase in molecular weight, and the settling rate achieved will be higher.

Even though it is not easy to predict the optimum dose, Qian et al. [311] have given a theoretical approach to relate the optimum dose and critical concentration of the polymer for a given concentration of suspended solids (C_{ss}) in a given system. According to them, a linear relationship between C_{od} and $(C^* \cdot C_{ss})^{0.5}$ is obtained, and could be expressed as follow:

$$C_{ad} = 5763.9(C^* \cdot C_{ss})^{0.5} - 4.2$$

The degree of flocculation achieved can be markedly affected by dose and the mixing [312-314] conditions. Flocculation in a given system cannot be increased beyond a certain optimum dosage of polyelectrolyte, and further additions result in decreased efficiency. It has been found [315] that for high solids concentrations and relatively low polymer doses, flocculation occurs rapidly, but the flocs are not stable and can break at moderate stirring rates. By reducing the rate of stirring shortly after polymer dosing, floc size (and settling rate) can be held at plateau levels, without subsequent decline. It has been suggested that [316,317] optimum flocculation occurs when half the area of solid is covered with polyelectrolytes. At higher concentration, the degree of flocculation decreases and the particles may be completely covered by the absorbed polymer layer. Thus overdosing can be a serious mistake in that it may create a well established suspension that is extremely difficult to separate. But in principle, a substantial degree of flocculation can be obtained with much lower polymer dosage than is usually required. Hydrodynamic factors [318,319] arising from mechanical agitation play a significant role in flocculant adsorption. Vigorous agitation of flocculating

suspension causes floc breakage and the exposure of fresh surfaces to polymer adsorption thereby increasing adsorption capacity. At the same time, increased agitation leads to the production of smaller flocs, indicating that enhanced adsorption does not compensate for increased floc breakage. In fact, the general rule seems that the actual amount adsorbed varies inversely with the extent of flocculation.

2.13.3 Conformation of Polyelectrolyte in Solution

It was observed [320] that, in the flocculation of clays by two high molecular weight PAMs of different degrees of hydrolysis, the high molecular weight with 30 % hydrolyzed polymer will perform better. The flocculation performance diminishes beyond an optimum concentration, which can be explained by bridging mechanism. The higher molecular weight polymers can adsorb in configurations with loops of greater length extending from particle surface, increasing collision probability. Particles bridged by 30 % hydrolyzed polymer perform better because the charge not only affects the particle-polymer interaction but also causes an extension of the solvated polymer chain. At 30 % hydrolysis, a balance is reached between the effects of like charge repulsive forces of the polymer and the particle surface. The concentration effects are due to the need for vacant surface sites on which a bridging polymer can adsorb. In a similar study Yu et al. [321] have established that polymer conformational changes have a beneficial effect on the flocculation of alumina [322].

2.13.4 Solution Properties

2.13.4.1 Effect of Ionic Strength

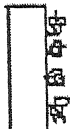



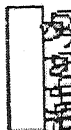

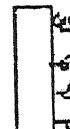
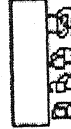

The configuration of polyelectrolytes in solution is significantly affected by ionic strength and this affects flocculation. This is indicated by the increased viscosity of a polyelectrolyte solution as ionic strength decreases. Similar charges on the polymer chain tend to expand the chain as a result of mutual charge repulsion. As ionic strength increases, these charged sites are shielded and allow the polymer to fold and assume a smaller hydrodynamic volume, as indicated by a decrease in solution viscosity. These effects manifest themselves in the flocculation mechanism. In a high solids system to be flocculated by a high molecular weight charged polymer, decreasing ionic strength expands the polymer in solution and enhances bridging by increasing the effective particle radius. In systems where the electrostatic patch mechanism predominates, the effect of ionic strength is less well understood. On the other

hand, when charge-neutralization mechanism is operative the effect of ionic strength is realized through double layer compression in systems where flocculant and surface are oppositely charged.

2.13.4.2 Effect of pH

The pH of the pulp determines the surface charge. With inorganic flocculants, the effective species can be a solvated metal ion, which affect flocculation through double-layer compression and Schulze-Hardy effects. With increase in pH, these species become charged and the mechanism of action changes. When the colloids are hydrophilic, e.g. humic acids, pH affects protonation. In presence of ionizable acidic or basic groups, colloid surface charge is affected by pH changes. In organic polymer flocculation, pH can affect polymer activity and the mechanism. The pH also controls the degree of ionization of the polymer and, therefore, varies the amount of charge on the polymer chain. This determines the degree of extension of the molecule and affects the degree of bridging. Therefore, flocculants can only function over a certain pH range. A schematic representation of the effect of solution pH on the conformation of the polymeric flocculants is given in Table 2.1.

Table 2.1 Schematic representation of the conformational state of adsorbed polymer at different pH [323].

pH	Non Ionic	Anionic	Cationic
2.3			
6.4			
10.95			

The table is showing that at lower pH the non-ionic polymer chains coils up and showed lower flocculation efficiency. With increase in pH of the medium, the polymer chains stretched. This conformation favours polymer bridging.

Anionic flocculants showed most coiled conformation when the solution pH is very low but it stretched when the solution pH increases.

Cationic polymers showed just the opposite behaviour. They show most coiled conformation at higher pH value but at lower pH value the polymer chains stretched to a considerable extent.

2.13.4.3 Effect of Particle Size

The importance of particle size variation with regard to flocculation has been investigated by many researchers [324]. Moudgil et al. [325] have reported that there exists a strong correlation between aggregation of a given size and the molecular weight of the flocculant. They have explained the correlation between particle size and flocculant molecular weight in terms of floc formation forces provided by polymer bridging and floc-breaking forces (e.g. turbulence) encountered in an agitated system. In a similar report Mishra et al. [326] have reported the decreasing settling rate of coal suspensions with decreased particle size. This has been attributed to an increase in surface area that decreases the charge neutralization capacity of the coal surface by the flocculant.

2.13.4.4 Effect of Temperature

It is generally thought that an increase in temperature improves flocculation, although this is not always the case. A change in temperature will exert different effects on different systems. The rate of diffusion of flocculant and the rate of collision of particles increases with a rise in temperature. But the adsorption step, which is exothermic, must be unfavorably affected by higher temperature. The linear extension of the polymer molecules may vary with change in temperature depending on the nature of the solvent-solute interactions. Thus, it is difficult to accurately predict the effect of temperature in a given system.

2.14 APPLICATIONS OF FLOCCULANT

2.14.1 Water Clarification

Flocculants are used for clarification of potable and industrial process water. Their principal function is the removal of suspended solids, which cause turbidity. The flocculants are also used in gravity separation and flotation processes for industrial and municipal water clarification. For waste-water, containing mainly inorganic compounds, anionic flocculants are preferred whereas for organic compounds cationic flocculants are most often applied. Polymeric flocculants are employed for waste-water treatment in the metals, chemicals, pulp and paper, food processing, petroleum refining and textile industries. Zemaitaitiene et al. [327] reported the role of anionic substances in removal of textile dyes from solution using cationic flocculant. Zhong et al. [328] studied the treatment of oily wastewater using flocculation and ceramic membrane filtration.

2.14.2 Paper Making

In the process of production of paper from wood and pulp, fillers such as clays, titanium dioxide, calcium carbonate etc. are used to provide opacity and whiteness to paper. However, a significant percentage of the fillers added as well as fibre fines may be lost during draining of the wet paper web. The loss of valuable fillers and fines during drainage is significantly reduced by addition of flocculants, the type of which is dependent on the history of the pulp. Both alum and cationic polymers are used to neutralize the negative paper fibres. Because the alum forms small, easily sheared flocs, it may be used in conjunction with a high or ultrahigh molecular weight cationic or anionic polymer. Starch and cationic starch also function as flocculants when added to fibre slurry to increase the wet strength. An additional benefit of using the flocculants as retention aids in paper industry is that, the residual polymer left in the stream is very effective in clarifying the "white effluent" formed in the process. Cationic starches are widely used as wet-end additives in paper making [329]. Whipple et al. [330] reported the adsorption characteristics of a fluorescent cationic poly (acrylamide) flocculant to clean fibre.

2.14.3 Mineral Processing

In all mining operations, solids and liquids must be separated, which can be facilitated by flocculants in the thickening of froth flotation, concentration and clarification steps. In most mineral processing, the suspended fines are impurities arising from crushing and grinding. They are separated as the solid phase rather than the mineral of interest, which remains in solution, coal being an exception. The coal industry is the largest user of flocculants. Both cationic and anionic flocculants [331] are used including some natural polymers. Cationic polymers are of quaternary ammonium type, e.g. poly (DADMAC) or polyamine especially in the recovery of coal. The principal anionic synthetic flocculants are poly (acrylamide-acrylate) copolymers although nonionic PAM is also utilized. Among natural polymers used are starch, GG, animal glue, lignin (sulfonate) etc.

2.14.4 Selective Flocculation

One of the applications that have shown considerable promise in the beneficiation of mineral fines is selective flocculation [332-335]. This process involves flocculating particles of one type from a well-dispersed suspension of the ore or mixture, followed by separating the flocs by either froth flotation or sedimentation. Selective flocculation, like flotation, takes advantages of the differences in the physico-chemical properties. But unlike flotation, flocculation does not depend entirely on the wettability characteristics of the particle surfaces. The selective flocculation involves three steps: (i) dispersing the fine particles, (ii) selectively adsorbing the polymer on the active component (flocculating particles of interest) and forming flocs, and (iii) separating the flocs. The major applications of selective flocculation have been in mineral processing but many potential uses exist in biological and other colloidal systems [334]. These include purification of ceramic powders, separating hazardous solids from chemical wastes and removal of deleterious components from paper pulp [336]. Industrial applicability of this process has so far been limited, e.g. processing of taconite and potash ores; because results obtained by selectively flocculating natural ores or complex synthetic mixtures often do not correlate with the selectivity observed in single component systems. Selective flocculation of desired fraction has become an active area of research in the field of flocculation [337-340].

A critical review on iron oxide/quartz separation using starch and poly acrylic acid indicates starch to be a more selective agent [341]. The presence of clays, particularly montmorillonite,

is known to have a detrimental effect on the selectivity of separation. To prevent heterocoagulation, sodium silicate is to be added. Ravisankar et al. [342] attempted selective flocculation of iron oxide-kaolin mixtures using a modified PAM flocculant containing hydroxamate functional groups.

Flourapatite, the phosphate fertilizer mineral, occurs in nature in association with silicate and carbonate minerals. During flotation separation of apatite, a significant proportion of P_2O_5 value is lost in the form of slimes. Selective flocculation appears to be promising for recovering the fine phosphate values. Pradip et al. [343,344] have successfully examined the feasibility of selective flocculation of tribasic calcium phosphate using hydrolyzed PAM and poly (acrylic acid) flocculants. Xiao et al. [345] developed organo-modified cationic silica nanoparticles/anionic polymer as flocculants. The synergistic effect of flocculation of cationic polymer microparticles and anionic polymer on fine clay has been reported [346]. Petzold et al. [347,348] studied interaction between the oppositely charged polyelectrolytes poly (dimethyldiallylammonium chloride) (PDMDAAC) and poly (maleic acid-co- α -methyl styrene) (P (MS- α -MeSty)) as flocculants in the presence of cellulose or a mixture of cellulose and clay.

2.15 PARTIAL ALKYLALYNE HYDROLYSIS

The partially hydrolyzed grafted copolymers were prepared by treatment with alkali. The use of alkali hydrolyzed the amide end groups to carboxylate groups. As the carboxylate groups are negatively charged they repel each other thus gives an extension of the chain. These extended chains can penetrate the double layer and can approach the particle surface close enough prior to effective adsorption.

But in experimental condition both of the polymer chain and the particles are negatively charged (as seen by their Zeta Potential). So, for an effective adsorption to occur between the polymer and the particle there must be some other mechanism rather than the electrostatic attraction. Observation [349-351] with iron oxide showed that it is the chemical groups and architecture of the macromolecules and their interaction with the metals oxides of the particles, which plays the important role for adsorption. A variety of studies showed that the anionic polymers were adsorbed at metal oxide surfaces [352,353] Vermöhlen et al. [354] found polyacrylic acid to co-ordinate with the surface of metal oxides using DRIFT spectroscopy and ab initio calculations. They concluded that the carboxylate oxygen of

polyacrylic acid bridges two Al^{3+} surface atoms in a ligand-exchanged inner sphere surface complex. Jones et al. [355] found polyacrylate to adsorb on iron oxide in an asymmetric bridging structure. The hydroxamate functional group also found to form complex with the metal ion (M) of the oxide surfaces [356-358]. A considerable amount of covalent character was found in the bond formed with the hydroxamate group compared with the ionic nature of the bond formed with carboxylate groups. When the polymer chain comes closer to the surface of the particle, the carboxylate group is believed to form a four membered ring or a complex with two metal oxides of the particles (**Figure 2.10**). Particles having higher Zeta Potential invite larger amount of polymer chains towards the surface. If the polymers have higher negative charges then they repel each other strongly. It is the attractive force between the particle and the polymer and the repulsive force among the polymer, which determines the fate of the flocculation performance. The detail of the synthesis, characterization and flocculation properties of the hydrolyzed graft copolymers are given in Chapter-V.

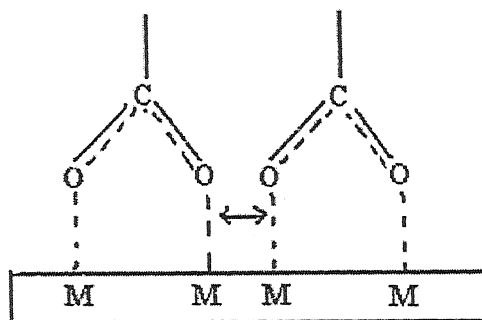


Figure 2.10 Schematic representation of anionic polymer-particle interaction

2.16. CATIONIZATION

The cationization of polymer provides a unique technique for modifying polymers to meet desirable end use requirements. The cationized polymers are of additional interest because of their potential use as viscosifier in enhanced oil recovery operations, as flocculants and in beneficiation and treatment of mining and wastewater sludges. An important advantage of cationic polymers is that the polymeric substrate or backbone polymer and the inserted cationic moiety are held together by chemical bonding allowing the two polymers to be intimately associated rather than as mere physical mixtures. The method of cationization of

polymer has been utilized as a special technique in the recent decades for synthesizing new class of polymeric materials by modifying the physical and chemical properties of synthetic and natural polymers. The mechanism for flocculation with cationized copolymers may be given as follows: It is well accepted that cationic polymers are adsorbed via coulombic interactions between the cationic groups on the polymer and the negative charged particle surface.

Durand Piana et al. [359] and Denoyel et al. [360] described the influence of charged density of polycation on the interaction with the particles. They reported that for a polymer having fixed molecular weight, the amount of adsorbed polymer decreases with increase in cationicity. Indeed they found that the time to reach equilibrium depends on the cationicity insofar as it took minimum time when cationicity is maximum.

Denoyel et al. [360] found that for adsorption of polycation onto particle surface the enthalpy of exchange for a cationic unit was, for a given molecular weight, particularly independent of the surface coverage. This is marked contrast to the behaviour of non-ionic polymers where the enthalpy has generally been found to decrease with surface coverage [361]. This contrast indicates that the chain conformation is largely independent of the surface coverage. They proposed that the polycation chains, which arrive when a significant portion of the surface is coated with polycation, might only be attached to the surface through a few cationic centers. All the above results suggests that the density of cationic groups on the clay surface increased rapidly with increase in cationicity upto a certain value at which the surface charge is completely saturated. As the cationicity increased, the dense packing of the chains on the surface was prevented by electrostatic repulsions and chain stiffness.

Durand Piana et al. [359] also suggested that if the cationicity of the polymer is very low then the bridging would be the major adsorption mechanism rather than the charge neutralization and for this case flocculation will depend on the polymer chain length because long chain can able to bridge more particles.

The flocculation of the suspended particles with cationic polymer can be represented schematically as follows: When both the polymers and the particles have higher charge, a stiffer extended conformation of polymer chain, which lies close to the surface with few loops and trains results with thin layer of polycations when the polymer loading is low (Figure 2.11, a). Here the flocculation is solely depends on the charge neutralization mechanism. But when the particles have lower surface charge, the polycations have fewer

contact points on the surface. Thus the adsorbed polymer layer is much thicker (Figure 2.11, b). When the particles have lower charge density and smaller size, the possibility of bridging is much higher (Figure 2.11, c).

For polycations having lower charge density than the particles, flocculation occurs through a new mechanism called "electrostatic patch mechanism" (Figure 2.12). This occurs when a polycation rich patch comes closer to an anionic patch.

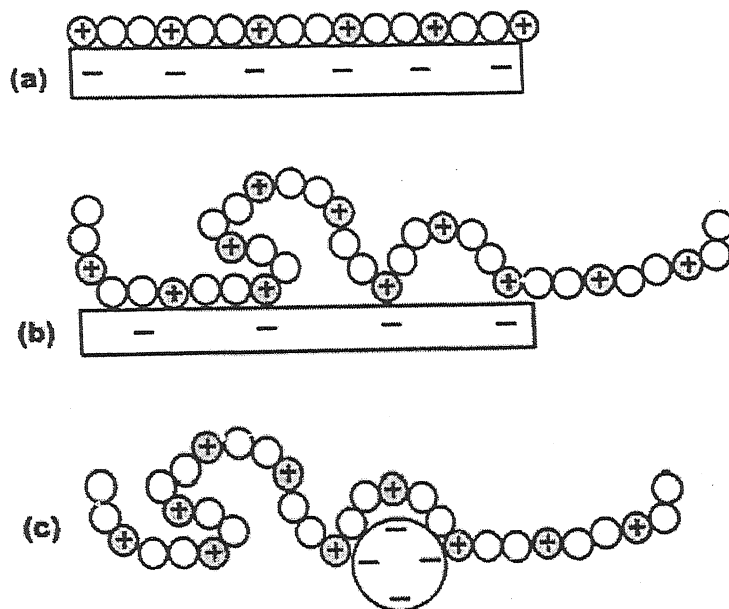


Figure 2.11 Schematic illustration of the adsorbed polycation conformation for (a) highly charged polycation on a highly charged anionic surface; (b) highly charged polycation on a surface of low anionic charge; (c) highly charged polycation on a small, negatively charged particle

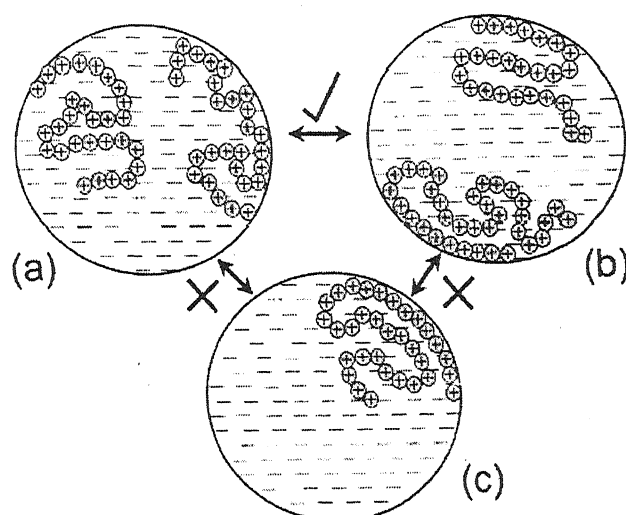


Figure 2.12 Schematic illustration of electrostatic patch flocculation mechanism.

Flocculation occurs when polycation-rich surfaces collide with polycation free surfaces

Water-soluble cationized polymers are a class of polyelectrolytes that derive their unique properties from the density and distribution of positive charges along the macromolecular backbone. These cationized polymers draw much attention in the field of wastewater and paper making process due to strong attraction with the negatively charged colloidal particles. A vast quantity of research effort has been directed towards the development of cationized polymer, the polysaccharide is the majority of them. The detail of the synthesis and properties are given in Chapter –VI.

2.17 SUMMARY

Chitosan is a biopolymer found in the exoskeleton of crustacean animals. It is cationic in nature due to the presence of amino groups. Chitosan is soluble in mild acid solution. The investigation was confined to the grafting of the PAM onto the backbone of chitosan by CAN as a redox initiator. So, throughout the literature review, the main emphasis is on the physiochemical properties of chitosan and different ways of synthesizing polysaccharide based graft copolymers. Upon this emphasis, this research study had attempted to find the flocculation performance of the graft copolymers. A portion of the literature review is dedicated to the flocculation and coagulation performance of natural and synthetic polymers. This chapter describes the properties of particles and critical polymer concentration to flocculate them. It also describes the parameters affecting the flocculation performance of the particles. This chapter also reviewed the flocculation performance of partially hydrolyzed graft copolymer and cationised polysaccharides.

CHAPTER-III

**SYNTHESIS AND
CHARACTERIZATION**

3.1 MATERIALS

Chitosan was a kind gift from Central Institute of Fisheries Technology, Cochin, India. Acrylamide was procured from E.Merck, Germany. CAN was obtained from Loba Chemie, Mumbai, India. Acetone and Hydroquinone were procured from S.D. Fine Chemicals, Mumbai. Kaolin was procured from B.D. Pharmaceuticals, Howrah, India. Iron ore was a gift from Joda Mines, India. Silica was obtained from Jyoti Chemicals, Mumbai, India. Bentonite was procured from Merck Limited, Worli, India. Chitosan and all the other chemicals were used as they were supplied without further purification.

3.2 SYNTHESIS

The chitosan based graft copolymers were synthesized by solution polymerization technique using ceric ion induced redox initiation method [56,362]. The entire reaction was carried out at room temperature. As oxygen inhibits the polymerization of the vinyl monomer, the grafting was performed in an inert atmosphere of N_2 . The details of the synthesis process are as follows:

First, 2 grams of supplied chitosan was poured into a reactor containing 200 ml of 1% aqueous acetic acid solution. It was then stirred for several hours (app: 4 hours) to get a clear solution. Calculated amount of acrylamide was then dissolved into 75 ml of distilled water and the solution was poured in the reactor containing chitosan solution. The reactants were mixed by continuous stirring. N_2 gas was purged through the mixture for about 25 minutes to remove the oxygen. At this stage, calculated amount of CAN was dissolved in 25 ml freshly prepared distilled water. The CAN solution was added to the reaction mixture without further delay. The mixture was again stirred for another 15 minutes. While stirring, N_2 gas purging was continued to remove even the last traces of oxygen. After 15 minutes of purging, the stirring was stopped and the reaction was allowed to continue for next 24 hours. Then saturated aqueous solution of hydroquinone was added to terminate the reaction. The mixture was then poured into a beaker containing 1000 ml of distilled water to produce homogenous slurry. The slurry was poured in excess of acetone to precipitate the product. The product was then kept overnight in acetone to assure that the last portion of the water was removed from the product. The product was filtered out and dried at controlled temperature ($60^{\circ}C$), in vacuum oven for 2 hours. Subsequently it was pulverized and sieved. In this similar way, all the grades were prepared. By varying the acrylamide and CAN concentration, seven grades

of chitosan based PAM graft copolymers were prepared (Chito-g-PAM1 to Chito-g-PAM7). The details of the synthesis parameters are summarized in **Table 3.1**.

Table 3.1 Synthesis details of the graft copolymers

Sl. No.	Polymer	Moles of MSU ^a	Acrylamide (mole)	Amount of CAN mole x 10 ³	% Conversion ^b	Intrinsic viscosity (dl/g)	Molecular weight ^c (M) X 10 ⁵ In 0.01(M) NaCl
I	Chito-g-PAM1	0.005	0.05	1.8	82.85	2.452	1.27
II	Chito-g-PAM2	0.005	0.10	1.8	86.31	3.021	1.7
III	Chito-g-PAM3	0.005	0.20	1.8	88.45	4.653	2.92
IV	Chito-g-PAM4	0.005	0.30	1.8	82.66	3.453	2.44
V	Chito-g-PAM5	0.005	0.20	0.126	84.26	5.625	4.07
VI	Chito-g-PAM6	0.005	0.20	0.090	89.88	8.09	6.77
VII	Chitp-g-PAM7	0.005	0.20	0.054	87.34	7.598	6.20

a. Calculated on the basis of Monosaccharide units (MSU)

b. % Conversion = [$\frac{\text{Wt. of graft copolymer}}{\text{Wt. of polysaccharides}} \times \frac{\text{Wt. of acrylamide monomer}}{100}$]

c. Viscosity average molecular weight

3.3 PURIFICATION OF THE GRAFT COPOLYMERS BY SOLVENT EXTRACTION

The extraction of the occluded polyacrylamide was carried out by solvent extraction using a mixture of formamide and acetic acid (1:1 by volume) solution [363] as given in **Figure 3.1**. The procedural details are as follows: 3 grams of grafted copolymer was taken in a 250 ml beaker. 100 ml of the prepared solvent was added to it. The mixture was kept at room temperature for around 12 hours. After that the mixture was filtered using Buchner funnel. The residue was washed with the same solvent mixture for ten times and every time, the filtrate was checked with acetone whether there was a precipitation of polyacrylamide or not. After which the polymer was again washed with acetone and kept into it for 24 hours to remove the solvent. The filtered polymer was then dried in vacuum oven.

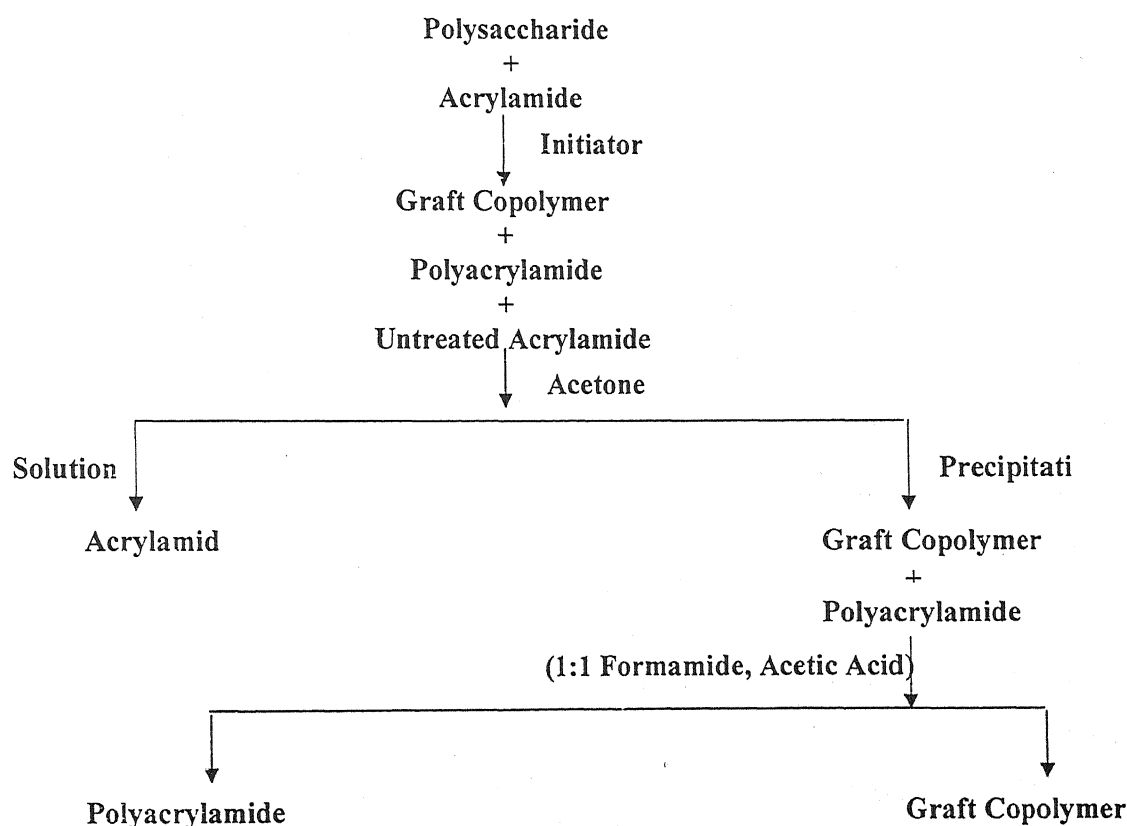


Figure 3.1 Schematic representation of the purification of the graft copolymer

3.4 CHARACTERIZATION OF THE GRAFT COPOLYMERS

3.4.1 Elemental Analysis

The elemental analysis of chitosan and all the graft copolymers was performed using a Carlo Erba 1108 Elemental Analyzer. The estimation of only three elements namely, carbon, hydrogen and nitrogen were undertaken.

3.4.2 Measurement of Intrinsic Viscosity

Viscosity measurement of polymer solutions was carried out with the help of Ubbelohde Viscometer (CS/S. 0.00386). Intrinsic viscosity of all the graft copolymers and chitosan was determined from the point of intersection of two extrapolated (to zero concentration) plots [364] i.e., inherent viscosity versus concentration (η_{inh} vs. C) and reduced viscosity versus concentration (η_{red} vs. C). For the measurement of intrinsic viscosity of chitosan and all the graft copolymers, 0.125 grams of the polymer was dissolved in freshly prepared distilled water with slow stirring at room temperature (33°C). 1% aqueous solution of acetic acid was also added to the mixture for complete dissolution. The resulting solution was taken and the volume was made up to 100 ml. This was the polymer stock solution. From the stock solution different concentrations of the polymer solutions were prepared. The capillary viscometer was properly cleaned with chromic acid solution and washed several times with tap water. Finally it was rinsed with freshly prepared distilled water. This cleaning method was repeated after each measurement and before taking a polymer solution of a different concentration into the viscometer. The viscometer was introduced into constant temperature bath (maintained at $30 \pm 0.1^{\circ}\text{C}$) and clamped to a stand to hold it vertically. About 25 ml of freshly prepared distilled water was introduced into the viscometer and the viscometer was kept into the bath for about 20 minutes so as to allow the distilled water to come to thermal equilibrium with the bath. The distilled water was suctioned into the upper bulb of the viscometer through the capillary and time of flow in between the two marks was noted. Three consecutive readings were noted before taking the average value. This was noted as t_0 , the time of flow of distilled water (solvent for the polymer). In the similar way, the time of flow of the polymer solutions at various concentrations were measured. The time of flow for the polymer solution was recorded as t ,

the time of flow of polymer solution at concentration C. The reduced viscosity and inherent viscosity were calculated by using the following equations.

$$\eta_{rel} = t/t_0$$

$$\eta_{sp} = \eta_{rel} - 1$$

$$\eta_{red} = \eta_{sp}/C$$

$$\eta_{inh} = (\ln \eta_{rel})/C .$$

The intrinsic viscosities of all the graft copolymers are reported in Table 3.1.

3.4.3 IR Spectroscopy

The IR spectra of chitosan, PAM and all the graft copolymers were recorded in solid state using KBr pellet. A Perkin-Elmer-630 IR spectrophotometer was used to record the spectra in the range of 4000-400 cm^{-1} wave numbers.

3.4.4 Thermal Analysis

DSC analysis of all the polymers was performed using Perkin Elmer, PYRIS, Diamond DSC (USA). TG and DTG analysis was done with Staton Redcroft (STA-625) Thermal Analyzer. The DSC, TG and DTG analysis was performed starting from room temperature at nitrogen atmosphere. A uniform heating rate, 10 $^{\circ}\text{C}/\text{min}$ was maintained in this experiment.

3.4.5 Scanning Electron Microscopy (SEM)

For SEM study of the polymer samples, JEOL, JSM-6360, SEM, (Model-7582) made in England was used. For this study, chitosan and all the graft copolymers were used in small granular forms.

3.4.6 X-ray Diffraction Analysis (XRD)

Chitosan and grafted chitosan were subjected for XRD analysis. A PW 1840 diffractometer and PW-1716 X-ray generator (Phillips, Holland) were used for this study producing $\text{CuK}\alpha$ radiation. The powdered polymer samples were packed into the hole of 2 mm diameter in a

small container made of Perspex about 1.5 mm thick. The scattering angle (2θ) was varied from 10 to 50 degree.

3.5 RESULTS AND DISCUSSION

3.5.1 Synthesis

The synthesis details of the graft copolymerization reaction based on chitosan and percentage of grafting are given in **Table 3.1**.

The synthesis parameters like, amount of acrylamide and CAN were varied in order to observe the effect with varying the number or length of the grafted PAM chains. Two series of graft copolymers, a total of seven grades of graft copolymers were synthesized by grafting acrylamide onto the chitosan backbone. In the first series (I-IV) the amount of chitosan and CAN were kept fixed. Only the acrylamide concentration was changed. In the second series (V-VII) the amount of chitosan and acrylamide were kept constant whereas the amount of CAN varied. The mechanism of ceric ion initiated reaction involves in the formation of chelate complexes [71]. CAN decomposes to generate free radical sites on the chitosan backbone [73,110]. The active free radical thus created reacts with acrylamide monomers and generate PAM side chains onto the backbone of chitosan. The average number of grafting sites per backbone molecule depends on the ratio of the concentration of the ceric ion to chitosan. Following a simplistic approach, a low concentration of initiator should initiate a few grafting sites resulting longer polyacrylamide chains as against a high concentration of initiator that will initiate a large number of grafted sites thus making the average polyacrylamide chains shorter for the same acrylamide concentration. This is reflected in the graft copolymers in the series (**Table 3.1**).

Table 3.1 shows that there is an increase in percentage of conversion upto a certain value of the increase in the monomer concentration. Thereafter, the percentage of conversion decreases with increase of monomer concentration. This may be attributed to the limited number of active centers available for grafting on the backbone and more monomer units competing for the same sites. The decrease in the percentage of conversion with an increase in monomer concentration indicates the termination reactions will be more favourable after the saturation of the grafting sites.

The table (**Table 3.1**) also indicates that with the increase of initiator concentration, the percentage of conversion increases upto a certain value then it decreases with further

increase in the initiator concentration. This may be attributed to the fact that at higher initiator concentration, the active sites for grafting increases onto the backbone of the chitosan molecules but at the same time some of the initiator could be used in the termination reactions thereby decreasing percentage of conversion.

It should be noted here that the chitosan powder is not dissolving in neutral water. It is dissolving only in dilute acidic solution (not in all acids). This solution can be kept in bottle for few months if the bottle is amber coloured. The effectiveness of chitosan as flocculant improves on storage. This may be attributed for the slow dissolution of the chitosan moieties accompanying the weakening of the association between the polymer chains.

Eromosele [365] described that the percentage of grafting increases with increase in acetic acid concentration between 0.5 % and 1 % and then the grafting yield decreases with increase in acetic acid concentration. The maximum percentage of grafting obtained when the chitosan is dissolved in 1 % acetic acid. The increase in the grafting yield with increase of acetic acid concentration (upto 1 %) may be due to the kinetics, which favours redox reaction between chitosan backbone and the monomer units. Further increase of the acetic acid concentration may be partially terminating the radical formation on the chitosan backbone, resulting in reduction of the graft yield.

It is well known that an amide moiety loses an equivalent of ammonia upon heating and is condensed to an imide. These intermolecular moieties will have larger agglomeration and they are resistant to solvents. This type of polymer solution may be less effective as a flocculant according to the bridging mechanism. PAM heated over 175 °C will undergo imidisation. Even drying at moderate temperature for prolonged time will initiate imidisation. So, to prevent all these problems, drying was undertaken at 60 °C for about 2 hours.

Elvan et al. [366] observed that even in the absence of monomer there was an increase in the mass of the chitosan. This effect must be due to the precipitation of the insoluble cerium salts in the medium. It should also be noted that chitosan has an affinity towards metal ions [19, 21]. It may be probable that some sort of complexation between chitosan and free ceric ions also occurs during grafting. They concluded that it is not possible to separate ceric ions from grafted chitosan, since their solubility behaviour is similar. So, there is always a possibility of unavoidable increase of viscosity of the graft copolymers even when they are in the storeroom.

3.5.2 Elemental Analysis

The results of elemental analysis of chitosan and the graft copolymers are given in Table 3.2. It was found that the percentage of nitrogen increases with increase in grafting. Among the graft copolymers, Chito-g-PAM6 and Chito-g-PAM4 have the highest percentage of nitrogen. Even though the content of nitrogen is same in both Chito-g-PAM4 and Chito-g-PAM6, the flocculation performance of Chito-g-PAM6 is better. This may be due to the PAM chain length. In Chito-g-PAM6, the length of PAM chain may be higher than that in Chito-g-PAM4. The higher intrinsic viscosity of Chito-g-PAM6 (Table 3.1) also indicates the longer chain length in Chito-g-PAM6.

Table 3.2 Elemental analysis of chitosan and grafted chitosan

Polymer	Carbon (%)	Hydrogen (%)	Nitrogen (%)
Chitosan	40.36	6.68	7.65
Chito-g-PAM4	41.60	7.09	16.22
Chito-g-PAM5	41.61	7.19	15.83
Chito-g-PAM6	41.58	7.32	16.22
Chito-g-PAM7	41.60	7.48	15.85

3.5.3 Intrinsic Viscosity

The intrinsic viscosity of a polymer is the measure of its hydrodynamic volume in solution, which in turn depends upon its molecular weight, structure and nature of the solvent and the temperature of the medium. Keeping the other factors constant, for two polymers of approximately similar molecular weight, a branch polymer will have lower hydrodynamic volume and hence lower intrinsic viscosity in comparison with its linear counterpart. Furthermore, along a series of branch copolymers the longer the branches are, the higher will be the intrinsic viscosity and vice-versa. This has been observed in practice.

The intrinsic viscosity of Chito-g-PAM4 to Chito-g-PAM6 increases with decrease in amount of CAN concentration (Table 3.1). This is due to the formation of very small number of active sites onto the backbone of the chitosan molecule. Acrylamide molecules

were only grafted at those active sites and the PAM side chain length increases. The increase in the PAM side chain length increases the hydrodynamic radius of the copolymer and this is the reason for the increase in the intrinsic viscosity of the graft copolymers from Chito-g-PAM4 to Chito-g-PAM6. The intrinsic viscosity of chitosan and PAM was found to be 31.668 dl/g and 6.269 dl/g respectively (in 0.01M NaCl solution). The higher intrinsic viscosity of chitosan is assumed to be due to the rigid backbone structure and lower solubility. The plot of intrinsic viscosity chitosan and PAM are shown in **Figure 3.2** and **Figure 3.3** respectively.

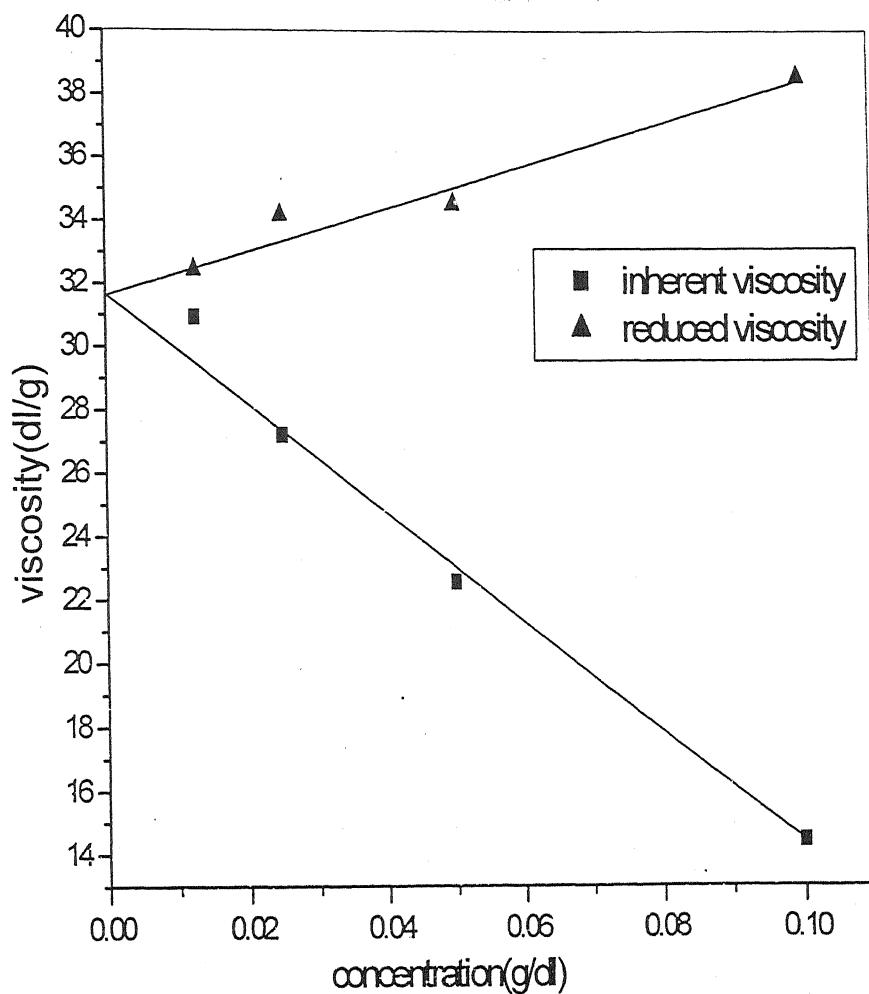


Figure 3.2 Variation of viscosity of chitosan with concentration

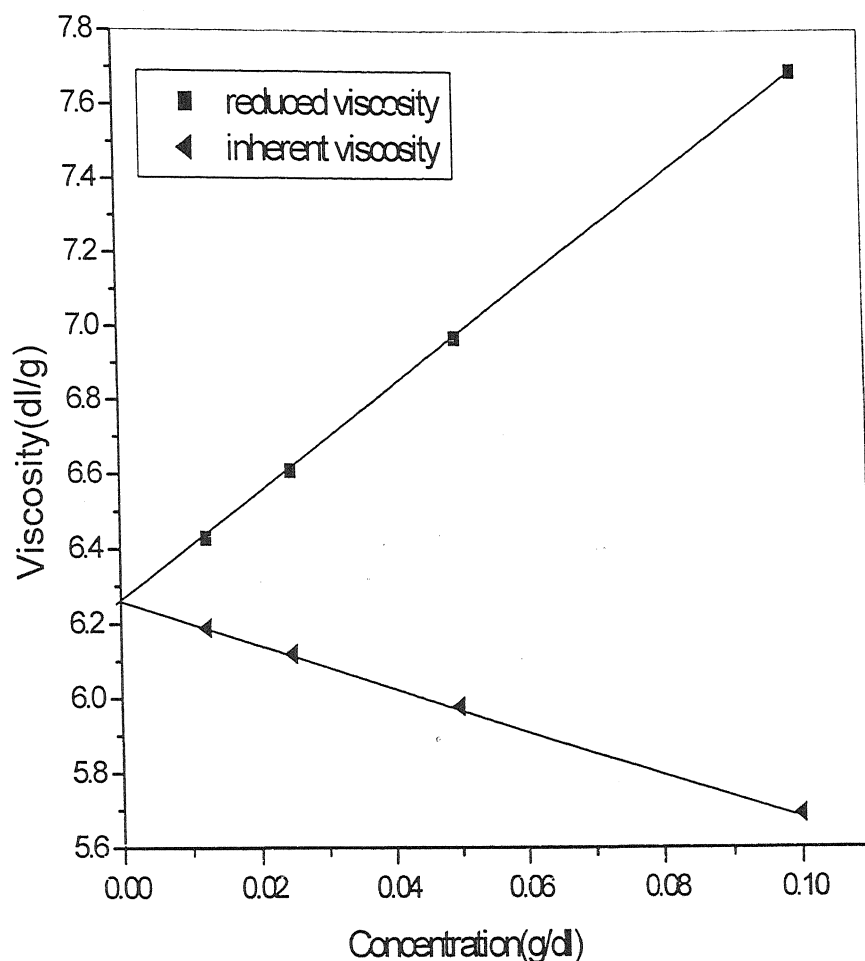


Figure 3.3 Variation of viscosity of PAM with concentration

3.5.4 Calculation of Approximate Molecular Weight

Molecular weight of the polymer samples can be estimated from the intrinsic viscosity $[\eta]$ value. The Mark-Houwink equation, $[\eta] = KM^\alpha$ is generally employed for the estimation of the molecular weight $[M]$ of the linear polymers. Where, K and α are constants for a given polymer/ solvent / temperature system.

For Polyacrylamide the value of K and α are given below [90-92].

$$[\eta] = 6.8 \times 10^{-4} (M_n)^{0.66}$$

$$[\eta] = 6.31 \times 10^{-5} (M_w)^{0.80}$$

Where M_n is the number average molecular weight and M_w is the weight average molecular weight.

Graft copolymers were synthesized following two steps. The first step is associated with opening of the chitosan ring and generation of free radicals at the ring opening sites. The second step is associated with the grafting of acrylamide monomers onto those free radicals so generated. The open ring structure imparts slight flexibility to the backbone. Moreover the percentage of polysaccharide in graft copolymer is small in comparison with the PAM. Hence in case of grafted polysaccharides; several workers [114,115] have used the Mark-Houwink equation to estimate approximate molecular weight, which is applicable for linear polymers. The same has been done in the present case. In the present calculation, the values of K and α have been taken from the second chapter (2.4.2). The approximate viscosity average molecular weights of the graft copolymers are given in **Table 3.1**.

3.5.5 IR Spectroscopy

The grafting of PAM onto the backbone of chitosan was confirmed by IR spectroscopy. The IR spectra of chitosan, PAM and product are shown in **Figures 3.4 -3.6**. **Figure 3.4** is showing the characteristic bands of O-H and N-H at 3429 cm^{-1} and 3292 cm^{-1} respectively. The broad pyranose ring characteristic band of chitosan is clearly observable in 1081 cm^{-1} region. The band at 2882 cm^{-1} is due to C-H stretching vibration. The presence of bands around 1420 cm^{-1} and 1381 cm^{-1} are assigned for $-\text{CH}_2$ scissoring and $-\text{O-H}$ bending vibrations respectively. The presence of a band at around 1033 cm^{-1} is due to the stretching of ether linkage ($-\text{CH}_2-\text{O}-\text{CH}_2-$).

In the IR spectra of PAM (**Figure 3.5**), a broad band at 3432 cm^{-1} is observed. This band is assigned for the N-H stretching of the NH_2 group. Two bands around 1691 cm^{-1} and 1642 cm^{-1} are due to amide-I (carbonyl group) and amide-II (NH bending). The bands around 1342 cm^{-1} and 2930 cm^{-1} are for the C-N and C-H stretching vibrations respectively. Other bands at 1450 cm^{-1} and 1320 cm^{-1} are attributed to CH_2 scissoring and CH_2 twisting respectively.

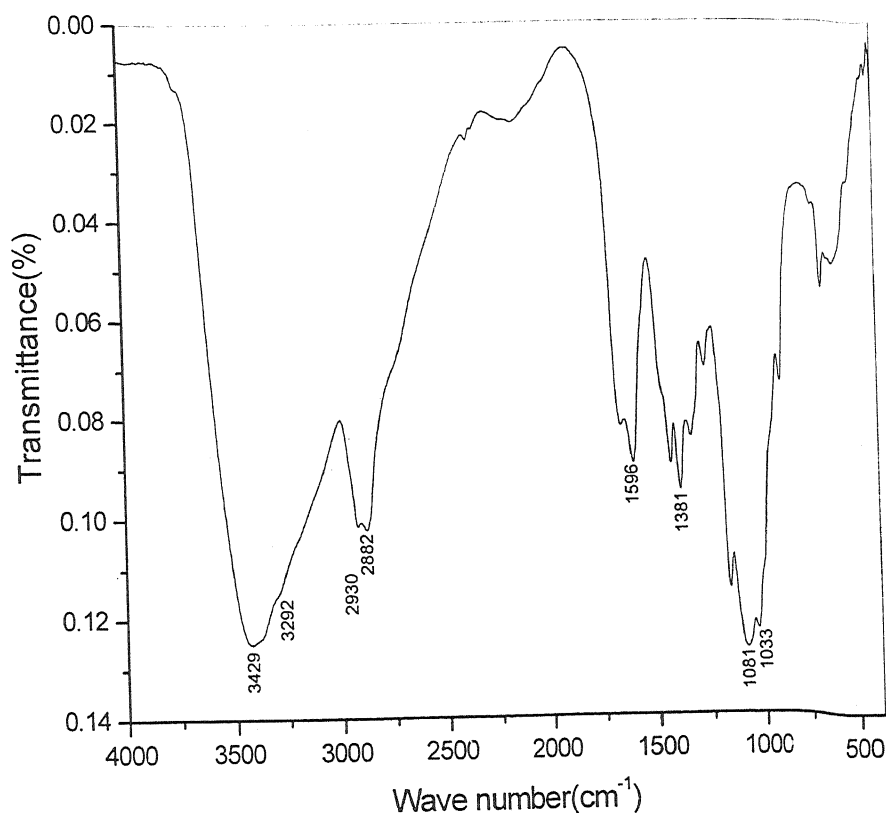


Figure 3.4 IR spectra of chitosan

Figure 3.6 shows the IR spectra of product. The presence of a broad absorption band at 3445 cm^{-1} is due to the overlapping of -O-H stretching band of chitosan and -N-H stretching band of the amide group of PAM. Two bands at around 1653 cm^{-1} and 1603 cm^{-1} are due to the amide-I and amide-II bending respectively.

The absence of a sharp absorption band around 3450 cm^{-1} indicates the absence of free -OH groups of chitosan, which probably is involved in some hydrogen bonding. The absorption frequency of -O-H is shifting from 3429 cm^{-1} in chitosan to 3445 cm^{-1} in product, which indicates more hydrogen bonding in product in comparison with chitosan. The ether linkage ($\text{-CH}_2\text{-O-CH}_2\text{-}$) band is observed at 1118 cm^{-1} . The presence of the above bands in the product is strong evidence of the grafting.

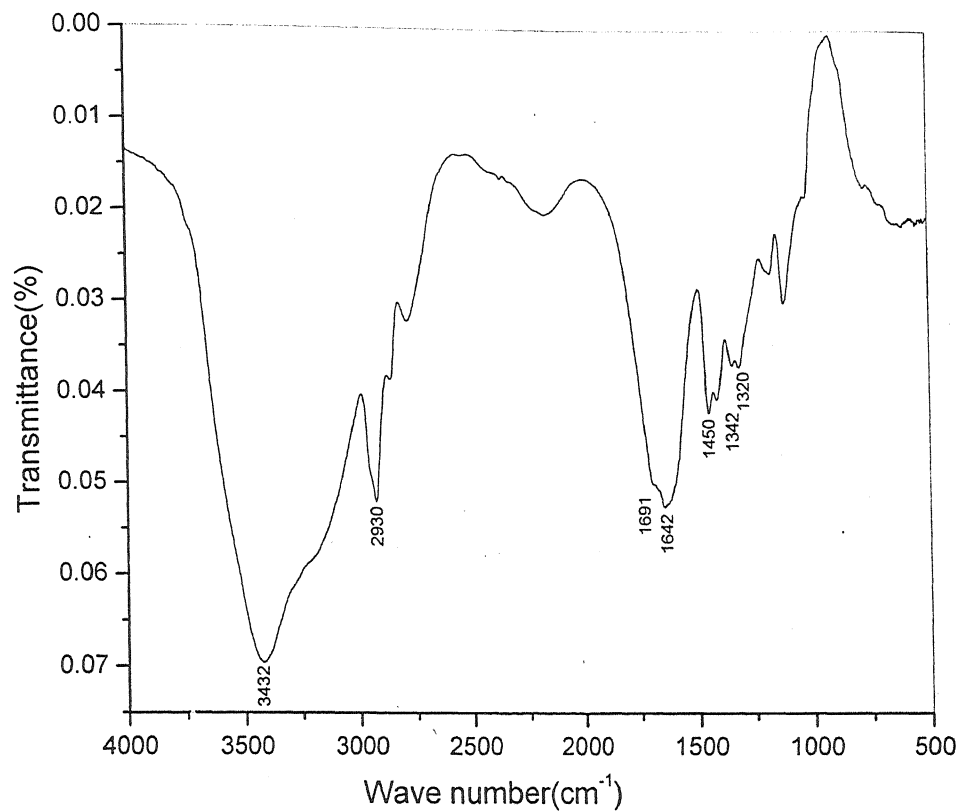


Figure 3.5 IR spectra of PAM

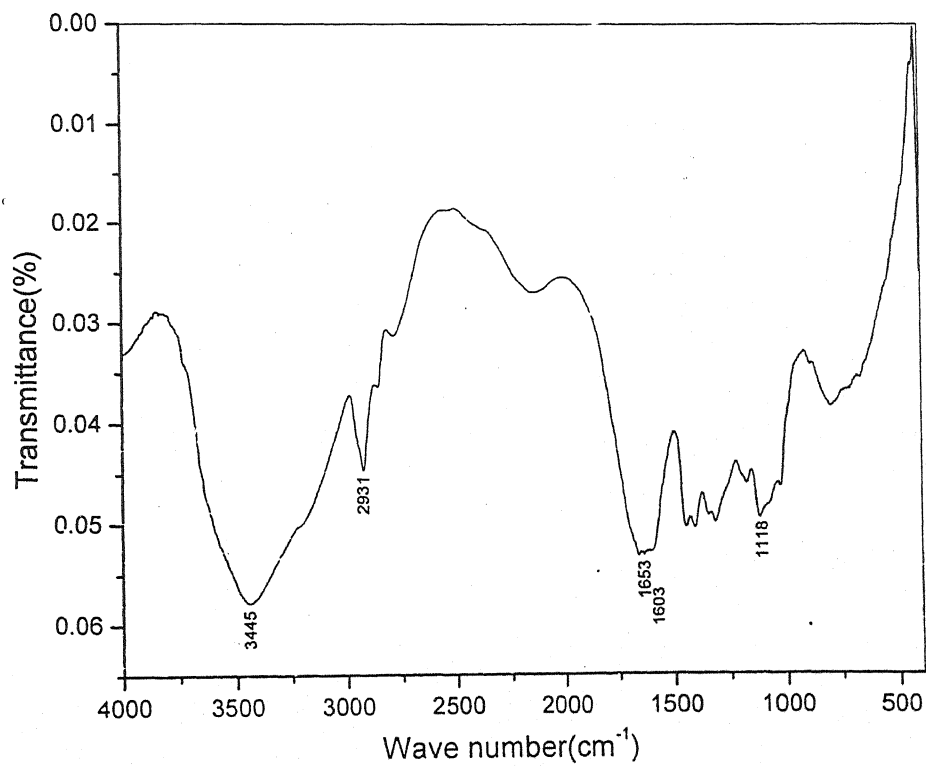
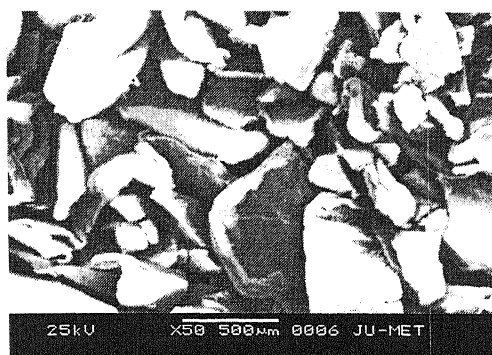


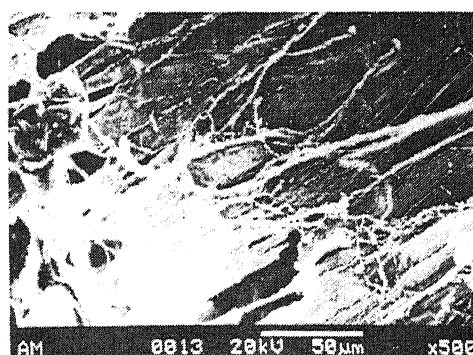
Figure 3.6 IR spectra of product

3.5.6 Scanning Electron Microscopy (SEM)

Figure 3.7 shows the SEM of chitosan; PAM and PAM grafted chitosan copolymer. The figure shows that the surface morphology of chitosan has been remarkably changed by the grafting of PAM onto the backbone of chitosan.



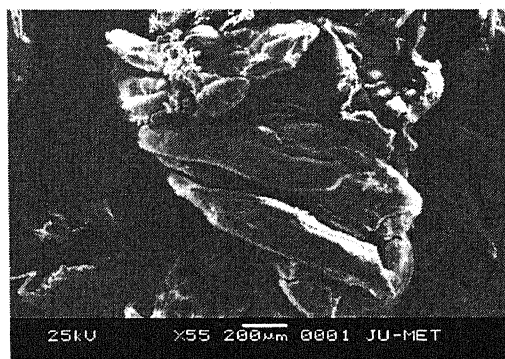
(a)



(b)



(c)



(d)

Figure 3.7 Scanning Electron Micrographs of (a) chitosan, (b) PAM and (c and d) grafted chitosan

3.5.7 Thermal Analysis

3.5.7.1 Differential Scanning Calorimetry (DSC)

The differential scanning calorimetric measurement (**Figure 3.8**) was done in nitrogen atmosphere. For chitosan the first thermal event registered in the sample was a wide endothermic peak centred at 125-147 °C with an onset at 70-117 °C. The onset of the endothermic peak may be related to pressure build up because of water evaporation inside the pans.

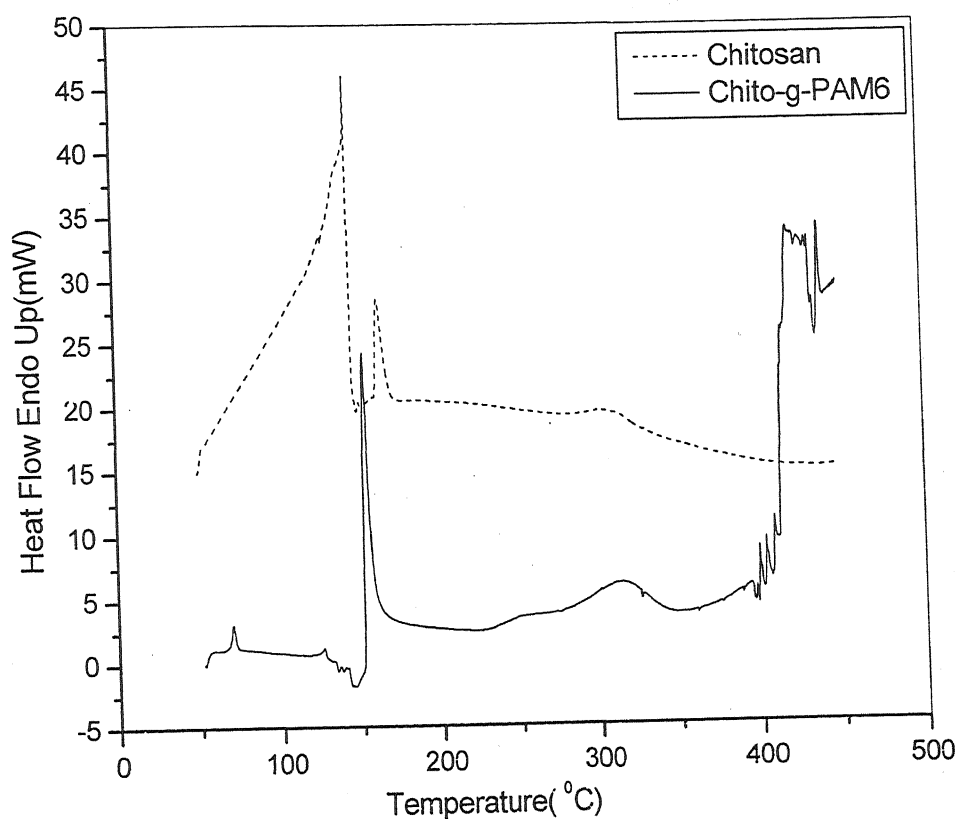


Figure 3.8 DSC curves of chitosan and Chito-g-PAM6

Polysaccharides usually having a strong affinity for water and in the solid state these macromolecules may have disordered structures, which can be easily hydrated. As is known, the hydration properties of these polysaccharides depend on the structures. Therefore, the endotherm related to the evaporation of water is expected to reflect the

physical and molecular change during N-deacetylation. There is a change in the slope appearing just before the endotherm. Pizzoli et al. [367] described that the origin of this transition was interpreted due to the local relaxation of the backbone chain of the polysaccharide. The endothermic peak at around 163°C is due to the evaporation of the bound water associated with the hydrophilic groups of the chitosan [367].

As for the Chito-g-PAM6, the endothermic peak shifted to higher value range depending on the length of the side chains. This could be attributed to the much stronger interaction between the water and the grafted chitosan chains, since the crystallinity of chitosan has been largely decreased after grafting. The endothermic peak at 162°C , which is seen in chitosan, is hidden under the broad endotherm in Chito-g-PAM6 copolymer.

A peak at 253°C is due to the loss of ammonia. It has been reported that PAM degrades in the temperature range of 175°C to 300°C by the formation of imide group via cyclization [368]. The peak at 390°C is for the decomposition of the cyclized imide groups.

3.5.7.2 Thermogravimetric Analysis (TG and DTG)

The TG curves of chitosan and Chito-g-PAM6 are shown in **Figures 3.9 and 3.10**. In case of chitosan, two distinct zones are observed where the weight is being lost. The initial weight loss starts at 34°C and continues upto 223°C , which is due to the loss of small amount of adsorbed and bound moisture in the sample. The second loss is due to the degradation of the chitosan and it will continue upto 409°C .

The Chito-g-PAM6 undergoes weight loss in three distinct stages. The first weight loss, which occurred between 34°C and 230°C , is due to the loss of adsorbed and bound water in the sample. There is nearly 10 % weight loss due to the liberation of water. The second weight loss starting from 230°C to 348°C with about 22.6 % weight loss is due to the degradation of the chitosan in the graft copolymer. The third loss, which continues upto 490°C with a weight loss of 71%, is due to the degradation of the polymer grafted by random chain scissoring.

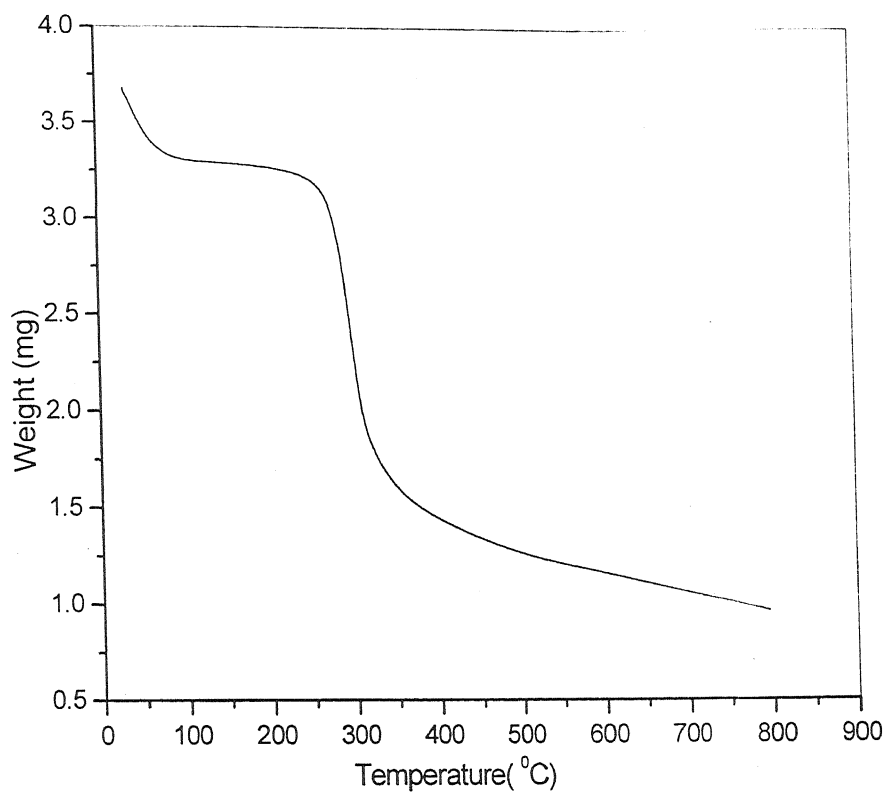


Figure 3.9 TG curve of chitosan

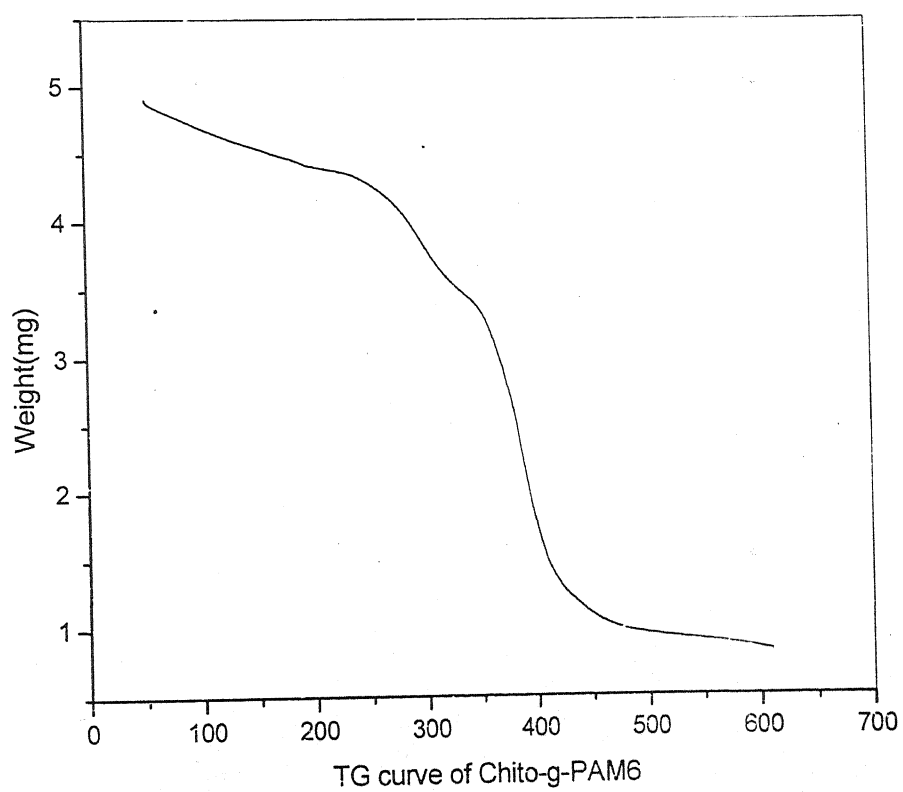


Figure 3.10 TG curve of Chito-g-PAM6

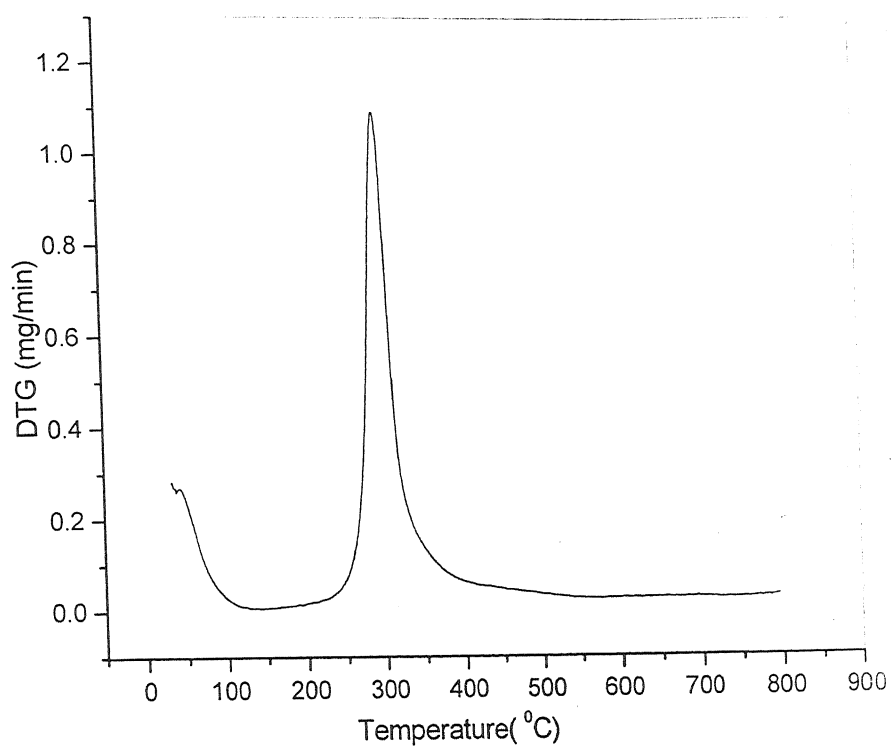


Figure 3.11 DTG curve of chitosan

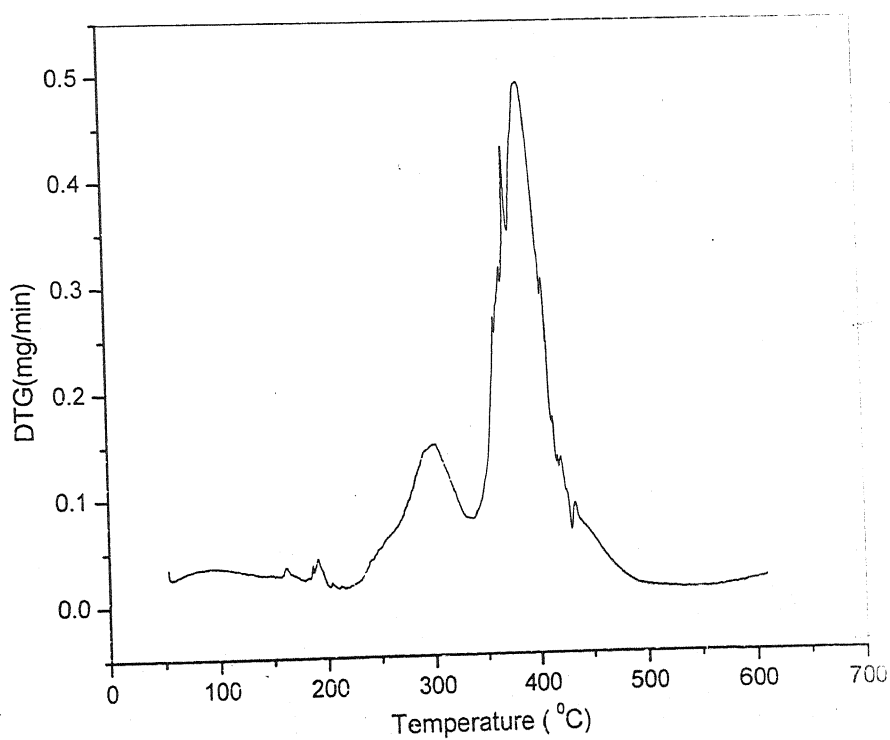


Figure 3.12 DTG curve of Chito-g-PAM6

Differential thermogravimetric analysis curves (Figures 3.11 and 3.12) shows the thermal decomposition behaviour of the two distinct polymers in details. The maximum decomposition temperature of chitosan appeared at 295°C , is ascribed to the dehydration of the polysaccharide rings and depolymerisation of the acetyl and deacetylated units of the polymer. The same decomposition peak is also observed in Chito-g-PAM6 copolymer with a little shift to the higher temperature. Another sharp peak in DTG curve of Chito-g-PAM6 at 387°C is attributed to the decomposition of the cyclized imide rings [264,266,373]. So it can be concluded from the above discussion that the Chito-g-PAM6 has higher thermal stability than the chitosan itself.

3.5.8 X-ray Diffraction

X-ray diffraction patterns of chitosan and Chito-g-PAM6 are described in Figures 3.12 and 3.13 respectively. The X-ray diffraction pattern shows a sharp peak at 24 degree which is attributed due to the crystallinity. The crystallinity decreases with the incorporation of the PAM into the backbone of the chitosan can be seen from the hump in X-ray diffraction pattern of Chito-g-PAM6 copolymer.

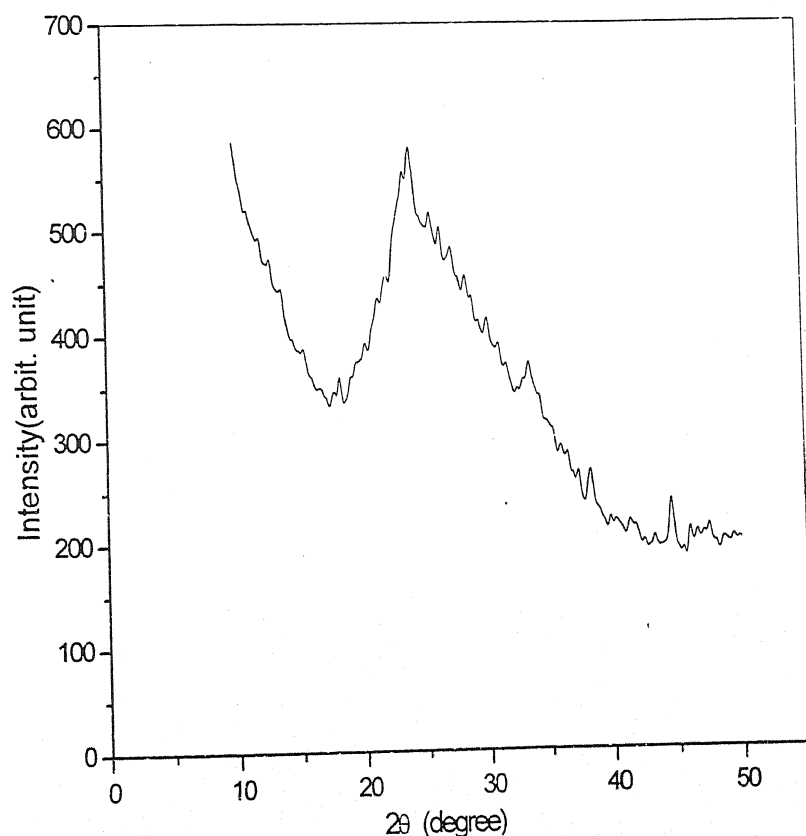


Figure 3.13 X-ray diffraction pattern of chitosan

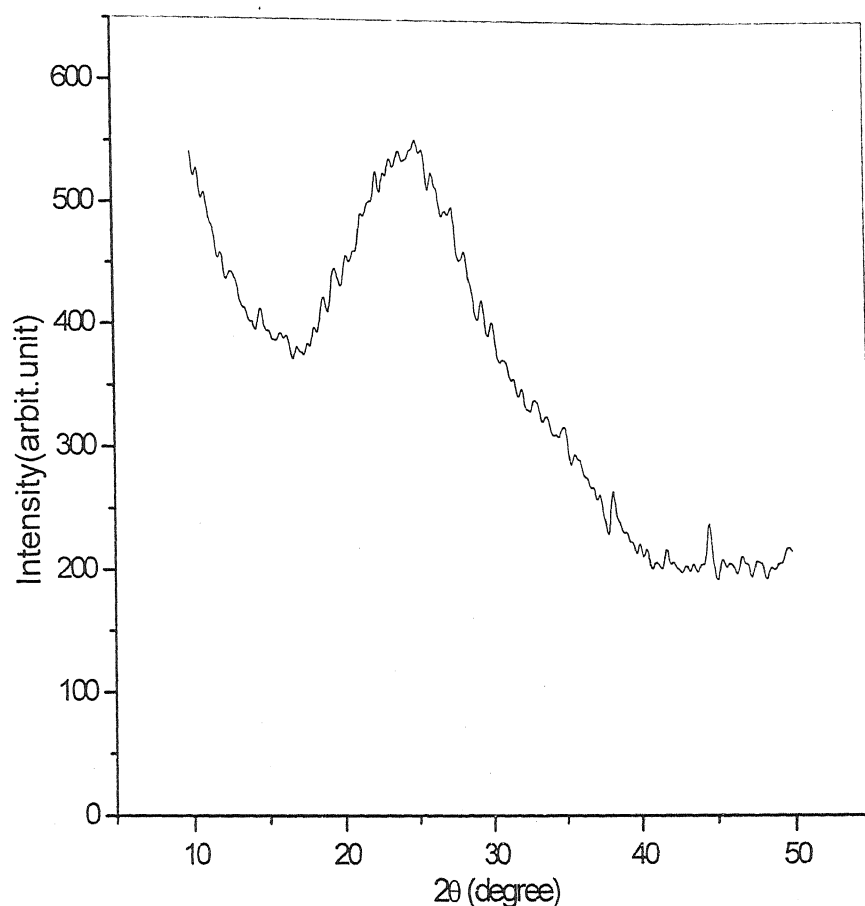


Figure 3.14 X-ray diffraction pattern of Chito-g-PAM6

3.6 SUMMARY

Through this chapter, the main emphasis is on the synthesis of a series of graft copolymers (Chito-g-PAM1–Chito-g-PAM7) and their characterization. PAM was grafted onto the backbone of chitosan. The grafting was confirmed by different material characterization techniques such as elemental analysis, IR spectroscopy, SEM, thermal analysis and XRD analysis. Elemental analysis shows that with the increase in acrylamide concentration, the percentage of nitrogen increases and reaches a maximum value. The intrinsic viscosity of Chito-g-PAM6 was found highest among all the graft copolymers. It indicates the higher hydrodynamic radius of the graft copolymers which is a proof of longest PAM side chain. Comparing the thermal stability of chitosan and Chito-g-PAM6, it was found that the thermal stability of graft copolymer is higher than the chitosan. The higher thermal stability

of the graft copolymer is due to the presence of the PAM chains. The PAM chains, upon heating, release ammonia and form imide rings. The X-ray diffraction pattern shows that grafting decreases the percentage of crystallinity. The decrease in crystallinity is due to the incorporation of the PAM chains, which breaks the intermolecular attraction among the chitosan molecules and also disturbs the regularity of chitosan chain due to random nature of PAM grafting onto the backbone of chitosan main chains.

CHAPTER-IV

**FLOCCULATION
STUDIES**

4.1 MATERIALS

Kaolin was supplied by B.D. Pharmaceuticals works, Howrah, India. Iron ore was obtained from Joda Mines, India. Silica was produced from Jyoto Chemicals, Mumbai, India. Bentonite was obtained from Marck limited, Worli, India. All the other chemicals used in this study were laboratory grades.

4.2 EXPERIMENTAL

4.2.1 Measurement of Zeta Potential

Zeta potential was measured by Particle Micro Electrophoresis (Apparatus Mark-II) made in England. The details of the procedure for the measurement are outlined below.

4.2.1.1 Measurement Procedure

Suspensions of fine solids were prepared by the dispersion of 50 grams of the samples in 100 ml of distilled water. The pH levels were adjusted by adding either hydrochloric acid or sodium hydroxide. The samples were then digested for few hours to get equilibrium. The clean liquid from the top of each beaker was poured into the cell and the electrodes were introduced into it. After switching on the illumination beam, its position was adjusted to illuminate the top of the surface of the sample cell. Then the illuminating object was moved until the particles were visible on the monitor screen. The time (t) taken by a particle to cross a grid was observed. The particles were timed successively in opposite direction (by changing the field of direction) on minimizing the polarization effect. It was usually considered necessary to time at least ten particles at each direction and take a mean velocity. Knowing the average value of t, under the applied voltage V, the Zeta potential is calculated. The sign of Zeta potential was governed by the direction of the movement of the particles with respect to the applied field. The formula of Zeta potential by which it can be measured is given in the literature section (Chapter-III). The results are shown in **Table 4.1**.

4.2.2 Measurement of Particle Size Distribution

Particle size distribution was measured on Malven 3601 Particle Size Analyzer, made in England. The particle analyzer works on the principle of laser diffraction. The particles were introduced to the analyzer beam in liquid dispersion in the sample cell. Particles were well dispersed ultrasonically. The scattered light fell on a special design detector, in the form of a

series of 31 concentric annular rings. The detector, provided with an electric output signal, proportional to the light energy measured over 31 separate solid angles of collection. The computer read the signal and performed the time averaging by successively reading the detector over a period of time set by the operator and summing the data. The computer gave the output in the form of a histogram and cumulative percentage of size distribution. The result is shown in **Table 4.2**.

Table 4.1 Zeta potential of the colloidal suspensions

Name of the Colloidal Suspension	pH	Zeta Potential (mV)
Kaolin	Neutral	-2.3
Iron Ore	Neutral	-38.0
Silica	Neutral	-51.98
Bentonite	Neutral	-50.1

Table 4.2 Average particle size of the colloidal suspensions

Name of the Colloidal Suspension	Average Particle size (nm)
Kaolin suspension	102
Iron ore suspension	700
Silica suspension	250
Bentonite suspension	220

4.2.3 Average Chemical Composition of the Colloidal Particles

The average chemical composition of kaolin, iron ore, silica and bentonite particles are given in Table 4.3.

Table 4.3 Average chemical composition of the colloidal particles

Particles	SiO ₂ (%)	Al ₂ O ₃ (%)	Fe ₂ O ₃ (%)
Kaolin	46.25	39.13	0.25
Iron ore	7.48	7.01	56.37
Silica	77.12	6.75	2.12
Bentonite	57.77	18.80	3.95

4.2.4 Scanning Electron Micrograph Analysis of Particles

The surface structure of all these particles used in this study were observed using SEM. **Figure 4.1(a, b)** shows the characteristics flaky nature of the kaolin particles. The sharp spikes are believed to be the collapsed structure of the typically layered cards found in kaolin particles.

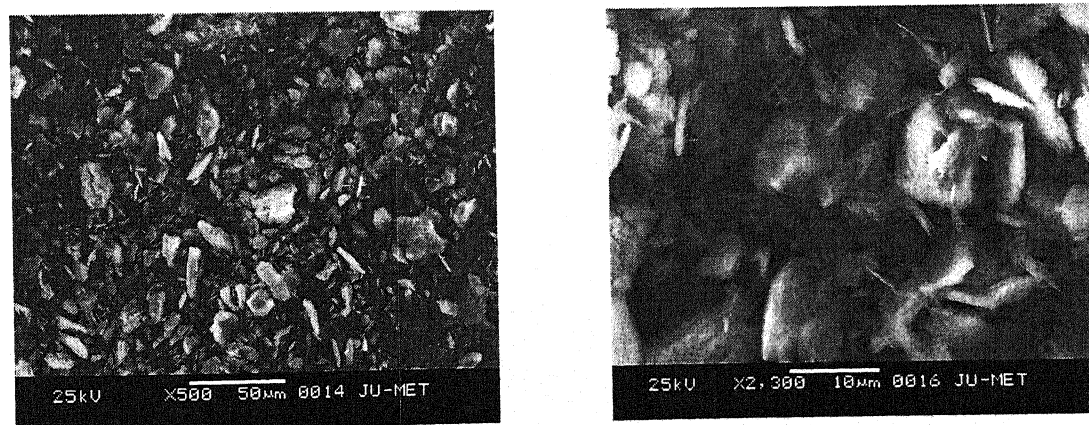


Figure 4.1(a, b) Scanning electron micrograph of kaolin powder

The iron ore has long-range particle size distribution. It can be easily seen from **Figure 4.1(c, d)**. In iron ore the adhesion of the small particles on large particles may be due to the hydrophobic attraction force and presence of moisture on the particle surface.

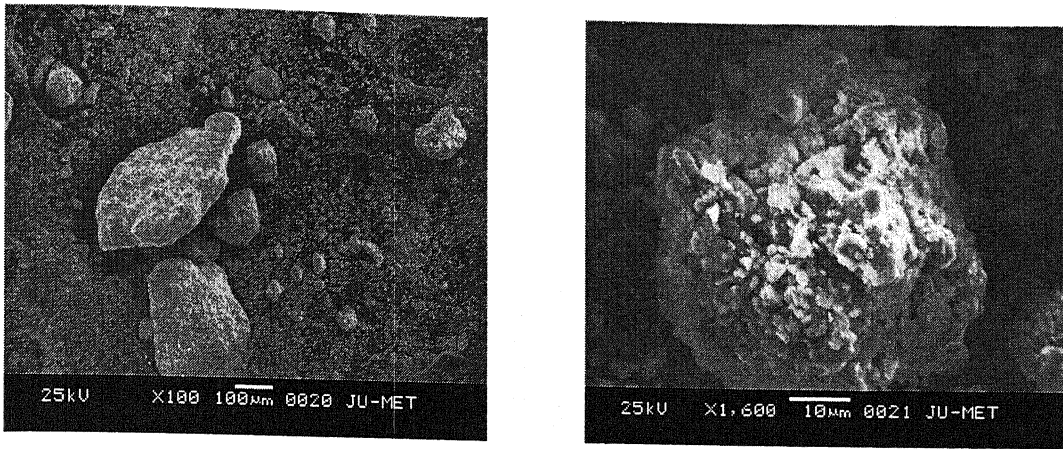


Figure 4.1 (c, d) Scanning electron micrograph of iron ore

The silica particles have irregular and broken structure. It has smooth surface texture, can be seen from the SEM micrograph (Figure 4.1 (e, f)).

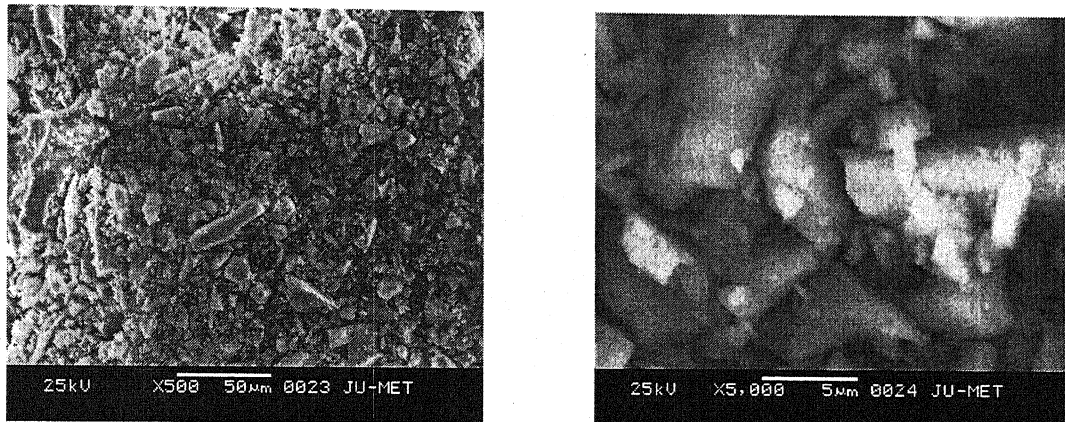
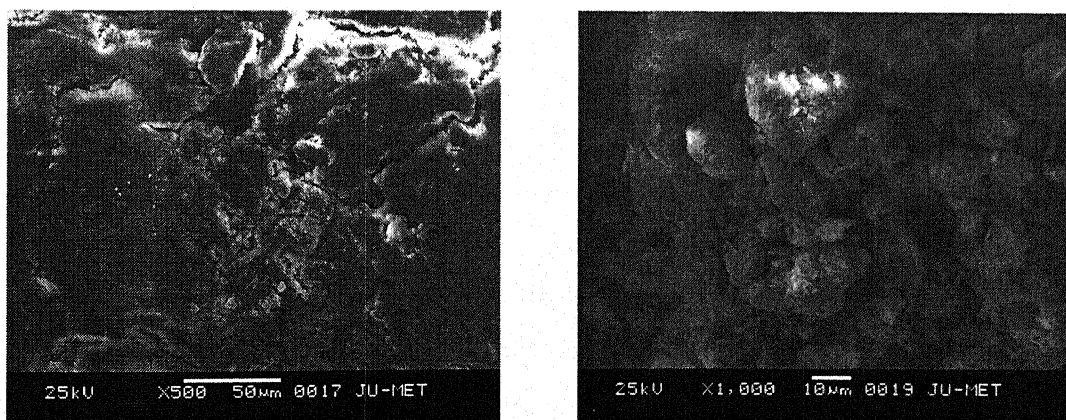


Figure 4.1 (e, f) Scanning electron micrograph of silica powder

Bentonite has spherical structure with small flakes attached to the big particles. This can be seen from the Figure 4.1(g, h, i).



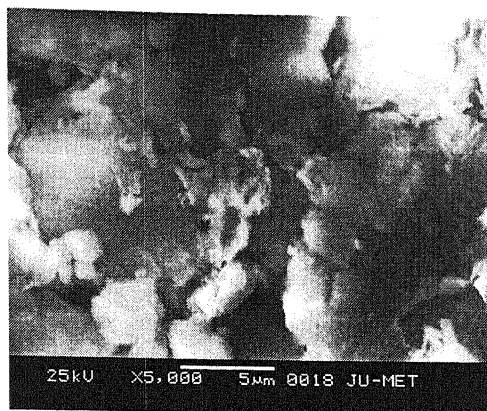


Figure 4.1 (g, h, i) Scanning electron micrograph of bentonite powder

4.2.5 Flocculation Studies

The flocculation characteristics of chitosan, PAM and all the graft copolymers were investigated using the column settling and jar test methods.

4.2.5.1 Settling Test

This test employs a 100 ml stoppered graduated cylinder and a stopwatch. First of all, the slurry sample is taken in the cylinder and then polymer solution is added to it. The cylinder is inverted 10 times for thorough mixing. After that the cylinder is set upright and the height of interface between water and settling solid bed is measured over time.

4.2.5.2 Jar Test

The flocculator was supplied by M.B. Flocculators, Mumbai, India. It consists of six pedals on a bench connected to each other by gear mechanism. All the pedals rotate simultaneously by a motor with the provision of speed control. The following procedure was adopted uniformly in all the cases. 400 cc of different effluent suspensions were taken in one-liter jars. The jars were placed on the flocculator bench dipping the stirrer blade in the suspensions. A polymer stock solution was prepared. From the stock solution, desired amount of polymer solution was added to each jar. Immediately after addition of polymers to all the jars, the mixtures were stirred at a constant high speed of 75 rpm for two minutes. This allows the polymers to mix properly with the suspensions. The mixtures were then stirred at a constant speed of 25 rpm for another five minutes. This allows the polymers to form flocs. The flocs were allowed to settle for next ten minutes. After that, supernatant liquid was

drawn from each of the jars and its turbidity was measured by digital Nephelo Turbidity Meter. The turbidity is expressed in Nephelo Turbidity Unit (NTU). The turbidity versus polymer dosage graph shows the flocculation efficiency of a particular polymer for a particular suspension.

4.2.6 Measurement of Supernatant Turbidity

Before measuring the turbidity of the test suspension, the turbidity meter is calibrated with the standard Formazin Suspension. Formazin polymer has been used as a reference turbidity standard suspension, because it is easy to prepare and its light scattering property is more reproducible than clay or turbid natural water.

The turbidity of the supernatant liquid was measured with a Systronics Digital Nephelo Turbidity Meter-132, supplied by Systronic, Ahmedabad, India. The principle of operation of the instrument is based on the well-known Tyndal Effect. A beam of light passing through a turbid liquid being tested scatters the light, which is collected at right angles by a photocell and is indicated on a digital display. The amount of scattered light is proportional to the turbidity of the solution under test.

4.2.6.1 Preparation of Stock Turbidity Suspension

One gram of hydrazine sulfate, $[(\text{NH}_2)_2\text{H}_2\text{SO}_4]$ was dissolved in 100 ml freshly prepared distilled water. 10 grams of hexamethylene tetramine, $[(\text{CH}_2)_6\text{N}_6]$ was dissolved in 100 ml of distilled water. 5 ml of each of the above solutions were taken in a 100 ml volumetric flask and the mixture was allowed to stand for 24 hours. The volume was made up 100 ml. This was a stock solution for 400 NTU.

4.2.6.2 Preparation of Standard Turbidity Suspension

10 ml of this turbidity suspension was diluted to 100 ml with distilled water. The turbidity of this suspension was defined as 40NTU.

4.2.6.3 Measurement Procedure

A. Calibration of the Turbidity Meter

The following procedure was used after installation of the instrument. The calibration was made for the range of 0-40 NTU.

- I. Calibration control was set to maximum.

- II. The measuring cell with distilled water was introduced into the cell holder and was covered with the light shield.
- III. The set zero controls were adjusted till the meter indicates zero reading.
- IV. The cell was removed and the distilled water was replaced with a standard solution of 40 NTU. Care has been taken to align the cell properly with the marking on the cell holder.
- V. The calibration control was now adjusted such that the turbidity of the standard solution (40 NTU here) was shown in the digital panel meter. This position of the calibration control was kept fixed for this range (0-40 NTU), unless a separate calibration was necessary for a different range (say, 0-100 NTU).
- VI. The instrument was ready for testing samples. Cell containing the unknown test sample was replaced and the reading was noted from the digital panel meter.

B. Measurement of Turbidity less than 40 NTU

For such test suspensions, the turbidity was directly noted from the instrument digital panel. Care was taken that suspension was free of bubbles.

C. Measurement of Turbidity above 40 NTU

For highly turbid suspensions, the samples were diluted with distilled water until turbidity values were reduced to less than 20 NTU.

The turbidity of the original suspension was computed from the turbidity of diluted sample and the dilute factor.

Calculation:

$$\text{Nephelometric Unit (NTU)} = \frac{a(a+b)}{c}$$

Where, a = NTU found in diluted sample.

b = Volume of dilution water in ml.

c = Sample volume taken for dilution in ml.

4.3 RESULTS AND DISCUSSION

4.3.1 The Settling Test Results

The settling test of chitosan, PAM and all grafted copolymers were carried out in four different suspensions namely, kaolin, iron ore, silica and bentonite. The flocculation performance of these suspensions has been studied at various concentrations for distinct observation. In each case the settling time was plotted against the height of interface. The flocculation performance of a particular polymer could be correlated with the settling velocity for a particular suspension. The greater the velocity of the floc containing particles, the better will be its flocculation performance.

4.3.1.1 Flocculation of the Kaolin Suspension

The flocculation performance of all the PAM grafted chitosan (Chito-g-PAM4 to Chito-g-PAM7) was studied in 3wt% kaolin suspension. The result was given in **Figure-4.2**. The optimal polymer dose for flocculation was calculated and it was taken 10 ppm. From the figure it can be clearly observed that Chito-g-PAM6 is showing better flocculation performance among all the graft copolymers.

Furthermore, the flocculation efficiency of Chito-g-PAM6 was compared with native chitosan and PAM solutions (**Figure-4.3**). It was observed that the flocculation efficiency of the graft copolymer is better than both the ungrafted chitosan and PAM solutions. This may be due to the dangling PAM side chains onto the backbone of chitosan. In case of graft copolymers the branches are able to come closer to the suspended particles in a better way as per Singh's Easy Approachability Model [14].

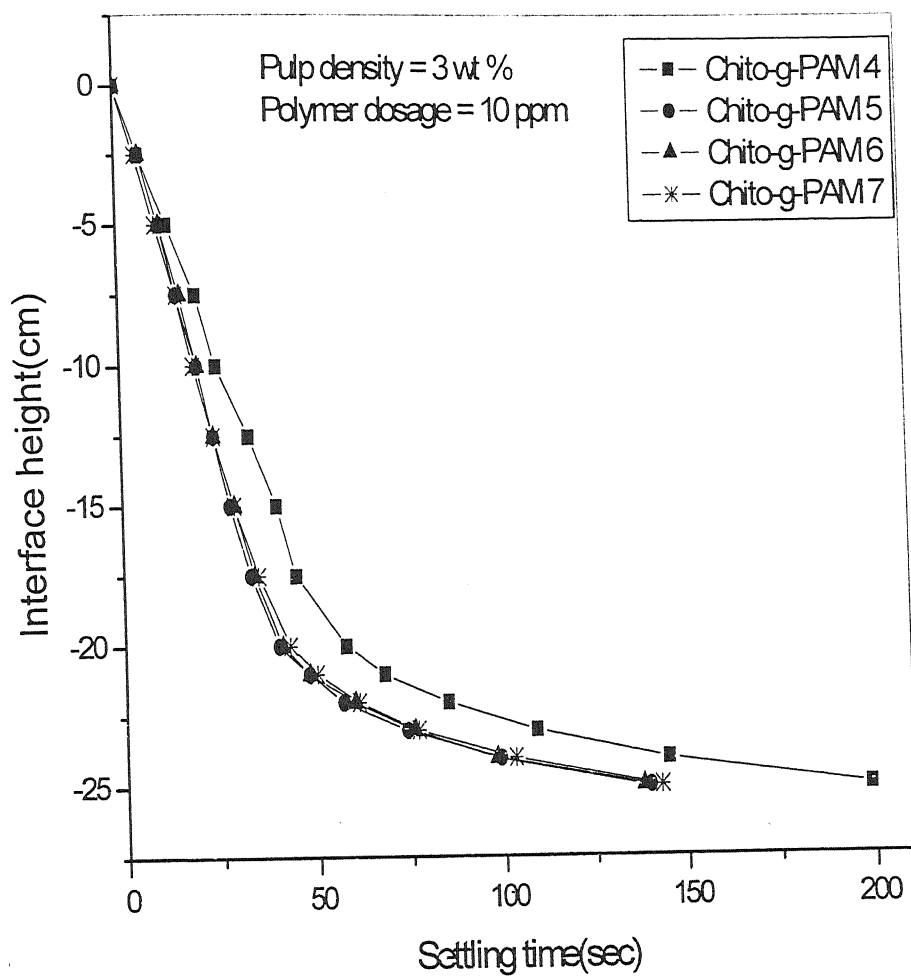


Figure 4.2 Settling curves for kaolin suspension with addition of PAM grafted chitosan copolymers

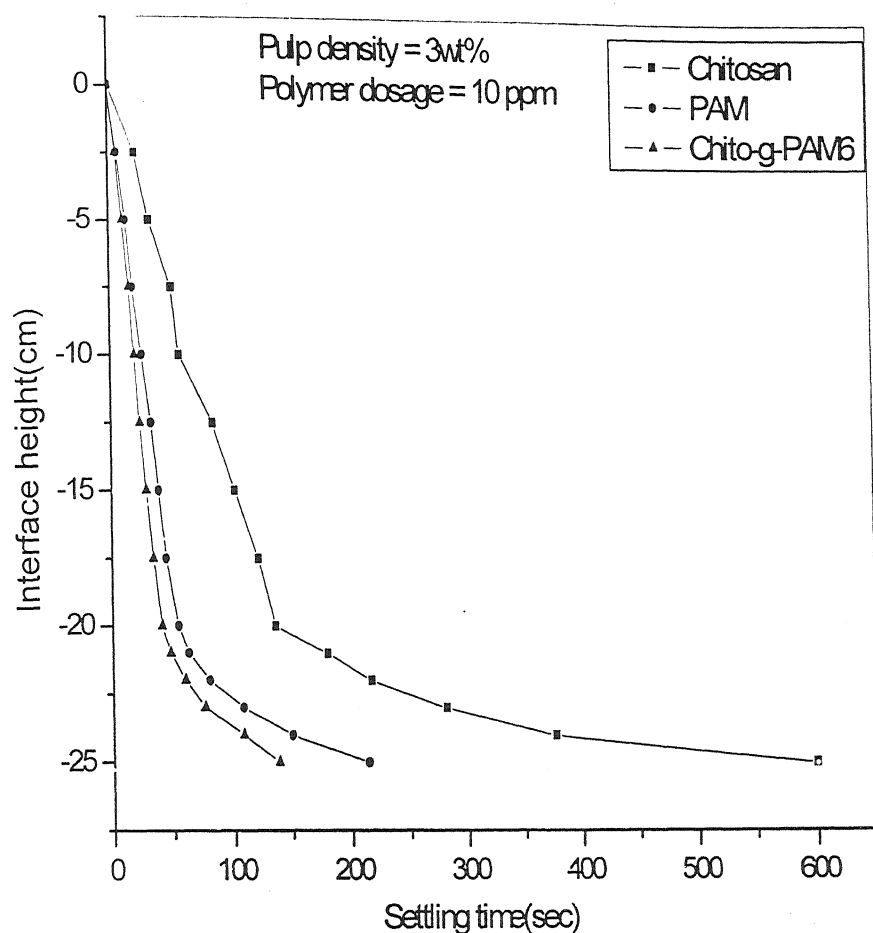


Figure 4.3 Settling curves for kaolin suspension with addition of chitosan, PAM and Chito-g-PAM6

The enhancement of flocculation characteristics of the graft copolymers is believed to be due to the greater polymer bridging [369-371]. The controversy concerning the bridging and charge neutralization mechanism of aggregating aqueous suspensions by the adsorption of water-soluble polymers was of long standing. In the early experimental and theoretical investigations, La Mer [288] and his group were prominent in advocating bridging. For effective bridging to occur, the length of the grafted chain should be longer so as to adsorb on a particle surface to another particle surface. Hence, the graft copolymer with longer side chains would be more effective as a flocculant than that with shorter chains, which has been observed by different research scholars [320, 8].

From the settling curves (Figures 4.2 and 4.3); it is observed that the fall of interface is linear for a considerable height before it becomes non-linear. This means that the rate of fall of the interface is constant initially, after which it gradually declines. Initial settling rate is

calculated from the slope of the initial portion of the curves. In the flocculation study of the graft copolymers for kaolin suspension, a satisfactory linearity was maintained for about 20 cm fall of the interface.

4.3.1.2 Flocculation of the Iron Ore Suspension

Figure 4.4 represents the flocculation efficiency of all the grades of PAM grafted chitosan copolymers (Chito-g-PAM4 to Chito-g-PAM7) in 3 wt% iron ore suspension. It has been observed that Chito-g-PAM6 shows better flocculation performance among all the graft copolymers.

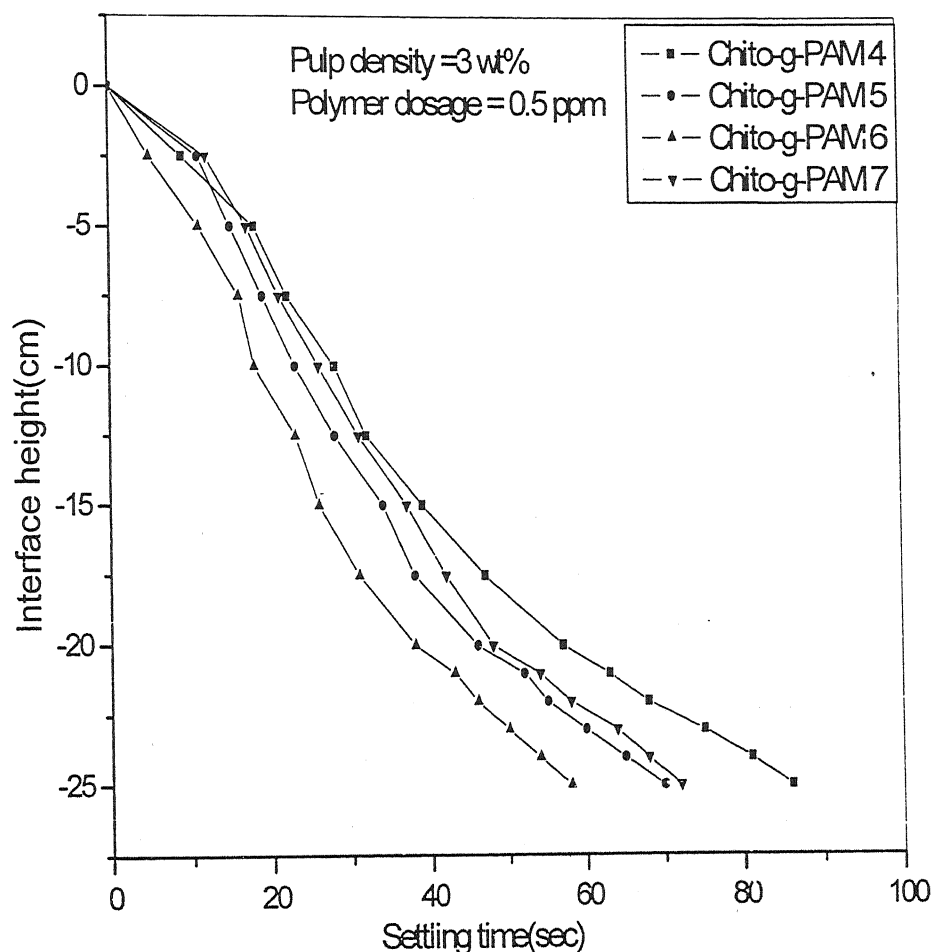


Figure 4.4 Settling curves for iron ore suspension with addition of PAM grafted chitosan copolymers

Figure 4.5 compares the flocculation efficiency of Chito-g-PAM6 with chitosan and PAM solution. It can be easily observed from the curves that Chito-g-PAM6 is far better flocculant than both the chitosan and PAM solutions in iron ore suspension.

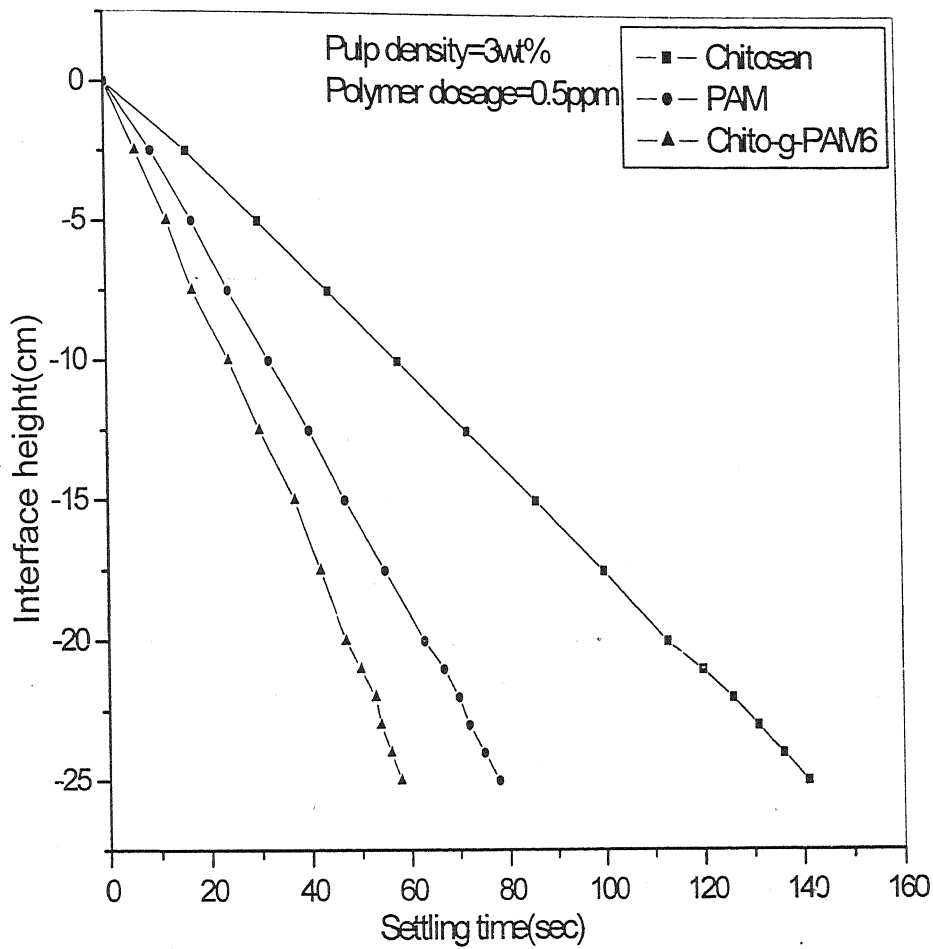


Figure 4.5 Settling curves for iron ore suspension with addition of chitosan, PAM and Chito-g-PAM6

4.3.1.3 Flocculation of the Silica Suspension

The flocculation characteristics of all the graft copolymers (Chito-g-PAM4 to Chito-g-PAM7) in 3 wt% silica suspension are shown in **Figure 4.6**. The flocculation characteristic of the Chito-g-PAM6 is better than all the graft copolymers.

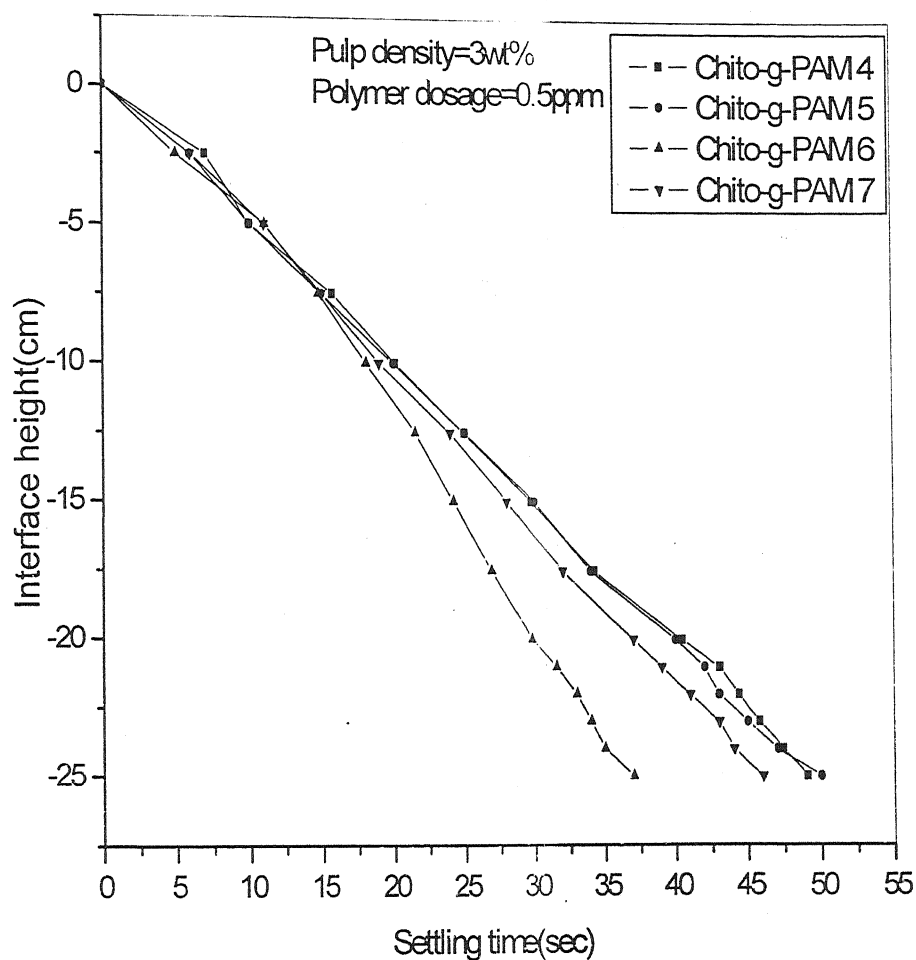


Figure 4.6 Settling curves for silica suspension with addition of PAM grafted chitosan copolymers

Again, the grafting efficiency of Chito-g-PAM6 is compared with chitosan and PAM solutions. The results are given in **Figure 4.7**. It has been observed that Chito-g-PAM6 is showing better flocculation performance than both the chitosan and PAM solutions.

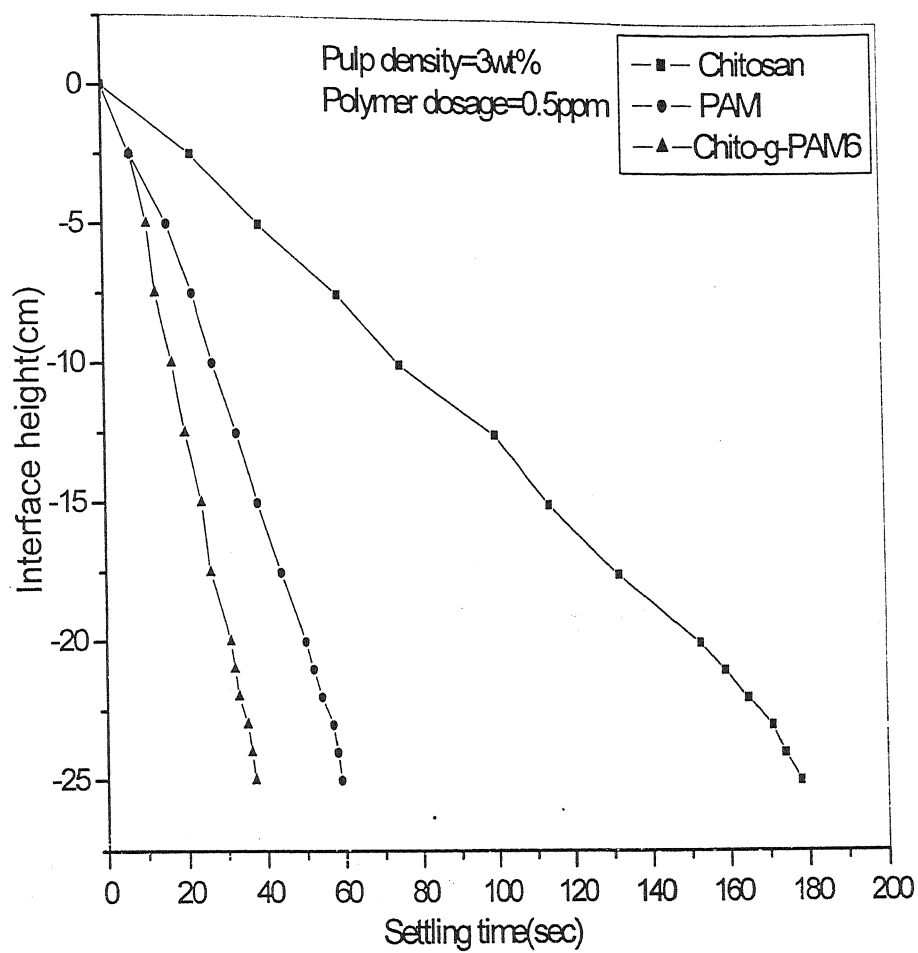


Figure 4.7 Settling curves for silica suspension with addition of chitosan, PAM and Chito-g-PAM6

4.3.1.4 Flocculation of the Bentonite Suspension

The flocculation characteristics of all the graft copolymers (Chito-g-PAM4 to chito-g-PAM7) in 1 wt% bentonite suspension were compared and shown in **Figure 4.8**. The flocculation characteristic of the Chito-g-PAM6 is best among all the graft copolymers.

Again, the flocculation efficiency of a Chito-g-PAM6 was compared with native chitosan and PAM solutions in bentonite suspension and the results are shown in **Figure 4.9**. Results show that Chito-g-PAM6 is better flocculant than both the native chitosan and PAM solutions.

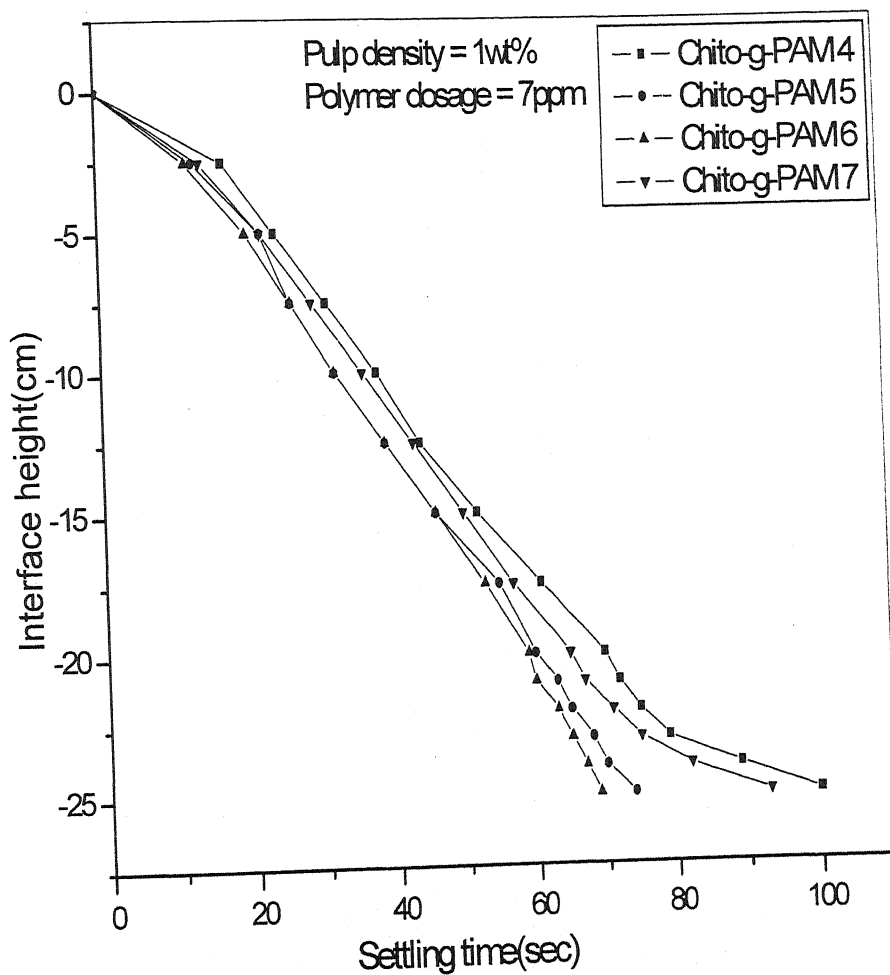


Figure 4.8 Settling curves for bentonite suspension with addition of PAM grafted chitosan copolymers

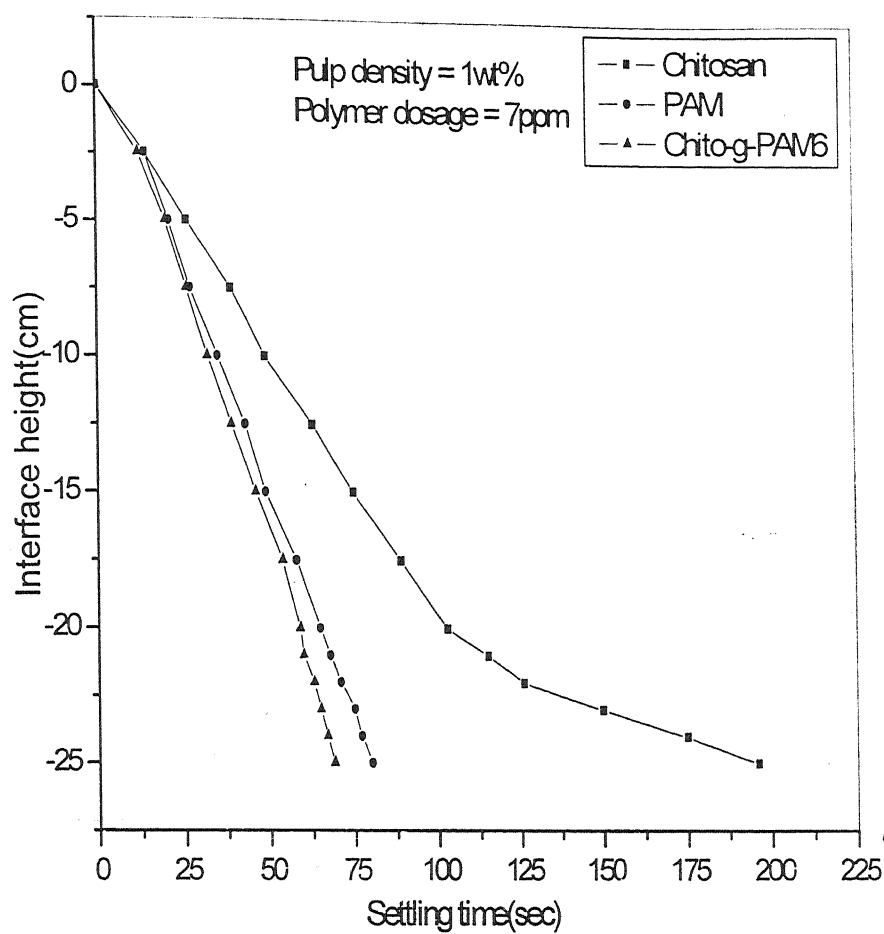


Figure 4.9 Settling curves for bentonite suspension with addition of chitosan, PAM and Chito-g-PAM6

4.3.2 Jar Test Results

4.3.2.1 Flocculation of the Kaolin Suspension

In the jar test method the flocculation efficiency of all the PAM grafted chitosan copolymer was compared with 0.25wt% kaolin suspension. The turbidity of the supernatant liquid after flocculation has been measured by plotting turbidity versus polymer dosage. The enhancement of the flocculation efficiency of the PAM grafted chitosan copolymer was believed to be due to polymer bridging [369,370].

It has been observed from **Figure 4.10** that Chito-g-PAM6 shows better flocculation performance than other graft copolymers in jar test for kaolin suspension. This is because of the presence of the fewer but longer PAM chains in Chito-g-PAM6.

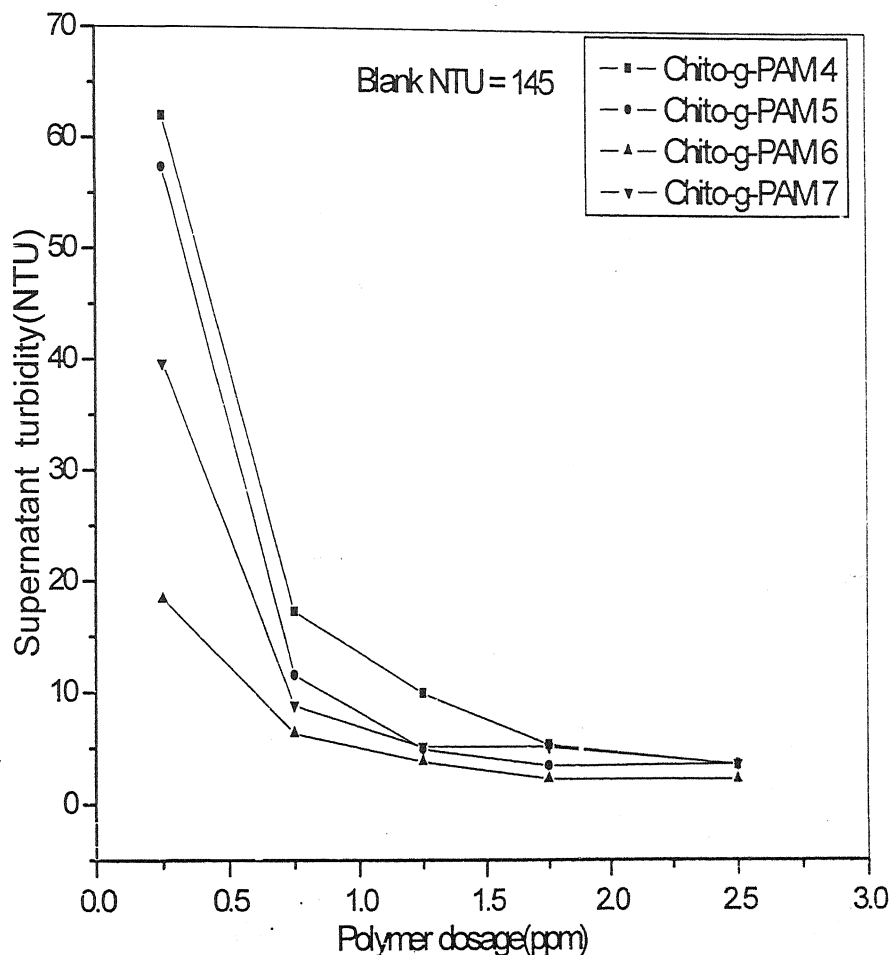


Figure 4.10 Jar test results for kaolin suspension (0.25wt %) with addition of PAM grafted chitosan copolymers

4.3.2.2 Flocculation of the Iron Ore suspension

Figure 4.11 represents the flocculation efficiency of all the graft copolymers in 0.25wt% iron ore suspension. Here also, Chito-g-PAM6, which is believed to have longer PAM chains, shows better flocculation performance than the other graft copolymers. At 1ppm polymer dose, almost all the graft copolymers shows their corresponding minimum turbidity value (**Figure 4.11**) and after that increase in the polymer dosage increases the turbidity values due to deflocculation effect.

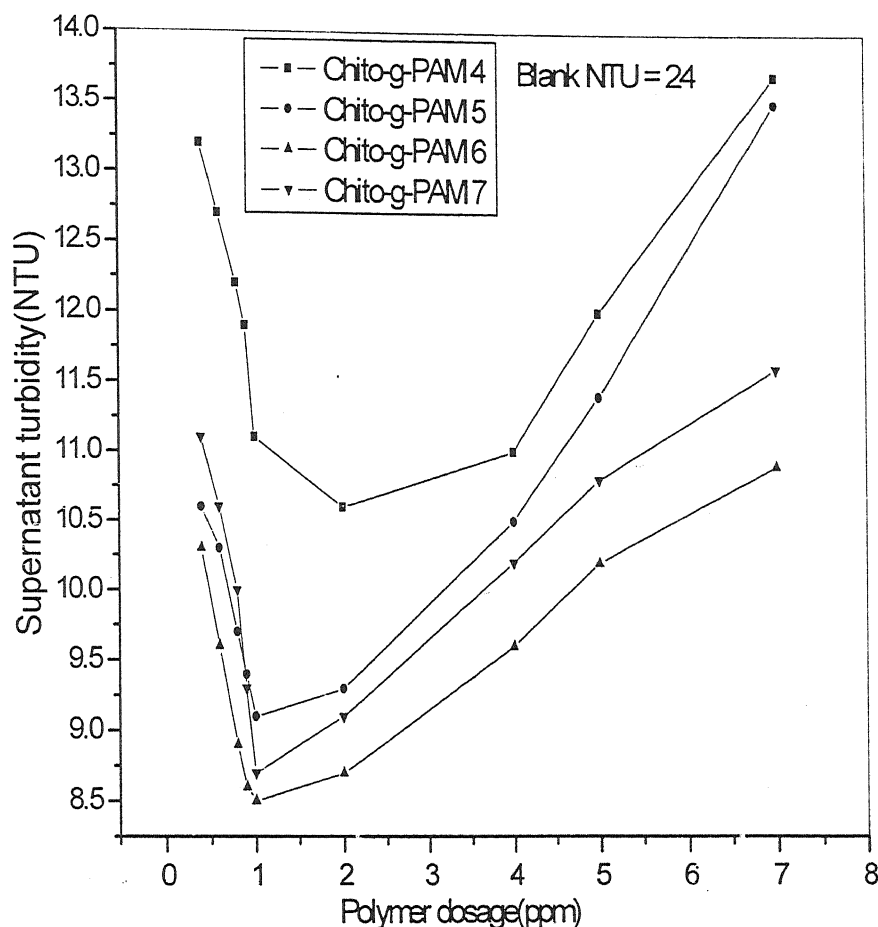


Figure 4.11 Jar test results for iron ore (0.25wt %) suspension with addition of PAM grafted chitosan copolymers

4.3.2.3 Flocculation of the Silica Suspension

In Figure 4.12 flocculation efficiency of all the graft copolymers were compared in 0.25wt% silica suspensions. Here, Chito-g-PAM6 again shows best flocculation performance among all the PAM grafted chitosan copolymers.

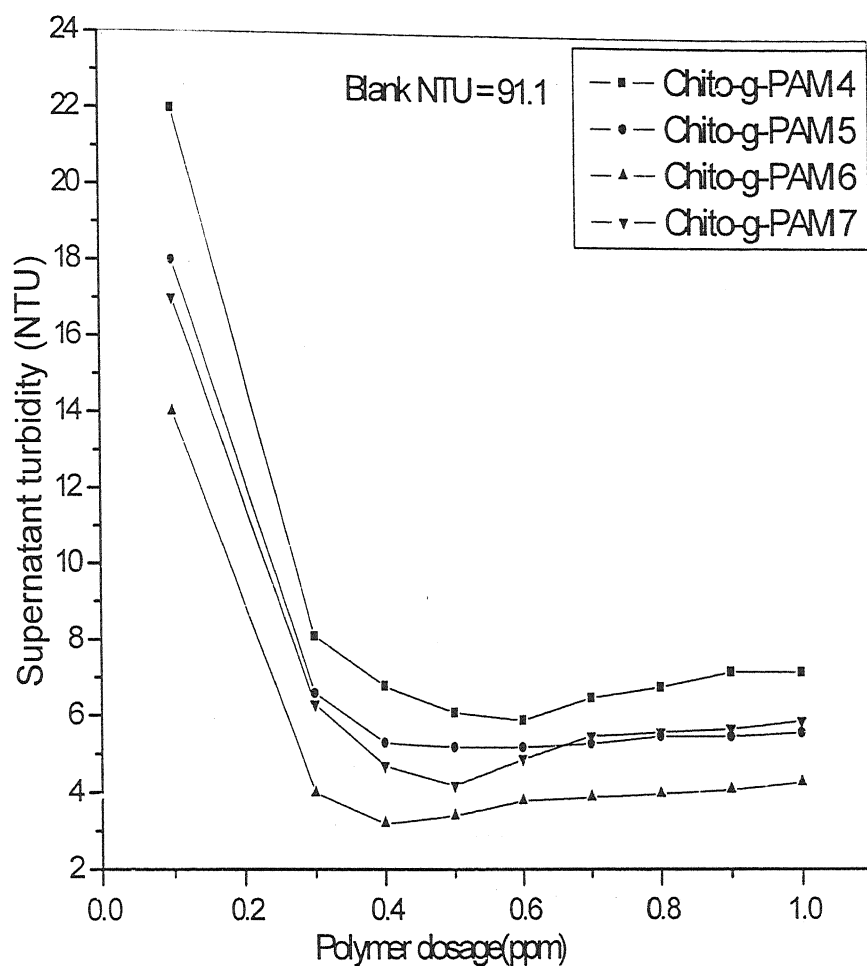


Figure 4.12 Jar test results for silica suspension (0.25wt %) with addition of PAM grafted chitosan copolymers

4.3.2.4 Flocculation of the Bentonite Suspension

In Figure 4.13 flocculation efficiency of all the graft copolymers was compared in 0.25wt% bentonite suspension. Here, Chito-g-PAM6 shows best flocculation performance among all the PAM grafted chitosan copolymers. It should be noted here that not only the nature of the polymeric flocculants, structure and molecular weight but also the nature of the colloidal particles and their surface properties plays an important role in flocculation.

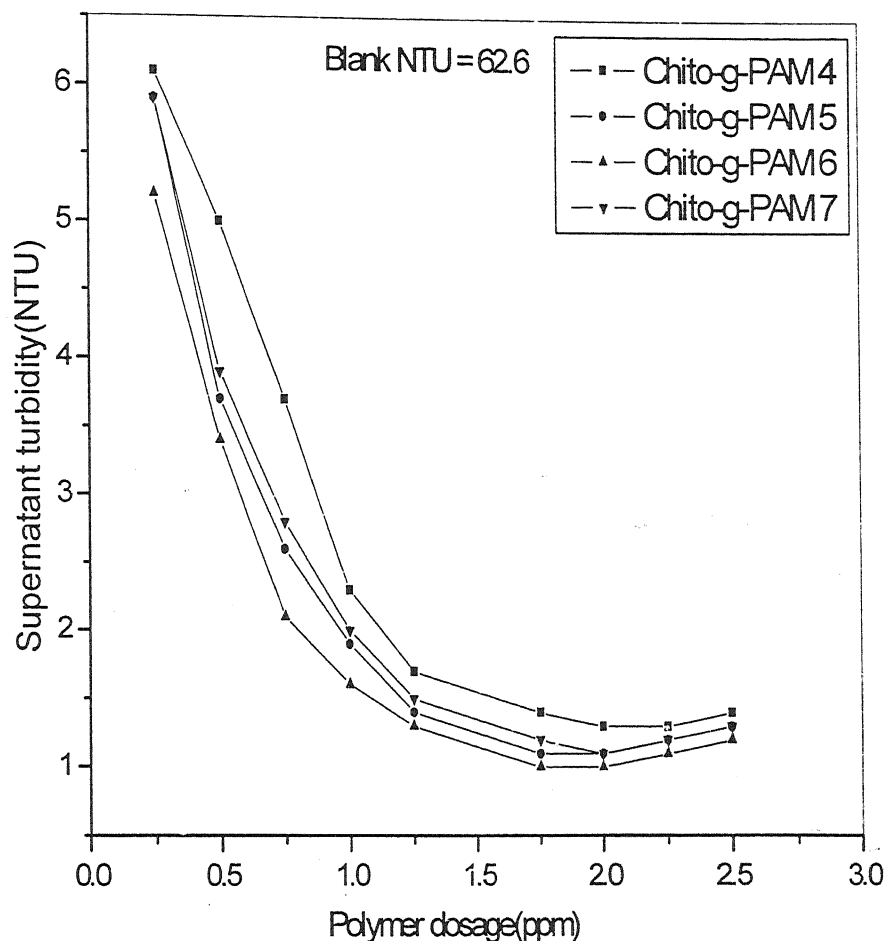


Figure 4.13 Jar test results for bentonite suspension (0.25wt %) with addition PAM grafted chitosan copolymers

4.4 SUMMARY

This chapter emphasis on the flocculation performance of all the PAM grafted copolymers. To investigate the flocculation performance, different grades of graft copolymers (Chito-g-PAM1 to Chito-g-PAM7) were made varying the concentration of acrylamide and CAN. The flocculation performance of the graft copolymers (Chito-g-PAM4 to Chito-g-PAM7) was determined with kaolin, iron ore, silica and bentonite suspensions. It was found that the flocculation efficiency of the graft copolymers is better than the ungrafted chitosan. Among all the graft copolymers Chito-g-PAM6 shows best flocculation performance. This may be due to the presence of a few but longer PAM chains, dangling from the chitosan backbone. Measuring the settling rate can prove the same results. **Table 4.4** represents the settling rate of chitosan and PAM grafted chitosan copolymers. It can be seen from the table (**Table 4.4**) that the settling rate is highest for Chito-g-PAM6 among all the graft copolymers.

Table 4.4 Settling rate of chitosan and PAM grafted chitosan copolymers

Polymer	Settling Rate (cm /sec)			
	Kaolin	Iron Ore	Silica	Bentonite
Chitosan	0.150	0.1735	0.128	0.192
Chito-g-PAM4	0.387	0.371	0.4968	0.277
Chito-g-PAM5	0.519	0.447	0.498	0.310
Chito-g-PAM6	0.580	0.549	0.654	0.337
Chito-g-PAM7	0.580	0.402	0.539	0.298

CHAPTER-V

**PARTIAL ALKALINE
HYDROLYSIS**

5.1 INTRODUCTION

It has been observed that on grafting PAM onto the polysaccharide backbone, the flocculation characteristics enhances tremendously. This is because of the easy approachability of the polyacrylamide chains grafted onto the rigid robust polysaccharide backbones to contaminant particles in the effluents. Many researchers [216,369] have also investigated the flocculation by partially hydrolyzed PAM. The partially hydrolyzed product showed better performance than PAM itself. Huguenard et al. [216] studied the aggregation kinetics of hematite in the presence of neutral and hydrolyzed polyacrylamide at low hydrolysis ratios and showed that the hydrolyzed polyacrylamide has been performing better than the PAM. On hydrolysis, the $-CONH_2$ groups of the PAM are converted to $-COO^-$ groups and the hydrolyzed products acquire a polyelectrolyte character. The repulsion among the $-COO^-$ groups expands the polymer coils and thus increases the solution viscosity of the hydrolyzed products. The expansion of the coils also enhances the flocculation characterization.

Keeping this in mind, PAM grafted chitosan copolymers were partially hydrolyzed. The hydrolysis reaction was carried out with sodium hydroxide. By varying the amount of sodium hydroxide, various grades of partially hydrolyzed products were synthesized. This section describes the flocculation efficiency of the partially hydrolyzed copolymers having straightened and expanded side PAM chains in details. As it has been observed that among all the graft copolymers, Chito-g-PAM6 showed the best flocculation performance, therefore, only this graft copolymer was partially hydrolyzed.

5.2 MATERIALS

Chitosan was a gift from Central Institute of Fisheries Technology, Cochin, India. Sodium hydroxide was procured from E. Merck, Mumbai, India. The other chemicals used here were referred in Chapter -III and IV.

5.3 ALKALINE HYDROLYSIS OF Chito-g-PAM6

Among the various grades of graft copolymers based on chitosan, the best performing Chito-g-PAM6 was chosen for the hydrolysis and the partially hydrolyzed products are referred as Chito-hyd-1 to Chito-hyd-5.

Alkaline hydrolysis of Chito-g-PAM6 was performed as follows:

One gram of Chito-g-PAM6 was dissolved in 250 ml of distilled water. Calculated amount of 1(N) NaOH was added to the solution at a particular temperature. The mixture was then stirred with a magnetic stirrer for an hour. At the end of the proposed reaction time, the content of the flask was poured in to the excess of acetone. The precipitated product was filtered and washed with acetone several times. It was then dried and pulverized. Five different partially hydrolyzed grades were synthesized by varying the experimental conditions. The details of the synthesis parameters are given in Table 5.1.

Table 5.1 Synthesis details of alkaline hydrolysis of Chito-g-PAM6

Polymer	Volume of 1(N) NaOH (ml)	Reaction Temperature (°C)	Reaction Time (Hr)
Chito-hyd-1	5.6	33	1
Chito-hyd-2	6.4	33	1
Chito-hyd-3	7.2	33	1
Chito-hyd-4	8	33	1
Chito-hyd-5	9	33	1

5.4 CHARACTERIZATION OF HYDROLYZED PRODUCTS

5.4.1 Determination of Neutralization Equivalent (N.E.) of the Hydrolyzed Copolymers

Neutralization equivalent (N.E.) is the equivalent of acid as determined by titration with standard base [370]. Neutralization equivalent of an acid can be determined by the following way:

Let X grams of a sample of an unknown acid required Y ml of z (N) NaOH for complete neutralization. Since each 1000 ml of the base contains Z equivalents and the number of equivalents of base required is equal to the number of the equivalent of acid present. The equivalent weight of the acid will be equal to,

$$\frac{X \times 1000}{Y \times Z}$$

The neutralization equivalent (N.E.) of the graft copolymers and all the hydrolyzed products were determined by the following procedure:

About 50 mg of each graft copolymer and the partially hydrolyzed products were dissolved in a 100 ml of distilled water in a conical flask. After that 25 cc of 0.0965 (N) HCl was added to each of the solution. The flasks were kept at room temperature for 5 hours under this condition. Then the solutions were back titrated with 0.0975 (N) NaOH solution. The difference between the titre value of only the HCl and the polymer solution gives the volume of alkali required for titrating the acid in the polymer.

5.4.2 Elemental Analysis

The elemental analysis of the partially hydrolyzed graft copolymers was performed using a Carlo Erba 1108 Elemental Analyzer. The estimation of only three elements i.e. carbon, hydrogen and nitrogen was done. The results are shown in Table 5.3.

5.4.3 IR Spectroscopy

The Infrared spectroscopy of Chito-hyd products were recorded in solid state using KBr pellet as discussed earlier. The results were compared with the IR spectrum of original corresponding graft copolymer.

5.4.4 Scanning Electron Microscopy (SEM)

The SEM of the partially hydrolyzed product was studied in granular form using the same instrument discussed in Chapter-III.

5.4.5 Thermal Analysis

DSC analysis of all the polymers was performed using Perkin Elmer, PYRIS, Diamond DSC (USA). TG and DTG analysis was done with Staton Redcroft (STA-625) Thermal Analyzer. The DSC, TG and DTG analysis was performed starting from room temperature at nitrogen atmosphere. A uniform heating rate, $10^{\circ}\text{C}/\text{min}$ was maintained in this experiment.

5.4.6 X-ray Diffraction

The XRD analysis of the partially hydrolyzed product (Chito-hyd-3) was recorded in a similar fashion and in the same instrument as discussed earlier (Chapter-III).

5.5 FLOCCULATION STUDIES

The flocculation studies of all the partially hydrolyzed graft copolymers were carried out using settling test and jar test methods in different aqueous suspensions. The detail of the methods was described in Chapter-III.

5.6 RESULTS AND DISCUSSION

5.6.1 Synthesis

In hydrolyzing the graft copolymers, the aim was to straighten the flexible polyacrylamide chains onto the backbone of chitosan and then investigate their effect as flocculants. During the treatment of the graft copolymers with alkali (NaOH solution), the following reactions were expected to occur; (i) saponification of the amide groups to carboxyl groups (ii) deetherification and depolymerization reactions of the PAM components of the graft copolymers [371]. The extent of these reactions depends on the reaction conditions. Khalil et al. [372] observed that the alkaline hydrolysis of PAM-starch graft copolymer using NaOH concentration upto 1(N) and temperature in between 80°C to 90°C leads only saponification reaction (conversion of $-\text{CONH}_2$ groups into $-\text{COO}^-\text{Na}^+$). While using higher concentration of alkali, deetherification and depolymerization reaction occurs simultaneously with the saponification reaction. From the past experience of our laboratory [373] the neutralization equivalent (N.E.) is found to be higher at near room temperature than at higher temperature for partially hydrolyzed products. So, to get a higher N.E., all the hydrolysis reactions were carried out at room temperature (33 °C).

5.6.2 Characterization

5.6.2.1 Neutralization Equivalent Value

The N.E. of the Chito-g-PAM6 and all its partially hydrolyzed products are given in **Table 5.2**.

Table 5.2 Determination of Neutralization Equivalent (N.E.) of Chito-g-PAM6 and its partially hydrolyzed products

Polymer	Volume of 0.0975(N) NaOH (V ₂) (ml)	(V ₁ *-V ₂) (ml)	N.E. (g)
Chito-g-PAM6	24	0.75	683.76
Chito-hyd-1	23	1.75	293.07
Chito-hyd-2	22.8	1.95	262.98
Chito-hyd-3	22.5	2.25	227.92
Chito-hyd-4	22.1	2.65	193.51
Chito-hyd-5	21.5	3.15	162.8

V₁* is the volume of 0.0975 (N) NaOH to neutralize 25 ml of 0.0965 (N) HCl =24.75 ml.

From the neutralization equivalent measurement of the partially hydrolyzed Chito-g-PAM6 and the unhydrolyzed product, it can be concluded that the carboxyl content of the hydrolyzed product depends upon alkali concentration. In case of the partial hydrolysis of Chito-g-PAM6, the N.E. value gradually decreases from Chito-hyd-1 to Chito-hyd-5, due to increase in carboxyl content.

5.6.2.2 Elemental Analysis

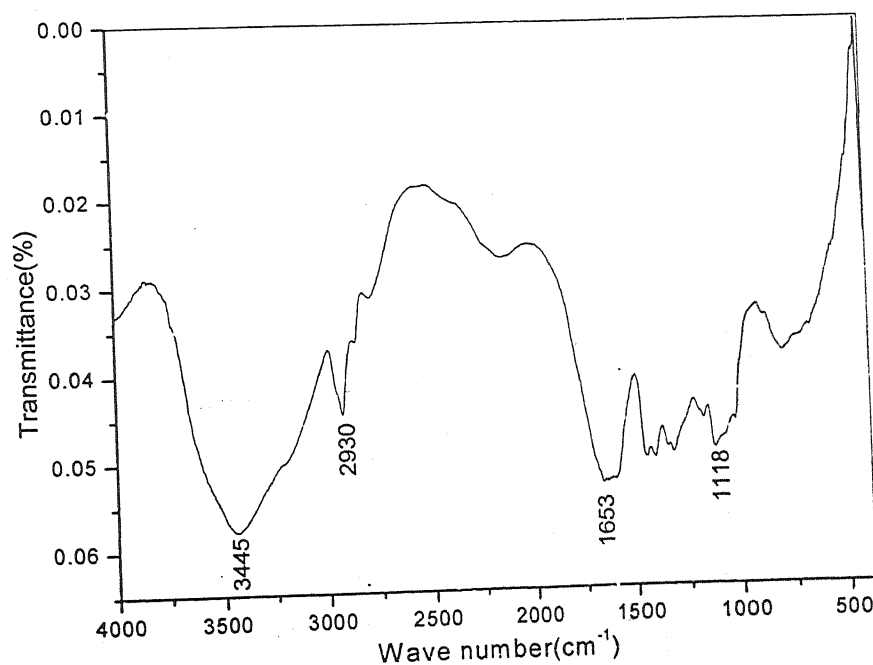
As on hydrolysis, some -CONH₂ groups of the graft copolymers are converted to the -COO⁻ groups and ammonia gas is also evolved during hydrolysis. Therefore, the % of nitrogen on the hydrolyzed products decreases. This is observed from **Table 5.3**.

Table 5.3 Elemental analysis of partially hydrolyzed and unhydrolysed Chito-g-PAM6

Polymer	Carbon (%)	Hydrogen (%)	Nitrogen (%)
Chito-g-PAM6	41.58	7.32	16.22
Chito-hyd-1	38.85	7.07	12.48
Chito-hyd-2	38.06	6.98	12.12
Chito-hyd-3	38.12	6.95	12.01
Chito-hyd-4	36.14	6.13	10.49
Chito-hyd-5	36.01	6.12	10.31

5.6.2.3 IR Spectroscopy

The IR Spectra of Chito-g-PAM6 and partially hydrolyzed Chito-g-PAM6 (Chito-hyd-3) are given in **Figure 5.1** and **5.2**. It has been observed that all the peaks present in Chito-g-PAM6 are also present in Chito-hyd-3 with a little change in intensity and frequency.

**Figure 5.1** IR Spectrum of Chito-g-PAM6

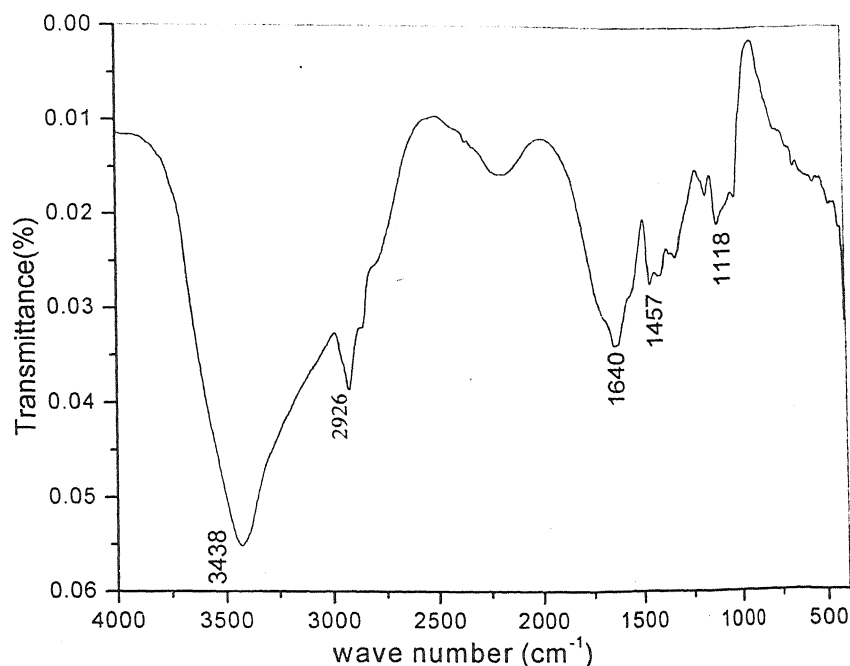


Figure 5.2 IR Spectrum of Chito-hyd-3

The formation of the carboxylate group can be proved by the presence of a strong asymmetric stretching at 1457 cm^{-1} and a strong symmetric stretching at 1640 cm^{-1} . These are the characteristic bands for carboxylate salts.

5.6.2.4 Scanning Electron Microscopy (SEM)

Figure 5.3 shows the scanning electron micrographs of unhydrolyzed Chito-g-PAM6 and partially hydrolyzed Chito-g-PAM6 (Chito-hyd-3). The surface morphology of the partially hydrolyzed graft copolymer has changed remarkably in comparison with the grafted one.

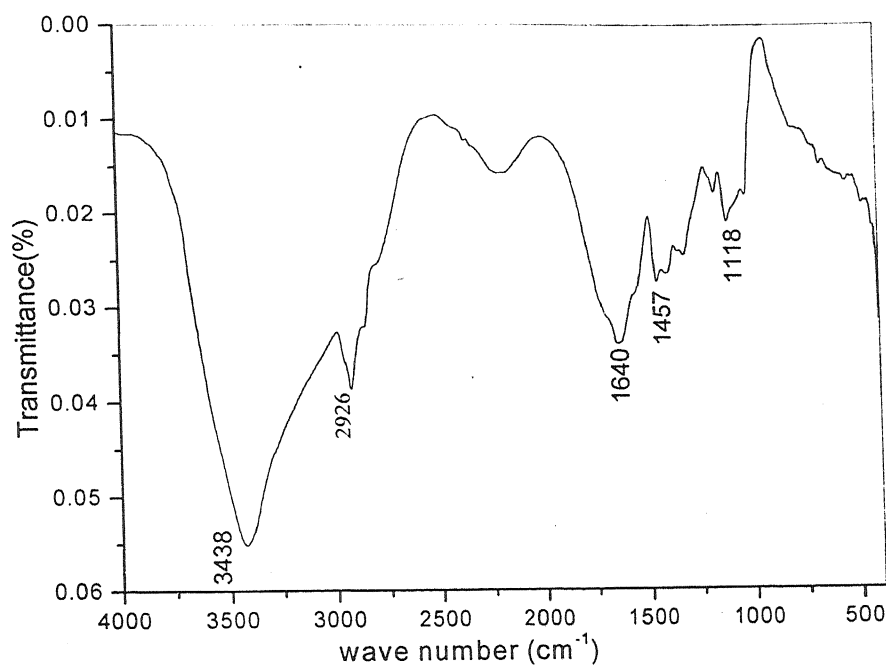
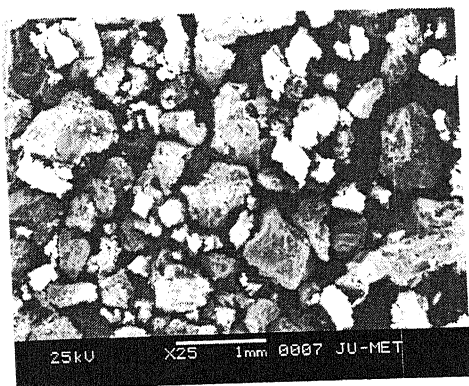


Figure 5.2 IR Spectrum of Chito-hyd-3

The formation of the carboxylate group can be proved by the presence of a strong asymmetric stretching at 1457 cm^{-1} and a strong symmetric stretching at 1640 cm^{-1} . These are the characteristic bands for carboxylate salts.

5.6.2.4 Scanning Electron Microscopy (SEM)

Figure 5.3 shows the scanning electron micrographs of unhydrolyzed Chito-g-PAM6 and partially hydrolyzed Chito-g-PAM6 (Chito-hyd-3). The surface morphology of the partially hydrolyzed graft copolymer has changed remarkably in comparison with the grafted one.



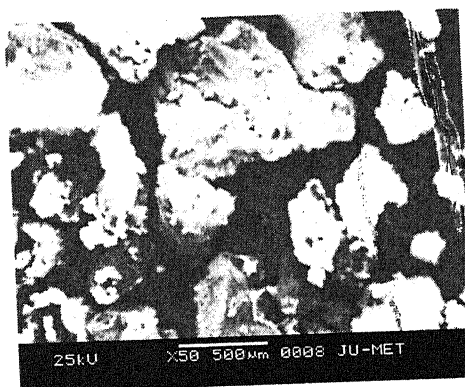
(a) Chito-g-PAM6



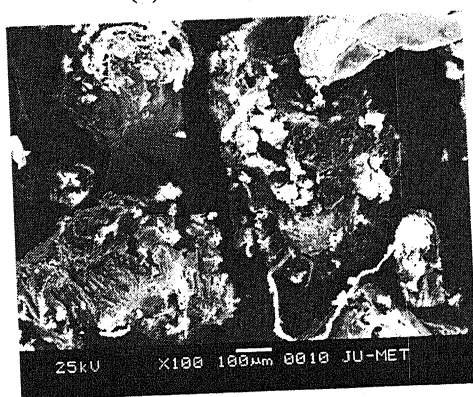
(b) Chito-hyd-3



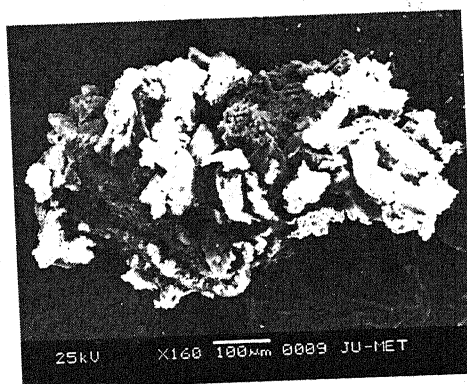
(c) Chito-g-PAM6



(d) Chito-hyd-3



(e) Chito-hyd-3



(f) Chito-hyd-3

Figure 5.3 SEM of Chito-g-PAM6 (a, c) and Chito-hyd-3 (b, d, e, f)

5.6.2.4 Thermal Analysis

5.6.2.5.1 Differential Scanning Calorimetry (DSC)

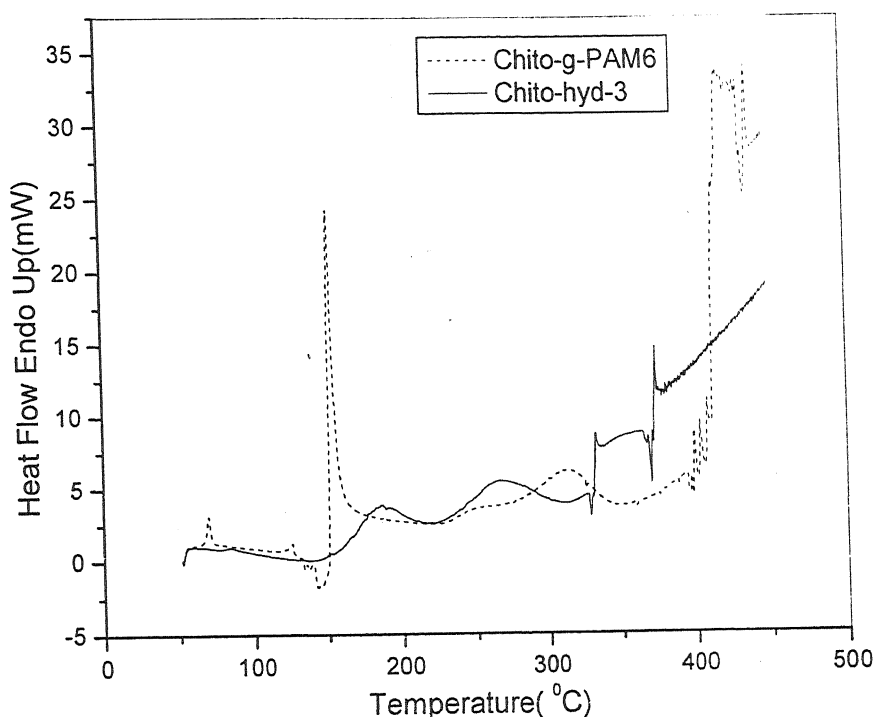


Figure 5.4 DSC curves of Chito-g-PAM6 and Chito-hyd-3

Figure 5.4 shows the DSC thermograph of Chito-g-PAM6 and Chito-hyd-3. From the graphs it can be seen easily that the hydrolyzed product decomposes at relatively lower temperature in comparison with the grafted one.

The presence of carboxylate moieties in the hydrolyzed products adsorbed more water compared to the unhydrolyzed graft copolymer. The presence of large amount of water molecules breaks the intermolecular attraction of the graft copolymer and thus lowered the crystallinity and shifted the endotherm for water adsorption to a higher value.

Hence, it can be concluded that hydrolysis does not favour thermal stability. It is believed that the negative charges generated due to the formation of the carboxylate group decreases the intermolecular attraction by charge repulsion and resulting in the decrease in the thermal stability.

5.6.2.5.2 Thermogravimetric Analysis (TG and DTG)

The TGA curves of Chito-g-PAM6 and Chito-hyd-3 in nitrogen atmosphere are shown in **Figures 5.5** and **5.6** respectively. The TG curve shows three distinct zones for decomposition.

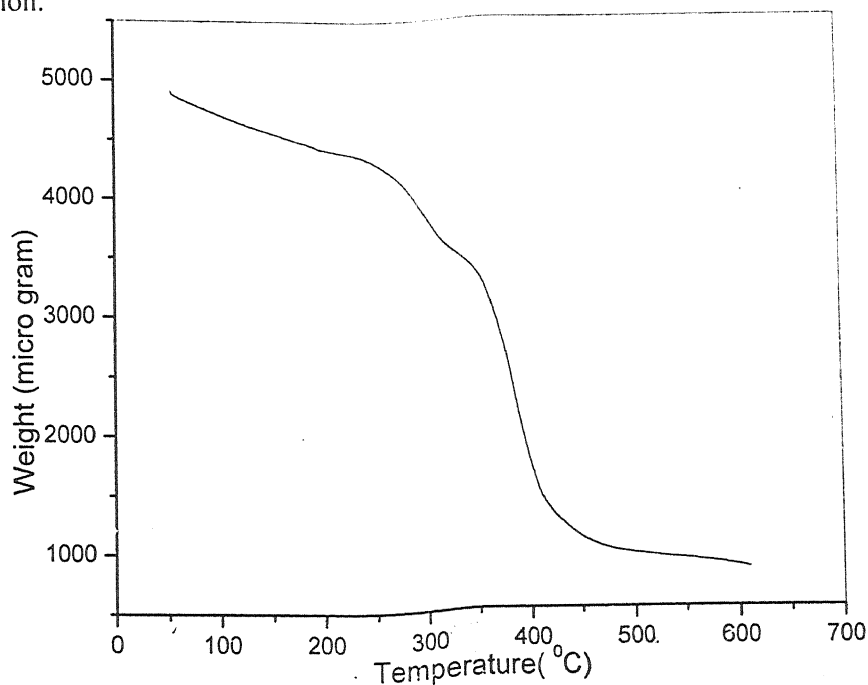


Figure 5.5 TG curve of Chito-g-PAM6

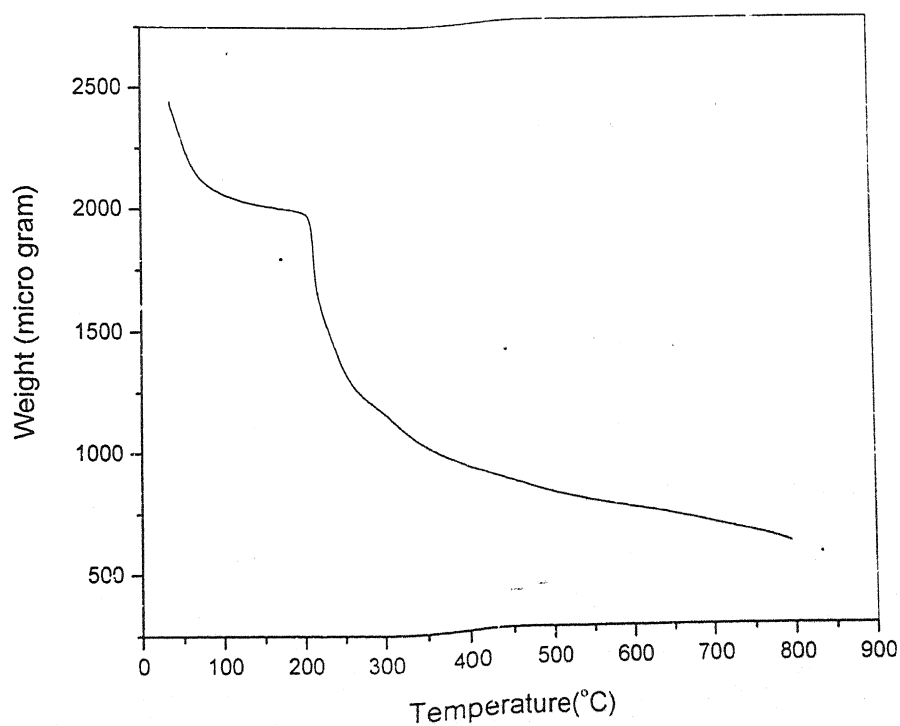


Figure 5.6 TG curve of Chito-hyd-3

The first zone is associated with the removal of water. The second zone is associated with the decomposition of the chitosan chain and the third one is associated with the decomposition of the Chito-g-PAM branches. These have been described in detail in the previous chapter (Chapter-III).

The Chito-hyd-3 has only two distinct steps for decomposition. The first weight loss is due to the liberation of the adsorbed and bound water in the product. Nearly 19 % weight loss is observed when the product was heated from room temperature to 196 °C. The second zone of weight loss is associated with the chain scissoring. It starts from 198 °C and ranges upto 469 °C. Nearly 58 % weight loss is observed in this zone.

The maximum temperature for decomposition of Chito-g-PAM6 and Chito-hyd-3 can be easily seen from the DTG curves presented in Figures 5.7 and 5.8 respectively.

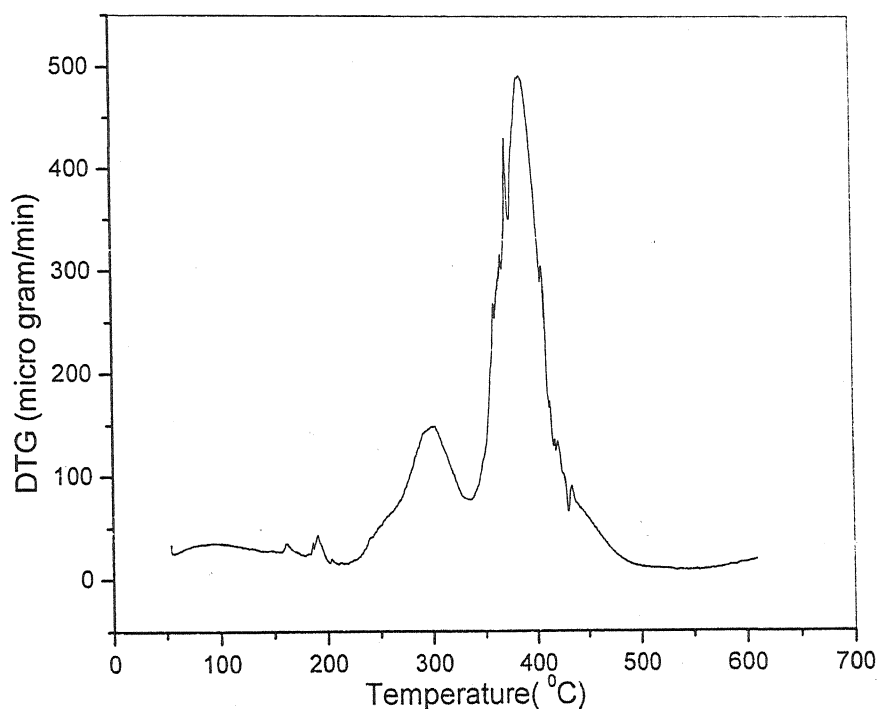


Figure 5.7 DTG curve of Chito-g-PAM6

The DTG curve of Chito-g-PAM6 shows two maximum points. It is described earlier in Chapter-III that the initial decomposition peak is associated with the decomposition of the degraded chitosan chain and the second one is associated with the decomposition of the cyclized imide moiety.

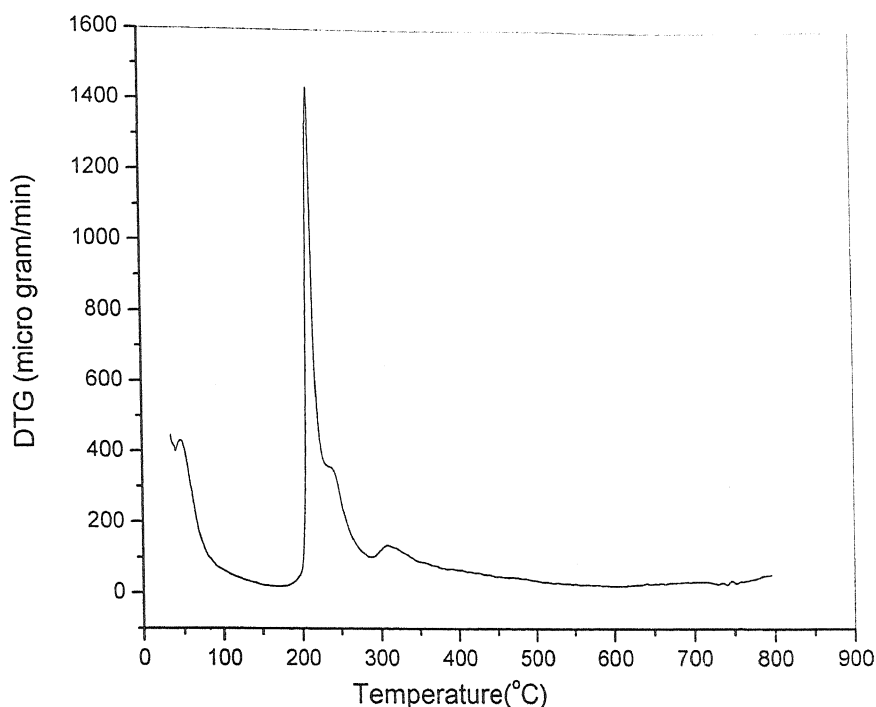


Figure 5.8 DTG curve of Chito-hyd-3

The DTG curve of Chito-hyd-3 shows three peaks. The first sharp peak is associated with the removal of the water molecules. The second and third are associated with the scissoring of the main chain and decomposition of the carboxylated branches.

From the TGA data, it can be concluded easily that the thermal stability of the hydrolyzed product is much lower than the unhydrolyzed one.

5.6.2.6 X-ray Diffraction

The X-ray diffraction patterns of the Chito-g-PAM6 and Chito-hyd-3 are presented in **Figures 5.9** and **5.10** respectively. The presence of PAM disrupts the intermolecular interaction among the chitosan chains and thus decreases the crystallinity of the Chito-g-PAM6. This has been discussed in Chapter-III. Partial hydrolysis of the grafted product introduced some new characteristics in the hydrolyzed product. The hydrolysed product has carboxylate groups, which are anionic in nature thus repels each other. Moreover they adsorb water molecules. These in return decreases the crystallinity of the hydrolyzed products. It can be easily seen from the **Figure 5.10**.

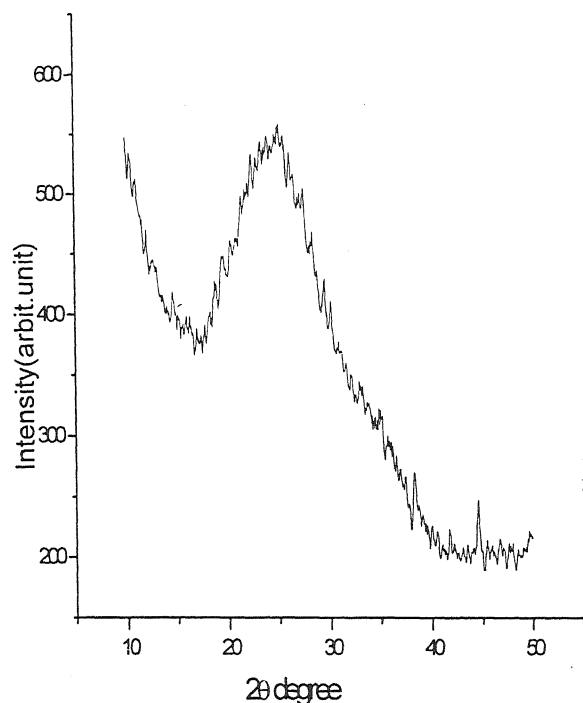


Figure 5.9 X-ray diffraction of Chito-g-PAM6

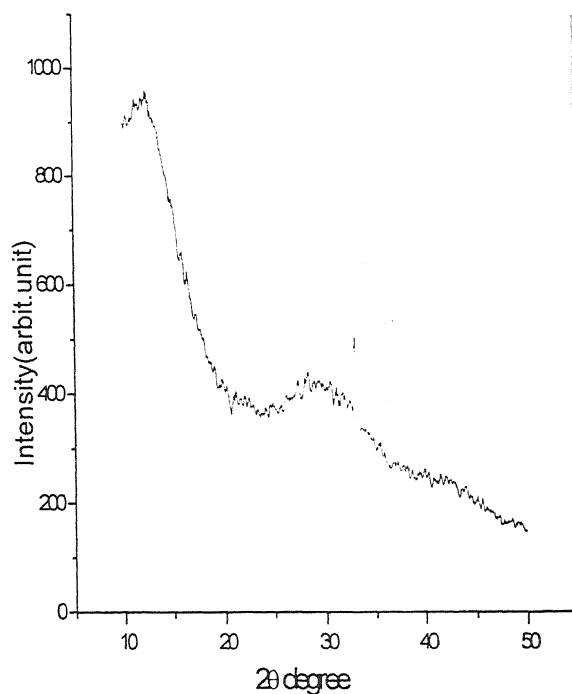


Figure 5.10 X-ray diffraction of Chito-hyd-3

5.7 FLOCCULATION STUDIES

5.7.1 The Settling Tests

Settling Test was done to see how fast the flocculant could remove contaminants from the liquid. To see how fast the flocculant removes suspended particles, a 100 ml stoppered graduated cylinder and a stopwatch have been used. Homogeneous slurry of the particles was taken in the cylinder and then the hydrolyzed copolymer was added to the slurry and the cylinder was then inverted 10 times to mix the polymer with the slurry. The cylinder was set upright and immediate after that the height of the interface between water and settling solid bed is measured over time.

5.7.1.1 Flocculation of the Kaolin Suspension

The flocculation performance of all the partially hydrolyzed products was compared with 3 wt% Kaolin suspension. It is presented in Figure 5.11. Chito-hyd-3 shows the best flocculating performance among all the partially hydrolyzed products.

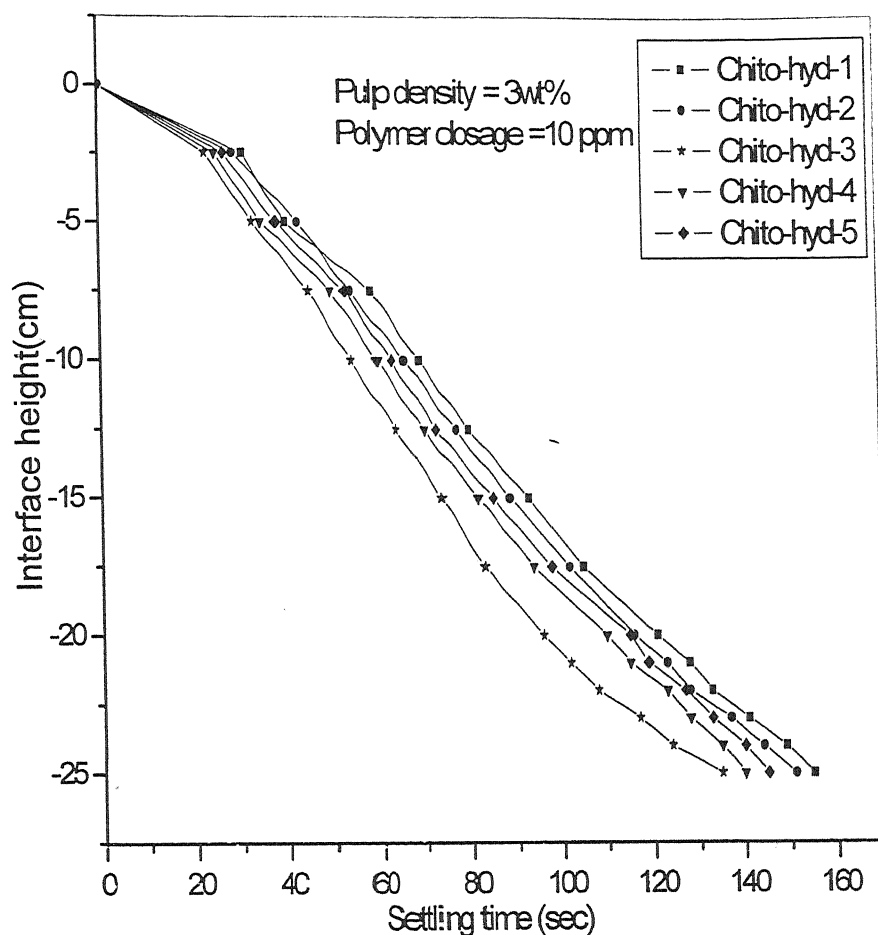


Figure 5.11 Settling curves for kaolin suspension with addition of partially hydrolyzed graft copolymers

Figure 5.12 represents the flocculation performance of chitosan, PAM, Chito-g-PAM6 and Chito-hyd-3 for 3 wt% kaolin suspension. It shows that even though the settling rate of Chito-g-PAM6 is higher than Chito-hyd-3, the overall time taken by the Chito-hyd-3 is less than Chito-g-PAM6. This is due to the higher time taken for concentration of the flocs in the case of Chito-g-PAM6 in comparison to Chito-hyd-3.

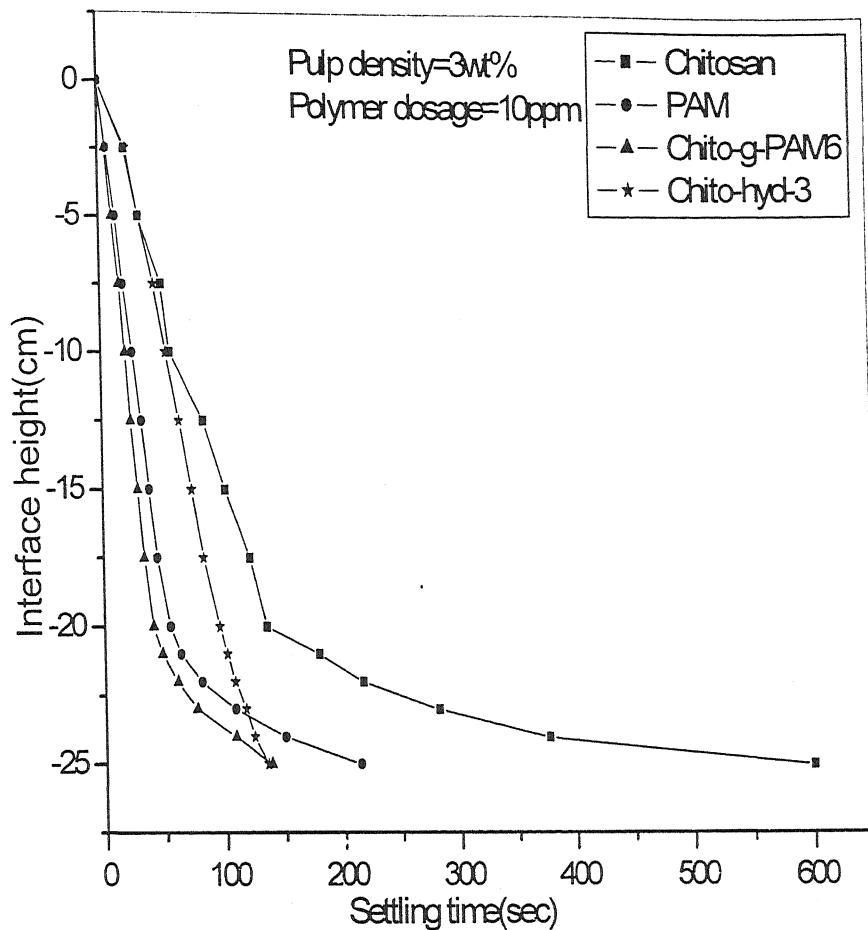


Figure 5.12 Settling curves for kaolin suspension with addition of chitosan, PAM, Chito-g-PAM6 and Chito-hyd-3

5.7.1.2 Flocculation of the Iron Ore Suspension

The flocculation efficiency of all the partially hydrolyzed products for iron ore suspension is represented in Figure 5.13. It is found that there is a steady decrease of interface height with no change of settling rate. This may be due to the larger particle size of the iron ore and higher specific gravity. Here Chito-hyd-3 shows better flocculation performance among all the partially hydrolyzed products

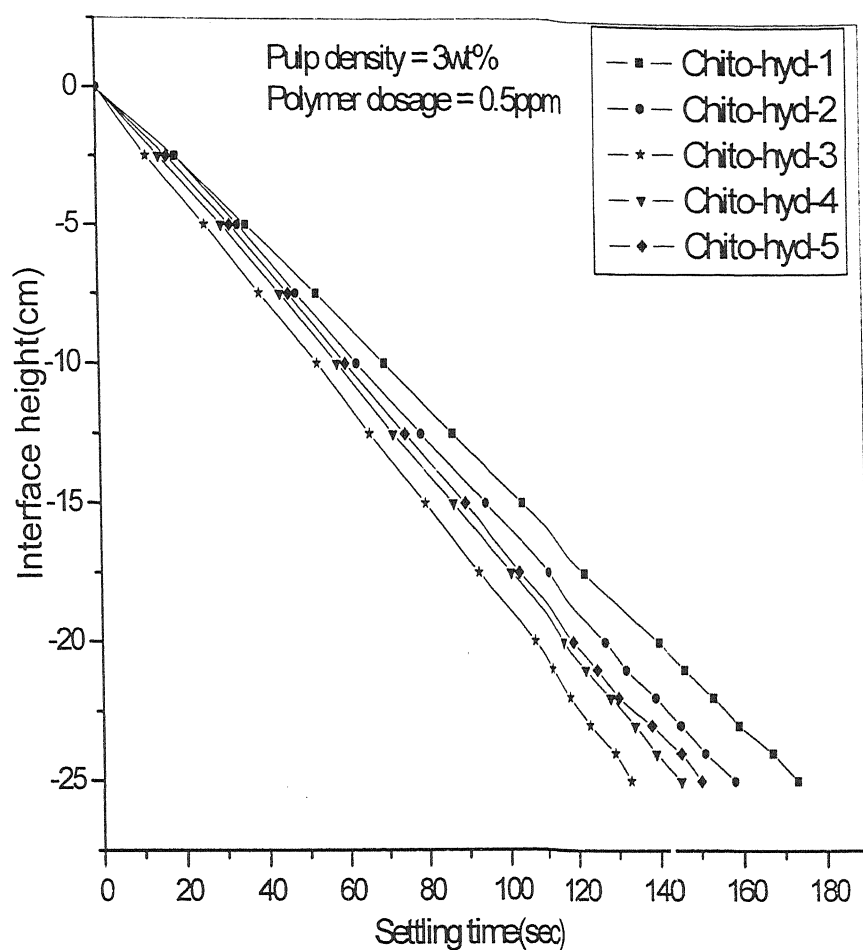


Figure 5.13 Settling curves for iron ore suspension with addition of partially hydrolyzed graft copolymers

Figure 5.14 describes the flocculation performances of Chito-hyd-3, chitosan, PAM and Chito-g-PAM6. It is evident from the curves that the flocculation efficiency of Chito-hyd-3 is better than chitosan but it is not showing better flocculation performance than either for PAM or Chito-g-PAM6.

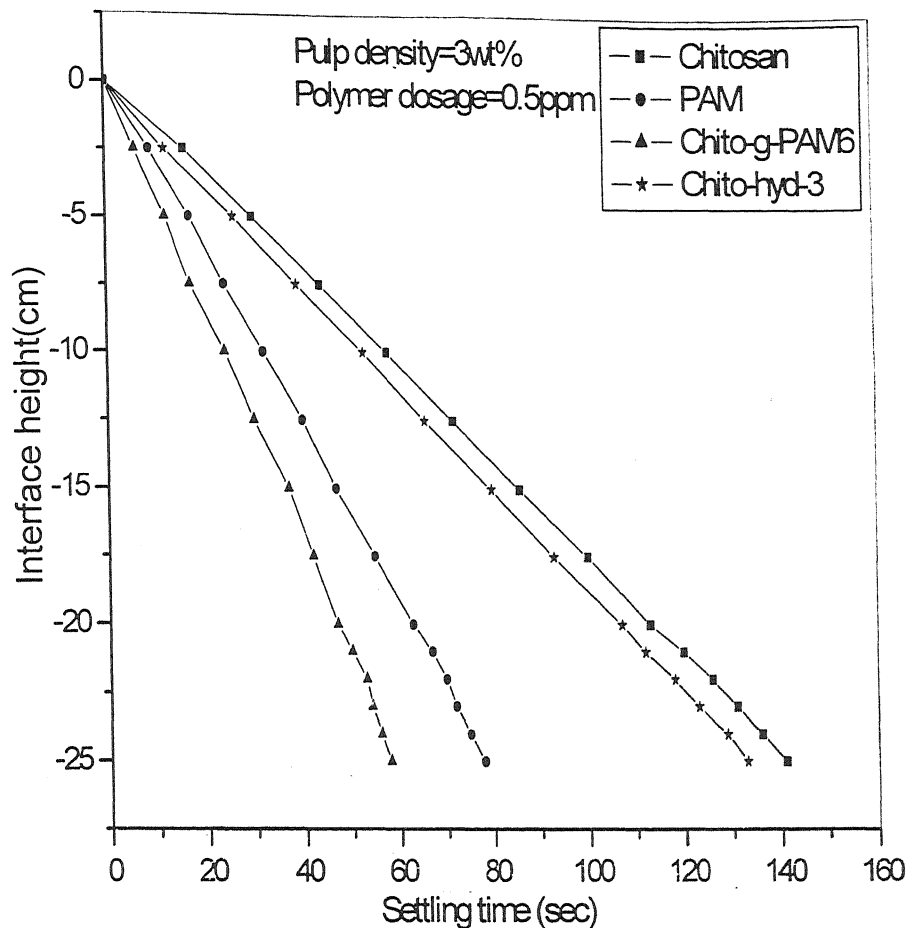


Figure 5.14 Settling curves for iron ore suspension with addition of chitosan, PAM, Chito-g-PAM6 and Chito-hyd-3

5.7.1.3 Flocculation of the Silica Suspension

The flocculation performance of all the partially hydrolyzed grades in 3wt% silica is described in Figure 5.15. It is found that the Chito-hyd-4 shows better performance among all the partially hydrolyzed copolymers. The reason for Chito-hyd-4 showing the best performance among all the grades and not the expected Chito-hyd-3 may be due to the competition between the approachability of the partially hydrolyzed copolymers towards the particle surface and the repulsion among the negatively charged polymer chains adsorbed onto the surface of the particle.

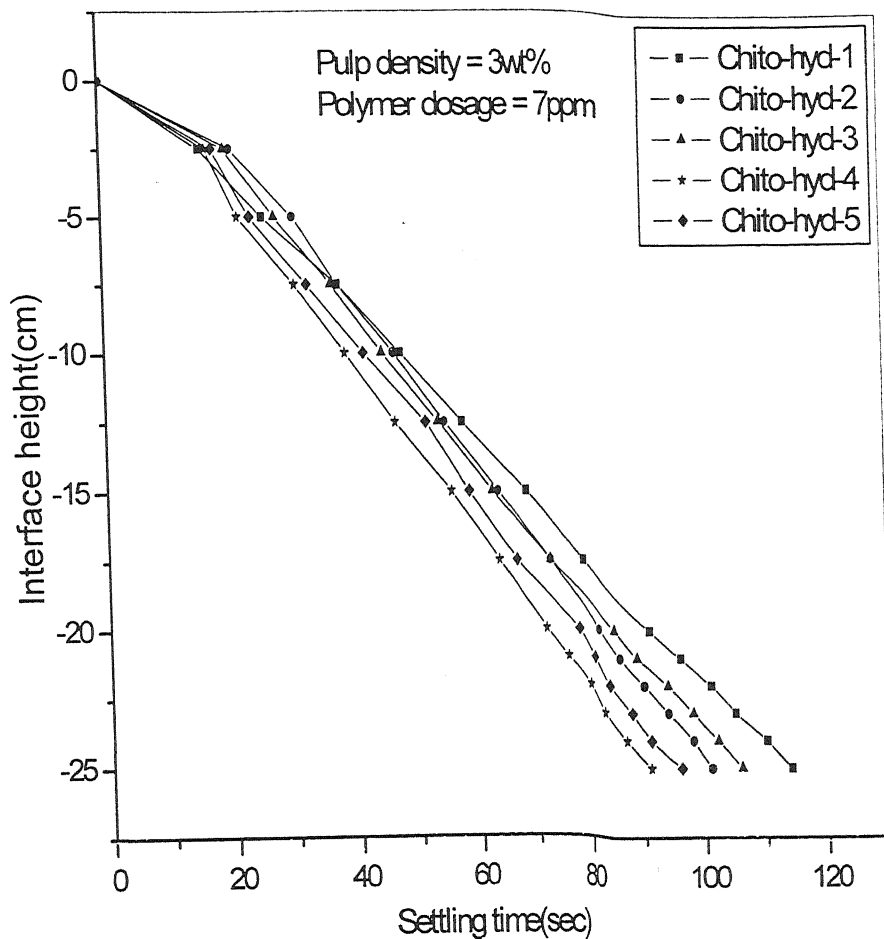


Figure 5.15 Settling curves for silica suspension with addition of Partially hydrolyzed graft copolymers

The flocculation performance of the Chito-hyd-4 is compared with the chitosan, PAM and Chito-g-PAM6 and it is depicted in **Figure 5.16**. In this figure Chito-hyd-4 is showing better flocculation performance than native chitosan solution but its settling rate is lower than both the PAM and Chito-g-PAM6 solutions.

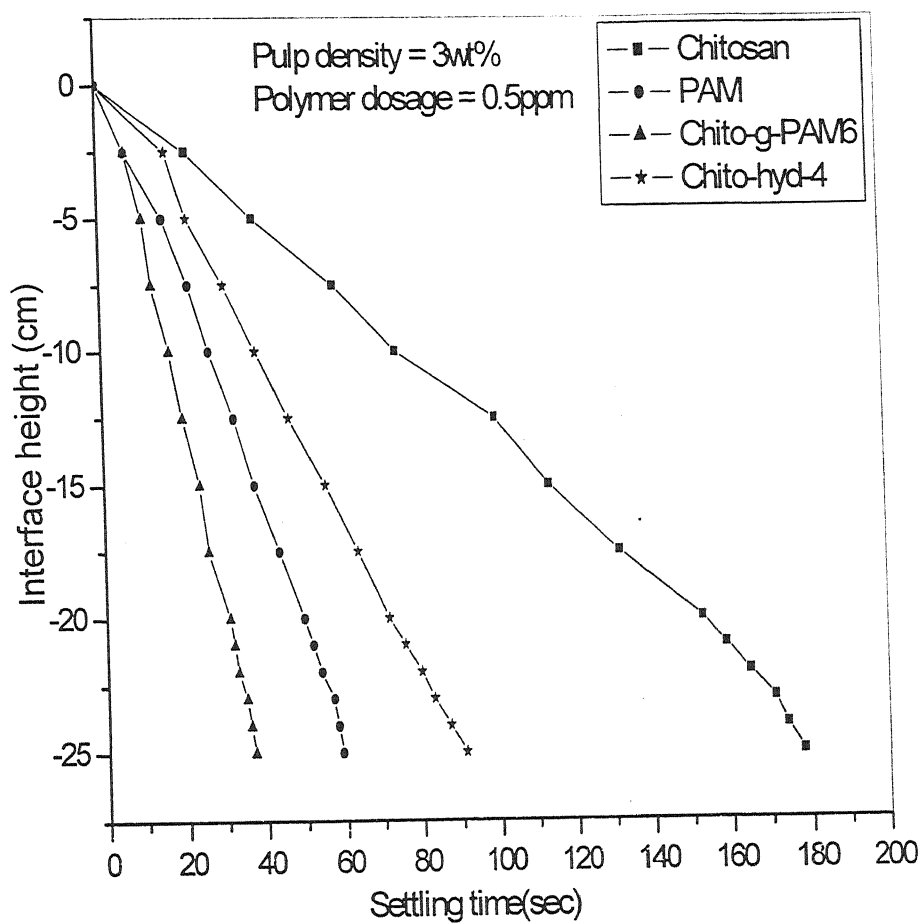


Figure 5.16 Settling curves for silica suspension with addition of chitosan, PAM, Chito-g-PAM6 and Chito-hyd-4

5.7.1.4 Flocculation of the Bentonite Suspension

The flocculation performance of the partially hydrolyzed products with bentonite suspension is described in **Figure 5.17**. Due to experimental problem; the test was carried out with 1wt% bentonite suspension. The polymer dosage for this experiment was a little bit higher than the expected to get a feasible settling rate. It is found that Chito-hyd-4 shows better flocculation performance among all the partially hydrolyzed grades.

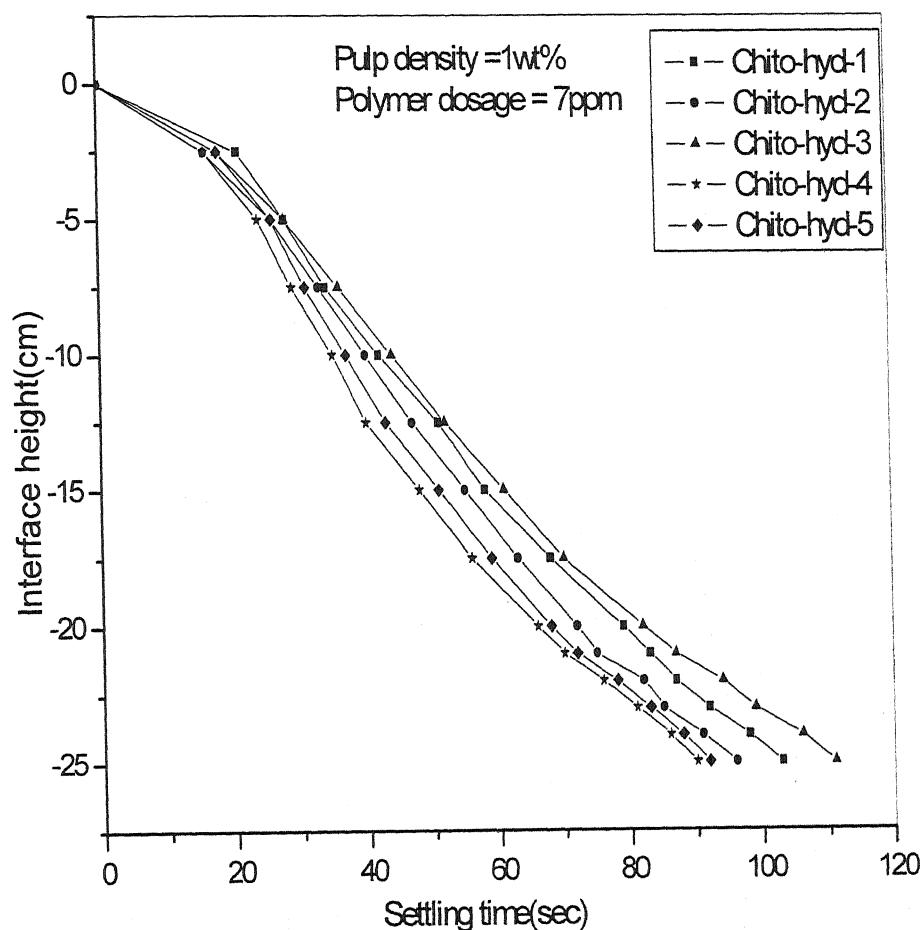


Figure 5.17 Settling curves for bentonite suspension with addition of partially hydrolyzed graft copolymers

Figure 5.18 compares the flocculation performance of the Chito-hyd-4 with chitosan, PAM and Chito-g-PAM6 in 1wt% bentonite suspension. The flocculation performance of Chito-hyd-4 is comparable to the PAM solution.

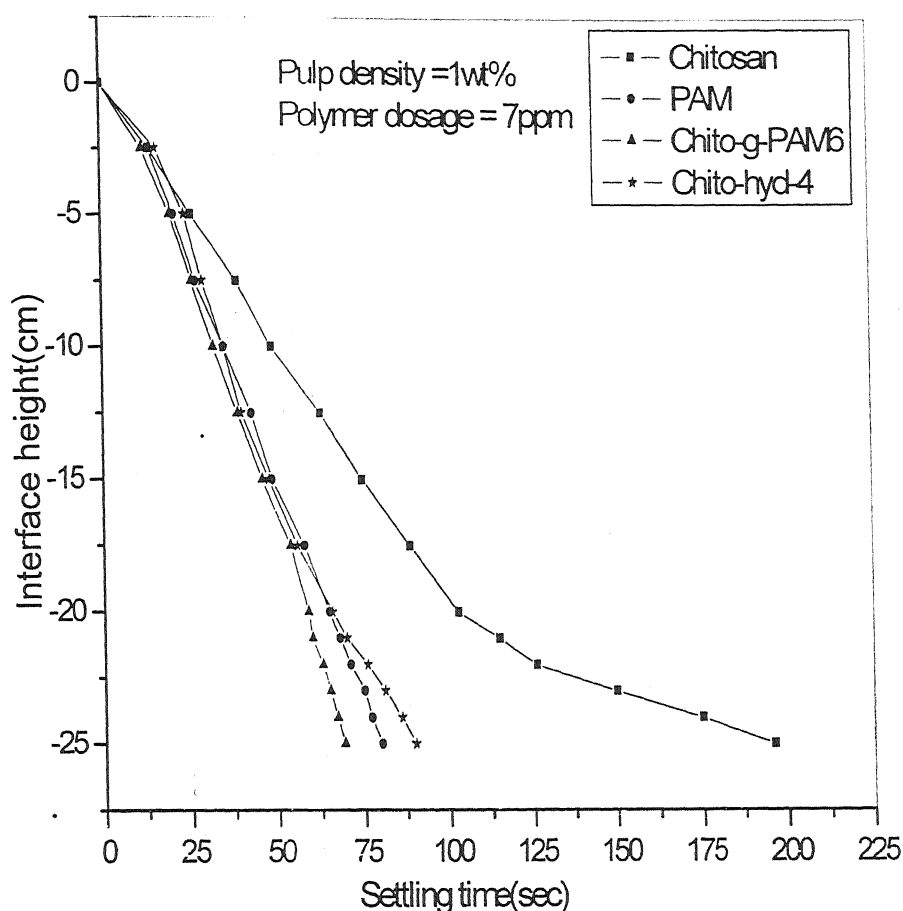


Figure 5.18 Settling curves for bentonite suspension with addition of chitosan, PAM, Chito-g-PAM6 and Chito-hyd-4

5.7.2 Jar Test Results

Jar Test measures the efficiency of a flocculant to clarify the liquid in a given time. We have used the same flocculator kindly supplied by M.B. Flocculators, Mumbai, India. The stirring condition was also the same as before. Immediately after addition of the polymer to the solution, the solution was stirred at a constant speed of 75 rpm for next 2 minutes to make a homogeneous mixing of the polymer then a slow stirring at 25 rpm for another 5 minutes, which allows the polymer to form flocs. The flocs so developed were allowed to settle for next 10 minutes. The supernatant liquid was then drawn from each of the jars and measured the turbidity in a pre calibrated Nephelo Turbidity Meter. The same experiment was repeated for each sample for two to three times so that an average value of the turbidity can be obtained.

5.7.2.1 Flocculation of the Kaolin Suspension

In jar test, the flocculation efficiency of the all the partially hydrolyzed graft copolymers was compared in 0.25wt% kaolin suspension. The value of the turbidity of the supernatant liquid after flocculation has been plotted against polymer dosage and is given in **Figure 5.19**. The jar test result shows that the Chito-hyd-3 has better flocculation efficiency among all the partially hydrolyzed graft copolymers. All the partially hydrolyzed graft copolymers show a minimum supernatant turbidity value at 2.5 ppm polymer dosage.

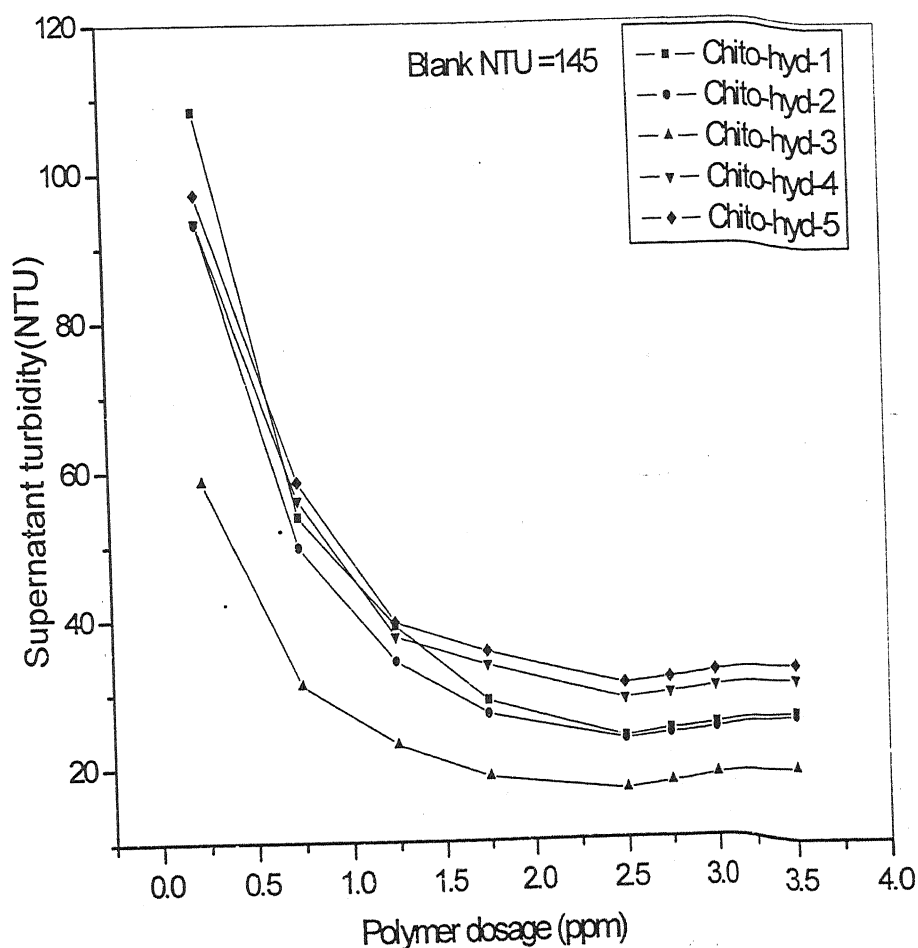


Figure 5.19 Jar test result for kaolin suspension (0.25wt%) with addition of partially hydrolyzed graft copolymers

5.7.2.2 Flocculation of the Iron Ore Suspension

In jar test, the flocculation efficiency of all the partially hydrolyzed graft copolymers was compared in 0.25wt% iron ore suspension. The turbidity of the supernatant liquid after flocculation has been plotted against polymer dosage and is given in **Figure 5.20**. The jar test results show that the Chito-hyd-4 has better flocculation efficiency among all the partially hydrolyzed graft copolymers. All the hydrolyzed graft copolymers show a minimum value of turbidity at 0.25 ppm polymer dosage. After the minimum value further increase in the polymer dosage rapidly increases the turbidity value of the supernatant liquid.

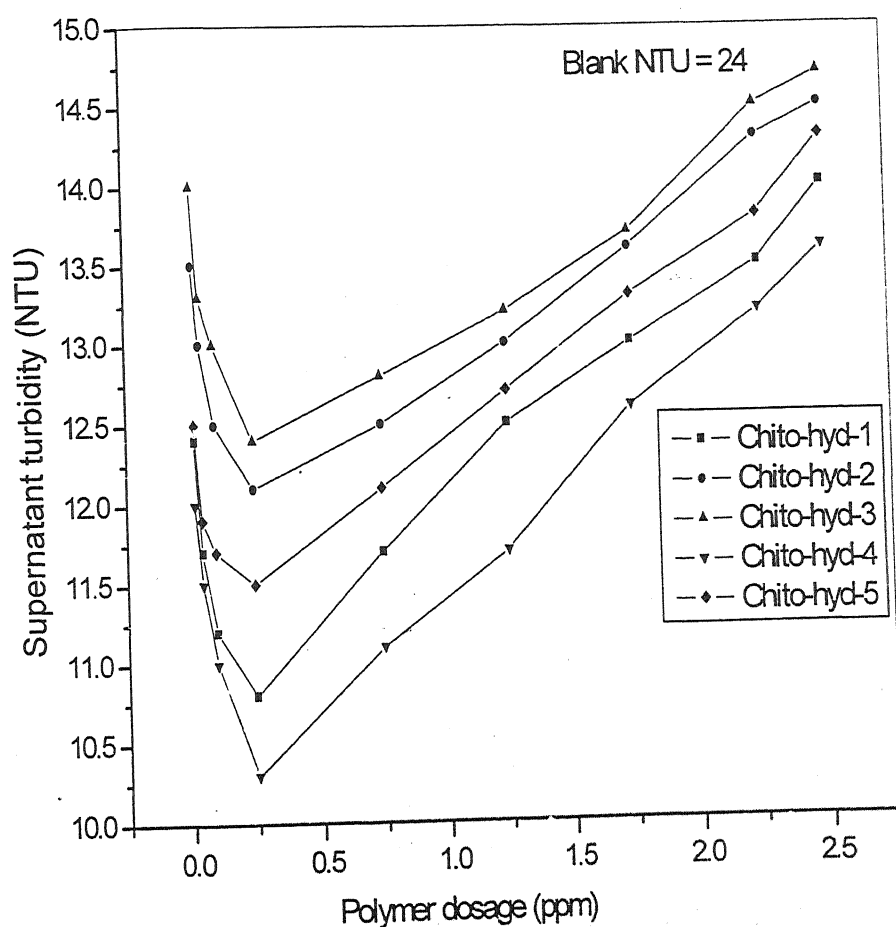


Figure 5.20 Jar test results for iron ore suspension (0.25wt %) with addition of partially hydrolyzed graft copolymers

5.7.2.3 Flocculation of the Silica Suspension

In jar test, the flocculation efficiency of all the partially hydrolyzed graft copolymers was compared in 0.25 wt% silica suspension. The turbidity of the supernatant liquid after flocculation has been plotted against polymer dosage and is given in **Figure 5.21**.

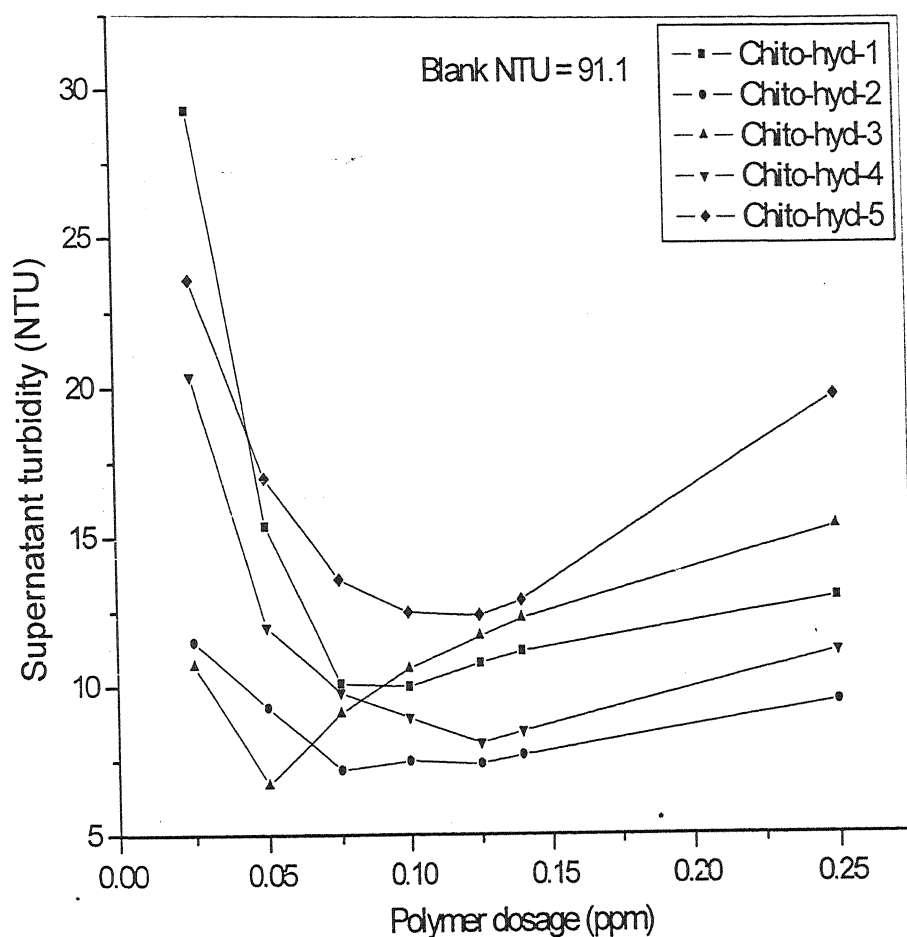


Figure 5.21 Jar test results for silica suspension (0.25wt %) with addition of partially hydrolyzed graft copolymers

The jar test results show that the Chito-hyd-4 has better flocculation efficiency among all the partially hydrolyzed graft copolymers. Here from the figure it can be easily seen that the partially hydrolyzed copolymers are not showing minimum value of turbidity at the same polymer dosage.

5.7.2.4 Flocculation of the Bentonite Suspension

In jar test, the flocculation efficiency of all the partially hydrolyzed graft copolymers was compared in 0.25 wt% bentonite suspension. The turbidity of the supernatant liquid after flocculation has been plotted against polymer dosage and given in **Figure 5.22**. The jar test results show that the Chito-hyd-4 has better flocculation performance among all the partially hydrolyzed graft copolymers. The curves show a minimum value of turbidity of the supernatant liquid for the bentonite suspension at 0.25 ppm. After the minimum value further increase in polymer dosage rapidly increases the turbidity value of the supernatant liquid.

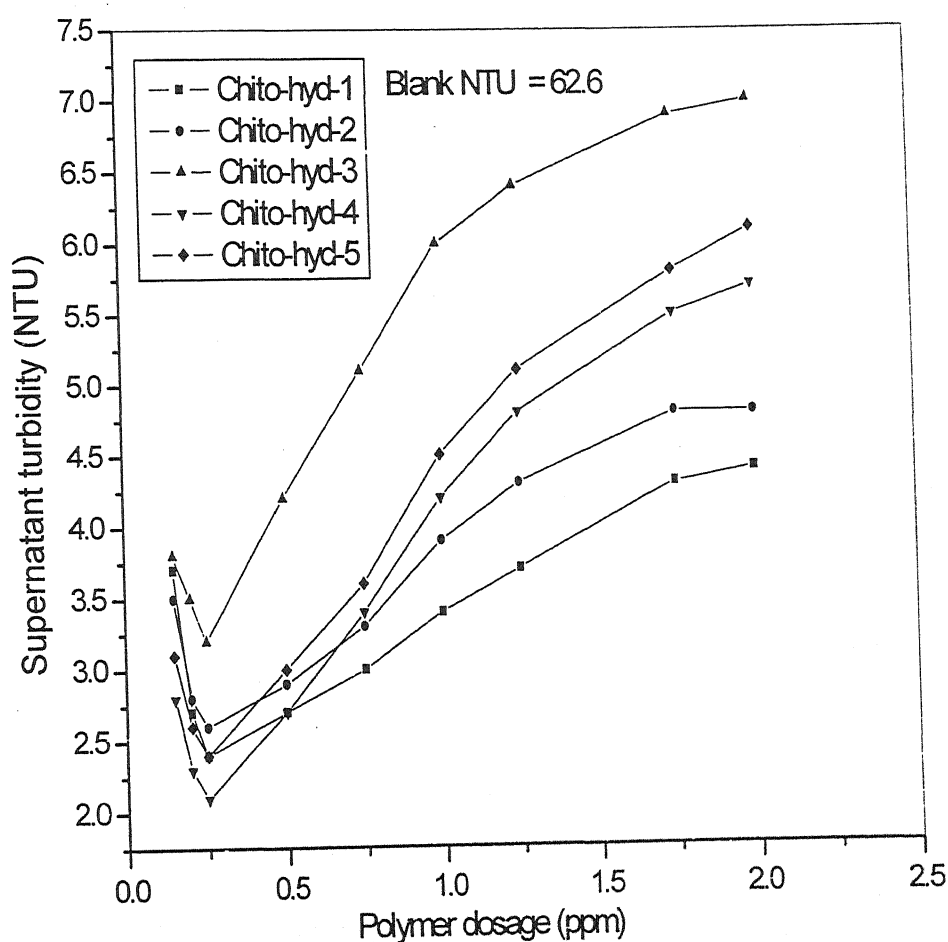


Figure 5.22 Jar test results for bentonite suspension (0.25wt %) with addition of partially hydrolyzed graft copolymers

5.8 SUMMARY

This chapter described the synthesis, characterization and flocculation properties of various grades of partially hydrolysed products. It is believed that hydrolysis straighten the polymer chain. To achieve closer approach of the hydrolyzed PAM chains to the suspended particles (*as per Singh's Easy Approachability Model*) various grades of products were prepared using different amount of NaOH solution. Here Chito-g-PAM6 was used as a base polymer for hydrolysis. The synthesized copolymers were characterized by different material characterization techniques such as elemental analysis, IR spectroscopy, SEM, thermal analysis, XRD. The above characterization techniques proved that hydrolysis has been accomplished. Thermal analysis showed that hydrolysis decreases the thermal stability of the product.

Figures 5.11 to 5.22 show that for kaolin and iron ore suspension, Chito-hyd-3 shows better flocculation performance among all the partially hydrolyzed graft copolymers and for silica and bentonite suspensions, Chito-hyd-4 shows better performance. These results can also be proved by settling rate measurement. Table 5.4 represents the settling rate of partially hydrolyzed graft copolymers for all the suspensions used. The table (Table 5.4) shows that Chito-hyd-3 has highest settling rate for kaolin and iron ore suspensions and Chito-hyd-4 has highest settling rate for silica and bentonite suspensions.

Table 5.4 Settling rate of Chito-g-PAM6 and partially hydrolyzed graft copolymers

Polymer	Settling Rate(cm /sec)			
	Kaolin	Iron Ore	Silica	Bentonite
Chito-g-PAM6	0.580	0.549	0.654	0.337
Chito-hyd-1	0.160	0.144	0.216	0.254
Chito-hyd-2	0.168	0.175	0.236	0.270
Chito-hyd-3	0.203	0.187	0.235	0.236
Chito-hyd-4	0.182	0.172	0.267	0.315
Chito-hyd-5	0.176	0.166	0.253	0.289

The Jar test result indicates that there is a competition between Chito-hyd-3 and Chito-hyd-4. Chito-hyd-3 shows lowest value of turbidity of the supernatant liquid for kaolin and silica

solutions and Chito-hyd-4 shows lowest turbidity value for iron ore and bentonite suspensions.

Experimental results show that there is a considerable amount of flocculation even though the polymer and contaminants are both highly negatively charged. This is because of the presence of negative charges on the polymer chains (due to the carboxylate groups). The electrostatic repulsion extends the polymer chains which causes increase in flocculation. Moreover, studies [349-358] showed that, the carboxylate groups of the hydrolyzed copolymers formed coordinate complex with the metal ions present on the particle surface. However, due to negative charges on the polymer chains and contaminant particles, there is tendency of electrostatic repulsion, which decreases the flocculation. Partially hydrolyzed graft copolymers cause flocculation due to these opposing effects and on optimum hydrolysis the maximum in flocculation obtained.

CHAPTER-VI

**CATIONIZATION
OF
CHITOSAN**

6.1 INTRODUCTION

Several methods have been used to remove inorganic and organic materials from water during wastewater treatments and a very common method is coagulation / flocculation followed by sedimentation or filtration.

Since organic and inorganic materials are nearly always anionic over a wide range of natural water pH, they interact strongly with cationic additives, especially hydrolyzed metal coagulant and cationic polymers.

The cationization of polymers provides a unique technique for modifying polymers to meet desirable end use requirements. The cationic polymers are of additional interest because of their potential use as viscosifiers in oil recovery operations, as flocculants and in beneficiation and treatment of mining and waste water etc. An important advantage of cationic polymers is that the polymeric substrate or backbone polymer and the inserted cationic moiety are held together by chemical bonding allowing the polymer backbone and cationic moiety to be intimately associated rather than as mere physical mixtures. The method of cationization has been utilized as a special technique in the recent decades for synthesizing new class of polymeric materials by modifying the physical and chemical properties of synthetic and natural polymers.

Water-soluble cationic polymers are a class of polyelectrolytes that derive their unique properties from the density and distribution of positive charges along the macromolecular backbone. These cationic polymers draw much attention in the field of waste water and paper making process due to strong attraction with the negatively charged colloidal particles. Vast quantities of research efforts have been directed towards the development of cationic polymer and the cationized polysaccharide being the majority of them. As a result, the study of the preparation and application of cationized polysaccharides has grown into a separate field of its own. A survey of literature based on cationic polysaccharides can be divided into three sections: (a) preparation, (b) characterization and (c) application.

Cationized polysaccharides have long been used to flocculate negatively charged colloidal particles from aqueous suspensions. For examples, Kerr and Neukon [374] reported the preparation of 2-aminoethyl ether derivative of starch, which readily flocculated aqueous suspensions of negatively charged colloids such as algin and carboxymethyl cellulose. Additionally, Paschall and Minkema [375] have described the preparation of cationized quaternary ammonium starch ether, which was found to be an excellent flocculating material in aqueous system. Audebert et al. [376] reported the flocculation behaviour of aqueous silica

suspensions by various cationized polyelectrolytes. They proposed that only bridging mechanism did not do the flocculation of silica. It was the electrostatic interactions, which played the main role in flocculation with cationic polyelectrolytes (patchwork model) [377].

According to the accepted theory [378], a two part electrical layer is formed at solid-liquid interface, when solid particles were in suspension. The first layer is called Stern Layer, whereas the second layer is called Diffused Layer. The potential difference between the Stern Layer and Diffused layer is known as Zeta Potential. When a cationic polymer enters into the suspension, it decreases the thickness of the Stern Layer and reduces the electrostatic repulsion between the particles. Thus it brings the particles close enough and it is the long chain polymer, which bridges the particles together and form flocs.

Ogedengbe [379] also confirmed that both the charge neutralization and bridging mechanism were playing significant role in flocculation by cationic polymers.

In paper making industries, cationic polymers are widely used as wet-end additives. They provide many benefits, which can be classified into four categories: (i) improvement of mechanical strength (ii) better retention of fines and fillers (iii) faster dewatering and (iv) reduction of wastewater pollution.

In this part of the study, a new series of cationic polymers was prepared by using chitosan as base material. N-(3-chloro-2-hydroxypropyl) trimethyl ammonium chloride (CHPTAC) was grafted onto chitosan. The synthesized material was characterized by several techniques.

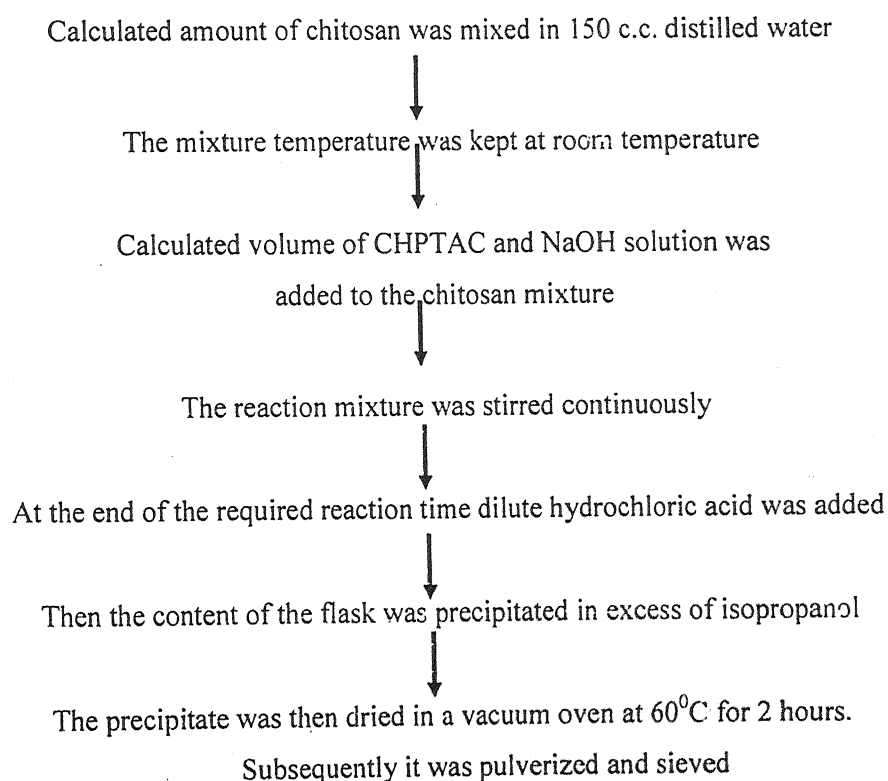
6.2 MATERIALS

Chitosan was a gift from Central Institute of Fisheries Technology, Cochin, India. N-(3-Chloro-2-hydroxypropyl) trimethyl ammonium chloride (CHPTAC) was procured from Lancaster Synthesis Company, England. Analytical grade of sodium hydroxide and hydrochloric acid were purchased from E Merck (India) Limited, Bombay, India. Isopropanol was supplied by S. D. Fine- Chem. Pvt. Ltd., India. All the above chemicals were used without further purification.

6.3 SYNTHESIS

Chitosan has been cationized by reaction between the chitosan and the cationic monomer N-(3-Chloro-2-hydroxypropyl) trimethyl ammonium chloride (CHPTAC) in presence of NaOH. The synthesis of cationized chitosan was performed in the following way:

Calculated amount of chitosan was poured into distilled water at room temperature with a constant stirring for 1 hour. A mixture of calculated amount of CHPTAC and NaOH was added to the polysaccharide mixture and the whole reaction mixture was stirred continuously for next 18 hours. The chitosan was cationized during the reaction. The initial pH of the reactants was 11. The pH was then lowered to 2 by adding hydrochloric acid to stop the cationization process [380]. The cationized product was then precipitated in isopropanol. It was then dried in a vacuum oven. Subsequently, it was pulverized and sieved. The synthetic route is shown in **SCHEME -I** (Figure 6.1).



SCHEME I

Figure 6.1 Schematic representation of the synthesis of cationized chitosan

In a similar way, various grades of cationized chitosan were synthesized by varying the reaction parameters. The details of synthetic parameters of cationized chitosan are summarized in Table 6.1.

Table.6.1 Synthesis details of cationized chitosan

Grades	Chitosan (MSU)	CHPTAC (mole)	Reaction Time (hr)	Reaction Temperature (°C)
Chito-cat-1	0.0044	0.00175	18hrs	33°C
Chito-cat-2	0.0044	0.0030	18hrs	33°C
Chito-cat-3	0.0044	0.00426	18hrs	33°C
Chito-cat-4	0.0044	0.0054	18hrs	33°C
Chito-cat-5	0.0044	0.0061	18hrs	33°C

6.4 CHARACTERIZATION OF THE CATIONIZED CHITOSAN

6.4.1 Elemental Analysis

Elemental analysis of cationized chitosan was undertaken with a Carlo Erba 1108 elemental analyzer. The estimation of only three elements, i.e. carbon, hydrogen and nitrogen, was undertaken.

6.4.2 Measurement of Intrinsic Viscosity

Viscosity measurements of polymer solutions were carried out with the help of Ubbelohde viscometer (CS/S: 0.00386). Intrinsic viscosities of all the cationized chitosan solutions were determined from the point of intersection of two extrapolated (to zero concentration) plots [381] i.e., inherent viscosity versus concentration (η_{inh} vs. C) and reduced viscosity versus concentration (η_{red} vs. C).

6.4.3 IR Spectroscopy

A Thermo Nicolet IR Spectrophotometer (Model – Nexus 870 FTIR) was used to study the infrared spectroscopy of the cationized chitosan. Spectroscopy grade KBr was used for pellet making.

6.4.4 Scanning Electron Microscopy (SEM)

The SEM study of the cationized product was performed in small granular forms. For this study JEOL, JSM-6360, SEM, (Model-7582) made in England has been used.

6.4.5 Thermal Analysis

The DSC analysis of all the samples was performed using Perkin Elmer, PYRIS Diamond DSC (USA). The TG/DTG analysis of all the samples was carried out with Stanton Redcroft (STA 625) thermal analyzer. Both the DSC and TGA analyses of the samples were performed starting from room temperature in an atmosphere of nitrogen. The heating rate was uniform in all cases at 10 deg/min.

6.4.6 X-ray Diffraction (XRD)

Cationized chitosan was subjected for XRD analysis. A PW 1840 diffractometer and PW 1729 X-ray generator (Philips, Holland) were used for this study producing CuK_α radiation. The powdered polymer samples were packed into a hole of 2 mm diameter in a small container made of Perspex [poly (methyl methacrylate)] about 1.5mm thick. The scattering angle (2θ) was varied from 10 to 50 degrees.

6.5. FLOCCULATION STUDIES

The flocculation studies for all the suspensions were carried out with addition of all the cationized products using settling test method and jar test method as described in the previous chapter (Chapter-IV & V).

6.6 RESULTS AND DISCUSSION

6.6.1 Synthesis and Intrinsic Viscosity Measurement

The synthesis details of cationized chitosan are in Table 6.1. Chitosan was cationized by incorporating a cationic moiety *N*-(3-chloro-2-hydroxypropyl) trimethyl ammonium chloride (CHPTAC) on their backbone in the presence of alkali. Various grades were developed for optimizing their flocculation characteristics. The synthesis parameter like amount of CHPTAC varied in order to observe the effect with varying number of inserted CHPTAC chains.

It should be mentioned here that even though CHPTAC has been grafted onto chitosan, all the CHPTAC grafted chitosan has lower intrinsic viscosity in comparison to the native chitosan polymer, [Table 6.2]. This may be due to the better solubility of the cationized chitosan. The CHPTAC grafted chitosan is quickly soluble in aqueous medium within a few minutes but chitosan is not fully soluble in aqueous medium. It is even not making solution easily in acid medium. The poor solubility of chitosan may be explained by partially crystalline structure and very tight hydrogen bonding between amino and hydroxyl groups [382].

Table 6.2 Intrinsic viscosities of various grades of cationized chitosan

Polymer	Intrinsic Viscosity (dl/gm) in 0.01(M) NaCl solution
Chitosan	31.668
Chito-cat-1	1.32
Chito-cat-2	1.51
Chito-cat-3	2.443
Chito-cat-4	2.736
Chito-cat-5	3.245

The mechanism for the cationization of the chitosan by CHPTAC is described in Figure 6.2. The reaction shows that the increase in the amount of the CHPTAC increases the number of branching on the backbone of the chitosan and thus making a comb like structure.

6.6.2 Elemental Analysis

The elemental analyses of different grades of CHPTAC grafted chitosan are given in **Table 6.3**. It is observed that there is an increase in the percentage of nitrogen in the CHPTAC grafted chitosan from Chito-cat-1 to Chito-cat-5, which can be accounted for by the presence of inserted CHPTAC chains. The higher percentage of nitrogen may be due to the increased CHPTAC content in the cationized product.

Table 6.3 Elemental analysis of cationized chitosan

Polymer	% of Carbon	% of Hydrogen	% of Nitrogen
Chitosan	40.36	6.68	7.65
CHPTAC	37.71	7.82	7.34
Chito-cat-1	29.1	6.45	6.01
Chito-cat-2	29.69	6.54	5.98
Chito-cat-3	29.31	6.50	5.96
Chito-cat-4	30.50	6.59	5.77
Chito-cat-5	29.65	6.57	5.51

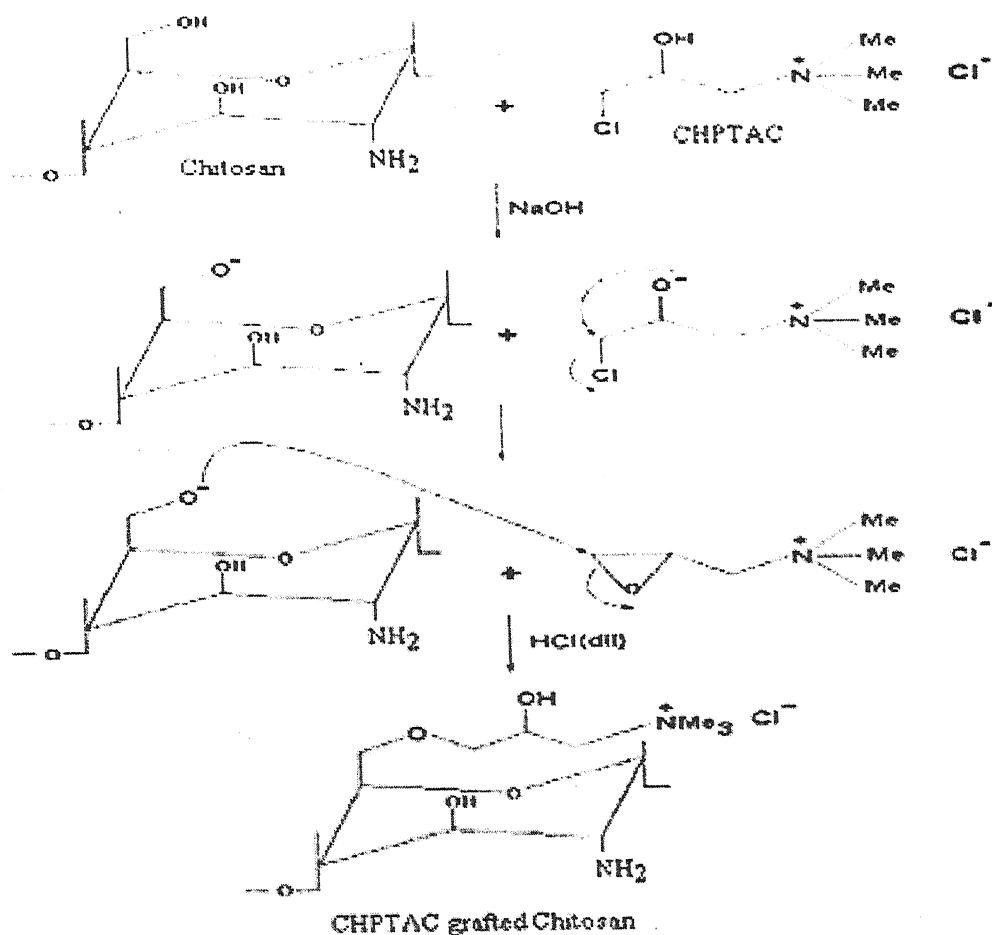


Figure 6.2 Mechanism for the synthesis of CHPTAC grafted chitosan

6.6.3 IR Spectroscopy

The cationisation of chitosan is conformed by IR spectroscopy. The IR spectra of CHPTAC, chitosan and CHPTAC grafted chitosan are shown in Figures 6.3, 6.4 and 6.5 respectively.

In CHPTAC, the broad band at $3206\text{--}3273\text{ cm}^{-1}$ is for O-H stretching vibration. The band has shifted to a little lower value due to the strong hydrogen bonding. The band around 2840 cm^{-1} is assigned to the C-H stretching. A strong band at 670 cm^{-1} is due to the C-Cl absorption band. In CHPTAC grafted chitosan, the broad band at 3435 cm^{-1} is due to the stretching mode of O-H groups. The broad band of O-H stretching absorption somewhat overlaps the N-H stretching band. The IR spectra of cationized chitosan showed a sharp peak at 1020 cm^{-1} , which is the characteristic peak of C-N bond. There is another peak at 1158 cm^{-1} . This is the characteristic peak for alkyl ether. The same peak is also present in chitosan due to the six

membered ring with oxygen but with a lower intensity. These peaks are evidence of chemical bonding of CHPTAC onto the backbone of chitosan.

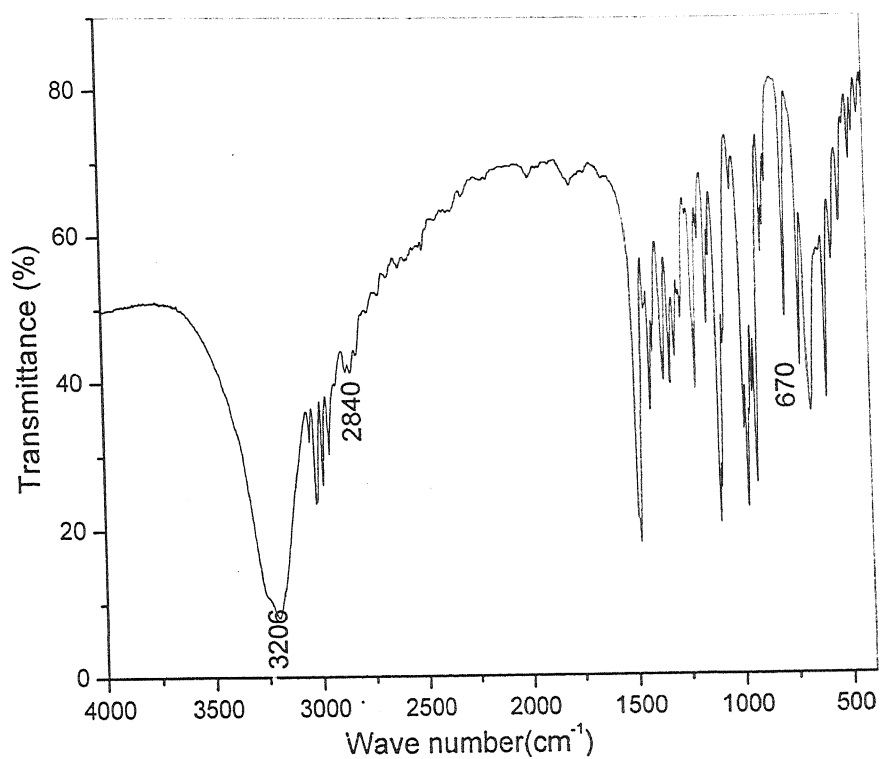


Figure 6.3 IR Spectrum of CHPTAC

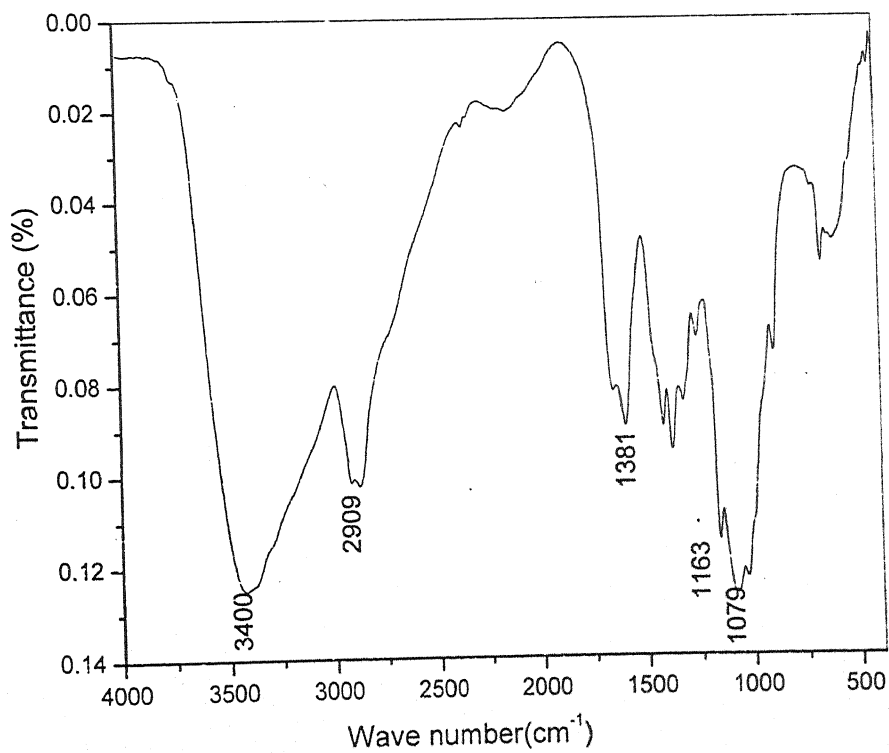


Figure 6.4 IR Spectrum of chitosan

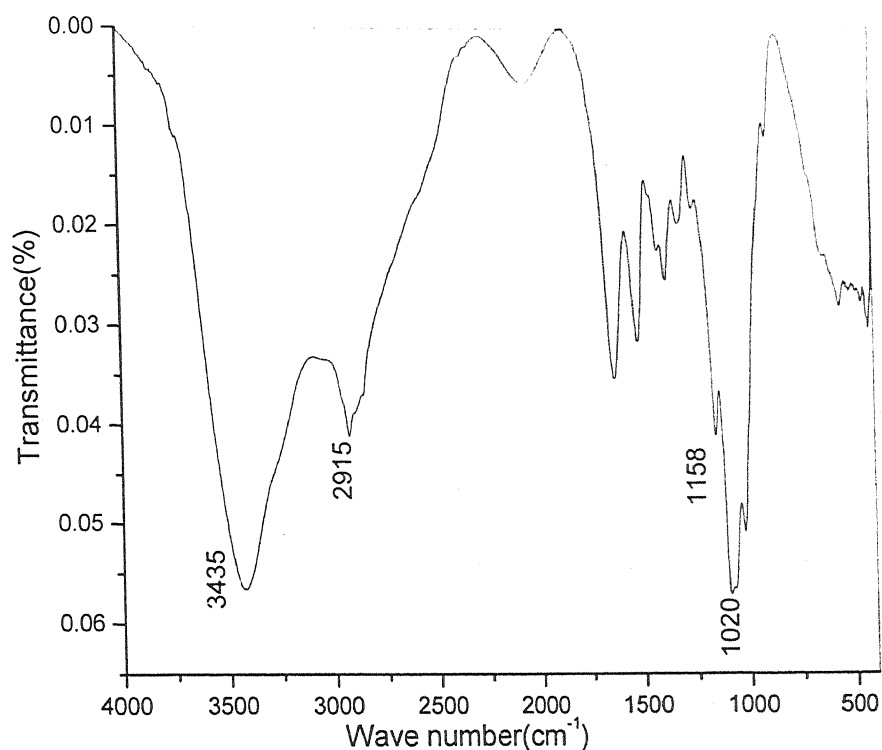


Figure 6.5 IR Spectrum of CHPTAC grafted chitosan

6.6.4 Scanning Electron Microscopy (SEM)

Figure 6.6 shows the scanning electron micrographs of the CHPTAC grafted chitosan copolymers. It can be easily seen from the figures that the grafting of CHPTAC considerably changes the surface morphology of the chitosan. SEM observation of the native chitosan reveals the flaky nature, wherein fibre strands deposition over the surface is visible. The flaky and fibrous nature of the chitosan was totally modified in the grafted materials. A discernible difference is seen in their surface topography. CHPTAC grafted chitosan shows a soft porous structure.

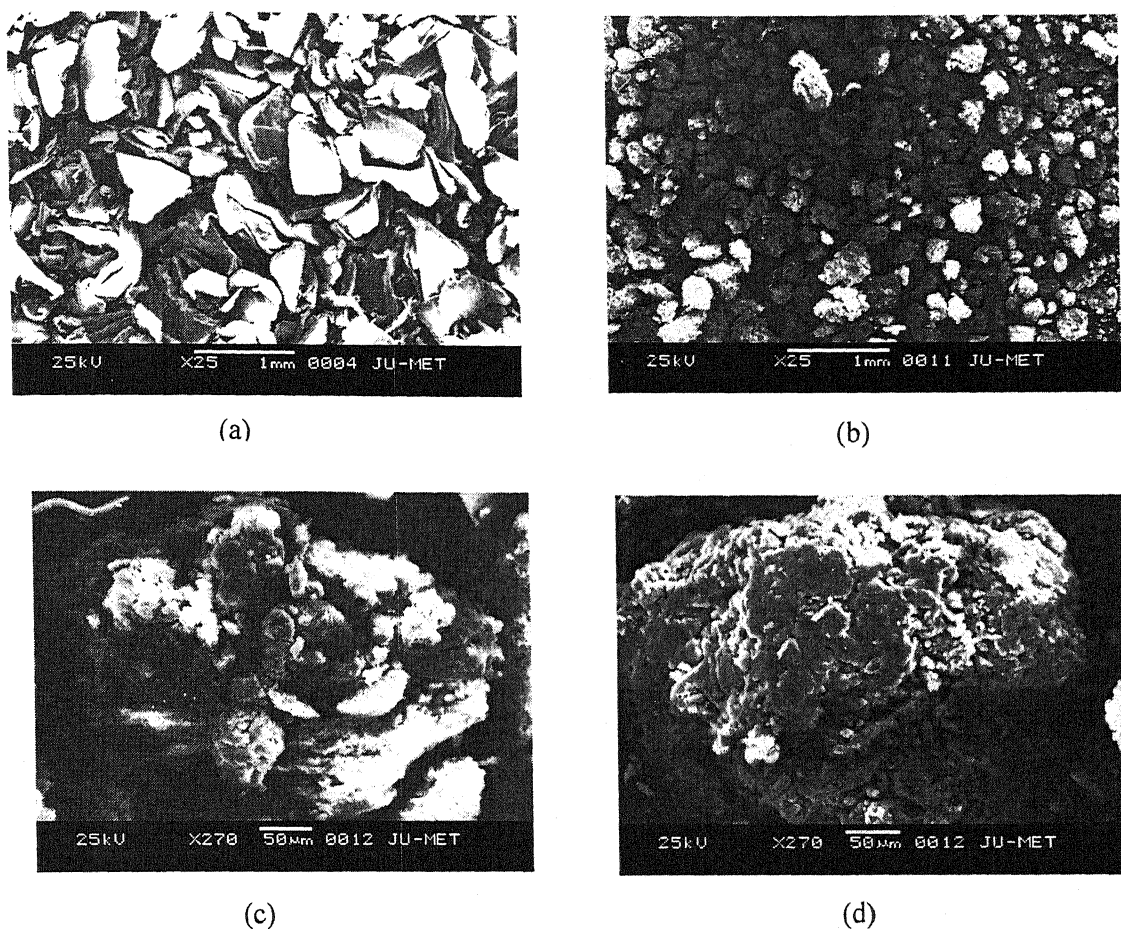


Figure 6.6 SEM of chitosan (a) and Chito-cat-2 (b, c, and d)

6.6.5 Thermal Analysis

6.6.5.1 Differential Scanning Calorimetry (DSC)

The **Figure 6.7** shows the DSC curve of chitosan and Chito-cat-2. The initial endothermic peak in chitosan represents the loss of water. Chitosan shows two endothermic peaks at around 144°C and 162°C . Chito-cat-2 shows one sharp peak at 147°C , which corresponds to the evaporation of the sorbed and bound moisture from the sample. A sharp endothermic peak at around 212°C is due to the decomposition of the bonded CHPTAC moieties. There is a broad exothermic peak in the $231\text{--}309^{\circ}\text{C}$ range, which corresponds to the degradation of

the backbone chitosan. An endothermic peak in the range of 317-450 °C is due to the decomposition of the degraded products.

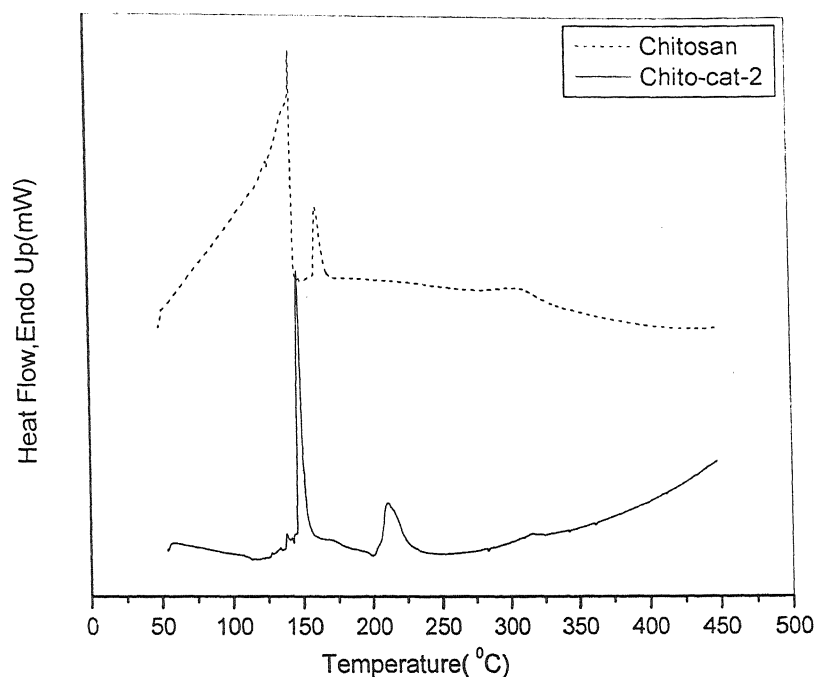


Figure 6.7 DSC Thermograph of chitosan and Chito-cat-2

6.6.5.2 Thermogravimetric Analysis (TG and DTG)

The TG curves of chitosan and the Chito-cat-2 are shown in Figure 6.8. The initial weight loss at approximately 147 °C was due to the evaporation of water. When CHPTAC was grafted onto chitosan, the thermal stability of the cationized product shifted to a lower value in comparison with chitosan. In order to examine the thermal behaviour of decomposition in detail, differential thermogravimetric (DTG) curves of these two polymers were compared. (Figure 6.9). The maximum decomposition temperature of chitosan appeared at 298 °C. This is ascribed to a complex process including dehydration of the polysaccharide rings and depolymerization of the acetylated and deacetylated units of the polymer [383,384]. The Chito-cat-2 decomposes at a lower temperature (206 °C, 243 °C). This could be attributed to the disintegration of the intermolecular attraction among the chitosan chains by incorporation of the CHPTAC moiety.

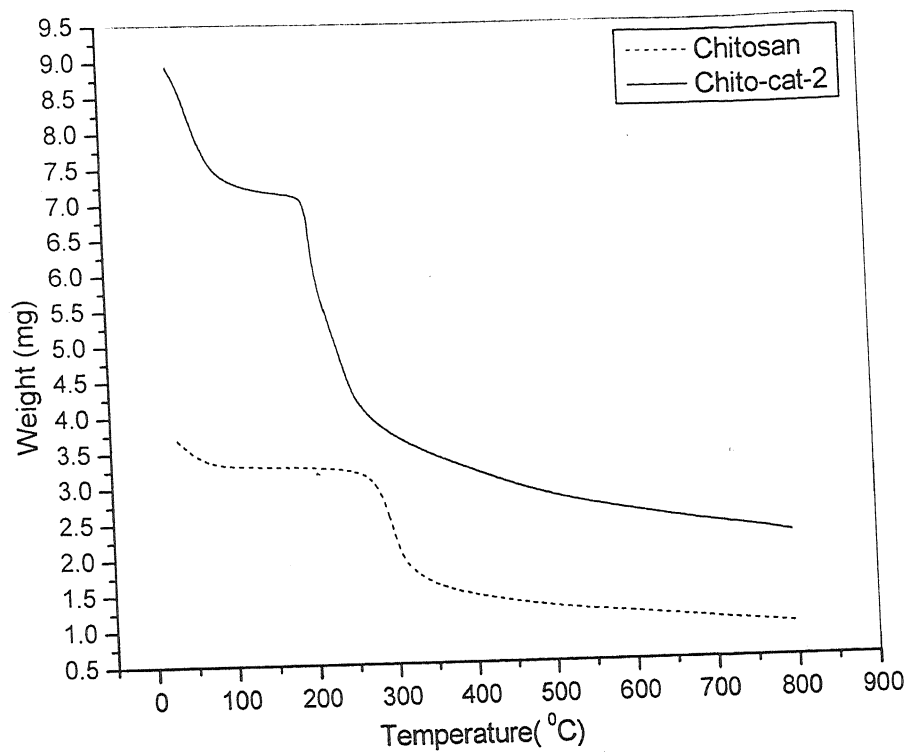


Figure 6.8 TG Curves of chitosan and Chito-cat-2

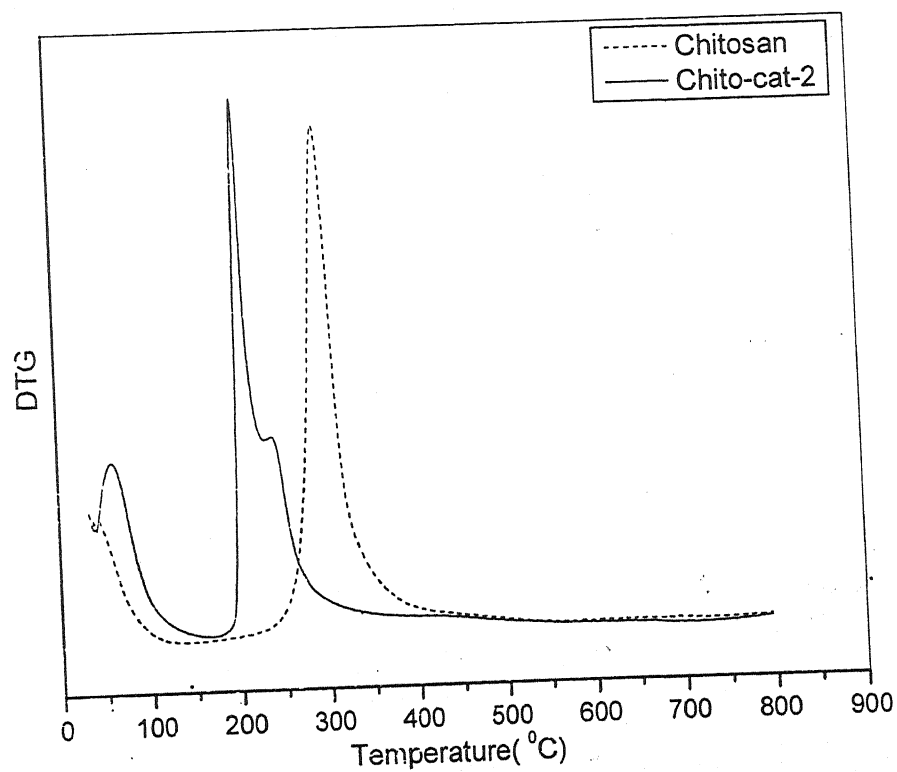


Figure 6.9 DTG Curves of chitosan and Chito-cat-2

6.6.6 X-ray Diffraction

Figure 6.10 (a, b and c) shows the X-ray diffraction pattern of chitosan, CHPTAC and CHPTAC grafted chitosan respectively.

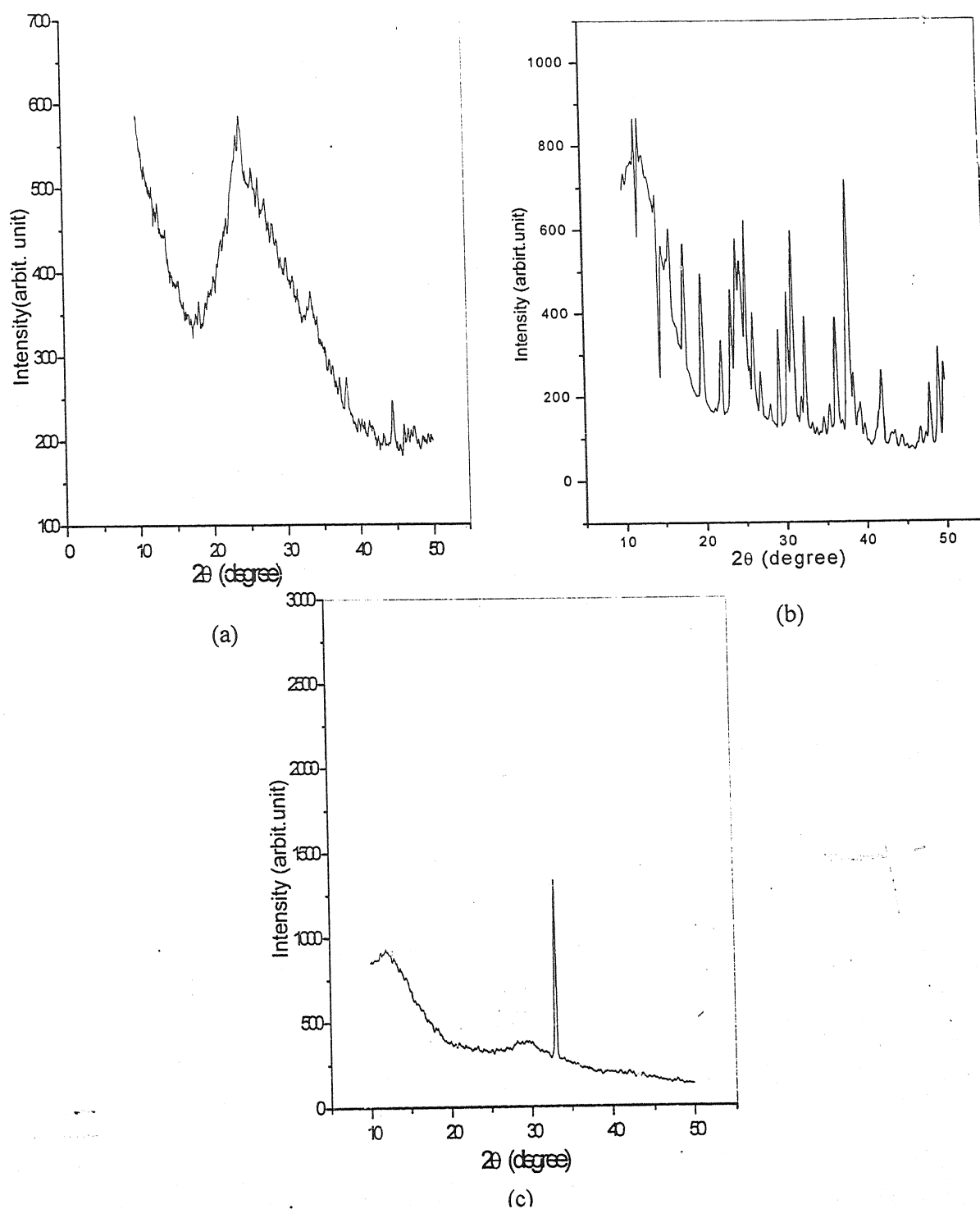


Figure 6.10 X-ray diffraction of (a) chitosan, (b) CHPTAC and (c) Chito-cat-2

From **Figure 6.10 (a)**, it is obvious that chitosan exhibits low crystallinity and is showing a characteristic broad peak at around 20 degree. A peak at 33 degree indicates the presence of hydroxyapatite salt [23-25]. However, the cationized product [**Figure 6.10 (c)**] does not have any peak at around 20 degree, which indicates the amorphous nature of the cationic material, but it has a sharper peak at 33 degree, which indicates the presence of crystalline hydroxyapatite. It should be noted here that with treatment of alkali, the crystallinity of the hydroxyapatite salt increases. This indicates the random chemical linkage of CHPTAC onto the backbone of chitosan, destroying its partial crystallinity. The crystallinity of this inorganic salt also increases with heating. The sharp peaks found in CHPTAC monomer [**Figure 6.10 (b)**] are also absent in the cationic product.

6.7. FLOCCULATION STUDIES

The flocculation performances of all the cationized chitosan (Chito-cat-1 to Chito-cat-5) were compared in kaolin, iron ore, silica and bentonite suspensions. The characteristics of all the suspensions are given in Chapter-IV.

6.7.1 The Settling Tests

The settling tests for synthesized cationized polysaccharides were carried out in all the four colloidal suspensions, namely, kaolin, iron ore, silica and bentonite. In each case, the settling time was plotted against the height of interface. The flocculation performance of a particular polymer could be correlated with the settling velocity. The higher the settling velocity of the floc containing contaminants, the higher will be its flocculation performance.

6.7.1.1 Flocculation of the Kaolin Suspension

Figure 6.11 represents the flocculation behaviour of various grades of cationized chitosan in 3 wt% kaolin suspension. It has been observed that the flocculation performance of Chito-cat-2 is better than all the other cationized chitosan solutions.

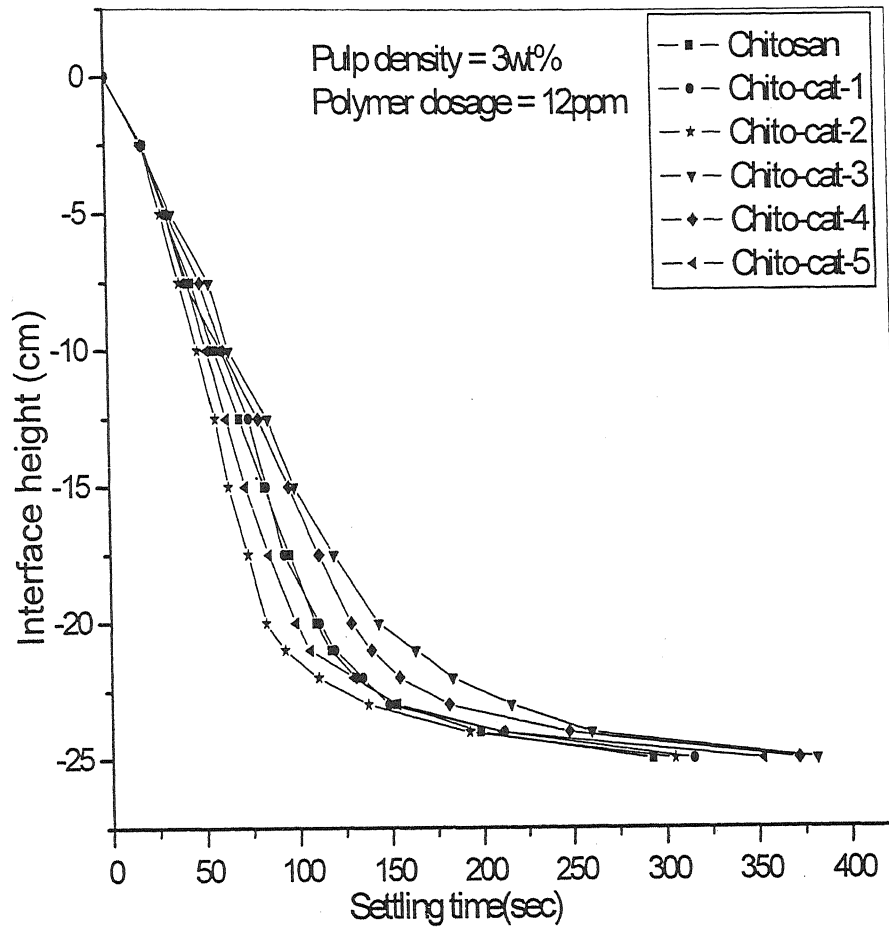


Figure 6.11 Settling curves for Kaolin suspension with all the cationized chitosan solutions

6.7.1.2 Flocculation of the Iron Ore Suspension

The flocculation performance of iron ore suspensions was measured with all the grades of cationized chitosan solutions. The pulp density was fixed at 3wt% and the optimum polymer dose was experimentally determined 5 ppm. It can easily observe from the curves (Figure-6.12) that the settling behaviour of iron ore is faster with the addition of chito-cat-2 compared to other cationized chitosan solutions.

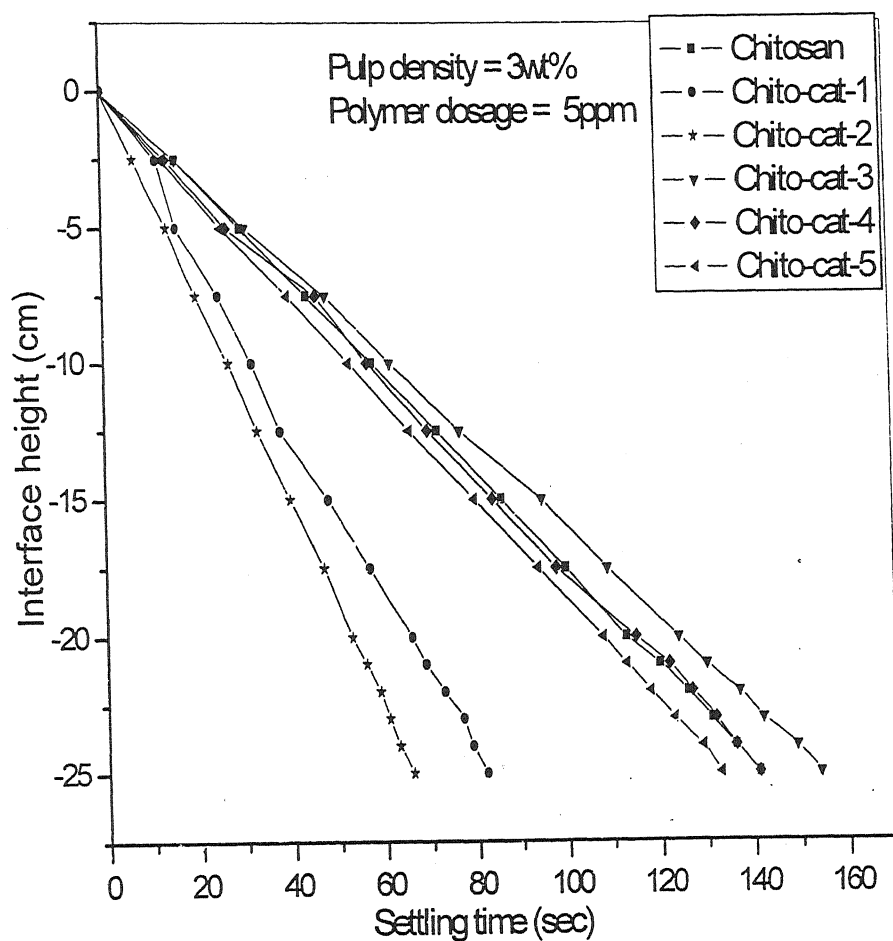


Figure 6.12 Settling curves for iron ore with addition of all the cationized chitosan solutions

6.7.1.3 Flocculation of the Silica Suspension

The flocculation performance for the Silica suspension was done with addition of all the cationic graft copolymers. Figure 6.13 represents the flocculation performance of all the cationic copolymers for Silica suspension. The pulp density was made fixed at 3wt% and the polymer dosage was optimized at 4ppm. Here it can be seen from the figure that Chito-cat-2 shows better performance than all the other copolymers.

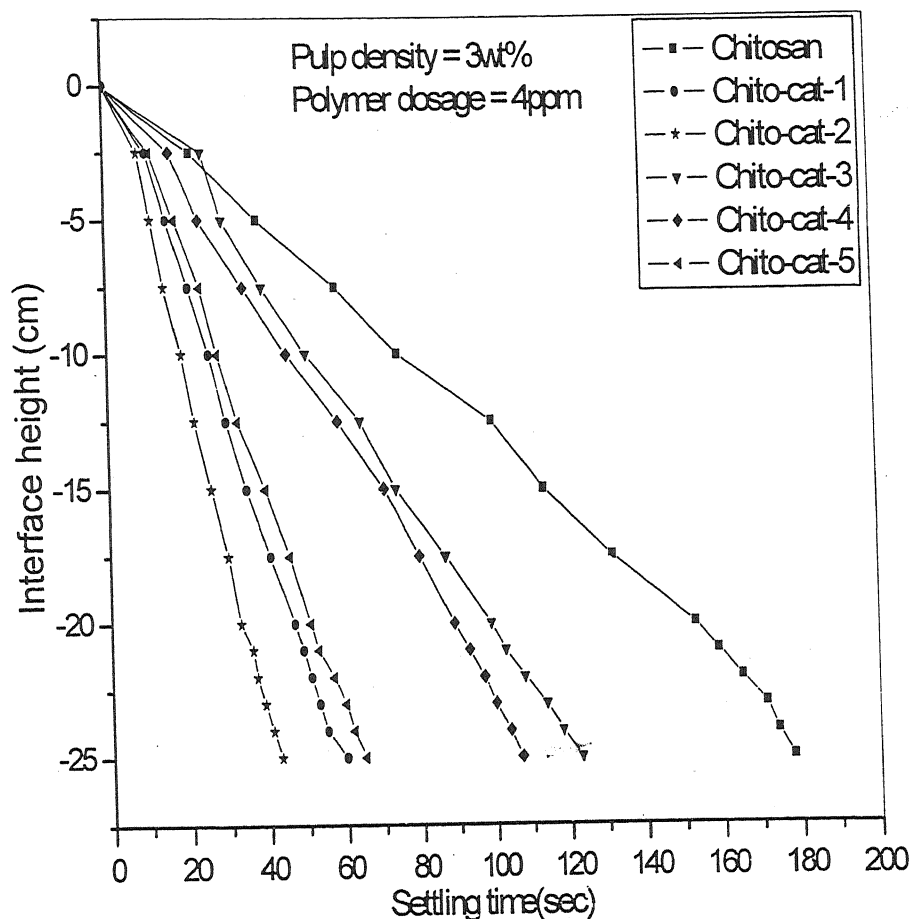


Figure 6.13 Settling curves for silica suspension with addition of all the cationized chitosan solutions

6.7.1.4 Flocculation of the Bentonite Suspension

The flocculation efficiency for the bentonite suspension is represented in Figure 6.14. To achieve a measurable settling rate the pulp density was taken 1 wt%. Here it can be observed from the figure that Chito-cat-2 shows better flocculation performance for bentonite suspension than other cationized chitosan solutions.

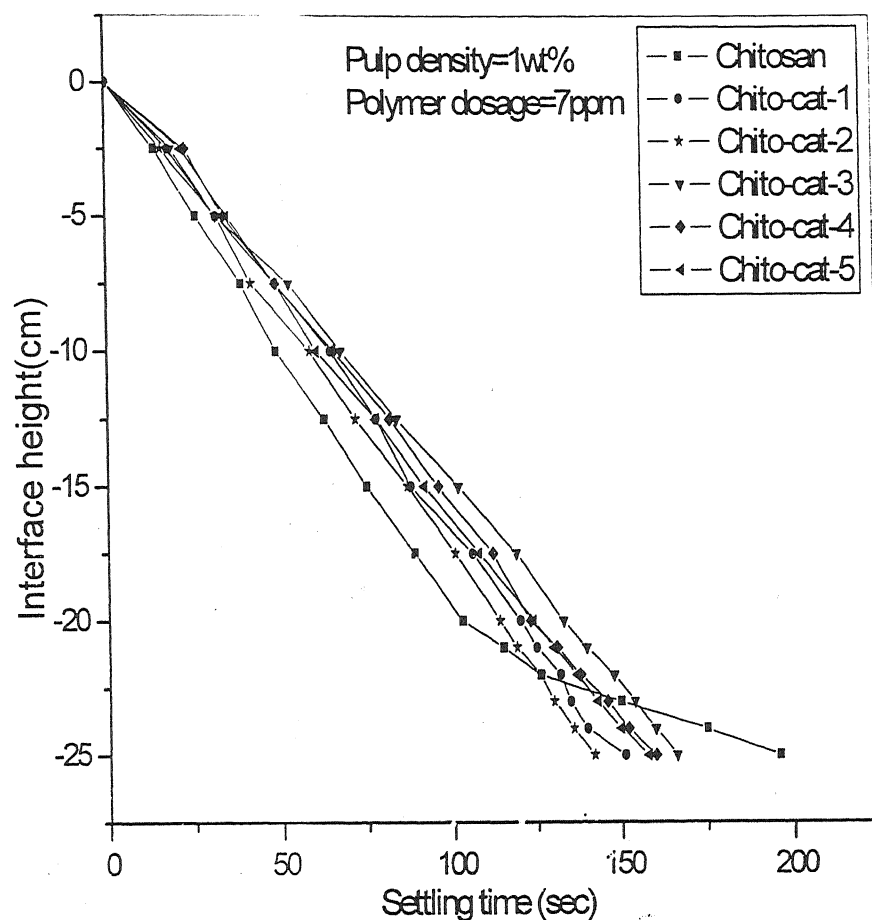


Figure 6.14 Settling curves for bentonite suspension with addition of all the cationized chitosan solutions

It can be seen from Figure 6.14 that the initial rate of settling of chitosan is higher in comparison to Chito-cat-2. But after 20 cm of interface height the settling rate of chitosan decreases. This could be due to the large but loose flocs, which hinder the settling rate of the bentonite suspension.

6.7.2 Jar Tests

In Jar Test method the flocculation efficiency of all the cationized chitosan was compared in 0.25wt% of all the suspension. The turbidity of the supernatant liquid after flocculation has been plotted against cationized chitosan dosage at room temperature (33 °C).

6.7.2.1 Flocculation of the Kaolin Suspension

The jar test for kaolin suspension was performed with addition of all the cationized chitosan solutions (Figure 6.15). It is found that the Chito-cat-5 shows better flocculation performance among all the cationized chitosan in kaolin suspension. The flocculation efficiency increases with increase of polymer dosage and reaches at minimum turbidity value, after that, increase in polymer dosage increases turbidity value.

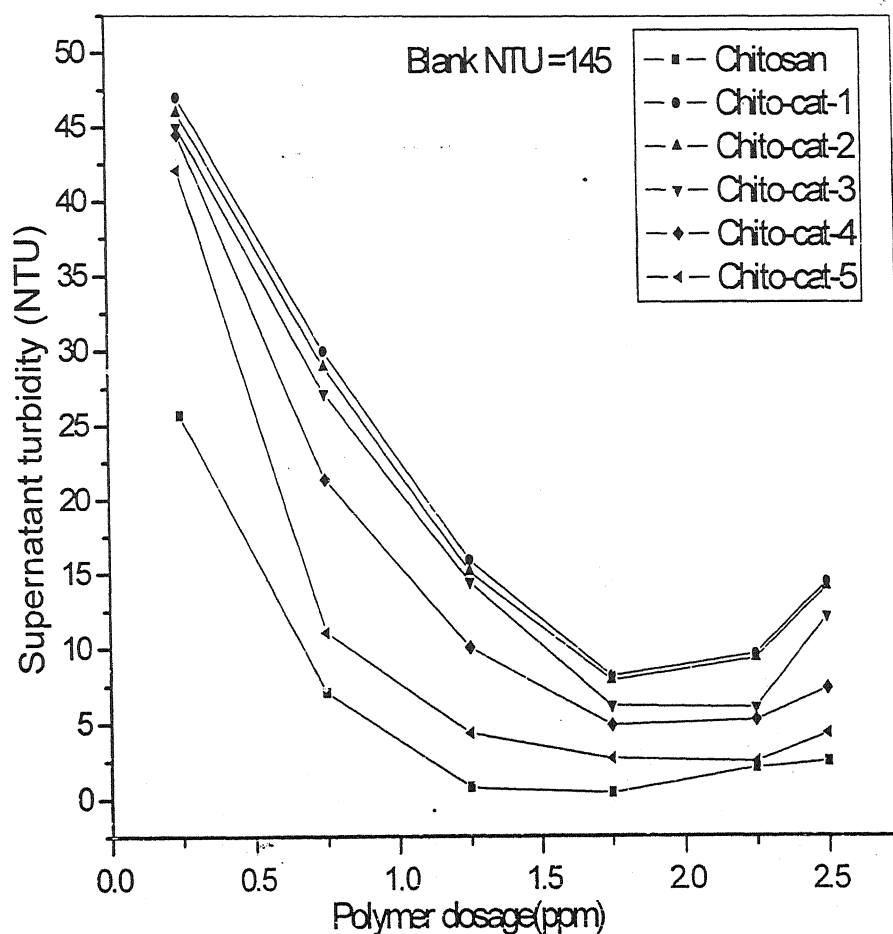


Figure 6.15 Jar test results for kaolin suspension (0.25wt%) with addition of all the cationized chitosan solutions

6.7.2.2 Flocculation of the Iron Ore Suspension

Figure 6.16 represents the flocculation efficiency of the cationized chitosan solutions in 0.25wt% iron ore suspension. Here Chito-cat-2 shows better flocculation performance among all the cationized chitosan solutions. It can be easily observed from the figure that the flocculation performance of the cationized chitosan increases with increase with the polymer dosage upto a certain value and after that increase in polymer dosage decrease the flocculation efficiency rapidly.

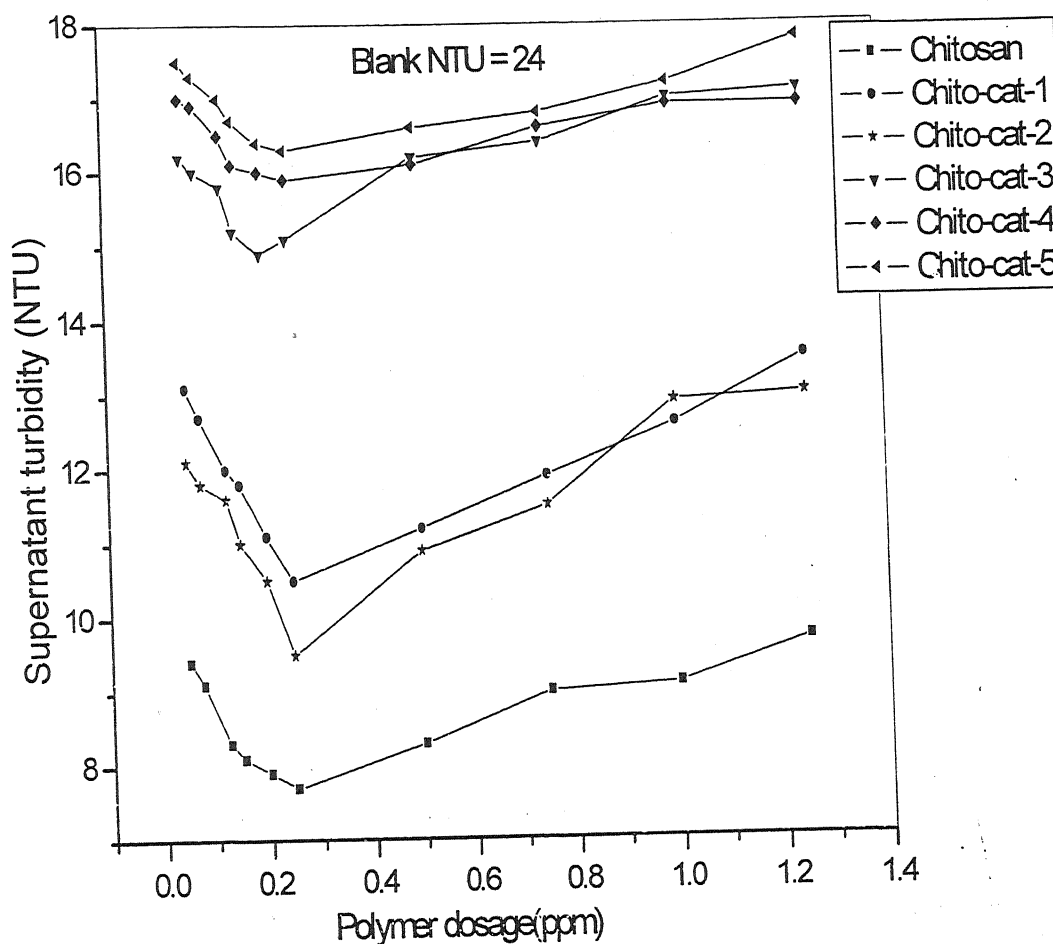


Figure 6.16 Jar test results for kaolin suspension (0.25wt%) with addition of all the cationized chitosan solutions

6.7.2.3 Flocculation of the Silica Suspension

Figure 6.17 represents the flocculation efficiency of all the cationized chitosan solutions in silica suspension.

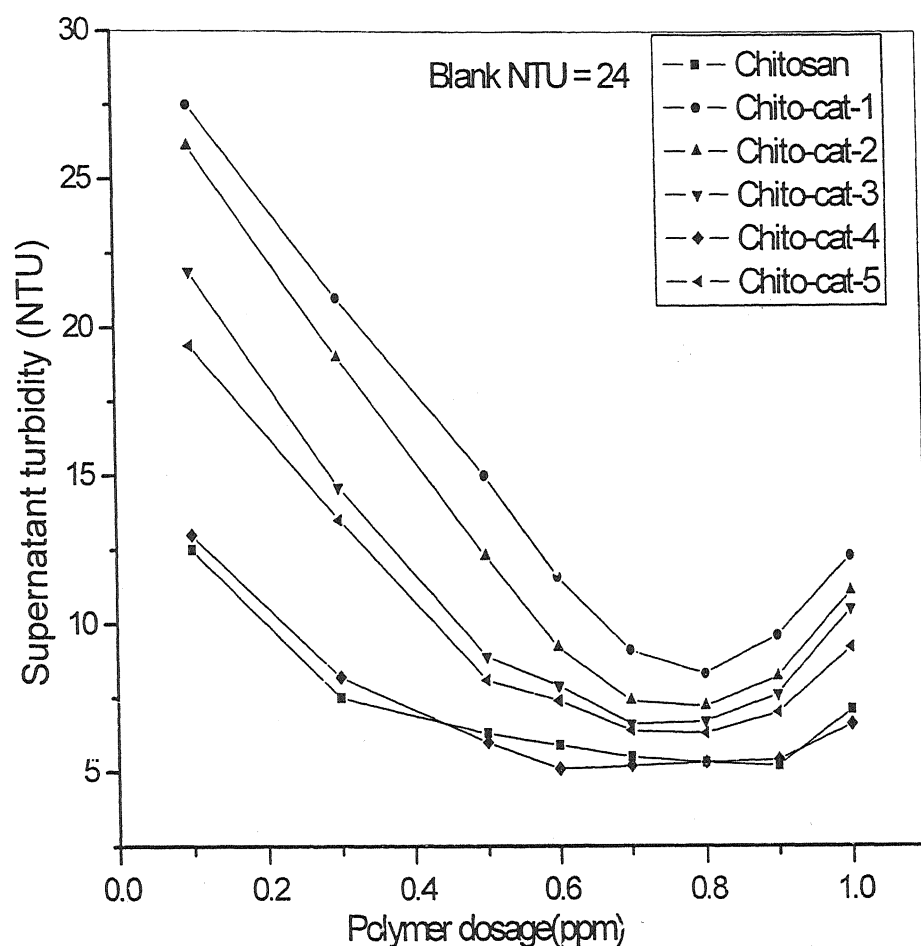


Figure 6.17 Jar test results for silica suspension (0.25wt%) with addition of all the cationized chitosan solutions

It can be seen from the Figure 6.17 that Chito-cat-4 shows the best performance among all the cationized chitosan solutions. For silica suspension, the best clarification of the supernatant liquid is seen at relatively higher polymer dosage.

6.7.2.4 Flocculation of the Bentonite Suspension

The flocculation performance of all the cationized chitosan solutions was studied in bentonite suspension and represented in **Figure 6.18**. A closer look shows that Chito-cat-2 is showing relatively better performance among all the cationized chitosan solutions.

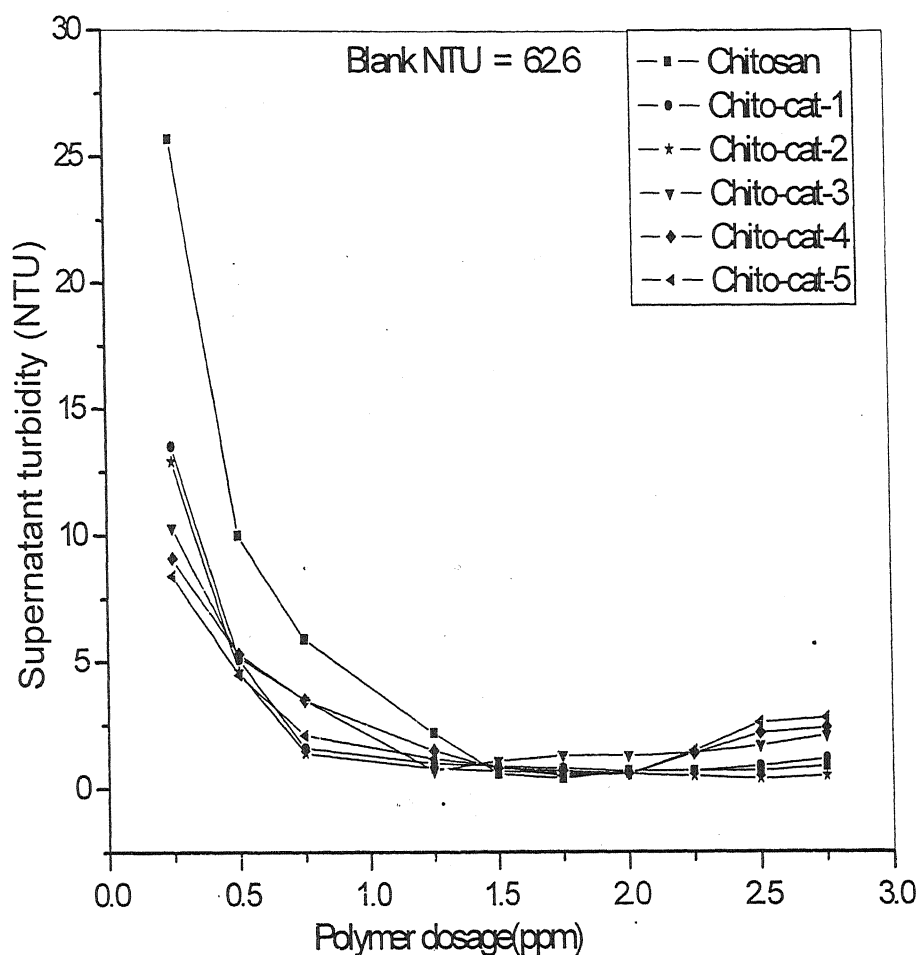


Figure 6.18 Jar test results for bentonite suspension (0.25wt) with addition of all cationized chitosan solutions

It can be seen from all the above figures (**Figure 6.15 - 6.18**) that the flocculation efficiency of all the cationized chitosan increases with increase in polymer dosage upto a certain value and after that further addition decreases the flocculation.

6.8 SUMMARY

This chapter described the synthesis of different grades of cationized chitosan. N-(3-chloro-2-hydroxypropyl) trimethyl ammonium chloride (CHPTAC) has been chemically bonded onto the chitosan backbone. The reaction was carried out in alkaline medium. The reaction parameters were varied to get better flocculent. The best grade was characterized with different material characterization techniques such as elemental analysis, IR spectroscopy, SEM, thermal analysis, etc. The change in elemental analysis along with the presence of C-N band in IR spectrum clearly proved the grafting of CHPTAC onto chitosan backbone. Thermal analysis indicates that the thermal stability of chitosan decreases with grafting of CHPTAC moiety.

Flocculation properties of all these cationized products were investigated by settling test and jar test measurement method. Here four different types of particles (kaolin, iron ore, silica and bentonite) were used for flocculation measurement. Chito-cat-2 showed faster settling rate among all the cationized products (Table 6.4). But jar tests results indicates that chitosan is a better water-clarifying agent than all the CHPTAC grafted chitosan. This may be due to the amine groups in the chitosan backbone, which has higher affinity towards the particles.

Table 6.4 Settling rate of chitosan and cationized chitosan

Polymer	Settling Rate (cm /sec)			
	Kaolin	Iron Ore	Silica	Bentonite
Chitosan	0.150	0.1735	0.128	0.192
Chito-cat-1	0.187	0.306	0.430	0.166
Chito-cat-2	0.236	0.377	0.582	0.172
Chito-cat-3	0.145	0.162	0.200	0.148
Chito-cat-4	0.156	0.177	0.220	0.154
Chito-cat-5	0.207	0.187	0.370	0.162

CHAPTER-VII

**CONCLOSIONS
AND
FUTURE SCOPES**

7.1 CONCLUSIONS

Chitosan has wide variety of applications in mineral processing, biomedical industries and agriculture industries etc. It has been established in the group of R.P.Singh that physical properties of polysaccharides can be drastically improved by grafting and cationization of polysaccharides. In the present investigation alternate has been made to improve the flocculation characteristics of chitosan. Two series of graft copolymers were synthesized by varying acrylamide and CAN concentration. The graft copolymers were characterized with a number of material characterization techniques such as elemental analysis, IR spectroscopy, SEM, thermal analysis, viscometry and XRD. The flocculation characteristics of chitosan and all the graft copolymers were studied in aqueous suspension of kaolin, iron ore, silica and bentonite particles.

On hydrolysis of the graft copolymers, the amide groups on the graft copolymers are converted to carboxylate groups. As the hydrolyzed grafted chitosans have negative charge, they repel each other and straighten the side chains. To investigate the effect of hydrolyzed graft chitosan on flocculation performance, a series of hydrolysed grades (Chito-hyd-1 to Chito-hyd-5) were prepared using the graft copolymer having the best flocculation characteristics (Chito-g-PAM6). The hydrolyzed products were also characterized by various material characterization techniques mentioned above.

It is found that in aqueous suspension, both organic and inorganic contaminants are mostly anionic. They interact strongly with cationic additives, especially cationic polymers. To investigate the effect of cationic polymers on flocculation performance, CHPTAC has been grafted onto the backbone of chitosan. To examine the effect of cationicity, a series of CHPTAC grafted chitosan (Chito-cat1 to Chito-cat-5) were prepared by varying the CHPTAC concentration. All these cationized copolymers were characterized by various material characterization techniques.

The following conclusions are drawn from these investigations.

1. The variation in the synthesis parameters such as monomer and initiator concentration leads to the variation in the intrinsic viscosity of the graft copolymers (Chito-g-PAM1 to Chito-g-PAM7). A low concentration of initiator (CAN) creates a fewer number of radical sites on the backbone of chitosan as against a high concentration of CAN. As a result, for the same moles of acrylamide, the grafted chains should be longer in case of former than shorter in case of the latter. For two polymers of approximately same

molecular weight, a branched polymer will have a lower intrinsic viscosity value, which can be attributed to the lower hydrodynamic volume as compared to its linear counterpart. Further, along a series of branched polymers, the longer the branches, higher will be the intrinsic viscosity and vice versa. This has been experimentally observed that Chito-g-PAM6 has highest intrinsic viscosity (8.09 dl/g) among the graft copolymers.

2. During partial alkaline hydrolysis of PAM grafted chitosan, it is possible to control the carboxyl content by varying the reaction parameters like concentration of alkali, reaction time and temperature.
3. Results of elemental analysis show that chitosan has considerable amount of nitrogen content (7.65 %). The nitrogen content is due to the presence of amino groups in chitosan. It has also been found that there is a considerable increase in the percentage of nitrogen in the graft copolymers, which is accounted due to the presence of grafted PAM chains. The elemental analysis study of the hydrolysed products indicated that the percentage of nitrogen decreases in comparison with the corresponding graft copolymer (Chito-g-PAM6) as the amide groups are converted to carboxylate groups, which has also been observed in measuring the N.E values. The elemental analysis of the cationized products showed that there is a gradual decrease in the percentage of the nitrogen from Chito-cat-1(6.01%) to Chito-cat-5 (5.51%). This is due to the fact that with incorporation of the CHPTAC monomer on the backbone of chitosan, both the amount of carbon and nitrogen increases. But the increase of the amount of carbon is higher than the amount of nitrogen.
4. The hydrolyzed products are not giving a homogenous solution in aqueous medium and therefore it is found not feasible to measure the intrinsic viscosity of these polymers with the viscometer. The cationic products are readily soluble in aqueous medium and showed lower intrinsic viscosity than the corresponding chitosan polymer.
5. Comparison of the IR spectra of chitosan, PAM and PAM grafted chitosan (Chito-g-PAM6) proves the grafting of PAM onto chitosan. The hydrolysis of the grafter product is proved by the presence of the characteristic peaks for the carboxylate groups at 1457 cm^{-1} and 1640 cm^{-1} . The IR spectrum of cationized chitosan shows a sharp peak at 1020 cm^{-1} , which is the characteristic peak of C-N bond. There is another peak at 1158 cm^{-1} , which is the characteristic peak for alkyl ether. The same

peak is also present in chitosan due to the six membered rings with oxygen but with a lower intensity. These all peaks are evidence of grafting of CHPTAC onto chitosan.

6. Scanning electron micrograph of Chito-g-PAM6 shows a distinctive change of surface morphology in comparison to chitosan. On hydrolysis, the fibrous structure of Chito-g-PAM6 changes remarkably. Cationization of chitosan changes the flaky structure of chitosan to soft porous structure.
7. Thermal analysis of PAM grafted chitosan shows an improvement of thermal stability of the grafted product in comparison to chitosan. DSC thermograph of chitosan shows a slope just before the endothermic peak around 70 °C-125 °C. The slope is believed to be due to the local relaxation of the chitosan backbone. This slope is absent in Chito-g-PAM copolymer. The local relaxation of chitosan molecules was interrupted by the random attachment of PAM chains on the backbone of the chitosan. Hydrolyzed products have lower thermal stability than Chito-g-PAM6. Cationic chitosan is thermally less stable in comparison to native chitosan.
8. X-ray diffraction study shows that the crystallinity decreases in all graft copolymers, hydrolyzed graft copolymer and cationized chitosan in comparison to chitosan.
9. Results of the flocculation studies indicate that the graft copolymers have better flocculation performance in comparison to the ungrafted chitosan. The better flocculating performance of the graft copolymers over the chitosan is due to the presence of long dangling PAM chains in the graft copolymers, which gives effective bridging. Bridging takes places by adsorption of polymer molecules at more than one site on a particle or at sites on different particles. In the case of graft copolymers due to the easier approachability of the PAM chains, as per Singh's Easy Approachability Model, can easily bind the colloidal particles through bridging and can form flocs. This type of intense bridging is not possible in case of linear polymers. When all the graft copolymers were compared, Chito-g-PAM 6 exhibits best flocculation performance among all the grafted products. This may be due to the presence of fewer but longer PAM chains, which enhances the flocculation efficiency.
10. The hydrolyzed products have lower flocculation performance than the corresponding graft copolymer (Chito-g-PAM6). Among all the hydrolyzed graft copolymers, Chito-hyd-3 shows better flocculation performance for kaolin and iron ore suspensions. Whereas Chito-hyd-4 shows better flocculation characteristics for silica and bentonite

suspensions. This is due to the competition between the attraction and repulsion interactions among the polymer and particles.

11. Cationized chitosans can approach closer to the particle surface and can bound the particles tightly as in aqueous solution most of the particles remain negatively charged in neutral pH. Among the cationized chitosan, Chito-cat-2 shows best flocculation performance in aqueous suspension of all the particles. The settling rate of cationized chitosan is higher compare to chitosan. But in case of jar test the native chitosan is better than the cationized chitosan.

7.2 FUTURE SCOPE OF THE WORK

In future the work will be comprised of the following:

1. Comparison of the flocculation performance of unhydrolyzed, hydrolyzed and cationized chitosan with commonly available flocculation.
2. Investigation of the rheological properties of unhydrolyzed hydrolyzed and CHPTAC grafted chitosan.
3. To study of molecular weight distribution of unhydrolysed, hydrolyzed and cationized chitosan.

REFERENCES

REFERENCES

1. Sorensen, J. and Larsson, S.G. (1992). Chemical of Water and Wastewater treatment II, Proceedings of the Fifth Gothenburg Symposium, Nice, France, 181.
2. Lawler, D.F. (1997). *Water Sci Technol*, (36), 15.
3. Stauber, J.L.; Florence, T.M.; Davies, C.M.; Adams, M.S. and Buchanan, S.J. (1999). *J Am Water Works Assoc*, 91 (II), 84.
4. McLachlan, D.R.C. (1995). *Environmentrics*, (6), 233.
5. Singh, R.P. (1990). In Encyclopedia of Fluid Mechanics: Polymer Flow Engineering, I.P. Cheremisinoff (Ed), Gulf Publishing Houston, USA, (9), 425.
6. Singh, R.P. (1995). Polymers and Other Advanced Materials: Emerging Technologies and Business Opportunities, J.E. Mark and T.J. Fai (Eds), Plenum Press, New York, 227.
7. Singh, R.P.; Karmakar, G.P.; Rath, S.K.; Karmakar, N.C.; Tripathy, T.; Panda, J.; Kanan, K.; Jain, S.K. and Lan, T.N. (2000). *Poly Eng Sci*, (40), 46.
8. Singh, R.P.; Tripathy, T.; Karmakar, G.P.; Rath, S.K.; Karmakar, N.C.; Pandey, S.; Kanan, K.; Jain, S.K. and Lan, T.N. (2000). *Current Science*, (78), 798.
9. Rath, S.K. and Singh, R.P. (1997). *J. Appl Polym Sci*, (66), 1721.
10. Deshmukh, S.R.; Chaturvedi, P.N. and Singh, R.P. (1985). *J Appl Polym Sci*, (30), 4013.
11. Nayek, B.R.; and Singh, R.P. (2001). *J Appl Polym Sci*, (81), 1776.
12. Mishra, A.; Rajani, S.; Agarwal, M. and Dubey, R. (2002). *Polym Bulle*, (48) 439.
13. Tripathy, T.; Pandey, S.R.; Karmakar, N.C.; Bhagat, R.P and Singh, R.P. (1999). *Eur Polym J*, (35), 2057.
14. Deshmukh, S.R.; Sudhakar, K. and Singh, R.P. (1991). *J Appl Polym Sci*, (43), 1091.
15. Singh, R.P. and Biswal, D.R. (2003). Patent Application No: 196/KOL/2003.
16. Dambies, L.; Guimon, C.; Yiacoumi, S.; Guibal, E. (2001). *Colloids and Surface A: Physicochemical and Engineering Aspects*, (177), 203.
17. NO HK, Meyers SP. (1986). In Muzzarelli, C.J.; Peter, M.G.; (Eds), Chitin Handbook, New York; Plenum Press; 475.
18. Dutkiewicz J.K. (2002). *Journal of Biomedical Research (Applied Biomaterials)*, (63), 373.
19. Gyliene, O.; Rekertas, R.; Salkauskas, M. (2002). *Water Research*, (36), 4128.
20. Kumar. M.N.V.R. (2000). *Reactive and Functional Polymers*. (46), 1

21. Ngah, W.S.W.; Isa, I.M. (1998). *J Appl Polym Sci*, (67), 1067.
22. Tikhonov, V.; Radigina, L.A.; Yamskov, Y.A. (1996). *Carbohydrate Research*, (296), 33.
23. Muzzarelli, R.A.A. (1977). "Chitin". Pergamon Press, Oxford.
24. Muzzarelli, R.A.A.; Jeauniaux, C. and Gooday, G.H. (1989). "Chitin in Nature and Technology". Plenum Press, New York.
25. Skjak-Braek, G.; Anthonsen, T. and Sandford, P. (Eds). "Chitin and Chitosan". Elsevier Applied Science, London.
26. Blair, H.S.; Guthrie, J.; Law, T.K. and Turkington, P. (1987). *J Appl Polym Sci*, (33), 641.
27. Grant, S.; Blair, H.S. and McKay, G. (1988). *Polym Commun*, (29), 342.
28. Daly, W.H. (1991). In *Polymers from Biobased Materials*, (81), Chum, H.L. (Ed.) Noyes Data Corporation, New Jersey.
29. Mima, S.; Miya, M.; Iwamoto, R. and Susumu, Y. (1989). *J Appl Polym Sci*, (28), 1909.
30. Knorr, D. (1984). *Food Technol*, 38.
31. Huang, C.; Chen, Y. (1996). *J Chem Tech. Bioleth.* (66), 227.
32. Kurita, K.; Hasimoto, S.; Ishii, S.; Mori, T.; Nishimura, S. (1996). *Polym J*, (28), 686.
33. Kurita, K.; Hasimoto, S.; Ishii, S.; Mori, T. (1996). *Polym Bull*, (36), 681.
34. Hiraoka, K.; Yokoyama, T. (1997). *Nippon Gomu Kyokaishi*, (70), 155.
35. Tomalia, D.A.; Baker, H.; Dewald. (1985). *Polym J*, (17), 117.
36. Chellapandian, M.; Krishnan, M.R.V. (1998). *Process Biochemistry*, (33), 595.
37. Kojima, K.; Yoshikuni, M. and Suzuki, T. (1979). *J Appl Polym Sci*, (24), 1587.
38. Shigeno, Y.; Kondo, K. and Takemoto, K. (1982). *J Macromol Sci Chem A* (17), 571.
39. Kurita, K.; Yoshida, A. and Koyama, Y. (1998). *Macromolecules*, (21), 1579.
40. Shepherd, R.; Reader, S.; Falshaw, A. (1997). *Glycoconjugate J*, 14(4): 535.
41. Roberts, G.A.F. (1992) *Chitin Chemistry*. London: Macmillan, 350.
42. Broussignac, P. (1968). *Haut Polymère Naturel Connu dans l'Industrie: Le Chitosane*. *Chimie Industriel Genie, Chimie*, 99(9): 1241.
43. Batista and Roberts G.A.F (1990). *Makromolecular Chemistry*, (191), 429.
44. Ogawa, K.; Yui, T. (1993). *Bioscience Biotechnology and Biochemistry*, 57(9): 1466.
45. Ogawa, K. (1991). *Agricultural and Biological Chemistry*, 55(9): 2375.
46. Piron, E.; Accominotti, M.; Domard, A. (1997). *Langmuir*, (13), 1653.
47. Kurita, K.; Koyama, Y.; Chikaoka, S. (1988). *Polymer Journal*, (20), 1083.

48. Guibal, E.; Milot, C.; Roussy, J (1999). *Water Environment Research*, 71(1): 10.
49. Tilton, H. (Ed). (1998). *OPD Chemical Buyers Directory*, New York, Schnell Publishing Co., 206.
50. Peniston, Q.P.; Johnson, E. (1980). US patent No. 4, 195, 175, 5.
51. FDA (1999). Guideline for Drug Master Files (with list of Drug Master Files as of April 1999).
52. Felt, O.; Buri, P.; Gurny, R. (1998). *Drug Dev. Ind. Pharm.* 24 (11): 979.
53. Stannett, S.V. (1981). *Rad Phy Chem*, (18), 215.
54. Duke, F.R.; Forist, A.A. (1949). *J Am Chem Soc*, (71), 2790.
55. Duke, F.R.; Bremer, R.F. (1951). *J Am Chem Soc*, (73), 5179.
56. Mino, G.; Kaizarman, S. (1958). *J Polym Sci*, (31), 242.
57. Mino, G.; Kaizarman, S.; Rasmussen, E. (1959). *J Am Chem Soc*, (81), 14945.
58. Athawala, V.D.; Rathi, S.C. (1996). *J Polymer Material*, (13), 335.
59. Iwakura, Y.; Kurusaki, T.; Imai, E. (1965). *J Polym Sci, A*, (3), 1185.
60. Schwab, E.; Stannet, V.; Rakowitz, D.H.; Margane, J.K. (1962). *Tappi*, (45), 390.
61. Tripathy, T.; Pandey, S.R.; Karmakar, N.C.; Bhagat, R.P.; Singh, R.P. (1999). *Eur Polym J*, (35), 2057.
62. Iwakura, Y.; Kurosaki, T.; Imai, I. (1965). *J Polym Sci A*, (3), 1185.
63. Kurlyankina, V.I.; Molotokov, V.A.; Koz'mina, P.O.; Khripunov, A.K.; Shetennikova, I.N. (1967). *Eur Polym J Suppl*, 445.
64. Kurlyankina, V.I.; Koz'mina, P.O.; Khripunov, A.K.; Molotokov, V.A.; Novoselova, T.D. (1967). *Dokl Akad Nauk U.S.S.R*, 172,344(CA66: 66906V).
65. Kulkarani, A.Y.; Meheta, P.C. (1967). *J Appl Polym Sci B*, (5), 209.
66. Kulkarani, A.Y.; Meheta, P.C. (1968). *J Appl Polym Sci*, (12), 1321.
67. Ogiwara, Y.O.; Ogiwara, Y.V.; Kubota, H. (1968). *J Polym Sci A*, 1 (6): 1489.
68. Terasaki, I.; Matsuli, M. (1962). *Sen-I Gakkaishi*, (18), 147(CA 56:14505h).
69. Gupta, K.C.; Sahoo, S. (2001). *J Appl Polym Sci*, (79), 767.
70. Mino, G.; Kaizerman, S.; Rasmussen, E. (1959). *J Am Chem Soc*, (81), 1494.
71. Hinz, H.L.; Johnson, D.C. (1967). *J Org Chem*, (32), 556.
72. Muhammad, S.S.; Rao, K.V. (1963). *Bull Chem Soc, Japan*, (36), 949.
73. Pottenger, C.R.; Johnson, D.C. (1978). *J Polym Sci, A* (8), 301.
74. Zhang, J.; Yuan, Y.; Shen, J.; Lin, S. (2003). *Eur Polym J*, (39), 847.
75. Singh, H.; Thampy, R.T.; Chipalkatti, V.B. (1965). *J Polym Sci, A* (3), 4289.
76. Duke, F.R. (1947). *J Am Chem Soc*, (69), 2885.

77. Mehrotra, R.; Ranby, B. (1977). *J Appl Polym Sci*, (21), 1647.
78. Mehrotra, R.; Ranby, B. (1977). *J Appl Polym Sci*, (21), 3407.
79. Mehrotra, R.; Ranby, B. (1978). *J Appl Polym Sci*, (22), 2991.
80. Mehrotra, R.; Ranby, B. (1978). *J Appl Polym Sci*, (22), 3003.
81. Brockway, C.E.; Moser, K.B. (1963). *J Polym Sci, A* (1), 1025.
82. Brockway, C.E. (1964). *J Polym Sci, A* (2), 3721.
83. Uri, N. (1952). *Chem Revs*, (50), 375.
84. Brockway, C.E.; Esters, R.R.; Smith, D.R. (1963). US Pat: 3095391.
85. Mehrotra, U.S.; Mushran, S.P. (1970). *J Ind Chem Soc*, (47), 41.
86. Kimura, S.; Takitani, T.; Imoto, N. (1962). *Bull Chem Soc, Japan*, (35), 2012.
87. Imoto, M.; Morita, E.; Ouchi, T. (1980). *J Polym Sci, Polym Symp*, (68) 1.
88. Imoto, M.; Reeks; Ouche, T. (1973). *Die Makromol Chem*, (157), 353.
89. Nayek, P.L.; Lenka, S.; Pati, N.C. (1973) *J Appl Polym Sci*, (23), 1345,
90. Nayek, P.L.; Lenka, S.; Pati, N.C. (1979). *J Polym Sci, Polym Chem Ed*, (17), 3425.
91. Samal, R.K.; Mohanti, T.R.; Nayek, P. (1967). *J Macromol Sci, Chem A*, (10), 1239.
92. Nayek, P.L.; Lenka, S. Mishra, M.K. (1980). *J Appl Polym Sci*, (25), 1323.
93. Mishra, M.K.; Tripathy, A.K.; Lenka, S.; Nayek, P.L. (1981). *J Appl Polym Sci*, (26), 2769.
94. Lenka, S.; Nayek, P.L.; Mishra, M.K. (1980). *J Appl Polym Sci*, (25), 1323.
95. Mohanty, A.K.; Patnaik, S.; Singh, B.C. (1989). *J Appl Polym Sci*, (37), 1171.
96. Dimov, K.; Pavlov, P. (1969). *J Appl Polym Sci A* (7), 2775.
97. Ray Chaudhuri, D.K.; Hermans, J.J. (1960). *J Appl Polym Sci*, (48), 159.
98. Schurz, R.J.; Jacob, W. (1966). *Monatsh Chem*, (97), 1142.
99. Hebeish, A.; Khalil, M.I.; El-Rafir, M.H. (1975). *Angew Makromol Chem*, 1677.
100. Bendak, A.; Hebeish, A. (1965). *J Appl Polym Sci*, (17), 1953.
101. Kasting, E.G.; Naarmann, H.; Reis, H.; Berding, C. (1965). *Angew Chem*, (77), 313.
102. Tripathy, A.K.; Lenka, S.; Nayak, P.L. (1981). *J Appl Polym Sci*, (26), 1413.
103. Hofreiter, T. (1977). *J Appl Polym Sci*, (21), 761.
104. Lokhande, H.T.; Varadarajan, P.V.; Nakhane, N.D. (1993). *J Appl Polym Sci*, (48), 495.
105. Abdel, F.I.; Barker, P.; Lullirie, J.T. (1980). *Macromol Chem*, (181), 2063.
106. Shukla, S.R.; Gopala Rao, G.V.; Athalya, A.R. (1992). *J Appl Polym Sci*, 45(8), 1341.
107. Gangopadhyay, R.; Ghosh, P. (1999). *J Appl Polym Sci*, (74), 1623.

108. Morita, Y.; Sugahara, Y.; Iboni, M.; Takahashi, A. (1999). *J Appl Polym Sci*, (71), 189.
109. Angier, J.; Ceresa, R.J.; Waston, W.F. (1950). *J Polym Sci*, (34), 699.
110. Reys, Z.; Rist, C.E.; Russel, C.R. (1966). *J Appl Polym Sci*, A (4), 1031.
111. Fanta, G.F.; Burr, R.C.; Russel, C.R.; Rist, C.E. (1966). *J Appl Polym Sci*, (10), 929.
112. Brockway, C.E.; Seaberg, P.A. (1967). *J Appl Polym Sci*, A (1), 1313.
113. Mendelson, R.A. (1969). *Polym Eng Sci*, (9), 350.
114. Erciyes, A.T.; Erim, M.; Hazer, B.; Yagic, Y. (1992). *Angew Macromol Chem*, (200), 163.
115. Tripathy, T.; Karmakar, N.C.; Singh, R.P. (2000). *Int J Polym Mater*, (46), 81.
116. Ogiwara, Y.; Uchiyama, M. (1969). *J Polym Sci A* (7), 1479.
117. Eremeeva, T.E.; Bykova, T.O. (1998). *Carbo Polym*, (36), 319.
118. Diego Gómez-Díaz.; Navaza, José. (2003). *J Food Eng.*, (56), 387.
119. Okieimen, E.F.; Egharevba, F.; Jideonwo, A. (1991). *Die Angew Makromol Chemie*, 184, 1-6(Nr.3029).
120. Henderson, M.; Rudi, A. (1982). *J Appl Polym Sci*, (27), 4115.
121. Okieimen, E.F.; Egharevba, F. (1992). *Eur Polym J*, 28(4), 415.
122. Liyod, P.J.; Ward, A.S. (1975). *AIChE Symp Ser*, n17173, 6.
123. Tadors, M.E.; Mayes, I. (1980), Somasundaran, P. (Ed.), *Proc Int Sym on Fine Particle Processing*, Las Vegas, NV, 1583.
124. Rong, R.X.; Hitchins, J. (1995). *Mineral Eng*, 8(3), 293.
125. Dolina, L.F.; Kaminski, V.S. (1994). *Coke Chem (USSR)* (1), 8.
126. Ayub, A.L.; Sheppard, J.D. (1986). *Colloids and Surfaces*, (18), 43.
127. Henderson, A.F.; Cornell, C.F.; Dunyon, A.F.; Dahlstrom, D.A. (1957). *Trans AIME* (204), 349.
128. Gray, V.R. (1958). *J Inst Fuel*, 91.
129. Wakeman, R.J. (1975). Elsevier, Amsterdam, 144.
130. Wakeman, R.J. (1976). *Int J Miner Process*, (3), 193.
131. Ruston, A.; Hosseini, M.; Hassan, I. (1980). *J Sep Process Technol*, (1), 35.
132. McCall, M.T.; Tandros, M.E. (1980). *Colloids and Surfaces*, (1), 161.
133. Wheelock, T.D.; Drzymala, J. (1991). *Filtration and Separation*, (28), 351.
134. Brown, G.G.; Foust, A.S.; Katz, D.I.; Schneidewind, R.; White, R.R.; Wood, W.P.; Brown, G.M.; Brownell, L.E.; Martin, J.J.; Williams, G.B.; Banchemo, J.T.; York, J.L. (1966). *Unit Operations*, John Wiley & Sons, New York.

135. La Mer, V.K.; Smelie Jr.R.H. (1962). *Clay Miner.* (9), 295.
136. Healy, T.W.; La Mer, V.K. (1962). *J Phys Chem*, (66), 1835.
137. Hogg, R.; Healy, T.W.; Fuersteanau, D.W. (1966). *Trans Faraday Soc*, (62), 638.
138. Hogg, R. (1984). *J Colloid Interface Sci*, (102), 232.
139. Cohen Stuart, M.A.; Fler, G.D.; Lyklema, J.; Norde, W.; Scheutjens, J.M.H.M. (1991). *Adv Colloid Interface*, (34), 477.
140. Cosgrove, T.; in: Th.F.Tadros (Ed.). (1987). *Solid/Liquid Dispersions*, Academic Press, London, 131.
141. Fler, G.M.; Scheutjens, J.M.H.M.; Cohen Stuart, M.A. (1988). *Colloids Surf*, (31), 1.
142. Fler, G.M.; Cohen Stuart, M.A.; Scheutjens, J.M.H.M.; Cosgrove, T.; Vincent, B. (1993). *Polymer at Interfaces*, Chapman & Hall, London.
143. Scheutjens, J.; Fler, G.J. In: Th.F. Tadros (Ed.) (1982). Academic Press, London.
144. Lyklema, J.; In: Moudgil, B.; Samasundaran, P. (Eds.) (1985). *Flocculation, Sedimentation and Consolidation*, Engineering Foundation.
145. Tadros, Th.F. (1982). Academic Press, London.
146. Vincent, B. (1974). *Adv Colloid Interfac*, (4), 193.
147. Dickinson, E.; Eriksson, L. (1974). *Adv Colloid Interfac*, (34), 1.
148. Paul, J.; Snowden, M. (1996). *Adv Colloid Interfac*, (68), 57.
149. Somasundaran, P.; Sivakumar, A. (1988). *Colloids Surf*, (30), 401.
150. Onoda, G.Y.; Somasundaran, P (1987). *J Colloid Interface Sci*, (118), 169.
151. Gregory, J.; in: Th.F.Tadros (Ed.). (1987). *Solid/Liquid Dispersions*, Academic Press, London, 163.
152. Gregory, J. (1973). *J Colloid Interface Sci*, (42), 448.
153. Gregory, J. (1988). *Colloids Surf*, (31), 231.
154. Pelssers, E.G.M.; Cohen Stuart, M.A.; Fler, G.J. (1989). *Colloids Surf*, (38), 15.
155. Pelssers, E.G.M.; Cohen Stuart, M.A.; Fler, G.J. (1990). *J Colloid Interface Sci*, (137), 350.
156. Pelssers, E.G.M.; Cohen Stuart, M.A.; Fler, G.J. (1990). *J Colloid Interface Sci*, (137), 362.
157. Smoluchowski, M.Von. (1916). *Phys Z*, (17), 557.
158. Smoluchowski, M.Von. (1919). *Phys Z*, (17), 585.
159. Smoluchowski, M.Von. (1917). *Z Phys Chem*, (92), 129.
160. La Mer, V.K.; Healy, T.W. (1963). *Rev Pure Appl Chem*, (13), 112.
161. Hogg, R. (1984). *Colloid Int Sci*, 102 (1), 232.

162. Deason, D.M.; In: Attia, Y.A. (Ed), (1982). *Elsevier, Amsterdam*, 21.
163. Moudgil, B.; Shah, B.D. (1986). "Selection of Flocculant for Solid-Liquid Separation Processes", In: Moraliidhara (Ed). Battelle Press, Columbus, 191.
164. Sengupta, D.K.; Attia, Y.A.; Hamza, H.A. (1994). *Fluid/Particle Sep J.7* (4), 165.
165. Montgomery, J.M. (1985). John Willey & Sons, New York. 116.
166. Kruyt, H.R. (1952). *Colloid Sci*, (1), Elsevier, New York.
167. Deryagin, B.V.; Landau, L.D. (1941). *Acta Physicochim U.S.S.R*, (14), 733.
168. Verway, E.J.W.; Overback, J.Th.G. (1948). Elsevier, Amsterdam.
169. Banarjee, A.K.; Tscharnuter, W.W.; Weiner, B.B.; Gokhale, Y.B. (1996). *Chemical Industry Digest*, 116.
170. Friend, J.P.; Kitcheners, J.A. (1973). *Chem Eng Sci*, (28), 1071.
171. Operating Instruction and Manual on Particle Micro-Electrophoresis (Apparatus Mark-II), Rank Brothers, High Street, Bottisham, Cambridge, Cb59da, England.
172. Gregory, J. (1985). Proc of the Engineering Foundation Conference on Flocculation Sedimentation and Consolidation, the Cloister, Sea Island, Georgia, USA, 125.
173. Moss, N.; Dymond, B. (1978). *Mine and Quarry Journal*, 7(5), 57.
174. Richardson, P.F.; Connely, L.J. (1988). "Industrial Coagulants and Flocculants". Reagents in Mineral Technology, Somasundaran, P.Modugil, B.M. (Eds.), *Surfactant Science Series*, (27), 519.
175. Mangravite, F.J.; Leitz, C.R.; Galick, P.E. (1985). Proc of the Engineering Foundation Conference on Flocculation, Sedimentation and Consolidation, the Cloister, Georgia, USA, 139.
176. Black, A.P.; Birkner, F.B.; Morgan, J.J. (1965). *J Am Water Works Assoc*, 57(12), 1457.
177. Black, A.P.; Chen, C.L. (1965). *J Am Water Works Assoc*, 57(3), 354.
178. Stratton, R.A. (1983). *Tappi J.*, 66(3), 141.
179. Lindstrom, T.; Glad-Nordmark, G. (1984). *Colloids and Surfaces*, 8(4), 337.
180. Lindstrom, T.; Glad-Nordmark, G. (1984). *J Colloid & Interface Sci*, 97(1), 62.
181. Petaja, T. (1980). "A Fundamental Study of the Influence of Timing of Polyelectrolyte Dosage and Agitation on Retention with Dual Polymer System". Ph.D. Thesis. University of Oulu, Finland.
182. Ayyala, S.; Pugh, R.J.; Forssberg, E. (1985). *Mineral Processing and Extractive Metallurgical Review*, (12), 165.
183. Sun, S.F. (1994). *Wiley-Interscience*. New York.

184. Yu, X.; Somasundaran, P. (1996). *J Colloid Interface Sci*, (177), 283.
185. Chem Mark Rep, 6(Oct.29, 1991).
186. Chem Mark Rep, 3(Dec.24, 1990).
187. Finch, C.A. (Ed). (1993). Plenum Press, New York, 4th edition.
188. Davison, R.L.; Sittin (Eds), (1962). 2nd Edition, Reinhold, New York.
189. Molyneaux, P. (1984). (1/2) CRC Press, Inc., Boca Raston.
190. McCormick, C.L.; Bock, J. (1987). Mark, H.F.; Bikales, C.G.; Overberger, George, Kroschwitz, J.I. (Eds). John Wiley & Sons, (17), 730.
191. Bolto, B.A. (1995). *Prog Polym Sci*, (20), 987.
192. McDonald, C.J.; Beavar, R.H. (1979). *Macromolecules*, (12), 203.
193. Pelton, R.H. (1979). *J Polym Sci Polym Chem Ed*, (22), 3955.
194. Tanaka, H. (1979). *J Polym Chem Ed*, (17), 1239.
195. Tanaka, H. (1986). *J Polym Sci, Polym Chem Ed*, (24), 29.
196. Mabire, F.; Audebert, R.; Quivoron, C. (1984). *Polymer*, (25), 1317.
197. Solberg, D.; Wagberg, L. (2003). *Colloids and Surfaces A: Physicochem. Engg Aspects*, (219), 161.
198. Besra, L.; Sengupta, D.K.; Roy, S.K.; Ay, P. (2003). *Separation and Purification Technology*, (30), 251.
199. Butler, G.B.; Angelo, R.J. (1957). *J Am Chem Soc*, (73), 3128.
200. Lancaster, J.E.; Baccei, L.; Panzer, H.P. (1976). *J Polym Sci B*, (14), 549.
201. Zemaitaitiene, R.J.; Zliobaite, E.; Klimaviciute, R.; Zemaitaitis, A. (2003). *Colloids and Surfaces A: Physicochem Engg Aspects*, (214), 37.
202. Gill, R. I. S.; Herrington, T. M. (1987). *Colloid Surf*, (25), 297.
203. Gill, R. I. S.; Herrington, T. M. (1989). *Colloid Surf*, (42), 23.
204. Boothe, J.E.; Flock, H.G.; Hoover, F.M. (1970). *J. Macromol Sci-Chem A* (4), 1419.
205. Wandrey, C.; Jaeger, H.M.W. (1984). *Acta Polym*, (36), 100.
206. Lin, Y.; H. P. Jr.; Butler, G.B. (1988). *J. Macromol Sci-Chem A*, 25 (8), 999.
207. Deng, Y.; Xiao, H.; Pelton, R. (1996). *J Colloid Inter Sci*, (179), 188.
208. Petzold, G.; Mende, M.; Lunkwitz, K.; Schwarz, S.; Buchhammer, H.M. (2003). *Colloids and Surfaces A: Physicochem Engg Aspects*, (218), 47.
209. Ishikawa, M. (1976). *J Colloid Inter Sci*, (56), 596.
210. Cardoso, J.; Orta, T.; Manero, O. (1991). *Polymer Preprints*. 32 (3), 323.
211. Asanov, A.A.; Barulina, V.R.; Akhmedov, K.S. (1995). *Dokl Akad Nauk Resp Uzb*, (9-10), 31.

212. Mpofu; Addai-Mensah, J.; Ralston, J. (2003). *J Colloid Inter Sci*, (261), 349.
213. Besra, L.; Sengupta, D.K.; Roy, S.K.; Ay, P. (2002). *Int J Min Proc*, (66), 1.
214. J. C. Petzold, J.C.; Herrington, T.M. (1990). *Clay Miner*, (191), 1067.
215. Taylor, M.L.; Morris, G.E.; Self, P.G.; Smart, R.S.C. (2002). *J Colloid Interface Sci*, (250), 28.
216. Zhang, J.; Huguenard, C.; Scarnecchia, C.; Menghetti, R.; Buffle, J. (1999). *Colloids and Surfaces A: Physicochem. Engg Aspects*, (151), 49.
217. Walles, W.E. (1971). *J Colloid Interface Sci*, (37), 364.
218. Hoover, M.F.; Butler, G.B. (1974). *J Polym Sci, Polym Symp*, (45), 1.
219. McCormick, C.K.; Chen, G.S. (1982). *J Polym Sci, Polym Chem. Edn*, (20), 817.
220. Murfin, D.L.; Miller, L.E. (1969). U.S. Patent. 3, 478, 091.
221. Miller, L.E.; Murfin, D.L. (1970). U.S. Patent 3, 506, 707.
222. Qin, Z.; Yin, B.; Wen, L.; Zhang, L.; Yao, K. (1994). *Gaifenzi Cailao Kexue Gongcheng*, 10 (20), 73.
223. Yu, J.; Liu, H.; Chen, J. (2000). *Colloids and Surfaces A: Physicochem Engg Aspects*, (163), 225.
224. Abd-El Rahman, M. K. (2000). *Chem Eng Tech*, (23), 457.
225. Besra, L.; Sengupta, D.K.; Roy, S.K.; Ay, P. (2002). *Int J Min Proces*, (66), 203.
226. Lapick, L.; Alince, B.; Vande Ven, T.G.M. (1995). *J Pulp and Pap Sci*, 21(1).
227. Järnström, L.; Lason, L.; Rigdahl, M. (1995). *Colloids and Surfaces A: Physicochem Engg Aspects*, (104), 191.
228. Järnström, L.; Lason, L.; Rigdahl, M. (1995). *Colloids and Surfaces A: Physicochem Engg Aspects*, 104 (2/3), 207.
229. Weissenborn, P.K.; Warren, L.J.; Dunn, J.G. (1995). *Colloids and Surfaces A: Physicochem Engg Aspects*, (99), 11.
230. Weissenborn, P.K.; Warren, L.J.; Dunn, J.G. (1995). *Colloids and Surfaces A: Physicochem Engg Aspects*, (99), 29.
231. Weissenborn, P.K.; Warren, L.J.; Dunn, J.G. (1994). *Int J Miner Process*, (42), 191.
232. Nyström, R.; Hedström, G.; Gustafsson, J.; Rosenholm, G.B. (2004). *Colloids and Surfaces A: Physicochem Engg Aspects*, (234), 85.
233. Nyström, R.; Backfolk, K.; Rosenholm, J.B.; Nurm, K. (2003). *J Colloid Interface Science*, (262), 48.
234. Larsson, A.; Wall, S. (1998). *Colloids and Surfaces A: Physicochem Engg Aspects*, (139), 259.

235. Dahlberg, A.; Larsson, A.; Wall, S.; Akerman, B. (1999). *Colloid Polym Sci*, (277), 428.
236. Dahlberg, A.; Larsson, A.; Akerman, B.; Wall, S. (1999). *Colloid Polym Sci*, (277), 436.
237. Larsson, A. (1998). *Colloids and Surfaces B: Biointerfaces*, 12 (1), 23.
238. Larsson, A.; Walldal, C.; Wall, S. (1999). *Colloids and Surfaces A: Physicochem Engg Aspects*, (159), 65.
239. Deshmukh, S.R.; Chaturvedi, P.N.; Singh, R.P. (1985). *J Appl Polym Sci*, (30), 4013.
240. Deshmukh, S.R.; Singh, R.P. (1987). *J Appl Polym Sci*, (33), 1963.
241. Rodd, A.B.; Dunstan, D.E.; Boger, D.V. (2000). *Carbohydrate Polymers*, (42), 159.
242. Morris, E.R.; Morris, V.J.; Ross-Murphy, S.B. (1982). *J Polym. Sci: Polym Letters Edn*, (20), 531.
243. Rinaudo, M.; Milas, M. (1980). *International Journal of Biological Macromolecules*, (2), 45.
244. Ross-Murphy, S.B.; Morris, V.J.; Morris, E.R. (1983). *Faraday Symposium of the Chemical Society*, (18), 115.
245. He, M.; Horikawa, Y. (1996). *Soil Sci Plant Nutr.* (Tokyo), 42 (3), 603.
246. He, M.; Horikawa, Y. (1996). *Soil Sci Plant Nutr.* (Tokyo), 42 (3), 633.
247. Glass, J.E. (1986). *Am Chem Soc*, Washington, DC, 210.
248. Singh, R, P, D. R. Biswal, D, R (2003). Patent Application No. 196/KOL/2003.
249. Krishnamoorthi, S.; Mal, D.; Singh, R.P (2005). *Carbohydrate Polym.* (Article in Press)
250. Robyt, J.F. (1996). In *Enzymes for Carbohydrate Bioengineering*, Park, K.H.; Robyt, J.F.; Y. D. Choi, Y.D. (Eds.), *Amsterdam, Elsevier*, 1.
251. S, Pal.; Mal, D.; Singh, R.P. (2006). *Colloids and Surfaces A: Physicochem Eng Aspects*, 289(3), 193.
252. Rath, S.K.; Singh, R.P. (1997). *J Appl Polym Sci*, (66), 1721.
253. Karmakar, G.P.; Singh, R.P. (1998). *Colloids and Surfaces A: Physicochem Eng Aspects*, (133), 119.
254. Deshmukh, S.R.; Chaturvedi, P.N.; Singh, R.P. (1985). *J Appl Polym Sci*, (30), 4013.
255. Nayak, B.R.; Singh, R.P. (2001). *J Appl Polym Sci*, (81), 1776.
256. Mishra, A.; Rajani, S.; Agarwal, M.; Dubey, M.R. (2002). *Polymer Bulletin*, (48), 439.

257. Tripathy, T.; Pandey, S.R.; Karmakar, N.C.; Bhagat, R.P.; Singh, R.P. (1999). *Eup Polym J*, (35), 2057.
258. Deshmukh, S.R.; Singh, R.P. (1986). *J Appl Polym Sci*, (32), 6163.
259. Deshmukh, S.R.; Singh, R.P. (1987). *J Appl Polym Sci*, (33), 1963.
260. Deshmukh, S.R. (1986). "Turbulent Drag Reduction Effectiveness, Shear Stability and Biodegradability of Graft Copolymers". Ph.D Thesis, IIT, Kharagpur, India.
261. Karmakar, G.P. (1994). "Flocculation and Rheological Properties of Grafted Polysaccharides". Ph.D Thesis, IIT, Kharagpur, India.
262. Rath, S.K. (1997). "Water-Soluble Polymers based on Grafted Amylopectin: An Investigation on their Flocculation Characteristics". Ph.D Thesis, IIT, Kharagpur, India.
263. Singh, R.P.; Karmakar, G.P.; Rath, S.K.; Karmakar, N.C.; Tripathy, T.; Panda, J.; Kannan, K.; Jain, S.K.; Lan, N.T. (2000). *Polym Eng Sci*, (40), 46.
264. Singh, R.P.; Tripathy, T.; Karmakar, G.P.; Rath, S.K.; Karmakar, N.C.; Pandey, S.R.; Kannan, K.; Jain, S.K.; Lan, N.T. (2000). *Current Science*, (78), 798.
265. Singh, R.P.; Nayak, B.R.; Biswal, D.R.; Tripathy, T.; Bariik, K. (2003). *Mat Res Innovat*, (7), 331.
266. Pal, S.; Mal, D.; Singh, R.P. (2004). *Carbohydrate Polymers*, 59(4), 417
267. Pal, S.; Singh, R.P. (2005). *Mat Res Innovat*, (25)315.
268. Fanta, G.F.; Burr, R.C.; Russel, C.R.; Rist, R.E. (1970). *J Appl Polym Sci*, (14), 2601.
269. Fanta, G.F.; Burr, R.C.; Doane, W.M.; Russel, C.R. (1972). *J Appl Polym Sci*, (16), 2835.
270. Jones, D.A.; Jordan, W.A. (1971). *J Appl Polym Sci*, (15), 2461.
271. Hoover, M.F.; Sinkovitz, G.D. (1973). U. S. Patent 3, 734, 820.
272. Walldal, C.; Wall, S.; Biddle, D. (1998). *Colloids and Surfaces A: Physicochem Eng Aspects*, (131), 203.
273. Levy, N.; Garti, N.; Magdassi, S. (1995). *Colloids and Surfaces A: Physicochem Engg Aspects*, (97), 91.
274. Gu, L.; Hrymak, A.N.; Zhu, S. (1999). *J Appl Polym Sci*, (74), 1412.
275. Larsson, A.; Wall, S. (1998). *Colloids and Surfaces A: Physicochem Eng Aspects*, 139259.
276. Fort, D.J.; Stover, E.L. (1996). *Proc Ind Waste Conf*, 601.
277. Fort, D.J.; Stover, E.L. (1995). *Water Environ Res*, 67 (6), 921.
278. Gregory, J. (1983). *Effluent Treat J*, (23), 199
279. Angle, C.W.; Smith-Palmer, T.; Wentzell, B.R. (1997). *J Appl Polym Sci*, (64), 783.

280. Dahlstrom, D.A. (1980). *Engg & Mining J*, 181(6), 123.
281. Hogg, R.; Klimpel, R.C.; Dey, D.T. (1987). *Mine Metal Process*, 108.
282. Keren, R.; Sparks, D.L. (1995). *Soil Science Society of America J*, 59 (2), 430.
283. Sastry, C.A.; Raghuveer, S. (1991). *Indian J Environmental Protection*, 11 (4), 269.
284. Szpak, P.; Woods, D.R.; Bouchard, K. (1996). *Water Qual Res J, Canada*, 31 (1), 51.
285. Farrow, J.B.; Swift, J.D. (1996). *Int J Miner Process*, 46 (3-4), 263.
286. Jung, S.J.; Amal, R.; Raper, J.A. (1993). *Off Proc Comb Conf, 6th Conf Asia Pac Confed Chem Eng, 21st Australas Chem Eng Conf*, 2, 89/2-93/2.
287. Jung, S.J.; Amal, R.; Raper, J.A. (1995). *Part Syst Charact*, 12 (6), 274.
288. La Mer, V.K.; Healy, T.W. (1963). *Rev Pure Appl Chem*, (13), 112.
289. Sandell, L.S.; Luner, P. (1974). *J Appl Polym Sci*, (18), 2075.
290. Adachi, Y.; Cohen Stuart, M.A.; Fokkink, R. (1995). *J Colloid Interface Sci*, (171), 520.
291. Das, K.K.; Somasundaran, P. (2003). *Colloid Surf A*, (223), 17.
292. Xiao, H.; Liu, Z.; Wiseman, N. (1999). *J Colloid Interface Sci*, (216), 409.
293. Tripathy, T.; Singh, R.P.; (2002). *Eur Polym J*, (36), 1471.
294. Kage, H.; Yoshizo, M.; Higashitani, K. (1988). *Can J Chem Engg*, 66(5), 728.
295. Tripathy, T.; Karmakar, N.C.; Singh, R.P. (2001). *Appl Polym Sci*, (82), 375.
296. Qian, J.W.; Qi, G.R.; Fang, Z.B.; Cheng, R.S. (1998). *Eur Polym J*, 33 (8), 1263.
297. Qian, J.W.; Qi, G.R.; Cheng, R.S. (1998). *Eur Polym J*, 34(3/4), 445.
298. Brostow, W.; Wolf, B.A. (1991). *Polym Commun*, (32), 551.
299. Qian, J.W.; Li, J.; Zhou, G.H.; Qi, G.R. (2000). *J Appl Polym Sci*, (78), 836.
300. Shen, J.G.; Wang, Y.; Qian, R.Y. (2002). *Acta Polym Sinica*, (1), 113.
301. Huang, D.G.; Yang, Y.M.; Zhuang, G.Q.; Li, B.Y. (2000). *Macromolecules*, (33), 461.
302. Dondas, A.; Papanagaopoulos, D. (1995). *Polymer*, 36 (2), 365.
303. Papanagaopoulos, D.; Dondas, A. (1995). *Polymer*, 36(2), 369.
304. Qian, R.Y.; Cao, D.; Cheng, R.S. (1983). *Sci China (ser B)*, (12), 1080.
305. Cheng, R.S.; Yan, X. (1991). *J Appl Polym Sci. Appl Polym Symp*, (48), 123.
306. Qian, J.W.; Li, J.; Yang, Y.S.; Qi, G.R. (1998). *Chin J Polym*, 16 (4) 327.
307. de Gennes, P.G. (1979). *Scaling Concepts in Polymer Physics*. Ithaca, New York: Cornell University Press: (Chapter-III).
308. Pispas, S.; Floudas, G.; Pakula, T.; Lieser, G.; Sakellariou, S.; Hadjichristidis, N. (2003). *Macromolecules*, (36) 759.

309. Ward, A.S. (1996). Rushton, A.; Ward, A.S.; Holdich, P.G. (Eds). 1st Edition, VCH Publishers Inc.74.
310. Guibal, L.; Gregory, J. (1991). *Water Res*, 25(9), 1137.
311. Quan, J.W.; Xiang, X.J.; Yang, W.Y.; Wang, M.; Zheng, B.Q. (2004). *Eur Polym J*, (8), 1699.
312. Hogg, R.; Bunnaul, P.; Suharyono, H. (1993). *Min Metall Process*, 81.
313. Gregory, J.; Guibai, L. (1991). *Chem Eng Comm*, (108), 3.
314. Gregory, J.; Xing, L. (1994). *Dispersion Aggregation, Proc Eng Found Conf*, 427.
315. Young, Y.S.; Chiang, S.H.; Morsi, B.I. (1991). *Mines at Carriers*, (3), 39.
316. Ward, A.S. (1996). In *Solid-Liquid Filtration and Separation Technology*, A. Rushton, A. S. Ward, P.G. Holdich (Eds.), 1st edition, VCH Publishers Inc., 74.
317. Guibai, L.; Gregory, J. (1994). *Water Res*, 25 (9), 1137.
318. Hogg, R. (1992). Plenary Lecture Presented at Eng Foundation Conf on Dispersion Aggregation, Fundamentals and Applications, Palm Coasi, Florida.
319. Gregory, J. (1988). *Colloids Surfaces*, (31), 231.
320. Michaels, A.S. (1954). *Ind Eng Chem*, (46), 1485.
321. Yu, X.; Somasundaran, P. (1996). *J Colloid Interface Sci*, (178), 770.
322. Somasundaran, P.; Vasudevan, T.V.; Tjipangandjara, K.F. (1994). *Dispersion Aggregation, Proc Eng Found Conference*, Moudgil, B.M.; Somasundaran, P. (Eds.), Engineering Foundation, New York.
323. Besra, L.; Sengupta, D.K.; Roy, S.K.; Ay, P. (2004). *Separation and Purification Technology*, 37(3)237
324. Miller, R.K. (1971). *J Colloid Interface Sci*, 37 (2), 364.
325. Moudgil, B.M.; Behi, S.; Mehta, V. (1994). *Proc Eng Found Conference*, Moudgil, B.M.; Somasundaran, P. (Eds.), Engineering Foundation, New York, 419.
326. Mishra, K.P.; Gupta, K.D.; Tripathy, P.S.M.; Singh, N.M. (1996). *J Indian Chem Soc*, 73 (4-5), 223.
327. Zemaitaitiene, R.J.; Zliobaite, E.; Klimaviciute, R.; Zemaitaitis, A. (2003). *Colloids and Surfaces A: Physicochem Eng Aspects*, (214), 37.
328. Zhong, J.; Sun, X.; Wang, C. (2003). *Separation and Purification Technology*, (32), 93.
329. Nachtergaele, W. (1998). *Starch/Starke*, (41), 27.
330. Whipple, W.L.; Maltesh, C. (2002). *J. Colloid Interface Sci*, (256), 33.

331. Karol, R.H. (1987). In Encyclopedia of Polymer Science and Engineering, Mark, H.F.; Bikales, N.M.; Overberger, C.G.; Manges, G.; Kroschwitz, J.I. (Eds.), John Wiley & Sons.
332. Yasar, B.; Kitchner, J.A. (1970). *Trans Inst Min Metal*, (79), 23.
333. Sresty, G.C.; Raja, A.; Somasundaran, P. (1978). Li, N.N. (Ed.), CRC Press Vol. 4, 93.
334. Attia, Y.A. (1987). Attia, Y.A. (Ed), Elsevier, Amsterdam, 227.
335. Moudgil, B.M.; Mathur, S.; Prakash, T.S. (1995). Miner Process Recent Adv Future Trends, Proc Conference, Mehrotra, S.P.; Sekhar, R. (Eds.), Allied Publishers, New Delhi, 503.
336. Lindstrom, T.; Glad-Nordmark, G. (1983). *J Colloid Interface Science*, (94), 404.
337. Behl, S.; Moudgil, B.M.; Prakash, T.S. (1983). *J Colloid Interface Science*, (161), 414.
338. Behl, S.; Moudgil, B.M. (1993). *J Colloid Interface Science*, (161), 422.
339. Behl, S.; Moudgil, B.M. (1993). *J Colloid Interface Science*, (161), 430.
340. Somasundaran, P.; Das, K.K.; Yu, X. (1996). *Colloid Interface Sci.*, 1 (4), 530.
341. Ravisankar, S.A.; Pradip; Khosla, N.K. (1995). *Int J Mineral Processing*, (43), 235.
342. Ravisankar, S.A.; Pradip, Deo, M.G.; Kulkarni, R.A.; Gundiah, S. (1988). *Bulletin of Materials Science*, 10 (5), 423.
343. Pradip. Kulkarni, R.A.; Gundiah, S.; Moudgil, B.M. (1991). *Int J Mineral Processing*, (32), 259.
344. Pradip. Moudgil, B.M. (1991). *Int J Mineral Processing*, (32), 271.
345. Xiao, H.; Cezar, N. (2003). *J Colloid Interface Science*, (267), 343.
346. Xiao, H.; Liu, Z.; Wiseman, N. (1999). *J Colloid Interface Science*, (216), 409.
347. Petzold, G.; Buchhammer, H-M.; Lunkwitz, K. (1996). *Colloids and Surfaces A: Physicochem Eng Aspects*, (119), 87.
348. Petzold, G.; Nebel, A.; Buchhammer, H-M.; Lunkwitz, K. (1998). *Colloids and Polymer Science*, (276), 125
349. Li, H.; Liu, B.; Zhang, X.; Gao, C.; Shen, J.; Zou, G. (1999). *Langmuir*, (15), 2120.
350. Samoshima, Y.; Diaz, A.; Becker, Y. Nylander, T. (2003). *Colloids Surfaces A*, (231), 195.
351. Milling, A.J.; Kendall, K. (2000) *Langmuir*, (16), 5106.
352. Allara, D.L.; Nuzzo, R.G. (1985). *Langmuir*, (1), 52.
353. Weissenborn, P.K.; Warren, L.J.; Dunn, J.G. (1995). *Colloids Surfaces*, (99), 29.

354. Vermöhlen, K.; Lewandowski, H.; Narres, H.D.; Schwuger, M.J. (2000). *Colloids Surfaces*, (163), 45.
355. Jones, F.; Farrow, J.B.; Van Bronswijk, W. (1998). *Langmuir*, (14), 6512.
356. Fuerstenau, D.W.; Pradip, In: Jones, M.J.; Oblatt, R. (Eds.). (1984). *Reagents in the Minerals Industry*, The Institute of Mining and Metallurgy, London, 161.
357. Nagaraj, D.R. In: Somasundaran, P.; Moudgil, B.M. (Eds.). (1988). *Reagents in Mineral Technology*, Mercel Dekker, NY, 258.
358. Raghavan, S.; Fuerstenau, D.W. (1975). *J Colloid Interface Sci*, (50), 319.
359. Peniche-covas, C.; Argüelles-Monal, W.; San Roman (1993). *J Polym Deg Stab*, (39) 21.
360. Garcia, I.; Peniche, C.; Nieto, J.M. (1983) *L Therm Anal*, (21), 189.
361. Smellie, R.H.; La Mer, V.K. (1958). *J. Colloid Sci*, (13), 589.
362. Fanta, G.F. (1973). R.J.Ceresa (Eds), John Wiley & Sons. New York, (1), 1.
363. Fanta, G.F. (1973). "Synthesis of Graft and Block Copolymers of Starch, Block and Graft Copolymerization". R.J.Ceresa (Eds), John Wiley & Sons. New York, (1), 11.
364. Billmeyer, F.W.Jr. (1971). "Text Book of Polymer Science". John Wiley & Sons, N.Y. 84
365. Eromosele, I.C. (1994). *J Appl Polym Sci*, (53), 1709.
366. Hamit, C.; Hatice, H.; Osman, Y.; Elvan, Y. (1998). Graft Copolymerization of 4-Vinyl pyridine on to Chitosan -I By Ceric Ion Initiation.
367. Pizzoli, G.O.; Ceccorulli, G.; Scandola, M. (1991). *International Journal of Biological macromolecules*, (15), 281.
368. Conley, R.T. (1970). Conley, R.T. (Ed), Marcel Dekker, N.Y. (1), 254.
369. Gregory, J. (1987). Tadros, Th.F. (Ed), Academic Press (London) Ltd, London, Ch.8.
370. Gregory, J. (1996). Industrial water Soluble Polymers, Finch, C.A. (Ed), Royal Society of Cambridge, UK, 62.
371. Rey, R.E.; Varsanik, R.G. (1986). Glass, J.E. (Ed), 113.
372. Wing, R.E.; Donae, W.M and Russel, C.R. (1975). *J Appl Polym Sci*, (19), 847.
373. Morrison, R.T.; Boyd, R.N. (1995). Organic Chemistry, 6th edition, Prentice Hall Inc. Publishers, New Delhi, India, 744.
374. Khalil, M.I.; Farag, S.; Hebish, A. (1991). *Starch/Starke*, 43(2), 254.
375. Khalil, M.I.; Farag, S.ABD, S. Fattach, E.L. (1995). *J Appl Polym Sci*, (57), 335.
376. Biswal, Diptirani. (2003). "Flocculation and Rheological Investigations in Aqueous Solutions of Hydrolysed and Unhydrolysed Grafted Polysaccharide". Ph.D. Thesis, IIT, Kharagpur.

377. Kerr, R.W.; Neukom, H. (1952). *Die Stärke*, (4), 255.
378. Paschal, E.F.; Minkema, W.H. (1961). U.S. Patent 2,995,513 Chem Abstr 55, 26489.
379. Mobire, F.; Audebert, R.; Quivoron, C. (1984). *J Colloid Interface Sci*, (97), 120.
380. Mobire, F.; Audebert, R.; Quivoron, C. (1984). *Polymer*, (25), 1317.
381. Sennet, P.; Oliver, J.P. (1965). *Ind & Eng Chem*, (52), 32.
382. Ogedengbe, M.O. (1973). "Polyelectrolytes in the Treatment of Wastewaters". Ph.D. Thesis. Iowa State University.
383. Larsson, A.; Wall, S. (1998). *Colloids and Surfaces A: Physicochem Eng Aspects*, (139), 259.
384. Collins, E.A.; Bares, J.; Billmeyer, F.W. (1973). John Wiley & Sons, New York, 394.
385. Nishimura, S.I.; Kohgo, O.; Kurita, K. (1991). *Macromolecules*, (24), 4745.
386. Durand Piana, D.; Lafuma, F.; Audebert, R. (1987). *J Colloid Interface Sci*, (119), 474.
387. Denoyel, R.; Durand, G.; Lafuma, F.; Audebert, R. (1990). *J Colloid Interface Sci*, 139, 281.
388. Killman, E.; Berger, M. (1985). *Colloid Polym Sci*, (263), 338.

